Climatic Anomalies and their influence on Rainfall Trends in Vhembe District South Africa

SC Nenwiini

ORCID number: 0000-0002-3928-9935

Thesis submitted for the degree of Doctor of Philosophy in Geography at the Mafikeng Campus of the North-West University

Supervisor: Prof TA Kabanda

Graduation October 2017

Student number: 22706119

Declaration

I Miss Shandukani Confidence Nenwiini (Student No: 22706119) declare that this dissertation for the award of Doctor of Philosophy in Geography at the North West University, has not been previously submitted for a degree in this or other institutions, and that all the references contained in this study have been duly acknowledged.

Signature Date

Acknowledgement

This research was done while I was holding a study leave and a grant through AQIP (Academic Qualification Improvement Programme) program of UNISA (University of South Africa). I wish to register my sincere gratitude for the support I received. I am greatly indebted to my promoter Prof T.A. Kabanda for his academic guidance, counselling, encouragement and patience throughout the writing of this dissertation. I also value his tireless interest and vigour as a supervisor. It was partly through his ideas that the orientation of this study was conceived.

A special word goes to Mr. Andrew J. Smith of University of Reading England for proof reading and editing my work – always with a sense of humour. I sincerely, thank Dr TH Kabanda for drawing the study area map, which needed time and much precision. Prof T. Ruhiiga and Prof Palamuleni are acknowledged for their words of encouragements whenever they meet me. Those words kept me going, I thank you. The staff members of the Department of Geography and Environmental Sciences North West University (NWU) are gratefully acknowledged for various assistances. I would especially like to thank members of the Department of Geography at UNISA. All of you have been there to support me. Thanks to Mrs Segopotse Malema, Prof MD Nicolau, Prof Elizabeth Kempen for their support.

Lastly, and not least, the whole family of Nenwiini; my mother Ms. Sylvia Nenwiini, my late father Mr. Robert Nenwiini, my siblings Mulalo, Khathutshelo and my cousin Vhutshilo; are all acknowledged for their moral support. This work is dedicated to our children - Wanga, Dhahabu, Mukundi, Ondwela and Tshilidzi who are encouraged to study hard and attain high academic levels.

Abstract

The principal aim of this study was to relate the large-scale meteorological systems to the local seasonal rainfall characteristics (especially rainfall onset and variations/trends). In addition, the study established the relationship between the seasonal rainfall onset, mean climatological systems and anomalies and their respective dynamics in the north east of South Africa (Vhembe District). The two most significant forcings in Vhembe District that influence rainfall are the topographic effects and the large scale circulation, which are mutually interactive in some cases. Four steps of analyses were involved. In the first step humid and semi-arid climatic subdivisions of Vhembe District were assumed from earlier studies. The rainfall characteristics and trends for the local area were then analysed based on these climatic groups. This first step also included the task to determine seasonal rainfall onset changes over different decades and within decades from 1980 to 2009 for both humid and semi-arid areas. The results in this step were obtained using two techniques, namely Mann Kendal trend analysis and Sen's slope estimator, which were employed to test for the presence of statistically significant trends and magnitude respectively. The second step was to establish the degree to which the local gauge data captures the signal of large-scale climate forcing of the study area. This step was accomplished by examining rainfall estimated by global precipitation datasets (in this case Climate Prediction Centre (CPC)'s Merged Analysis of Precipitation (CMAP)) in order to compare and validate the seasonal rainfall onset obtained based on the analysis of local gauge data.

The third step was to establish relationships between seasonal rainfall onset and change and large-scale mean atmospheric circulation. This was accomplished by exploring meteorological systems and indicators of moisture transport and accumulation (specific humidity, moisture flux and vertical motion), that feature during seasonal rainfall onset. The final step, explores the time-varying large-scale meteorological anomalies associated with the evolution of local seasonal rainfall characteristics. The third and fourth steps used the data products of NCEP/NCAR reanalysis output.

The study has established differences and common denominators between humid and semi-arid zones during early and late seasonal rainfall onset in Vhembe District. For example, no large-scale moisture supply or convective activities are needed in the humid zone for seasonal rainfall to commence. While in the semi-arid zone, large-scale moisture supply and large-scale convective activities initiates seasonal rainfall onset.

Contents **Page No**

Chapter Six

Meteorological characteristics during the rainfall onset

Chapter Seven

Atmospheric Anomalies

List of Tables

List of Figures

Glossary

Atmospheric Circulation Model: A mathematical model for quantitatively describing, simulating, and analysing the structure of the circulation in the atmosphere and the underlying causes.

Anomaly: The deviation of a measurable unit.

Climate System (CS): The system consisting of the atmosphere (gases), hydrosphere (water), lithosphere (solid rocky part of the Earth), and biosphere (living) that determine the Earth's climate.

Climate variability: Refers to variations in the mean state and other statistics (such as standard deviations, statistics of extremes, etc.) of the ***climate*** on all temporal and spatial scales beyond that of individual weather events.

Composite: An average that is calculated according to specific criteria. For example, one might want a composite for the rainfall at a given location for all years where the temperature was much above average.

General Circulation Model: These computer simulations reproduce the Earth's weather patterns and can be used to predict change in the weather and climate

Outgoing Long-wave radiation (OLR): The energy that is radiated back to atmosphere by the earth surface. This takes place after the earth surface is heated by the short wave radiation from the sun; the radiation that arrives at the surface of the earth is partly reflected and partly absorbed.

ENSO (El Nino + Southern Oscillation (SO)): Term used to describe the full range of the SO that includes sea surface temperature (SST) increases (warming) as well as SST decreases when compared to that of a long-term average. It is basically an oscillation between a warm and a cold phase, commonly referred to above as El Nino and La Nina, respectively.

NCEP/NCAR Reanalysis Data: Is a continually updated gridded data set representing the state of the Earth's atmosphere, incorporating observations and numerical weather prediction (NWP) model output dating back to 1948. It is a joint product from the National Centre for Environmental Prediction (NCEP) and the National Centre for Atmospheric Research (NCAR).

Synoptic scale: Used to classify large-scale weather systems more than 200 km across.

Acronyms

CPC: Climate Prediction Centre
CMAP: CPC Merged Analysis of Precipitation
DAFF: Department of Agriculture Forestry and Fisheries
GPCP: Global Precipitation Climatology Project
GCM: Global Climate Model
ENSO: El Nino + Southern Oscillation
EAS: Earth-Atmosphere System
IPCC: Intergovernmental Panel for Climate Change
ITCZ: Inter Tropical Convergence Zone
LCL: Lifting Condensation Level
MAKESENS: Mann Kendall test for trend and Sen's slope estimates
NASA: National Aeronautics and Space Administration
NCEP: National Centre for Atmospheric Research
NCAR: National Centre for Environmental Prediction
NOAA: National Oceanic Atmospheric Administration
OLR: Outgoing Long-wave radiation
SAWS: South African Weather Service
WMO: World Meteorological Organization
TTT: Tropical Temperate Trough
SST: Sea Surface Temperature
SO: Southern Oscillation
QBO: Quasi Biannual Oscillation
SWIO: Southwest Indian Ocean
SAO: South Atlantic Ocean

Chapter One
Introduction

1.1 Overview of the Study

This study will give attention to the meteorological systems which are associated with long-term seasonal rainfall trends especially changes in rainfall onset (rainfall characteristics) in the north east of South Africa (Vhembe District). The main aim is to establish the relationship between the seasonal rainfall onset, mean climatological systems and anomalies and their respective dynamics. The study area is found north of the Tropical of Capricorn, and like most other tropical regions (in the lower latitudes), this area did not previously get much attention. According to Stringer (1972), modern climatology in many areas has put great emphasis on studying mid-latitude climates. Climatological concepts and principles applicable in temperate regions were then applied to the interpretation of climate developments in lower latitudes.

Vhembe District in South Africa occupies much of the former Venda homeland, which was one of the former designated homelands within South Africa. Four of these (Transkei, Bophuthatswana, Venda, and Ciskei) eventually became so-called independent with sovereign rights (Kaufman, 1998). The remaining six homelands KwaZulu, KwaNdebele, QwaQwa, KaNgwane, Gazankulu, and Lebowa-remained a part of the Republic of South Africa, but with self-governing rights within their borders.

The homelands never had the capacity for training and research into the climate prevailing in their areas and so were unable to understand the forcing factors that govern the climate variability and change in their respective homelands. Even for South Africa at large, the rainfall climatology of the former homelands never received much attention in the climate research. Therefore, there is little climate related literature that concerns the former homelands such as Venda, which date back before the 90s. Most of the studies that involve homelands are regional in scale (covering South Africa or southern Africa) and are not conducive for use operationally at a district level. For example, Kruger (2006) examined the spatial variations of trends in precipitation in South Africa from 1910 to 2004 and observed a significant decrease in annual precipitation of the northern part of Limpopo. The data used was smoothened using the whole South Africa averaged data. Moreover, the data used were not spatially representative, mostly are simulated data and not long enough to detect significant pattern of rainfall trend. Mason (1996) observed a decrease in rainfall in the Lowveld region of South Africa during the 1970s. David et al. (2007) described the nature of rainfall variability in the summer rainfall zone of South Africa from 1950 to 1999. However, in all of these studies, the distribution of rainfall stations was too sparse to capture the local effects.

Generally, all these studies, except Kabanda (2004) who studied drought climatology in Vhembe District, covered a large area. Nenwiini and Kabanda (2013) documented the changes in rainfall in Vhembe District using trend analysis. However, that analysis dealt with annual rainfall data instead of seasonal data. Mpandeli (2014) described the impact of rainfall variability in Vhembe District using annual rainfall data instead of seasonal data. According to Usman and Reason (2004), rainfall variability research that aim to provide climate information to users in the community such as farmers and resource managers need to provide more detailed information not just deviation from the mean state. The timing and consistency of seasonal rainfall during the growing season is crucial than the total amount received per season (Omotosho, 2000; Usman & Reason, 2004; Tadross et al., 2005; Camberlin et al., 2009; Dunning et al., 2016). Partal and Kahya (2006) advocated the use of seasonal data instead of annual data. They consider that annual trends should be interpreted with caution, as they may obscure large seasonal differences.

This study deals with changes in rainfall onset that affect the seasonal rainfall period (October to March) at a pentad scale. The pentad scale is deemed suitable for its ability to capture the tropical temperate troughs rain producing systems, which have been linked to most of the regional rainfall (Usman & Reason, 2004). This study also explores meteorological systems and indicators of moisture transport and accumulation (specific humidity, moisture flux and vertical motion and their anomalies), that feature during seasonal rainfall onset.

Lately, there has been an increase in dense spatial network of rainfall stations in the study area especially after the introduction of automatic weather stations (AWS) by South Africa Weather Service (SAWS). According to the South African Weather Services, countrywide observational network now consists of > 214 Automatic Weather Stations; 25 Climate Stations (1 x 1st order, 3 x 2nd order & 21 x 3rd order stations); 1277 Rainfall Stations and 131 Automatic Rainfall Stations (South African Weather

Service, 2011). Climate research recommend the use of dense network of data in order to filter irregularities in rainfall data and it is ideal for validating climate models.

Rainfall season characteristics – such as times of rainfall onset and cessation – show considerable changes and variability in Vhembe District (Kabanda, 2004; Nenwiini, 2012). A decrease of rainfall length of 50 days or approximately two months in recent years has been detected (Nenwiini, 2012) in the district.

There is a link between variations or trends in the rainfall climatology and global climate change (Hulme, Osborn & Johns, (1998)) or local anthropogenic climate change (Munyati & Kabanda, 2009; Kabanda & Munyati, 2010; Kabanda, 2011). However, there is no identification of weather systems and their anomalies that are associated with these variations and trends in the Vhembe District or at any local scale level the size of a district in South Africa. This shortfall renders the area's seasonal rainfall prediction difficult.

There are recent works that have added to the knowledge of Vhembe rainfall climatology (Reason, Hachigonta & Phaladi, 2005; Singo, 2008; Nenwiini, 2010; Kabanda, 2011; Nenwiini, 2012; Mpandeli, 2014; Mulugisi, 2015; Kabanda & Nenwiini, 2015). However, these are still not adequate to understand the area rainfall climatology fully, especially the dynamics of the rainfall producing systems. Also, lack of knowledge of the influence of the local characteristics on area rainfall still needs further exploration and understanding. For example, the orographic factors (Soutpansberg mountains) and geographical position of the Vhembe District (situated at the periphery of the southern and northern end of the tropics and subtropics respectively) has never been widely considered in previous studies. This could be the key information to explain the variability of Vhembe District spatial rainfall characteristics in seasonality and rainfall patterns. Therefore, this study will explore and quantify the climatological systems, their dynamics and their influence on the rainfall variation and trend. According to Kiangi (1989) and Makarau (1995), the study area and its environs are directly affected by the influential synoptic circulations (climatological systems) originating from the Indian Ocean and the central Africa subcontinent. From the subcontinent climate, developments are mainly associated with the Inter-Tropical Convergence Zone (ITCZ). Consequently, this study will thoroughly examine the climatological systems in terms of specific humidity, moisture flux and vertical motion that might influence the changes in rainfall onset.

The economy of Vhembe District is characterised by dual farming systems mainly subsistence farming, with emerging commercial farming and ecotourism sectors. Majority of the farmers in Vhembe District practise rain-fed subsistence farming (Moeletsi, 2013) with some small-scale and large commercial farmers who promote production through irrigation. Among these, agriculture is the most fundamental in the economic, social development and stability of the district. Agriculture in the study areas are in three subsectors: subsistence farming; commercial farming that is large scale fruit and nuts production and commercial forestry. Unpredictable variations in the onset and duration of the rainy season lead to uncertainties over planting dates and create stresses on agricultural production (Mabiru et al., 2012; Traore et al., 2013). Therefore, this study aims to establish the rainfall climatology of the district. According to Göbel et al. (1996), rainfall information is crucial for evaluating the agricultural production potential of a region and hence the sustainability of agricultural production systems. The Department of Agriculture, Forestry and Fisheries (DAFF) will be a beneficiary of the identified significant predictors that can support both commercial and subsistence farmers via extension officers and various publications.

1.2 Problem Statement

Fluctuations in the rainfall onset and cessation contribute to variation in seasonal rainfall length in Vhembe District. Changes in climate variation and trends have made it difficult to understand and determine the recurrence of extreme rainfall events such as floods; drought wet or dry spells especially at local-scale level. The implications of these changes are particularly significant for areas already under stress, such as regions that experience water shortage through a combination of dry climate and excessive water demands.

Rainfall characteristics are changing gradually (Nenwiini 2012; Nenwiini & Kabanda, 2013), and will negatively affect district agricultural production and development projects in the study area. Having sufficient rainfall information at local level will enhance water management planning and food security. Studying the rainfall climatology of the district is also essential in relation to the changing climate. Therefore, the study of synoptic-climatological systems and their anomalies in southern Africa in relation to rainfall variability and trend of Vhembe District will be the contribution or value added of this study to understand the rainfall climatology of the district and other areas of similar scales.

1.3 Research hypotheses

The base of the present study is on the following assumptions

(i) That the rainfall of the area is modulated by the synoptic circulation

(ii) That rainfall is further enhanced by the local features especially the orographic effect.

(iii) That the climatological anomalies related to seasonal variations of the location of the inter-tropical convergence zone (ITCZ), are instrumental in determining the changes and trends in the Vhembe District rainfall.

1.4 Research Aim and Objectives

The core aim of this research is to investigate a more meaningful association between the dynamics of synoptic meteorological systems and the rainfall characteristics in Vhembe District. This requires enhanced understanding of the significant characteristics and features of the meteorological systems' structure and evolution that influences the region (southern Africa in general) – namely the specific humidity, moisture flux and vertical motion. Very few studies so far have researched the specific effects of meteorological systems on the Vhembe District per se. These include that of Kabanda (2004) which provided the most comprehensive knowledge of the meteorological systems with respect to the climate of Vhembe District; although his study was concerning the climatology of drought in the district, which is not the main concern of this study. Lately, there has been an increase in studies on the perceptions of rural communities on climate change and variability in Limpopo province (Mpandeli, 2014; Mpandeli & Maponya, 2012 and 2014; Mpandeli, Nesamvuni & Maponya, 2015). However, lack of evidence-based (empirical) studies on the local rainfall variability proofs difficult to disentangle the impact of rainfall variability on livelihoods. Local scale climatology has received little attention in South African climate studies, although according to Wilbanks and Kates (1999), changes at a local scale in turn contribute to global changes and are affected by them. They have the opinion that improving the understanding of linkages between macroscale and microscale phenomena and processes is one of the intellectual challenges of our age in a wide range of sciences. This concept is not new; for example, Root and Schneider (1995) have suggested 'strategic cyclical scaling' as an approach to analysing interactions among processes operating at different climate and ecological scales. They advised that this would involve a continuing cycling of studies between large-scale associations that suggest small-scale investigations and smaller-scale associations in order to test the causes and driving forces of the large-scale patterns.

The study area is relatively small in comparison with South Africa but it covers an area of approximately 60,500 km^2, which is twice the size of Belgium - and climatological studies have been carried out in small countries such as Belgium, Burundi, Lesotho and others (Kabanda, 2004). Then it is high time to split bigger countries into small, manageable entities for climate research, and apply the well-researched large-scale driving climatologies to simulate and study local climates. This approach is starting to happen through downscaling. However, downscaling is computationally rigorous and very expensive. The majority of methods have been developed in developed countries where long-term data are available for model calibration and verification (Wilby, 1998; Haylock et al., 2006 Fowler, Blenkinsop & Tebaldi, 2007). Therefore, in the local settings such as Vhembe District in a developing country where data availability is still growing, downscaling is still a challenge.

The significance of small-scale (local-scale) climate analysis is concomitant with solving local community based problems. The current example, is the issues of supplying fog water for use in some Limpopo province (in particular Vhembe District) schools and the climate studies involved (Olivier & Van Heerden, 1999; Olivier & Rautenbach, 2002; Olivier & van Heerden, 2003).

1.4.1 What are the motivations behind this study?

- The scientific challenge – the complexity of the transition between tropical and subtropical systems (due to the latitudinal position of the study area), especially concerning synoptic meteorological systems, in terms of their forcing-effect on local rainfall.
- Gap in current knowledge exists. There is a lack of a thorough understanding of the local rainfall variability (onset) and seasonal fluctuation (trend) in the Vhembe District, especially when it comes to local influence (orographic effect) and synoptic features (meteorological systems). In addition, the lack of knowledge on

the climate of district (municipality) level in South Africa is another knowledge gap.

Through the following specific objectives, this study will achieve the intended aim and close the existing knowledge gaps in Vhembe District:

1. To identify characteristics of the local seasonal rainfall by analysing station-based rainfall trends and patterns
2. To relate local rainfall (rain gauge data) and Climate Prediction Centre Merged Analysis Precipitation (CMAP)
3. To explore time-varying large-scale meteorological systems associated with the evolution of local seasonal rainfall characteristics
4. To determine moisture features needed to initiate seasonal rainfall onset.

1.5 Description of the Study Area

1.5.1 Introduction

This section describes the environmental setting of the study area. It focuses on the physical components that influence rainfall in Vhembe District (Figure 1.1).

1.5.2 Description of the Study Area

Vhembe District is situated on the northern part of South Africa, extending from 22°S to 24°S and 29°E to 31.5°E. It covers an area of approximately 60,500 km^2 with a unique diverse topography, which has a significant influence on the climate of the area. According to Hanssen-Bauer et al. (1997), precipitation amount and variability may differ greatly over small distances, due to orographic effects that are sensitive to small differences in circulation patterns. The Soutpansberg is the most prominent mountain range in the study area. Generally, it runs northeast and southwest, perpendicular to the normal southeasterly - easterly flow of winds during the southern summer. When the moist wind from the Indian Ocean in the east flows up the eastern slopes (orographic lifting), the convection from daily heating coupled with the orographic lifting leads to the development of showers and thunderstorms that can build very rapidly (Sparrow, 1987; Olivier and Kabanda & Munyati 2010).

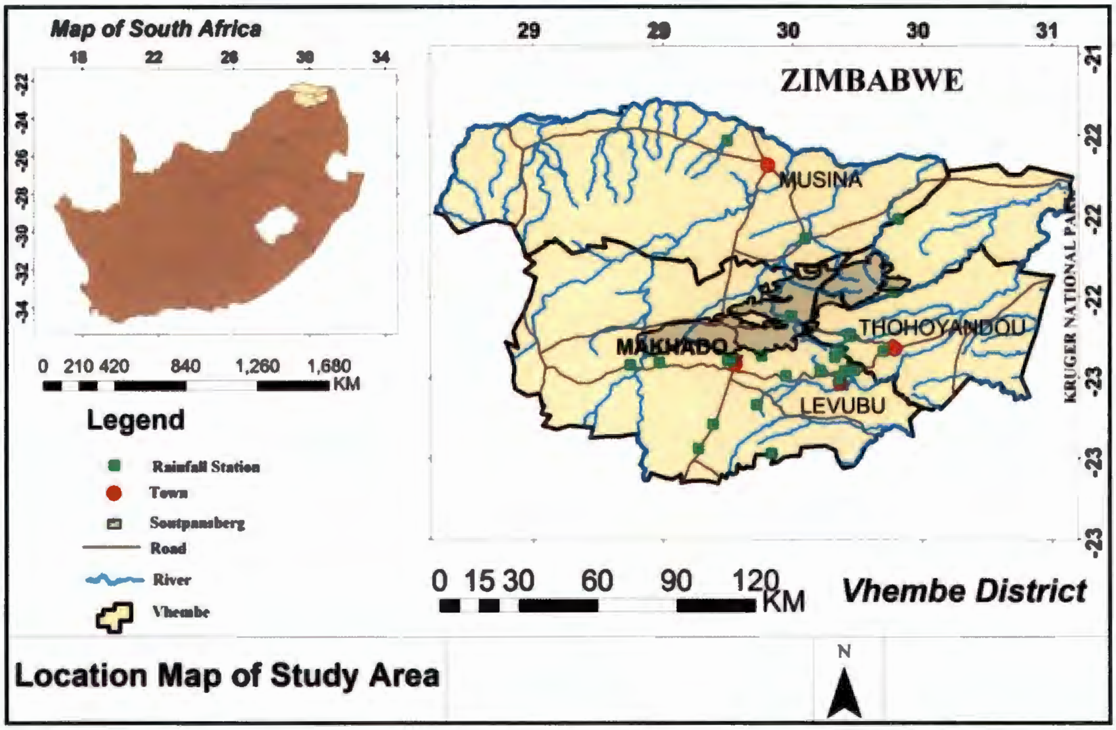

Figure 1.1: Map of Vhembe District showing rainfall stations, roads and rivers

1.5.3 Hydrology

Rivers and dams are important sources of moisture in order to maintain in-situ evapotranspiration that replenishes the area humidity. The rivers in Vhembe District are perennial. Major river catchments include Limpopo and Luvuvhu. The base flow of most Luvuvhu River catchment streams originates from the higher elevations, where higher precipitation and lower temperatures result in excess water being available during the winter season. This period is after the summer rainfall season that lasts for about five months (Singo, 2008). Most Luvuvhu River catchment streams generally lose all or part of their flow as they approach the end of the dry season. There are also smaller rivers like Tshirovha, Tshiombedi, Mukhase, Mbwedi, Madanzhe and Sterkstroom. The upper Luvuvhu, Sterkstroom, Latonyanda, Dzindi, Mukhase, Mbwedi, Tshinane and Mutshindudi are steep, narrow rivers dominated by cobblestones and occasional pools with a few bedrock rapids. The Tshirovha and Tshiombedi tributaries of the Mutale River are steep with both bedrock and fixed boulder rapids. Near the Kruger National Park border, in the Steep Lanner Gorge, the Mutale River joins the Luvuvhu River. The Luvuvhu River then joins the Limpopo River near Pafuri at Crook's Corner on the Mozambique border (State of Rivers Report, 2001).

Dams in the area include Albasini, Nandoni, Mambedi, Tshakhuma, Damani, Vondo and Phiphidi Dams. Vondo and Phiphidi Dams lie in the Mutshindudi River while Nandoni Dam is in the middle section of the Luvuvhu River east of the confluence with the Ḓzindi tributary. Dams play an important role in supplying moisture to the immediate lower atmosphere due to evaporation.

Wetlands found in the study area contribute to rainfall through evapotranspiration. Wetland habitats act as sponges that help to attenuate floodwaters and maintain a moist boundary layer with the air above. They are remarkably effective humidity-control agents because of their water retention capacity, which is ~0.94 mm; this is about twice that of uplands (average 0.43 mm) according to Liu (1998). Observations indicate that wetlands are drained to provide agricultural lands, space for urban development and to reduce risks of diseases such as malaria, or are being dammed (Sinthumule, 2001). This destruction of wetland habitats is one of the man-induced changes that may affect rainfall in the area.

1.5.4 Vegetation

According to Mucina and Rutherford (2006), the Soutpansberg mountains in Vhembe District consists of thick deciduous woodlands and evergreen montane forests with a poorly developed grassy layer, which follow the rainfall distribution in the area. Other parts feature a relatively open savannah type of vegetation. There are also different plant species, such as tree species that include the *Acacia tortolis*, as the main dominant species, *Adonsonia digitata, Sclerecaria birrea, Terminelia prunoides, Colophospermum mopane* (mopani) trees and some grass species including *Patilena cofandum*. Such types of vegetation have various significant roles to rainfall of the area; for example, by supply moisture through evapotranspiration, maintaining the moisture in the upper soil level and lowering the lifting condensation level (LCL) (Kabanda & Munyati, 2010). Vegetation is important, especially on the top of the mountain ranges, where it is able to pump moisture directly into the LCL thus contributing to cloud formation, development and rainfall.

Exotic species such as *Lantana camara* (Lantana) have invaded large areas of arable land in Vhembe District. Other alien plants include *Acacia saligna* (Port Jackson willow), *Acacia cyclops* (Rooikrans) and *Sesbania punicea* (Sesbania-red). Invasive species such as *Azolla filiculoids* (Water fern) and *Eichhornia crassipes* (Water hyacinth) are found in the wetlands and in other wet areas such as rivers, riverbanks and dams. These have displaced native species. They establish easily, and due to a lack of natural predators or competitors, are able to multiply rapidly and to out-compete indigenous vegetation (Sinthumule, 2001) causing ecological disruption.

Most of the alien plant species have leaf structures that promote high rates of evapotranspiration (for example, Solanaceae known as wild tobacco), which can lead to soil drying in the area (Netshitungulu, 2001).

1.5.5 Climate

According to Kabanda (2003), the climate of Vhembe District is distinctively divided into dry and wet seasons; the wet season encompasses the austral summer, while the dry season is the austral winter. Due to the east-west orientation of the Soutpansberg, the area experiences orographic rainfall. This phenomenon is due to moisture-laden air from the Indian Ocean, driven by the prevailing southeasterly winds. In addition, due to the extreme topographic diversity and altitude changes over short distances within the study area, climate varies dramatically. For example, Entabeni on the southern slopes of the Soutpansberg, receive an annual rainfall of 1,874 mm, which may increase to reach annual precipitation of 3,233 mm at times (Hahn, 2002; Olivier & Rautenbach, 2002). Also, temperatures vary considerably according to topography and seasonal conditions. The wet seasons are warm, with temperatures ranging from 16 – 40°C while dry seasons temperatures are mild, ranging from 12 – 22°C. Minimum dry season temperatures seldom drop below freezing point (Mostert, 2006). Moisture related climatic factors and their dynamics are expanded and explained further in later chapters.

1.5.6 Temperature

Temperature is found to vary from place to place and over time, and it is generally believed that the correlation between rainfall and temperature changes between months. For example, Rajeevan et al. (1998) examined the temporal relationship between land surface temperature and rainfall, and found that temperature and rainfall were positively correlated during January and May but negatively correlated during July. In addition, Huang et al. (2009) found a negative correlation between rainfall and temperature in the Yellow River basin of China. Variability of temperature distribution is influenced by a variety of factors. These factors include distance from water bodies, orography and nature of prevailing winds (Barry, 1992; Aguado & Burt, 2001). In Vhembe District , continentality and orography play a major role in influencing temperature. This causes daily temperature variation; also, variations are seen in mean weekly, monthly and annual scales. These temporal variations may lead to general rainfall variation, which is the main focus of this work.

Minimum temperature is highly affected by atmospheric disturbances near the ground (Tyson, 1986) than the maximum temperature. It is also found that temperature depends greatly on altitude and configuration of land and degree of continentality (Ayoade, 1983). Temperature variations are also influenced by the change in circulation system (Lengoasa, 1991). With the intensification of cyclogenesis and the possible increase of low pressure systems, moist air circulation over the tropical Indian Ocean would be directed to areas of enhanced surface convergence, leading to temperature fluctuations.

Temperature is closely related to cloud condition. When the amount of cloud is relatively high, maximum temperatures are relatively low. During relatively cold and rainy times of the year, correlation is seen between minimum temperature and mean cloudiness (Jones & Hulme, 1996). The prevalence of cloud bands and rainfall affects the extent of temperature anomalies depending on location and frequency of cloud band (Harrison, 1984). During the day, cloudless skies favour rapid heating and rapid loss of accumulated heat at night. Conversely, abundant clouds prevent rapid heating during the day and rapid cooling at night.

Temperature in Vhembe District is strongly associated with seasonal conditions: during wet seasons (December, January and February), temperatures are relatively warm, while in dry seasons (June, July and August) temperatures are associated with chilly cold conditions and clear sky in most instances. Dzivhani (1998) detected spatial and temporal fluctuation of temperatures in the district; he attributed the former to the influence of landscape features and the latter to seasonal forcing. The seasonal forcing is due to the influence of the movement of the sun, where the maximum influence is when the sun is overhead in the southern hemisphere. This situation is accompanied by strong insolation and high temperature that produces thermal heating and low-level convergence and rainfall, though with a fortnight to a month lag (Timiza, 2011).

1.6 Summary

This study focuses on investigating the relationship between the dynamics of synoptic meteorological systems and the rainfall characteristics in Vhembe District of Limpopo province. The focus is mainly to establish the onset of seasonal rainfall in relation to regional scale meteorological features. In this chapter, the background, research problem and hypothesis were discussed in order to justify the aim and objectives of the study.

Chapter Two

Literature Review: Synoptic Climatology and Methodological Approach

2.1 Introduction

High variability of onset and cessation of the rainy season is one of the many climate problems facing the population living in the semi-arid and sub-humid zones in Africa. Most people inhabiting these zones rely on subsistence farming of rain fed crops and pastoralism for their livelihood, which is dependent on an unreliable water supply in the form of rainfall. Vhembe District is characterised by high rainfall variability, and the majority of the population are reliant on subsistence farming, which depends on scarce rainfall water. Game farming, conservation and tourism are some of the activities that have recently been ventured into and which are contributing to the region's economy (Tshitangoni, 2010; Whitebread, 2011). All these activities depend on the performance of rainfall seasons. A delay in the onset of rainfall, early withdrawal, or short but intense rainfall events separated by long dry spells may cause seasonal rainfall to fail (Camberlin et al., 2009), which can lead to devastating impact on agriculture especially in areas where irrigation is underdeveloped.

Recently, there has been an improvement in the climate research in terms of predicting seasonal rainfall and climate variability. The General Circulation Model (GCM) has been developed and praised for its capability to predict seasonal and long term climate variability. However, the resolution of the GCM is too coarse with the seasonal predictions given at a scale of several hundred kilometres (Gong & Ho, 2003). In addition, the GCM models do not take into account the local land physiography, which is critical in modifying the local climate. Translating the GCM output to a small scale presents a challenge, so seasonal rainfall predictions based on the GCM are of little value to decision makers at the small-scale level such as a district, municipality or village.

Some efforts have been made to address the limitations affecting the GCM; a further downscaling has been done which is believed to yield relevant outputs at a regional level. Yet this does not address local area's needs. For instance, users at municipal and district level need reliable and accurate information on seasonal rainfall characteristics such as the onset, persistence and cessation in order to plan for activities such as agriculture, engineering and conservation management.

Information of the onset and the causes of rainfall season at finer scale taking into account both large scale dynamic features and the local features is required to cater for local specific needs. Studies on the seasonal variability of the regional rainfall have been undertaken, and some of these studies have been conducted as part of large scale research such as regional level (Reason et al., 2005; Mzezewa, Misi & van Rensburg, 2010), which is not sufficiently representative of the current study area (district level). Some of the studies were carried out a few years back and based on simulated rainfall data (Todd & Washington, 1999; Tennant & Hewitson, 2002; Fauchereau et al., 2003; Reason et al., 2005). Currently, there is a lack of information on the onset and the causes of the rainy season at a local scale. The effects of physiographic features on seasonal rainfall also require an in-depth understanding. The knowledge of the seasonal variability of rainfall in Vhembe District and the associated dynamic climatological features is of interest because of its importance in developing significant predictors that can help in making reliable predictions of the seasonal rainfall characteristics in order to ensure sustainable agricultural productivity, risk management planning, engineering, efficient water resource and conservation management practices.

2.2.1 Seasonal Rainfall Onset

One of the problems faced in identifying and predicting the onset of seasonal rainfall is the difficulty in differentiating between the true and false onset. According to Lima and Lall (2009), an isolated and unusual event of high rainfall in the beginning of the season may mask the onset of the rainy season in a region where wet-season rainfall is driven by deep convection. A false onset is often followed by a long dry spell (Goswami & Gouda, 2007) and can be mistaken as the true onset date. In effort to address this problem, a number of criteria to determine and distinguish true onset from false have been proposed. Various definitions of the season rainfall onset have been proposed based on varying criteria. They differ from one location to another due to the fact that particular onset dates are derived from the individual rainfall climatology.

Rainfall onset dates have been defined using rainfall amount, the number of rainy days, percentage cumulative mean rainfall, rainfall-evapotranspiration relation method, wind shear etc (Omotosho, 1990 & 1992; Odekunle, 2004; Guenang, 2012). Generally, the onset of the rainy season can be defined as the first day of the year in which the total daily rainfall is greater than a threshold value, which is commonly chosen subjectively

(Liebmann & Marengo, 2001; Lima, 2009). It is important to note that the definition of the onset date is adjusted based on the locations climatology and specific needs. A threshold value is the rainfall amount required for a day to be counted as a rainy day (Lima & Lall, 2009). The subjective adoption of threshold values has been criticised for its lack of robust conclusions. The rainy season onset, length and cessation have been shown to be sensitive to the rainfall threshold value (Marengo et al., 2001). A lower threshold means a longer season, starting earlier and finishing later, and a higher threshold gives a shorter season (Aviad, Kutiel & Lavee, 2004).

2.2.2 Rainfall Onset Criteria

Several methods have been developed to define the rainfall onset and cessation, and as a result, various models have been proposed. The onset method based on the analysis of daily rainfall data is the most commonly used and has received considerable attention (Ilesanmi, 1972a; Kowal & Knabe, 1972; Marengo et al., 2001; Liebmann & Marengo, 2001). Some studies have used the rainfall-evapotranspiration relation method (Cocheme & Franquin, 1967; Benoit, 1977) to determine the onset date. However, this method is not favoured in some regions because evapotranspiration data is not readily available, while in some areas evaporation exceeds precipitation, which implies that evapotranspiration does not always lead to precipitation.

Percentage cumulative mean rainfall method is another method employed in determining the rainfall onset dates (Ilesanmi, 1972b; Adejuwon et al., 1990; Ati, 2002; Odekunle, 2004). The use of total rainfall amount method has received considerable attention because it uses rainfall data, which is direct measurement and readily available, rather than other rainfall-associated variables (Olaniran, 1983). Although it has been commonly accepted, it has been criticised for its dependence on the amount of rainfall (Ati, 2002; Odekunle, 2004). Odekunle (2006) compared the effectiveness of the rainfall amount and rainy days method in determining the seasonal rainfall onset and cessation date in Nigeria. The observations showed that both methods produce similar mean onset and retreat dates. However, the use of rainy days was reported to be more effective because it produces rainfall onset and cessation dates that are more accurate than those produced by the rainfall amount method.

According to Camberlin et al. (2009), the performance of a rainy season, for ideal crop growth, does not merely depend only on the total amount of rainfall - an adequate distribution of rainfall during the rainy season is necessary. Isolated rainfall events (wet spells) that may occur early in the beginning of the rainy season may constitute the specified total amount of rainfall required for seasonal rainfall to be supposed to have started. Thus a wet spell in the beginning of the rainy season may be mistaken as true onset of seasonal rainfall, which is misleading. Rainfall frequency method, in terms of rainy days, was found to produce accurate onset and cessation dates because it required rainfall to be frequent enough to ensure that true seasonal rainfall onset date is identified (Walter, 1968; Ilesanmi, 1972a; Ojo, 1977; Adedokun, 1981; Hastenrath & Kutzbach, 1985; Odekunle, 2004; Taddros et al., 2007; Moeletsi et al., 2012; Amekudzi et al., 2015 and Beyer et al., 2016). In this study, the rainfall frequency method (in terms of rainy days) will be used to determine the seasonal rainfall onset.

Rainfall onset date derived purely on observed local station rainfall provides key information on the local variability and pattern of daily rainfall. However, local rainfall is affected by random convective events which might locally give enormous rainfall amounts, enough to shift the onset date by a few days or even weeks (Camberlin & Diop, 2003). The limitations of rainfall data derived from local stations have led to the development of various merged satellite and gauge precipitation products over the last few decades. Merged precipitation datasets offers comparison opportunities in the analysis of rainfall variability over space and time (New et al., 2001). Recently, studies have determined the rainfall onset based on local gauge and CMAP data (Tadross et al., 2005; Moron, Robertson & Beer, 2009). In this study, CPC Merged Analysis Precipitation estimates are compared with the amount of local station rainfall accumulated prior to and during the early and late seasonal rainfall onset date in the study area. Therefore, it is necessary to provide a short review of the gridded merged precipitation analysis.

2.2.3 Merged Analysis Precipitation (CMAP)

The development of gridded precipitation data has led to an improvement in climatology and hydrology research. Gridded precipitation products aim to estimate global and regional precipitation data using in-situ rain gauge data, satellite estimates, radar data, and model reanalyses or a combination of both. Various gridded precipitation products have been proposed with coverage ranging from regional to global scale. However, most gridded precipitation data products do not provide daily data at a global scale. The ENSEMBLES observations gridded data set (E-OBS), the Asian Precipitation Highly Resolved Observational Data Integration towards Evaluation of Water Resources project (APHRODITE's Water Resources), Baltex and Rhires are some of the products that provide data at regional scale. The estimates of daily precipitation from these products are derived solely from in-situ gauge observations (Schamm et al., 2014).

Rainfall observed by local station gauge and interpolated gridded data fields are important in obtaining area-averaged precipitation for the land surface, but they are marred by biases resulting from systematic measuring errors (Rudolph & Schneider, 2005). In some poorly populated and elevated areas, the rainfall stations are sparsely distributed, which can lead to underestimation of precipitation (Xie et al., 2007; Yatagai, Xie & Alpert., 2008). On the other hand, satellite data present the benefit of a very good spatial coverage relative to rain gauges that are somewhat sparse especially in developing countries and sparsely settled regions (Schamm et al., 2014). However, the accuracy of precipitation data derived from satellite is also questionable (AghaKouchak et al., 2011), in-situ gauge observations are the only source that is obtained through direct measurements (Vila et al., 2009) and they provide the most reliable observations of precipitation (Bowman, 2005). In order to improve the quality and coverage of the gridded precipitation products, scientists have merged biased corrected in-situ gauge data, radar data and satellite data. A combination of local gauge and satellite observations enhances the quality of the products (Schamm et al., 2014; Vila et al., 2009). According to Adler et al. (2003) merged local gauge data and satellite observations allows multi-satellite estimates to supplement data in areas where rain gauges are sparse.

Two precipitation data sets are widely used in climate variability studies. These are the Global Precipitation Climatology Project (GPCP) and CPC Merged Analysis Precipitation (CMAP) daily precipitation dataset. These products provide precipitation pentad analysis from 1979 to present at 2.5° x 2.5° spatial resolution. The datasets are constructed from an analysis of local gauge data and satellite derived precipitation estimates (Adler et al., 2003; Xie et al., 2007). According to New et al. (2001), CMAP product provides precipitation estimates at the same space and time scales as GPCP and uses a similar set of input data and a similar, but more complex, merging technique.

In this study, the CMAP pentad data that provides precipitation estimates on a 2.5° X 2.5° grid from 1979 to present (Xie et al., 2003) is used for comparison and validation of seasonal rainfall onset date observed based on in-situ local gauge data. Pentad CMAP analyses are produced through a combination of numerous kinds of individual data sources of precipitation. This includes in-situ gauge observations, satellite estimates, and precipitation fields from the NCEP/NCAR reanalysis (Xie et al., 2003). CMAP estimates smaller amounts of precipitation over some of the global land areas. This is attributed to differences in the algorithms used to define the merged analyses and the input data sources (Gruber et al., 2000).

CMAP pentad precipitation data have been widely accepted and used in climate and hydrology studies. The seasonal rainfall distribution in the East Asia monsoon region has been studied using CMAP and local rain gauge data from China and South Korea. The output of the local gauge rainfall data was compared with that of CMAP, and the results obtained from the two data sources were found to be very consistent (Qian, Corte-Real & Xu, 2002). Moron et al. (2009) analysed the austral-summer monsoon onset and post onset rainfall and their associated low-level winds in Indonesia using CMAP, Global Summary of the Day (GSOD) and CPC morphing technique (CMORPH) data. In South Africa and Zimbabwe, Tadross et al. (2005) determined the onset of maize growing season using CMAP and local station data from the Computing Centre for Water Research (CCWR). Both data sets reportedly produced similar estimates of the mean, standard deviation and trend of onset in South Africa.

2.3 Main Rain Bearing Systems in Southern Africa

The variability and distribution of seasonal rainfall is believed to be driven by the region climate regime (Aviad et al., 2004). Large-scale circulation systems associated with South African rainfall have been documented. The region's rainfall pattern is attributed to the tropical, subtropical and mid-latitudes circulation systems. Various studies have been conducted on the seasonal rainfall variability and the driving mechanisms

(Tadross et al., 2007; Moeletsi et al., 2013; Mzezewa et al., 2010; Kabanda & Nenwiini, 2015; Kephe et al., 2016; Kabanda, 2017). The cloud bands connecting the tropical circulations with mid-latitude cyclones were shown to be the dominant cause of the seasonal rainfall of the country, with a smaller contribution from the tropical and subtropical cyclones as categorised by Harrison (1984), in the classification of South African rain producing systems.

The timing of seasonal rainfall in the southern African region is considered to be highly variable across space and time. A Climate regime is attributed to the region's location between the tropics and the mid-latitudes, the two surrounding oceans and the steep orography give rise to the climate regime. The large and synoptic scale mechanisms that drive rainfall variability over southern Africa have been explored. A number of studies have tried to relate the variability with the large scale circulation systems, and most of these studies have identified the main factors responsible for producing rainfall over the region. The suggested factors include the El Niño–Southern Oscillation (ENSO) phenomenon, mid-latitude systems, subtropical high pressure systems and the seasonal migration of the Inter Tropical Convergence Zone (ITCZ). In South Africa, the cloud bands connecting the tropical circulations with mid-latitude cyclones has been ascertained to be the main systems responsible for summer rainfall over the interior of the country, with the tropical and subtropical cyclones having smaller impacts (Harrison, 1984).

This study aims to determine the seasonal rainfall characteristics and associated dynamic climatological features over the northern part of South Africa. The following sections present a review of various factors that are thought to determine rainfall over southern Africa region at different scales.

2.3.1 El Niño–Southern Oscillation (ENSO)

The relationship between Southern African rainfall and the El Niño-Southern Oscillation (ENSO) phenomenon has been noticed for a long time. Ropelewski and Halpert, (1987, 1989 & 1996) have shown a presence of positive correlation between the Southern Oscillation Index (SOI) and Southern African rainfall. Lindsay, (1988) observed the relationship/correlation between rainfall in South Africa and the Southern Oscillation Index. ENSO is a system of interactions between the equatorial Pacific Ocean and the atmosphere above that is indicated by the difference in sea level pressure between

Tahiti and Darwin. According to Allan (1996, 2000), the large-scale warming of the equatorial eastern and central Pacific has been known as El Niño by oceanographers since the 1960s - 1970s. This anomalous warming was related to the anomalies in the upper ocean thermal structure throughout the equatorial Pacific Ocean. Rasmusson and Carpenter (1982) recognised that the Southern Oscillation is closely related to the large-scale changes in the tropical Pacific Ocean. In brief, the Southern Oscillation represents the variability in the Indo-Pacific Walker circulation in the tropics, is manifested as a displacement of the convection over the maritime continent, and is associated with large-scale anomalies in the surface wind and sea level pressure throughout the tropical Pacific and into the Indian Ocean basins.

2.3.2 Mid-latitude Systems

The middle latitude weather systems influence the climate of northern South Africa through the migratory behaviour of the extra-tropical cyclones, anticyclones and frontal weather systems. As an example in this regard is the eastward propagating anticyclones that are responsible for the low level cold air incursion into Northern (Limpopo) Province of South Africa up to Zimbabwe (Kiangi, 1989). Mid-latitude frontal systems in South Africa show a quasi-biweekly (14-days) period of occurrence, and this characteristic affects the summer season due to the incursion of cool air observed at some regular intervals of approximately two weeks (Tyson & Preston-Whyte, 2000). When the cool moist air is heated from below by the warm surface of the northern region-Vhembe District (due to its close proximity to the tropics), the result is deep convective clouds and thunderstorms, which are often observed during the rainfall season. Heavy rain episodes that occur during the early stage of the rainy season (October-December) are often associated with the cut-off lows (cold-cored baroclinic systems originating in the middle and upper level westerlies) over South Africa (Taljaard, 1985; Singleton & Reason 2007). However, the area is deprived of rainfall if it experiences subsidence because of the anticyclones. The anticyclone is usually associated with convergence aloft and surface divergence. As the air subsides, warmed and dried, resulting in cloud free conditions and develop little vertical extent, thus rainfall hardly ever forms.

2.3.3 Tropical Temperate Trough

The tropical temperate trough (TTT) or Cloud Band is documented as the main system that is responsible for seasonal rainfall over the interior of South Africa (Harrison, 1984).

Cloud band formation is triggered by the arrival of an upper-level trough over southern Africa associated with the band of divergence east of its leading edge. Cloud bands form when a tropical disturbance such as an easterly low at the surface occurs in conjunction with the westerly low in the upper atmosphere (van der Heever, D'Abreton & Tyson, 1997). This situation is associated with an elongated trough that extends in the northwest to southeast direction across the sub-continent and the Southwest Indian Ocean (Harangozo & Harrison 1983; Harrison, 1986; Todd & Washington, 1999; Todd, Washington & Palmer, 2004). These events facilitate substantial energy, water vapour flux and momentum from the tropics into the mid-latitudes (van der Heever, 1997; Todd et al., 2004). The transport of moisture occurs along the TTT axis and is largely facilitated by changes to the streamfunction associated with a strengthening and eastward displacement of the Indian Ocean high, and the advent of midlatitude transients (Todd et al., 2004). It has been shown that TTT systems are major regions of moisture convergence; they are believed to contribute about 30% of the October and December rainfall totals, 60% of the January total and about 39% of the mean annual total rainfall (Harrison, 1984; Hart, Reason & Fauchereau, 2012). From all these observations, the general climatology of rainfall in South Africa can be claimed to have been studied in detail; what is not evidently known, however, is the driving force or systems concerned in the changes in rainfall at a local scale of a district level that are currently observed especially in the northeast of South Africa.

2.3.4 The Inter-Tropical Convergence Zone (ITCZ)

In South Africa, the most northern area is Vhembe District, which extends to approximately 23°S. This area enjoys a stronger influence of the tropical weather systems such as the Inter-Tropical Convergence Zone (ITCZ) than any other place in South Africa. This section will focus on reviewing and explaining the ITCZ and its influences. The ITCZ interacts with the southern Africa climate through a meridional circulation characterized by the Hadley cell. The ITCZ is a narrow low-latitude zone in which air masses originating in the northern and southern hemispheres converge and generally produce cloudy, showery weather. The characteristics of the ITCZ vary in space and time as observed by Barry and Chorley (1992). Its spatial and temporal variability depends on many factors such as maritime, continental and local effects, such as lakes, orography and vegetation cover. The position of the ITCZ varies seasonally, with the average January position at about 15°S during the southern hemisphere summer. However, the extreme southern position may oscillate to reach 22°S (Dhonneur, 1974). This situation provides tropical thermal forcing that can trigger trains of large-scale waves propagating into higher latitudes, thus influencing the climate there (Anyamba, Kiangi & Patnaik, 1982; Jury, Pathack & Sohn, 1992).

The variation of the ITCZ between 15°S and 22°S in southern Africa has not been well documented (Makarau, 1995) and it may be the missing link in understanding the droughts and wet/dry conditions or general variations in rainfall trends in the study area. The area is at the periphery of the southernmost position of the ITCZ during the southern summer (Makarau, 1995; Kabanda, 2004). In other parts of the world, it is well documented that year-to-year variations in the climatological location of the ITCZ produce surpluses or deficits of precipitation in regions; for example in the West African Sahel (Grist & Nicholson, 2001), northeastern Brazil (Biasutti, Battisti & Sarachik, 2003) and other regions throughout the tropics. However, these changes are not well understood in the case of South Africa rainfall.

The location of the ITCZ varies throughout the year and in the southern hemisphere, it can oscillate to 22°S at times. It has been the principal focus of many observational, modeling, and theoretical studies (Mitchell & Wallace, 1992; Waliser & Gautier, 1993; Xie, 1996) in some part of the world. A belt of low-level convergence and upper-level divergence with strong upward motion, deep penetrative convection, frequent cloudiness, and heavy rainfall (Wu, Liang & Zhang, 2003) characterises the ITCZ.

Determining trends of rainfall and the seasonal variations of convective activities (vertical motion), which are associated with the ITCZ; together with other climatological systems anomalies involved can be used to draw important conclusion that are useful for the study area.

Vhembe District has tropical and extra-tropical rainfall regimes that are influenced by large-scale features and different meteorological systems. However, the main rainfall regime is the summer-rainfall, which is centred on January (Rocha & Simmonds, 1997; Nenwiini & Kabanda, 2013). The extra-tropical rainfall regimes are associated with the winter season and arrive in the area in the form of light rain or drizzle, mainly due to frontal systems incursion into the north of South Africa from the south (Kabanda, 2004). It is also observed that during a wet summer, northeasterly flow laden with moisture is responsible for rainfall in southern Africa. These flows are enhanced by tropical disturbances moving south-westward in the northern Mozambique Channel, for example – tropical cyclone Eline (Reason & Keibel, 2004).

2.4 Local Climate of Vhembe District

There are some studies that concern climate and its related fields such as climatology, meteorology, agro-meteorology or any other branch of atmospheric science in Vhembe District and the few that do exist have appeared in recent years (late 1990s to date). Such studies are mostly unpublished material (dissertations and theses). Nevertheless, these studies give well-researched information and were supervised and examined by professionals and academicians in the relevant fields. Some of these include that of Dzivhani (1998) who detected spatial and temporal fluctuation of temperatures in the region; he attributed the former to the influence of landscape features and the latter to seasonal forcings such as the north-south oscillation of the overhead sun. Netshitungulu (1999) examined wind and its effects and detected areas of strong winds that render certain parts of Vhembe District susceptible to wind erosion. The effects were detected in the arid and semi-arid areas in the district where they affect large areas of croplands by removing topsoil, seeds and nutrients. According to Rose (1998), climatic factors such as rainfall, ambient humidity and extended drought modify wind erosion.

The study by Nenwiini (2010) was dedicated to delineating Vhembe District into homogeneous rainfall zones using principal component analysis. From the study, it emerged that the district features three major diverse climate zones - humid, sub humid and semi-arid, which explained 43%, 7.3% and 6.9% of the total variance respectively. On the seasonal rainfall onset and cessation, it was found that the rainfall season length in Vhembe District was getting shorter, such that over the last 60 years rainfall season length has decreased by 50 days (Nenwiini, 2012). Still, as far as rainfall mechanisms are concerned, there is still very limited understanding in terms of the timing of the rainfall onset and cessation.

The study area experiences drought of different magnitudes as observed by Kabanda (2004). He reported that, the more intense the drought becomes, the larger the area it affects. For example, the 1981-83 and 1991-92 droughts were the most intense and extensive in recent times, covering approximately two thirds of the whole district. It was also shown that extreme drought occurs once in approximately forty years while the severe category of drought could occur once in nearly every twenty years. The moderate drought is the most frequent and occurs once in nearly every ten years.

There are, however, few studies which appeared in scientific accredited sources; some are focusing on Vhembe District per se (Olivier & Rautenbach, 2002; Maponya & Mapndeli, 2012; Munyati & Kabanda, 2009; Kabanda & Munyati, 2010; Kabanda, 2011; Mpandeli et al., 2015) while others are using large area of study with Vhembe District embedded within. Nenwiini and Kabanda (2013) evaluated the rainfall trends and variability in Vhembe District South Africa. Their study employed Mann-Kendall trend analysis and Sen's slope estimator to determine trends in the rainfall climatology. They observed a significant negative trend that started in the mid-1990s, indicating that different local climate forcing came into play in the area during that period. Lately, Mpandeli (2014) investigated the impact of rainfall variability in Vhembe District based on monthly rainfall map over the study area. Their study noted the need for reliable and meaningful seasonal rainfall information, which can be useful to farmers at local scale.

Reason et al. (2005) examined the rainfall characteristics of the Limpopo region of northern South Africa. They investigated the interannual variability of dry spells within the rainy season over Limpopo and the onset dates of the rainfall season. Much attention was given to the possible relationships of these parameters with El Niño – Southern Oscillation (ENSO) and with regional circulation anomalies in order to detect predictability of those parameters. As explained earlier, Reason et al. (2005) combined Vhembe District with other areas, which feature different local characteristics that could influence the local climate.

A detailed study of how seasonal rainfall characteristics are changing in the Vhembe District has not been provided. Other studies in southern Africa that feature Vhembe District in their study domain include Nicholson & Selato, (2000); Shongwe et al. (2009) and Ambrosino et al. (2010). However useful they are for many applications, they do not reveal important aspects of how rainfall changes at a local scale level (district level).

2.5 Topography of the Study Area

The Soutpansberg is the most elevated part of the study area and is capable of modifying the local climate (Munyati & Kabanda, 2009). For an example during the wet season the area is warm, with temperatures ranging from 16 – 40°C, while during the dry season the temperatures are mild, ranging from 12 – 22°C. Minimum temperatures seldom drop below freezing point. The area experiences orographic rainfall. This phenomenon is due to moisture-laden air from the Indian Ocean, driven by the prevailing southeasterly winds onto the southern scarp of the Soutpansberg (Kabanda, 2003). Hahn (2002) observed that the north-south budding of the Soutpansberg in the central part tends to block the westerly movement of the atmospheric moisture, forcing it into the wedge created by the two mountains in the vicinity of Entabeni. Olivier and Rautenbach (2002) established that large amounts of rain are discharged onto the southern slopes of the Soutpansberg, resulting in Entabeni receiving an annual rainfall of 1,874 mm. At times, this may increase to annual precipitation of 3,233 mm when there is active orographic mist and fog along this southern slope or when the moisture over the area is enhanced by the presence of a tropical cyclone in the South West Indian Ocean. Hahn (2002) and Olivier and Rautenbach, (2002) associated the drying of western part of the Soutpansberg to the blocking effect of the moist flow in the middle area of the mountain range that creates a rain-shadow effect. Kabanda and Munyati (2010) inferred that the drying resulted from anthropogenic effects such as deforestation, settlement and urban sprawl in the eastern area of the Soutpasnberg. The main themes of this study are firstly, to detect the moisture level needed to trigger the rainfall onset in the areas that exhibit humid characteristics and those that reveal semi-arid features and secondly, to detect the quantity, trajectories, sources and sinks of moisture over Vhembe District in respect to rainfall changes in Vhembe.

2.6 NCEP/NCAR Reanalyses

In regions, which lack conventional observed data, the analyses greatly depend on model first guess. Various studies have investigated the effectiveness of NCEP/NCAR reanalysis data sets in climate and hydrological application and compared the output with that of other reanalysis datasets. Most of the studies reported biases and discrepancies in some of the field variables of these datasets - large and significant biases were found in the tropics. Trenberth and Guillemot (1995) evaluated the precipitable water and moisture budgets from the global analyses of European Centre for Medium Range Weather Forecasts (ECMWF), the US National Meteorological Center (NMC) (now NCEP) and NASA/Goddard, and examined the differences between output data. Their study observed critical dependence of the moisture budget on the veracity of the velocity field and horizontal divergence in the tropics. Similarly, Mo and Higgins (1996) compared NASA/DAO and NCEP reanalysis to station observations and satellite data in order to determine the range of uncertainty in the datasets. The study reported differences between the output data of the two analyses, with the largest differences found in the tropics.

2.7 Trend Analysis

Trend analysis can be defined as the use of an empirical approach to quantify and explain changes in a system over a period of time (Chandler & Scott, 2011). The analysis of trends in data can be performed using both parametric and non-parametric trend tests. Parametric tests assume that random variables are normally distributed and homogeneous (Hirsch, Alexander & Smith, 1991). According to the literature, non-parametric trend techniques proved to have advantages over parametric methods in terms of efficiency and power in the analysis of non-normal data sets. Önöz and Bayazit (2002) conducted a comparison study which estimated the power of parametric tests for trend detection for various probability distributions and compared this to the power of the non-parametric Mann-Kendall test. Their study established that the t test has less power than the non-parametric Mann-Kendall test when the probability distribution is strongly skewed, but the power ratio was ascertained to be close to one for moderately skewed distributions.

2.7.1 Mann-Kendall trend analysis

In this study, trend analysis will be performed using the Mann-Kendall non-parametric statistical test to detect if there is a trend in the rainfall time series. Mann-Kendall statistical analysis is well known to be effective in the detection of trends in hydrology and climatology studies (Partal & Kahya, 2006). In the current study rainfall is the main focus, and is regarded as a non-normally distributed climate variable. Therefore, the use of Mann-Kendall trend analysis is reliable since it has been proved to be successful in the analysis of non-normal variable such as rainfall.

Tomozeiu et al. (2000) used the Mann-Kendall test to detect trends in the summer precipitation of Emilia-Romagna in southern Europe for the period 1922 to 1995. In their study they established an increasing trend in summer precipitation in the northern, central and eastern part of the region studied with the climate signal more significant in the north-western, central and northeastern part of the region. In Sri Lanka, trends in annual and monthly precipitation were detected in the Kalu Ganga basin using the Mann-Kendall statistical test. A decreasing trend of -0.98 with an annual rainfall reduction of 12.03 mm/year was observed with strong decreasing trends in April and August, while July and November displayed strong increasing trends (Ampitiyawatta & Guo, 2009). A study by Esteban-Parra et al. (1998) used the Mann-Kendall trend test to analyse the spatial and temporal patterns of precipitation in Spain for the period 1880–1992 and detected significant long term decreases in precipitation for the Mediterranean and interior regions and an increase in precipitation for the Northern coastal region in Spain. Trend significance was assessed with the Mann-Kendall test. An investigation of the temporal variability of precipitation extremes in Estonia from 1961 to 2008 was undertaken using the Mann-Kendall test to assess the significance of the trends. It was observed that the frequency of both indices has increased with no significant negative trends. Paadam and Post (2011) observed an increase of 15.8 events over the 99th percentile per decade. Based on these results, the current study will employ the same method of determining trends in the study area.

In the current study, the Mann-Kendall trends analysis will be carried out based on an Excel template MAKESENS (stands for Mann-Kendall test for trend and Sen's slope estimates) application that was developed for detecting and estimating trends in the time series of the annual values of atmospheric and precipitation concentrations (Salmi et al., 2002).

2.8 Summary

In chapter 2, a synthesis of previous and earlier works on the local, regional and global climatology to support this study have been presented together with approaches relevant to the current study. The importance and need of information on the timing of seasonal rainfall in Vhembe District was emphasised. The main rain bearing systems that influence rainfall over the southern Africa and other local features that affect spatial and temporal distribution of rainfall were described. The chapter concludes with an overview of approaches of determining the onset date and dynamic meteorological features that are associated with rainfall over the study area.

Chapter Three
Data and Methods

3.1 Introduction

The preceding chapter presented a summarised review of rainfall climatology and the associated atmospheric circulation over southern Africa, with a specific reference to the local climate of Vhembe District. The current chapter outlines the data and methods used in this study in order to examine the rainfall climatology of Vhembe District and their associated anomalies. Section 1.4 introduced the main aims and objectives of the study, which to some extent represent gaps in the current knowledge that need to be filled. These are:

1. To identify characteristics of the local seasonal rainfall by analysing station-based rainfall trends and patterns
2. To relate local rainfall (rain gauge data) and Climate Prediction Centre Merged Analysis Precipitation (CMAP)
3. To explore time-varying large-scale meteorological systems associated with the evolution of local seasonal rainfall characteristics
4. To determine moisture features needed to initiate seasonal rainfall onset.

3.2 Data and Sources of Data

The study required high-quality rainfall data in order to construct an accurate description of seasonal rainfall characteristics. The main advantage that rainfall has over the other climate parameters such as temperature is that it is readily and widely available in the study area and it is a principal parameter while most other indicators are derived from it (Kabanda, 2004). From this perspective, rainfall in Vhembe District can be considered to be the carrier signal of various climate parameters. Other data used are the reanalysis data which are produced by the NCEP/NCAR Reanalysis project (Kalnay et al., 1996). The output variables considered in this study include the climatological mean and anomaly data.

3.2.1 Rainfall Data

Station based rainfall data of 60 years (1950 – 2009) were obtained for various stations in the Vhembe District from the South African Weather Service (SAWS). High spatial and temporal resolution data are essential in creating a time series for the study and long records are essential to determine the stability of statistical relationships, especially when trends in the data are studied. A total of 52 rainfall stations were considered in the beginning, however, upon data sampling and quality analysis, only 32 rainfall stations were found to be suitable for this study. The stations omitted had a large number of missing values and/or short period of observation; more explanation of the criteria considered in selecting the appropriate stations is provided in the methodology section (3.3).

3.2.2 Reanalysis Data

The atmospheric field data that were used in this study are produced by the National Centre for Environmental Prediction (NCEP) and National Centre for Atmospheric Research (NCAR). The field variables used include the climatological means, anomalies and composites of meteorological data. These data were obtained from the National Oceanic and Atmospheric Administration/ Climate Diagnostics Centre (NOAA/CDC) website http://wesley.wwb.noaa.gov/Reanalysis.html.

The NCEP/NCAR in collaboration with the National Oceanic and Atmospheric Administration (NOAA), have established a reanalysis using a frozen, state of the art analysis (Kalnay et al., 1996). The reanalysis project produced a retroactive record of more than 50 years of global analyses of atmospheric fields in effort to support research needs and those of climate monitoring communities (Kistler et al., 2001). These reanalysis data are generated using a "frozen, state of the art" global numerical weather forecasting model which assimilates past observation data onto a global three dimensional grid. Past observational data used for assimilation were obtained from ships, rawinsonde, pibal, aircraft, satellite and land based stations; additional global observational data were supplied by participating international organisations and countries. The output variables have been classified into four classes depending on the degree to which they are influenced by observations and/or the model (Kalnay et al., 1996). The first class of variables (A), which include the upper air temperatures, zonal and meridional wind components and geopotential height, are strongly influenced by the available observations and therefore considered to be the most reliable product of the reanalysis. The second class of variables (B) such as moisture variables, divergent wind and surface parameters are influenced both by the observations and by the model, and categorized as less reliable. The third class of variables (C) such as surface fluxes, heating rates and precipitation are entirely determined by the model, thus, they are derived from the assimilation of other observed variables. The fourth class of variables (D) are deridved from climatological data and are not dependant on the model. This study will use geopotential height, rotational winds and vorticity, which are considered to be highly reliable and specific humidity which said to be less reliable.

NCEP reanalysis data are quality controlled and assimilated with a data assimilation system that is kept unchanged over the reanalysis period in order to eliminate apparent climate jumps resulting from changes in the operational data assimilation system (Kalnay et al., 1996; Kistler et al., 2001). NCEP reanalysis gridded atmospheric data fields have been extensively used by researchers (e.g. Randel, Wu & Gaffen, 2000; Kostopoulou, 2003; Mulenga et al., 2003; Todd et al., 2004; Cook, Reason & Hewitson, 2004; Viguad et al., 2007; Fauchereau et al., 2008; Paltridge, Arking & Pook, 2009; Hart et al., 2010).

However, a number of concerns regarding the consistency and accuracy of outputs have been raised. Kalnay et al. (1996); Newman et al. (2000); Marshall and Harangozo (2000); Kistler et al. (2001); Reid et al. (2001) and Trenberth et al. (2001) assessed the consistency of the reanalysis output data. The noted inconsistencies have been linked with two major changes in the observing system on the reanalysis. Firstly, there is the establishment of the upper air network that occurred from 1948 to1957; consequently, the reanalysis prior to 1958 is considered to be the least reliable, especially in the Southern Hemisphere, because of the lack of observations during that period. Thus, the reanalysis for this period is entirely based on the model prediction. Secondly, the introduction of satellite data in 1979 resulted in a significant change in the climatology, and as a result the climatologies based on the years 1979 to present are considered most reliable (Kalnay et al., 1996; Kistler et al., 2001). This is supported by Tennant (2004) who quantified the extent to which the introduction of satellite data in 1979 impacts both daily and inter-annual scales of variability, and reported difference in the daily circulation statistics before and after 1979. The circulation statistics prior to 1979 were found to be typically based on the model climatology. In this study the climatological composite analysis is divided into two periods, 1950 – 1978 and 1979 –

2009. This will allow comparison of the results before and after the major changes in observation system because the climatology before 1979 is more dominated by the model climatology in data sparse areas such as the Southern Hemisphere (Kistler et al., 2001).

3.2.3 Mean and Anomalies Climatology Composites

This study focuses on the identification of suitable predictors that can be used for predicting the onset of seasonal rainfall in Vhembe District. The amount of rainfall over the area is largely determined by the moisture contained in the atmosphere especially in the lower (850hPa) and middle (500hPa) levels. Climatological data variables used to create composites for this study include long term mean of the following: Specific Humidity and Integrated Moisture Flux available from June 1974 to the present and relative vorticity components from National Centre for Environmental Protection/National Centre for Atmospheric Research NCEP/ NCAR reanalysis.

Atmospheric anomalies are given by the mean for 1980 – 2009 minus total mean of variables from the NCEP/NCAR reanalysis (1968 – 1996) as obtained from NOAA-CIRES Climate Diagnostics Centre.

3.3 Methodology

In this section, the analysis methods employed in this study are outlined. These methods are used in data sampling, analysing the seasonal rainfall data for a trend and the field significance of the trend, determining the rate of change that occurred per year, and the starting and end point of the observed trend. The seasonal rainfall data was subjected to a 5 year moving average to filter out the natural climate variability forcings before conducting the trend test. Trend analysis was then performed using the Mann-Kendall non-parametric statistical test for trend. The magnitude of change per year was determined using the non-parametric Sens' Slope estimator. A detailed explanation of each one of the analysis methods is presented in the following sections.

3.3.1 Statistical Methods

According to Von Storch and Navarra (1999), statistical analysis is required for the interpretation of observed and simulated data sets. The advantage of statistical approaches is that they allow one to deal directly with information about the real system. Statistical methods are sometimes the only way to shed light on some intricate processes generated from large data outputs. Statistical methods used here include correlation, cross-correlation analysis, moving average, Mann-Kendall analysis and Sen's slope estimator.

3.3.2 Correlation

Correlation is one of the statistical techniques that are used to quantify the strength of linear relationship between two random variables (Bewick, Cheek & Ball, 2003). The extent to which the variables relate is measured by a correlations coefficient which is denoted by "r". The correlation coefficient is measured on a scale ranging from +1 to -1. The stronger the correlation, the closer the correlation coefficient comes to ±1. A correlation coefficient of +1 indicates a direct relationship - that is, as one variable increases the other increases, while a negative correlation coefficient indicates an inverse relationship, thus, as one variable decreases the other increases. If a correlation coefficient is zero, there is no linear relationship that exists between two random variables (Swinscow & Campbell, 2002).

3.3.3 Cross-correlation Analysis

Cross-correlation analysis was used to sample the data from a large population of data. In this approach all the data were cross-correlated with each other using SPSS package, and stations were grouped based on the magnitude of their cross correlation. Thus, stations that share similar rainfall characteristics are highly correlated and can be grouped together.

3.3.4 Moving Average

To establish the temporal rainfall changes in Vhembe District, the data were first subjected to a 5-year moving average in order to filter out noise that can obscure the signal of climate change. A moving average uncovers trend information in historical data that a simple average would otherwise mask. In studies involving the detection of rainfall changes, the moving average is a traditional process that is used for long term trend depiction (Sneyers, 1992). The idea here was to analyse for climate-change forcing without confusing it with natural rainfall variability which was filtered out by using long term data (>60 years) and planetary scale forcing - ENSO (filtered by 5-year running mean). Once the data has been cleared of noise such as the natural climate variability and ENSO forcing, the Mann-Kendall trend analysis was employed to determine the temporal rainfall changes in Vhembe District.

3.4 Trend Analysis

Nenwiini (2012) and Nenwiini and Kabanda (2013) determined the rainfall trend in Vhembe District using annual rainfall data. In this study, the long-term trend in the summer season (October – March) is determined using monthly rainfall data obtained from SAWS rainfall stations scattered around study area. However, some rainfall stations in the study area had some gaps of missing data and varying record length. For instance, not all stations had continuous records from 1950 to 2008, and some rainfall stations had extended gaps simply because they started recording after 1950. Thus, there were 15 rainfall stations with records from 1950 to 2008, 21 stations with records from 1960 to 2008 and 25 stations with records from 1970 to 2008. Therefore, stations were arranged based on the different record length e.g. 60, 50, and 40 years. The division was done in order to enhance the quality of results; this is supported by Tomozeiu et al. (2000) who recognised sensitivity of trend analysis to the network density and recommended the use of long time series and high station density.

3.4.1 Trend Analysis Method

Mann-Kendall trend analysis is a non-parametric statistical technique that is used to detect trends in a time series. Partal and Kahya (2006) described Mann-Kendall analysis as a well-known statistical method that is effective in the detection of trends in hydrology and climatology studies. In the current study, the Mann-Kendall trends analysis was based on an Excel template MAKESENS application which was developed for detecting and estimating trends in the time series of the annual values of atmospheric and precipitation concentrations (Salmi et al., 2002).

The methodology explained in this section is a repetition of Tomozeiu et al. (2000) approach. However, in this study seasonal rainfall is the main focus since the synoptic systems which cause rainfall in South Africa vary from one area to the other. In this study, the interest is on the summer rainfall climatology, not the annual rainfall as described in (Nenwiini, 2012). Trend analysis was conducted using the Mann-Kendall non-parametric statistical test or trend, since it has been successfully used in other similar studies that look at trends in meteorological variables include that of Serrano et al. (1999), Tomozeiu et al. (2000) and Partal and Kahya (2006).

3.5 Composites Analysis Procedure

Composite analysis is a sampling technique based on the conditional probability of a certain event occurring (Fernando, Samita & Abeynayake, 2012). It involves identifying and averaging one or more categories of fields of a variable selected according to their association with key conditions (Folland, 1983). Compositing has an advantage over individual case study in that it emphasises commonly occurring features while smoothing out random noise (Williams & Kniveton, 2011). That is, it is expected that when the fields of a variable are averaged in relation to an event, the event features will remain and some noise will likely average out. Here, related events are averaged in order to identify and analyse potential predictors for the seasonal rainfall onset in the study area.

3.5.1 Composite Analyses

We use composite analyses of gridded NCEP/NCAR reanalysis fields with respect to the station based seasonal rainfall onset and cessation dates in order to identify typical atmospheric circulation patterns associated with wet and dry episodes within the rainy season in the district and the mechanisms that drive them.

3.5.2 Climatological-Dynamical Analysis

Evolution (sequential life cycle) of mean and anomalies of meteorological parameters (Section 3.2.1) are tracked based on the trends detected in the rainfall data. Each trend is analysed in chronological order so as to understand the dominant modulating factors. Through this technique, the study will be able to identify corresponding synoptic circulation patterns, sources and sinks of moisture and energy as well dynamic and thermodynamic variables and mechanisms associated with rainfall trends detected in Vhembe District.

3.5.3 Meteorological Indicators of Moisture Transport and Accumulation

This section will deal with composite patterns of operational meteorological parameters that include specific humidity, integrated moisture flux and vertical motion. The analysis domain extends from the study area to include the adjacent oceans, i.e. southwest

Indian Ocean in the east and southeast Atlantic Ocean in the west. The area of monitoring will reach 10°S to 40°S and extend from 0°E to 60°E. According to Kabanda (2004), weather systems that affect Vhembe District, especially those of the synoptic scale, seldom form in situ. Therefore, a larger area needs to be monitored in order to capture and highlight the geographical and temporal characteristics of the weather systems (source of activities) that enhance (or weaken) the moisture that arrive in the area and boost (or decrease) rainfall.

3.6 Summary

This chapter gave sufficient detail about the data and the methodology used in the study. The chapter provides a detail description of rainfall data and reanalysis data – including the mean and anomalies of meteorological variables such as specific humidity, integrated moisture flux and vertical motion. On statistical analysis, the Mann Kendal and Sen's Estimate are described in detail.

Chapter Four:
Seasonal Rainfall Trends and Onset

4.1 Introduction

Identifying the characteristics of the local seasonal rainfall trends and patterns for Vhembe District as outlined in the first chapter is one of the objectives of this study. However, it is not the main aim of the thesis. The core aim of this research is to investigate a more meaningful association between the synoptic meteorological systems, their dynamics and the local rainfall characteristics. In order to fully understand the relationships, it is important to establish a general overview of rainfall trends for the past 60 years. Any significant trends will provide important knowledge that will assist in understanding the relationships between the local rainfall of Vhembe District and the synoptic meteorological systems.

In this chapter, the results for the seasonal rainfall trend in Vhembe District are presented. The trends were computed for three different climatological periods (1950 to 2009, 1960 to 2009; and 1970 to 2009). The longer rainfall data series is composed of about 15 rainfall stations which started to report in 1950. The second data series feature additional 6 stations making a total of 21 stations. The third group contains many stations (31) that cover a bigger area of Vhembe District. Decadal scale trend analysis was done based on the third group of data (1970-2009).

The rainfall trends in Vhembe District are analysed to determine if the rate of change for different years was significant. If the regression line is statistically significant at ≥ 95% level of confidence, then the slope is significant and accepted as the rate of rainfall change per unit time. The results in this chapter were obtained using two techniques, namely Mann Kendal trend analysis and Sen's slope estimator, which were employed to test for the presence of statistically significant trends and magnitude respectively (Salmi et al., 2002). MAKESENS (Mann Kendall test for trend and Sen's slope estimates) template was employed in this application.

This chapter also analyses characteristics of seasonal rainfall onsets (of the selected years in different decades). The analysis investigates the seasonal rainfall onset in the humid and semi-arid areas of Vhembe District (Nenwiini, 2012). Figure 4.1 shows the monthly mean rainfall time series for the rainfall season in both humid and semi-arid areas. The rainfall pattern in both areas is similar, although the amount realised per month and eventually per season is different. The rainfall season in Vhembe consists of a series of consecutive rainfall months, starting in one calendar year and continuing into the next; for example, the 1970/71 season runs from October 1970 to March 1971.

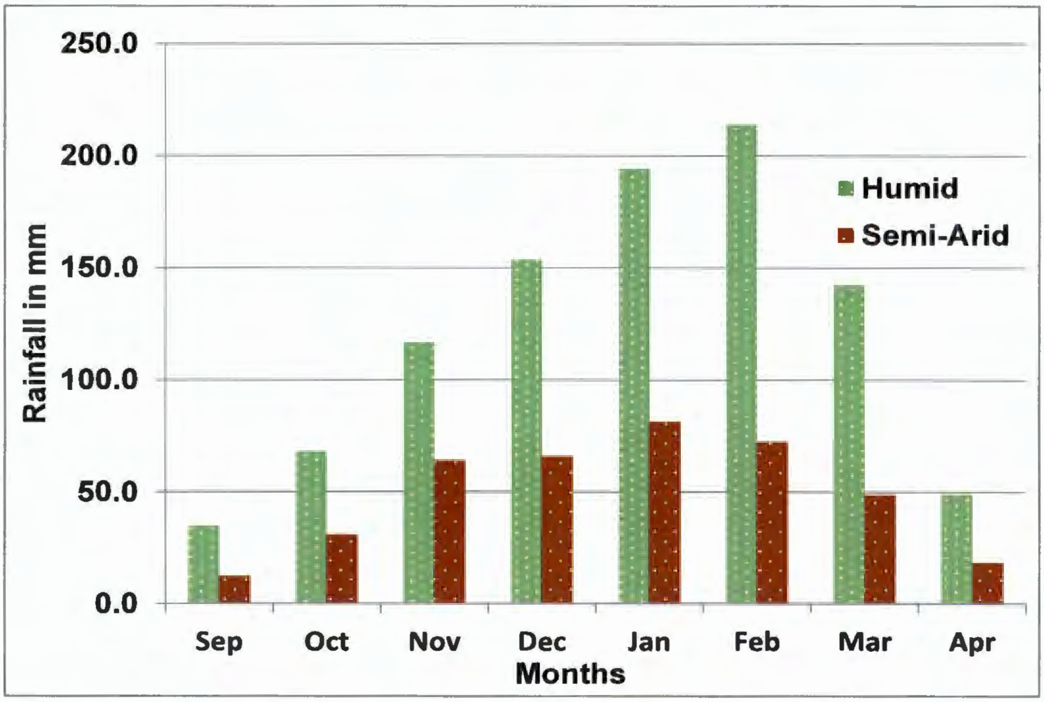

Figure 4.1: Seasonal rainfall comparison between humid and semi-arid areas in Vhembe District

The onset of seasonal rainfall over Vhembe District marks the beginning of a growing season during which the district receives water essential for agriculture, ecosystems and domestic use. The seasonal rainfall onset and cessation is reported to have changed in recent decades, reducing the length of the rainy season (Nenwiini, 2012; Kabanda & Nenwiini, 2015). However, the mechanisms that control the timing of the onset and its variability over this area are still unclear. According to Odekunle (2004), the rainy season starts when the rainfall becomes frequent and this can only take place when the atmosphere carries enough moisture to sustain a high rate of convection and overturning. The amount of moisture in the atmosphere is influenced by factors such as evaporation, air temperature and atmospheric transport of moisture (Barry & Chorley, 2010). These factors are manifested in different dynamical and thermo-dynamical atmospheric variables or meteorological systems (Goswami & Gouda, 2007). The influence of these meteorological systems on seasonal rainfall in Vhembe District will feature in chapter six.

Questions to be addressed in this chapter include:

- How seasonal rainfall onset have changed over different decades from 1980 to 2009 both in humid and semi-arid areas.
- Are statistically significant trends influencing rainfall onset?
- Are there distinct differences in seasonal rainfall onset between the seasons?
- Is there any similarity/difference between seasonal rainfall onsets in humid and semi-arid areas?

4.2 Results

4.2.1 Statistical Significance Test for Trends

Trends analysis is performed to determine if the rate of change of seasonal rainfall over Vhembe District over the years is significant. The null hypothesis is that the slope of each regression line is equal to zero (Thomas, 1983). If the regression line is statistically significant at ≥ 95% level of confidence, then the slope is significantly different from zero and the value is accepted as the change rate. The Mann-Kendall trend analysis technique and Sen's slope estimator based on MAKESENS template (Salmi et al., 2002) were employed and a table was produced. The table includes these columns: column A is assigned the stations used in the analysis, column B and C show the initial and final year of the time series considered in the computation of the trend. This is followed by a column D that represent the total number of years *(n)* in a time series and the computed Z test value is in column E. The absolute value of test Z shows presence of a trend at the selected level of significance (α); where a positive Z value indicates an upward trend while the negative value indicates a downward trend. The last column F constitutes the significance of the observed trends.

4.2.2 Seasonal Rainfall Trends from 1950 to 2009

Trend analysis results are presented in Table 4.1. The Mann Kendall trend test revealed a monotonous decreasing trend in the seasonal rainfall over most of the study area. Shefeera and Mara Pol experienced a steep decreasing rainfall trend, which was denoted by Z values of -3.98 and -3.25 respectively. UnaAgric (Z value of -2.37) and Matiwa (Z value of -2.11) followed them. Other stations in the study area observed gentle decreasing trend in rainfall.

It is worthwhile to point out that, statistical significant trends were observed in the stations that showed steep decreasing negative trends in general - for example;

Shefeera, Mara Pol, UnaAgric and Matiwa. While statistical significant increasing trend was observed in Klein Australie (Z = 2.45; α = 0.05). The observed increase of rainfall in this area may be attributed to agroforestry. Dense vegetation increases evapotranspiration and lower the Lifting condensation level (LCL) which enhances the formation of cloud and spill over precipitation to the surrounding area (Kabanda, 2011).

Table 4.1: Vhembe District 1950 to 2009 Mann Kendal seasonal trend analysis results

A	B	C	D	E	F
	Time Series Range				
	First Year	Last Year			
Mara Pol	1950	2009	60	-3.25	**
Legkraal	1950	2009	60	-0.07	
Mara	1950	2009	60	-0.51	
UnaAgric	1950	2009	60	-2.37	*
Bandelierkop	1950	2009	60	-1.63	
Hanglip	1950	2009	60	-0.96	
ElimHos	1950	2009	60	-1.57	
Goedehoop	1950	2009	60	0.19	
Shefeera	1950	2009	60	-3.98	***
Nooitgedacht	1950	2009	60	0.01	
Klein Australie	1950	2009	60	2.45	*
RoodewalBos	1950	2009	60	-0.44	
EntabeniBos	1950	2009	60	-1.48	
Matiwa	1950	2009	60	-2.11	*
Palmaryville	1950	2009	60	-1.32	

*** a trend at α = 0.001 level of significance, ** a trend at α = 0.01 level of significance
* a trend at α = 0.05 level of significance, + a trend at α = 0.1 level of significance

4.2.3 Season Rainfall Trends from 1960 to 2009

The trend test on seasonal rainfall based on 50-year time series (1960 – 2009) from 21 rainfall stations over the study area revealed increasing trends in the majority of rainfall stations (Table 4.2) with Mann Kendall test Z value ranging from 0.22 to 4.18. The exception were Bandelierkop, Shefeera, Mara Pol, Setali and Tshakhuma which recorded decreasing trends with test Z value ranging between -0.05 and -2.42. Nevertheless, only six rainfall stations registered statistically significant trends [Klein Australie (Z = 4.18; α = 0.001), Goedehoop (Z = 2.91; α = 0.01), Legkraal and Nooitgedacht Z = 2.47 and 2.12 at α = 0.05 respectively]. Sheffeera and Tshakhuma reported decreasing trends with test Z value of -2.42 and -2.32 respectively at α = 0.05 level of significance.

Table 4.2: Vhembe District 1960 to 2009 Mann Kendal seasonal trend analysis results

A	B	C	D	E	F
	Time Series Range				
	First Year	Last Year			
Mara Pol	1960	2009	50	-0.05	
Legkraal	1960	2009	50	2.47	*
Mara	1960	2009	50	1.01	
UnaAgric	1960	2009	50	0.26	
Bandelierkop	1960	2009	50	-0.16	
Hanglip	1960	2009	50	1.09	
ElimHos	1960	2009	50	0.46	
Goedehoop	1960	2009	50	2.91	**
Shefeera	1960	2009	50	-2.42	*
Nooitgedacht	1960	2009	50	2.12	*
Klein Australie	1960	2009	50	4.18	***
RoodewalBos	1960	2009	50	1.14	
EntabeniBos	1960	2009	50	0.42	
Matiwa	1960	2009	50	0.26	
Palmaryville	1960	2009	50	1.12	
Tshipise	1960	2009	50	0.22	
Setali	1960	2009	50	-0.77	
Tshakhuma	1960	2009	50	-2.32	*
Tsianda	1960	2009	50	-0.50	
Kruger	1960	2009	50	-0.28	
Folovhodwe	1960	2009	50	0.62	

*** a trend at α = 0.001 level of significance., ** a trend at α = 0.01 level of significance

* a trend at α = 0.05 level of significance, + a trend at α = 0.1 level of significance

4.2.4 Season Rainfall Trends from 1970 to 2009

Seasonal rainfall trends were computed from 40-year rainfall time series (1970 – 2009). Thirty-one key rainfall stations have been chosen to represent Vhembe District; they are spatially distributed across the study domain. As indicated in Table 4.3, a number of rainfall stations have experienced a decrease in seasonal rainfall. For example, Tshakhuma, which showed a reduction in rainfall ($Z = -3.19$; $\alpha = 0.01$), Pont Drift ($Z = -3.13$; $\alpha = 0.01$), Messina Pol and Tshipise ($Z = -2.18$ and $Z = -1.99$ at $\alpha = 0.05$). Other stations reported decreasing trends although not significant. On the other hand, there are some rainfall stations that registered upward trends: Klein Australie and Goedehoop reported statistically significant trends as indicated in the table.

Table 4.3: Vhembe District 1970 to 2009 Mann Kendal seasonal trend analysis results

A	B	C	D	E	F
	Time series Range				
	First year	Last Year			
Mara Pol	1970	2009	40	-0.64	
Legkraal	1970	2009	40	1.78	+
Mara	1970	2009	40	-0.52	
UnaAgric	1970	2009	40	-0.92	
Bandelierkop	1970	2009	40	-1.20	
Hanglip	1970	2009	40	-0.31	
ElimHos	1970	2009	40	0.38	
Goedehoop	1970	2009	40	2.37	*
Sheffeera	1970	2009	40	-1.11	
Nooitgedacht	1970	2009	40	0.94	
Klein Australie	1970	2009	40	2.64	**
RoodewalBos	1970	2009	40	-0.31	
EntabeniBos	1970	2009	40	-0.08	
Matiwa	1970	2009	40	0.45	
Palmaryville	1970	2009	40	1.06	
Soakmekar	1970	2009	40	1.96	+
Tshipise	1970	2009	40	-1.99	*
Pont Drift	1970	2009	40	-3.13	**
Messinal pol	1970	2009	40	-2.18	*
Folovhodwe	1970	2009	40	0.36	
Setali	1970	2009	39	-1.96	+
Levubu	1970	2009	39	-0.70	
Tshakhuma	1970	2009	39	-3.19	**
Tsianda	1970	2009	39	-0.	
Kruger	1970	2009	39	-1.	

*** a trend at α = 0.001 level of significance, ** a trend at α = 0.01 level of significance
* a trend at α = 0.05 level of significance, + a trend at α = 0.1 level of significance

4.3 Estimator of Trend Magnitude

The Sen's slope estimator is used to estimate trend magnitude – it is a very efficient nonparametric method of robust linear regression and is the median of all pairwise slopes in the data set (Salmi et al., 2002, Olofintoye, Adeyemo & Otieno, 2012). The advantage of Sen's slope estimator is that it competes well against simple least squares even for normally distributed data. It is also insensitive to the presence of outliers. It is significantly more accurate than simple linear regression for skewed data. Missing values are allowed and the data need not conform to any particular distribution.

A true slope of the observed trend is given by:

$$f(t)=Qt+B \qquad \text{Eq. 4.3}$$

where Q is the slope, B is a constant called the intercept, and t is time

In order to calculate a slope estimate of Q, the slopes of all data value pairs are first calculated as:

$$Q_i=\frac{x_j-x_k}{j-k} \qquad \text{Eq. 4.4}$$

where j > k

The median value is taken as the final slope of a trend. In the analysis of trend through MAKESENS, the statistical computation gives a high level of significance, with narrow angles between the confidence lines in cases where important significant trends are observed (Salmi et al., 2002). Then the field significance of the trend results is determined and a temporal analysis on the trend results is performed. The true slope of an existing rainfall trend and the magnitude of change over time are then estimated.

4.3.1 Rainfall Trend Magnitude

The results of the trend magnitude (Q) are shown in Table 4.4 and in the following figures (Figure 4.2, 4.3 and 4.4).

Table 4.4: Sen's slope estimator (Q mm/year) for seasonal rainfall (1950-2009, 1960-2009 and 1970-2009)

Station	**1950 - 2009**	**Signif.**	**1960 - 2009**	**Signif.**	**1970 - 2009**	**Signif.**
	Q mm/year		Q mm/year		Q mm/year	
Mara Pol	-0.348	**	-0.010		-0.053	
Legkraal	-0.014		0.265	*	0.269	+
Mara	-0.05		0.142		-0.110	
UnaAgric	-0.25	*	0.034		-0.154	
Bandelierkop	-0.128		-0.032		-0.204	
Hanglip	-0.168		0.219		-0.083	
ElimHos	-0.344		0.095		0.102	
Goedehoop	0.037		0.955	**	1.008	*
Sheffeera	-1.427	***	-1.230	*	-0.856	
Nooitgedacht	0.015		0.665	*	0.453	
Klein Australie	0.777	*	1.555	***	1.266	**
RoodewalBos	-0.13		0.282		-0.099	
EntabeniBos	-0.543		0.120		-0.044	
Matiwa	-0.724	*	0.095		0.318	
Palmaryville	-0.391		0.372		0.516	
Tshipise			0.037		-0.285	*
Setali			-0.166		-0.740	+
Tshakhuma			-1.108	*	-1.754	**
Tsianda			-0.188		-0.257	
Kruger			-0.050		-0.740	
Folovhodwe			0.082		-0.216	
Levubu					-0.257	
Tsianda					-0.294	
Soekmekaar					0.457	+
Messina Pol					-0.266	*
Pont Drift					-0.382	**
Mphephu						
Vondo Bos						
Saamboubrug						
Rammbuda						

*** a trend at $\alpha = 0.001$ level of significance, ** a trend at $\alpha = 0.01$ level of significance
* a trend at $\alpha = 0.05$ level of significance, + a trend at $\alpha = 0.1$ level of significance

4.3.2 Seasonal Rainfall in Vhembe District (1950 to 2009)

As seen in Table 4.4, an analysis of seasonal rainfall data from 1950 – 2009 revealed a declining trend in 12 rainfall stations. In other stations, the decreasing trend was not statistically significant while in others it showed high significance in the following order: -1.427mm/year for Sheffeera at α = 0.001 level of significance, -0.348mm/year for Mara Pol at α = 0.01 level of significance, and -0.724 for Matiwa and -0.25 for UnaAgric at α = 0.05 level of significance. Only one station (Klein Australie) in the whole study period showed a significant increasing trend (of less than 1mm/year) at α = 0.05 level of significance.

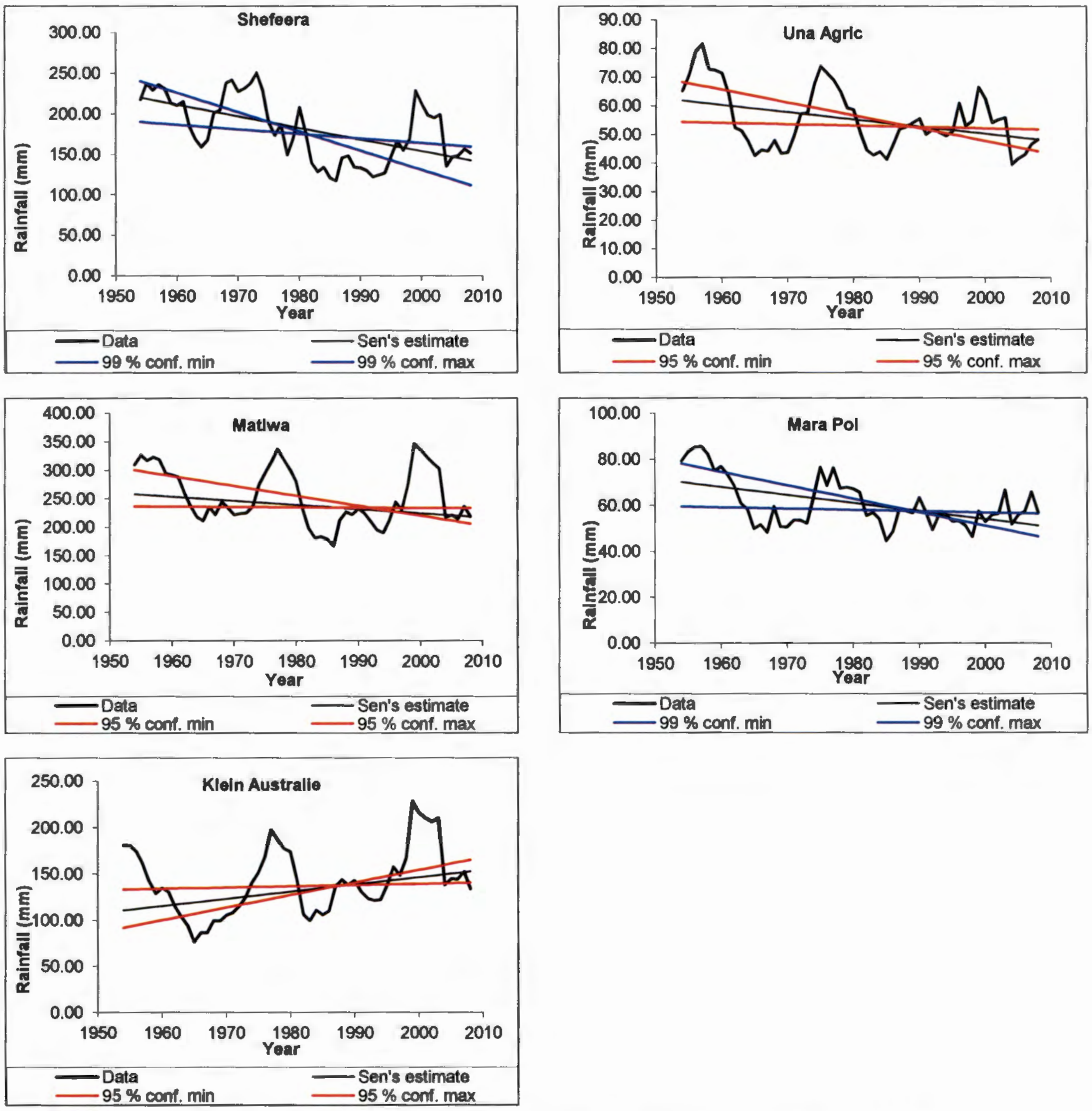

Figure 4.2: Seasonal rainfall trends in Vhembe District from 1950 to 2008

4.3.3 Seasonal Rainfall in Vhembe District (1960 to 2009)

The trend test results (Figure 4.3) based on rainfall data series from 1960 to 2009 (Table 4.4) showed an increasing trend in a number of stations. Klein Australie registered the highest increase of 1.555 mm/year at $\alpha = 0.001$ level of significance, followed by Goedehoop with 0.955 mm/year at $\alpha = 0.01$ level of significance, while Nooitgedacht and Legkraal showed an increase of 0.665 mm/year and 0.265 mm/year at $\alpha = 0.05$. Some other stations showed increasing rainfall although not statistically significant. The significant (at $\alpha = 0.05$) decreasing trends were reported in Sheffeera and Tshakhuma at -1.230 mm/year and -1.108 mm/year respectively.

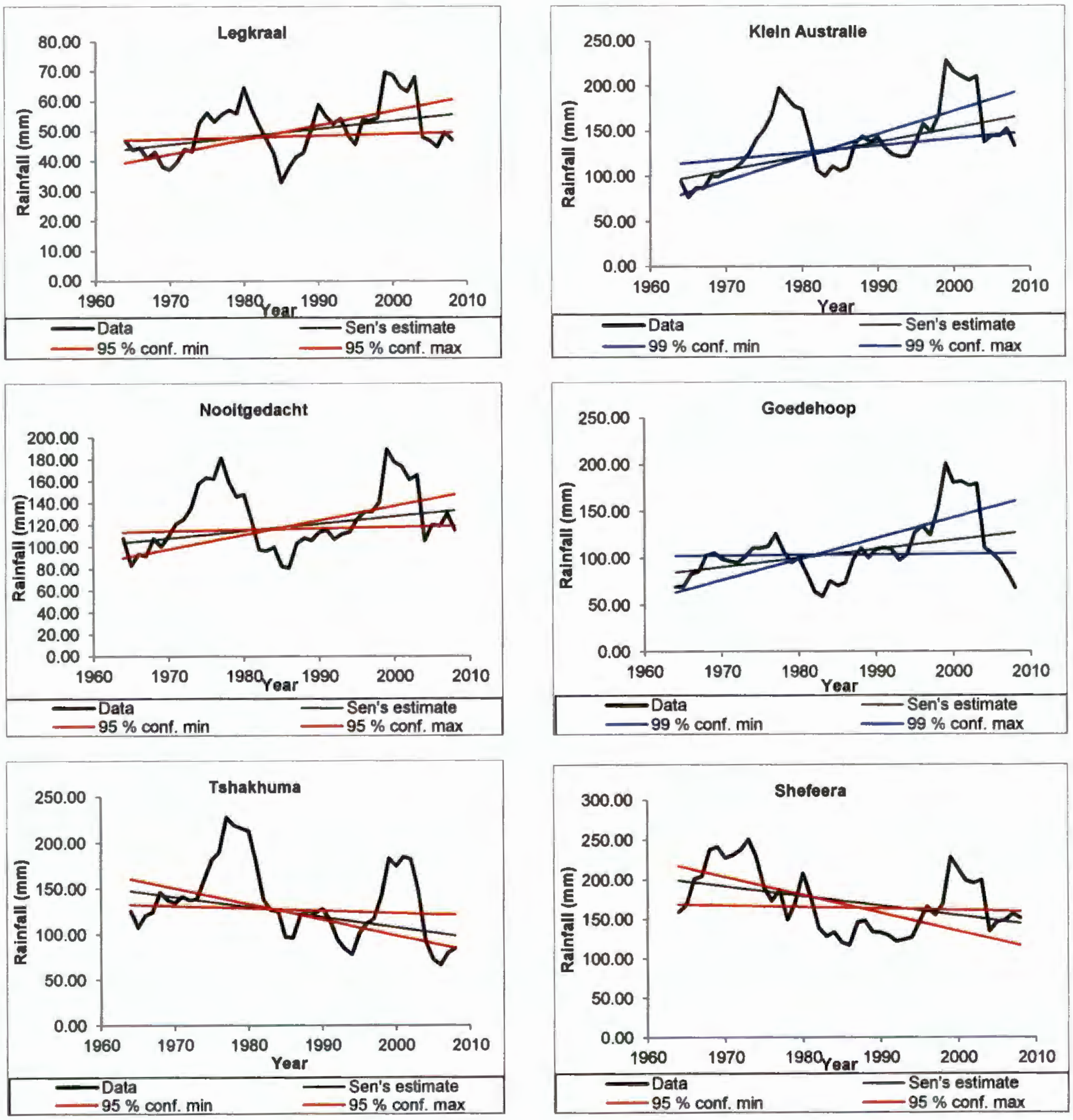

Figure 4.3: Trends test results for seasonal rainfall in Vhembe District (1960 to 2008)

4.3.4 Seasonal Rainfall in Vhembe District (1970 to 2009)

Figure 4.4 summarises the results of change per unit time of the trends detected in the period from 1970 to 2009 (Table 4.4). It shows a significant downward trend at Tshakhuma (Q = -1.754 mm/year at α = 0.01), Pont Drift (Q = -0.382 mm/year at α = 0.01), Messina Pol (Q = -0.266 mm/year at α = 0.05) and Tshipise (with -0.285 mm/year α = 0.05 level of significance). A relatively large decrease was registered in Sheffeera -0.856 mm/year and Setali -0.740 mm/year, although these observed changes were not statistically significant. There are, however, a small number of stations (out of a total of 31 stations) which revealed increasing trend in rainfall. The most conspicuous were Klein Australie and Goedehoop which showed the highest increases and the only statistically significant trends in the order of 1.266 mm/year at α = 0.01 level of significance and 1.008 mm/year at α = 0.05 level of significance.

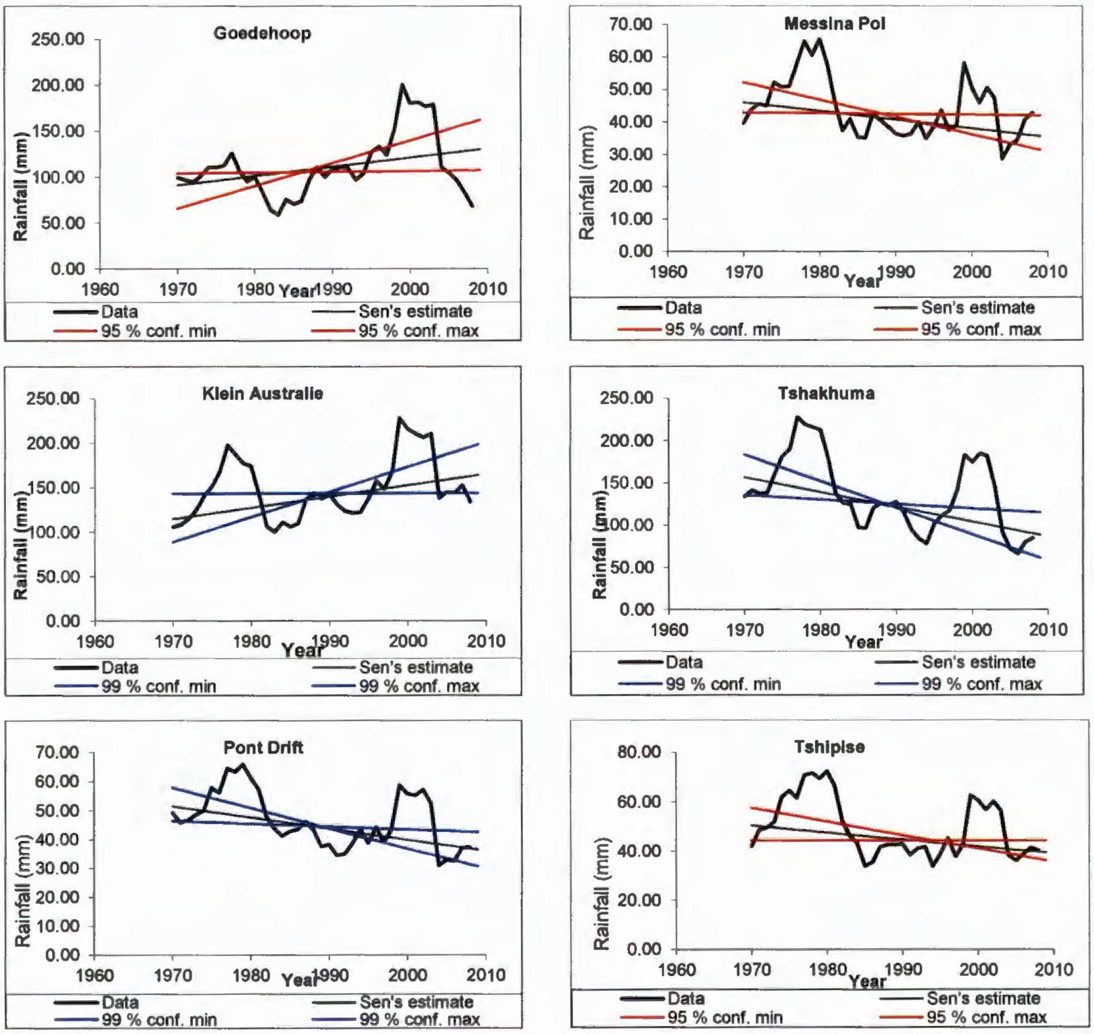

Figure 4.4: Trends test results for seasonal rainfall in Vhembe District (1970 to 2008).

4.4 Decadal Seasonal Rainfall Trend

The previous section analysed the seasonal rainfall pattern of Vhembe District based on three set of rainfall data with different time intervals (60, 50 and 40 years). A general decline in the seasonal rainfall was observed during the 1980-2009 period with a change point detected in the late 1980s. In order to provide an in-depth analysis of the pattern of seasonal rainfall at decadal scale and better spatial coverage, composite data sets of 31 stations in Vhembe District were subdivided into decadal scale (1980, 1990 and 2000). The following sub-sections present the analyses results of rainfall trend per decade.

4.4.1 Seasonal Rainfall Trend Analysis 1980 – 89 Decade

The Mann Kendall trend test (Table 4.5) shows a general decreasing trend of seasonal rainfall in most areas of Vhembe District during 1980 decade of Z value ranging between -0.18 and -2.33. But statistical significant decrease in rainfall at $\alpha = 0.05$ level of significance were observed in Elim Hos, Tshipise, Pont Drift, Messina Pol, Tshakhuma, and Kurgerwildstuin with Z values ranging between -1.97 and -2.33. The majority of these stations that experienced statistical significant trend are found in the semi-arid zone of the district. Overall, the largest reduction of rainfall (about -7.749 mm/year) during 1990 decade occurred in Tshakhuma. On the other hand, an increase in seasonal rainfall of magnitude ranging between 0.482 mm/year and 2.547 mm/year were reported in Una-Agric, Hanglip, Goedehoop and Klein Australie however; the observed trends were not statistically significant.

Table 4.5: Seasonal Rainfall Trend 1980 – 89 Decade Using the Mann Kendall Trend test

Station	Time Series Range		n	Test Z	Signific.	Q (mm/year)
	First Year	Last Year				
Mara Pol	1980	1989	10	-1.07		-1.147
Legkraal	1980	1989	10	-1.61		-2.534
Mara	1980	1989	10	-1.43		-2.481
Una Agric	1980	1989	10	0.54		0.482
Bandelierkop	1980	1989	10	-1.61		-1.433
Hanglip	1980	1989	10	0.72		1.000
Elim Hos	1980	1989	10	-1.97	*	-3.149
Goedehoop	1980	1989	10	1.07		2.547
Sheffeera	1980	1989	10	-1.07		-5.326
Nooitgedacht	1980	1989	10	-0.54		-2.386
Klein Australie	1980	1989	10	0.18		0.587
Roodewal Bos	1980	1989	10	-1.07		-1.223
Entabeni Bos	1980	1989	10	-0.72		-4.331
Matiwa	1980	1989	10	-0.72		-4.309
Palmaryville	1980	1989	10	-0.72		-3.786
Soekmekaar	1980	1989	10	-1.61		-4.529
Tshipise	1980	1989	10	-2.15	*	-3.410
Pont Drift	1980	1989	10	-2.33	*	-1.962
Messina Pol	1980	1989	10	-1.97	*	-2.388
Folovhodwe	1980	1989	10	-1.61		-1.764
Setali	1980	1989	10	-0.18		-0.641
Levubu	1980	1989	10	-1.43		-4.791
Tshakhuma	1980	1989	10	-2.33	*	-7.749
Tsianda	1980	1989	10	-0.54		-5.109
Kruger	1980	1989	10	-2.33	*	-3.21

*** a trend at α = 0.001 level of significance, ** a trend at α = 0.01 level of significance
* a trend at α = 0.05 level of significance, + a trend at α = 0.1 level of significance

4.4.2 Seasonal Rainfall Trend Analysis 1990 – 99 Decade

Interesting findings emerged from the analysis of seasonal rainfall during the 1990s decade (see Table 4.6 below); an increase in seasonal rainfall in almost all rainfall stations of Vhembe District is evident except in Mara Pol and Setali which showed decreasing trends. Out of 23 rainfall stations that registered an increasing trend, thirteen (13) rainfall stations showed statistically significant trends at level of significance ranging between α = 0.05 and 0.01. The biggest increase was observed in Entabeni which had an increase of about 9.7mm/year with a Z value of 1.9. Most stations located in the humid zone have shown statistically significant increases in seasonal rainfall; the exception were Matiwa, Tshakhuma and Tsianda.

Table 4.6: Seasonal Rainfall Trend 1990 – 99 Decade Using the Mann Kendall Trend test

Station	**Time Series Range**		**n**	**Test Z**	**Signific.**	**Q (mm/year)**
	First Year	Last Year				
Mara Pol	1990	1999	10	-1.43		-1.022
Legkraal	1990	1999	10	0.00		-0.071
Mara	1990	1999	10	2.33	*	1.819
Una Agric	1990	1999	10	1.43		0.777
Bandelierkop	1990	1999	10	0.54		0.716
Hanglip	1990	1999	10	1.97	*	4.256
Elim Hos	1990	1999	10	2.68	**	3.382
Goedehoop	1990	1999	10	2.33	*	6.389
Sheffeera	1990	1999	10	2.50	*	7.216
Nooitgedacht	1990	1999	10	2.68	**	4.987
Klein Australie	1990	1999	10	1.97	*	5.490
Roodewal Bos	1990	1999	10	2.15	*	6.525
Entabeni Bos	1990	1999	10	1.97	*	9.730
Matiwa	1990	1999	10	1.43		8.789
Palmaryville	1990	1999	10	2.86	**	6.326
Soekmekaar	1990	1999	10	1.79	+	4.707
Tshipise	1990	1999	10	0.72		0.609
Pont Drift	1990	1999	10	2.68	**	1.307
Messina Pol	1990	1999	10	1.79	+	0.724
Folovhodwe	1990	1999	10	1.25		0.718
Setali	1990	1999	10	-1.79	+	-3.582
Levubu	1990	1999	10	2.50	*	6.981
Tshakhuma	1990	1999	10	1.25		6.124
Tsianda	1990	1999	10	0.18		0.840
Kruger	1990	1999	10	2.15	*	2.43

*** a trend at α = 0.001 level of significance, ** a trend at α = 0.01 level of significance
* a trend at α = 0.05 level of significance, + a trend at α = 0.1 level of significance

4.4.3 Seasonal Rainfall Trend Analysis 2000 – 09 Decade

The results of trend analysis during the 2000s decade are presented in Table 4.7. In contrast to the observed pattern of seasonal rainfall trend in the 1990s decade, a general decline in the amount of seasonal rainfall is apparent during the 2000s decade. Most rainfall stations during this period showed statistically significant decreases in seasonal rainfall with the highest decrease seen in Entabeni Bos (-18.037 mm/year at α = 0.01 level of significance). Other stations that showed a declining trend, though not statistically significant, include Mara, Una-Agric, Banderlierkop, Sheffeera and Soekmekaar.

Table 4.7: Seasonal Rainfall Trend 2000 – 09 Decade Using the Mann Kendall Trend test

Station	**Time Series Range**		**n**	**Test S**	**Signific.**	**Q (mm/year)**
	First Year	Last Year				
Mara Pol	2000	2009	10	12		0.444
Legkraal	2000	2009	10	-22	*	-2.728
Mara	2000	2009	10	-16		-2.889
Una Agric	2000	2009	10	-10		-1.750
Bandelierkop	2000	2009	10	-16		-2.963
Hanglip	2000	2009	10	-20	*	-5.982
Elim Hos	2000	2009	10	-18	+	-5.960
Goedehoop	2000	2009	10	-32	***	-14.780
Sheffeera	2000	2009	10	-14		-7.728
Nooitgedacht	2000	2009	10	-22	*	-7.856
Klein Australie	2000	2009	10	-22	*	-10.515
Roodewal Bos	2000	2009	10	-18	+	-6.503
Entabeni Bos	2000	2009	10	-28	**	-18.037
Matiwa	2000	2009	10	-24	*	-14.744
Palmaryville	2000	2009	10	-20	*	-6.377
Soekmekaar	2000	2009	10	-15		-4.736
Tshipise	2000	2009	10	-18	+	-2.986
Pont Drift	2000	2009	10	-16		-2.808
Messina Pol	2000	2009	10	-12		-1.168
Folovhodwe	2000	2009	10	26	**	1.620
Setali	2000	2009	10	-26	**	-8.203
Levubu	2000	2009	10	-28	**	-9.076
Tshakhuma	2000	2009	10	-22	*	-16.327
Tsianda	2000	2009	10	-12		-4.559
Kruger	2000	2009	10	-22	*	-4.82
*** a trend at α = 0.001 level of significance, ** a trend at α = 0.01 level of significance * a trend at α = 0.05 level of significance, + a trend at α = 0.1 level of significance						

In each decade, the temporal and spatial variation of seasonal rainfall is apparent. A decreasing trend in seasonal rainfall has been observed in most rainfall stations over the study area during the 1980s and 2000s decade. On the other hand, the 1990s decade showed an increasing trend in seasonal rainfall. Yet, the relationship between the variation of seasonal rainfall amount and distribution over the study area is still not understood. According to Nandargi and Mulye (2012), the distribution of rainfall in time and space is an important factor in determining the economic status of a region. The amount and distribution of rainfall in any particular area is essential for crop planning (Singh & Sharma, 2003). Most importantly, the socio-economic activity such as planting depends on the onset of seasonal rainfall. Therefore, the subsequent sections will be dedicated to describing the spatial and temporal variation of seasonal rainfall onset characteristics.

4.5 Seasonal rainfall onset

The seasonal rainfall onset dates in the humid and semi-arid rainfall zones of Vhembe District were obtained based on the analysis of the daily rainfall. Kabanda and Nenwiini (2015) determined the seasonal rainfall onset in the same area by converting daily rainfall data into rainfall dekads, which is a 10 days total. In that study, the rainfall onset date was defined as the date after the beginning of October when the rainfall accumulated over 10 consecutive days is ≥10 mm provided that no dry spell within the following 30 days exceeds 10 days. This onset criterion is adopted here and the resolution is increased to pentad scale.

The use of pentads instead of dekads is to get a more precise date when the seasonal rainfall onset commenced – the five day average will indicate precisely the part of the dekad that contributed to the rainfall onset. This approach is in agreement with FAO (1995). In terms of pentads, the rainfall onset date is defined as the date after the beginning of September when the rainfall accumulated over 5 days is ≥5 mm provided that no dry spell within the following 30 days exceeds 5 days.

4.5.1 Seasonal rainfall onset dates in Vhembe District

Seasonal rainfall onset dates for the humid and semiarid rainfall zone in Vhembe District over three decades are presented in Table 4.8. The seasonal rainfall onset dates are based on pentad data. In three decades (30 years from 1980 to 2009) most rainfall seasons in the humid zone started earlier than in the semi-arid zone – between mid-September and early October (53 and 57 pentad). Some seasons reported late onset – the 1985, 1990, 1993, 1994, 1996, 1999, 2004, 2006 and 2007 seasons. Their range of rainfall onset was between early November and mid-December (62 and 71 pentad).

In the semi-arid zone rainfall onset was characterised by abnormally late onset dates that centred on November. In some instances, the onset was so late that it started between mid-December and early January of the following year, which are pentad 70 and 2 respectively. It should be noted that pentad 2 is late according to the rainfall season of Vhembe District (Kabanda, 2004) because the rainfall covers six months from October to April of the following year and January to April are the 2nd phase of the season. The seasons that had very late rainfall onset are 1981, 1991, 1997 and 2007.

Table 4.8: Onset Dates in Calendar Date Per Decade

	1980-1989 (Decade 1)		**1990-1999 (Decade 2)**		**2000-2009 (Decade 3)**	
Ten year period	**Humid**	**Semi-arid**	**Humid**	**Semi-arid**	**Humid**	**Semi-arid**
	59	63	68	?65	57	60
	55	1	58	?2	56	59
	57	?	61	?71	56	69
	56	62	66	62	59	60
	57	61	65	?66	65	63
	69	71	69	63	56	67
	54	66	62	?65	71	69
	54	67	60	?1	66	70
	57	?	53	?58	60	61
	57	64	63	65	61	?2
Mean Pentad	**57.5**	**66**	**62.5**	**66.4**	**60.7**	**65**
? indicate uncertainty of exact onset pentad						

From these observations, the seasonal rainfall in the study area is highly variable which makes it difficult to identify precisely the start of the rainfall season based on local-area rainfall alone. The difficulty in identifying the seasonal rainfall onset dates was more predominant in the semi-arid zone. For instance, in the 1990s, seasons onsets were inconclusive due to alternating dry spells coupled with large gaps in the daily rainfall data.

4.6 Chapter Summary

In this section, the chapter summary is presented, whereby the assessment of the observed seasonal rainfall trend pattern at different time scales is considered and comparisons between the rainfall onset dates of the humid and semi-arid zone have been summarised. Differences between seasonal rainfall onset dates in the humid and semi-arid zone are also presented. Generally, the seasonal rainfall onset in the humid zone is earlier and more well-defined than in the semi-arid zone although the rainfall patterns are similar.

The analysis of trend in 16 rainfall stations for the period from 1950 to 2009 has revealed a general decrease in seasonal rainfall of Vhembe District. This indicates that the amount of seasonal rainfall has declined during the past 60 years. Although the majority of rainfall stations in this set of data showed a decrease in rainfall, only four stations registered statistically significant trends. Two of these stations are found in the semi-arid zone while the other two are located within the humid and sub-humid zone.

The most conspicuous seasonal rainfall increase was displayed by Klein Australie which featured a consistently upward trend from 1950 to 2009 with level of significance ≥ 95% (1950 – 2009; Q = 0.777 mm/year at $\alpha = 0.05$, 1960 – 2009; Q = 1.555 mm/year at $\alpha = 0.001$ and 1970 – 2009; Q = 1.266 mm/year at $\alpha = 0.01$). Kabanda (2011) proposed that planting trees on the Soutpansberg mountains and increasing vegetation density will re-establish evapotranspiration hence lowering the lifting condensation level (LCL) closer to high humidity content (Vegetation Level) to enhance the formation of cloud and augment rainfall. This is observed in Klein Australie which is part of Matiwa/Entabeni forest complex (Symes, Venter & Perrin, 2000); it has maintained commercial afforestation at high altitudes and agroforestry crops and orchards at lower altitudes. The results are manifested in the persistent upward trend in rainfall.

On the other hand, statistically significant decreasing trends were observed in Tshakhuma at $\alpha = 0.05$ level of significance. Part of this may be attributed to the extensive degradation in the east of the Soutpansberg mountains environment (Mphaphuli, 1999, as cited in Fairhurst et al., 2000). Hence, shrinkage of the natural vegetation causes a decline in the rainfall patterns and a resultant change in the vegetation status. Apart from this degradation, the area is also experiencing urban sprawl and overpopulation. The findings drawn from this chapter are consistent with the findings of previous studies (Munyati & Kabanda, 2009; Kabanda & Munyati, 2010; Kephe, 2014 ;Kephe et al., 2015), which showed that vegetation plays a crucial role in rainfall distribution in Vhembe District.

It was established in this chapter that the 1980 – 89 decade showed a downward trend of seasonal rainfall - while mostly the 1990s decade showed a general increase in the rainfall over the study area, with statistically significant trends at a large number of stations. The period from 2000 to 2009 generally saw a negative trend at $\alpha = 0.05$ level of significance, with statistical significance particularly apparent in humid areas.

Regarding the seasonal rainfall onset, some interesting facts have emerged; these include temporal and spatial variability in the seasonal rainfall distribution. For example, different seasonal rainfall onset dates among the two rainfall zones (humid and semi-arid) within the district were observed both in terms of the early and mean onset. The humid zone showed earlier seasonal rainfall onset dates while the semi-arid appears to lag behind. For instance, during the 1980s decade, the average seasonal rainfall in the humid zone was found to occur in pentad 57.5 (08 - 12 October) which is approximately 9 pentads earlier than in the semi-arid zone which was found to start in pentad 67 on average.

During the 2000s decade, the seasonal rainfall onset dates were found to be occurring in later pentads in both the humid and semi-arid zones when compared with 1980 decade seasons. For instance, in the humid zone, the average onset date of seasonal rainfall during 2000 decade was recorded in pentad 60 (23 – 27 October) while that of 1980 decade was observed in pentad 57 (08 – 12 October). That is a delay in the onset of rainfall of about three pentads. The earliest seasonal rainfall onset during 2000 decade was recorded later in pentad 56 compared to pentad 54 during 1980 decade. The late seasonal rainfall onset during the decade was reported in pentad 71 (17 – 21 December) while in the 1980s decade it was reported two pentads earlier (in pentad 69, 07 – 11 December).

A similar pattern of seasonal rainfall distribution was observed in the semi-arid zone of the district. In the 2000 decade, seasonal rainfall for an average season was found to start in pentad 64 relative to pentad 62 in the 1980s decade. However, the earliest start of seasonal rainfall during the decade was recorded in pentad 59, which is two pentads earlier compared to the earliest of 1980 decade (pentad 61). This chapter indicated precisely the pentad in which the seasonal rainfall onset started. In Chapter 5, Climate Prediction Centre (CPC)'s Merged Analysis of Precipitation ("CMAP") data analyses are presented to highlight and validate the seasonal rainfall onset obtained based on the analysis of local gauge data (in the current chapter).

Chapter Five

Real-Time Daily Rainfall Analysis During the Rainfall Onset

5.1 Introduction

The previous sections dealt with the spatial and temporal analysis of the seasonal rainfall pattern of the study area based on local gauge data, and the observed variability of seasonal rainfall distribution in both time and space. As indicated at the end of Chapter 4, in order to establish the connection between Vhembe District seasonal rainfall onset with the synoptic scale atmospheric circulation systems, it is essential to compare the local gauge rainfall prior to and during the seasonal onset date with rainfall estimated by global precipitation datasets (in this case CMAP data). Thus, this chapter aim to establish the degree to which the local gauge data captures the signal of large-scale climate forcing of the study area.

Therefore, the purpose of this section is to examine the Climate Prediction Centre (CPC)'s Merged Analysis of Precipitation ('CMAP') data 20 days prior to and during the early, mean and late seasons rainfall onset in the humid and semi-arid zone in order to compare and validate the seasonal rainfall onset obtained based on the analysis of local gauge data. The evolution of CMAP estimated rainfall 20 days prior to and during early and late seasonal rainfall onset date is constructed at pentad scale and compared with the amount of rainfall accumulated prior to and during seasonal rainfall onset date obtained based on local station data.

According to Xie and Arkin (1997) the quality of the CMAP analysis is strongly dependent on the amount of gauge data available as well as the accuracy of the satellite estimates. Generally, the quality is best in the tropics and weakens as you move away. Datasets that represent the space/time variation of precipitation over the globe, including land and ocean, are essential for understanding the characteristics of global precipitation variability and for validating climate model simulations and projections (Arkin & Xie, 1994). However, since these data have advantages as well as shortcomings; the data set is generally best suited to identifying and quantifying in a relative manner the spatial and temporal variability of precipitation especially in the tropics (Xie, 1996). The NOAA/OAR/ESRL PSD, Boulder, Colorado, USA, provided CMAP Precipitation data from their web site at http://www.esrl.noaa.gov/psd/. For the description of the contents of CMAP see section 2.2.3 in Chapter Two.

This study used CMAP Precipitation data for the decades 1980 – 89 and 2000 – 09 in the analysis. The decade 1990 – 99 was excluded because of its high inconsistency and large gaps in daily rainfall data, which made it difficult to determine the date of onset. The window domain used is 10°S to 40°S and extends from 0°E to 60°E in order to capture typical patterns of the seasonal rainfall onset as they evolve. The location of the study area is indicated by a black square in the middle of the map. The temporal analysis considers 20 days prior to and during the early and late rainfall season onset for the humid and semi-arid zone in order to compare and validate the seasonal rainfall onset obtained based on the analysis of local rain gauge data. Also in consideration is the mean rainfall season onset for each zone.

5.2 Humid Zone

The humid zone in Vhembe District is considerably wetter than the semi-arid zone (Nenwiini, 2012) (see Figure 4.1 in Chapter 4). A typical seasonal rainfall mean onset in the humid zone began in pentad 57 during the 1980-89 decade. Rainfall seasons which started in pentad 57, include 1982, 1984, 1988 and 1989. The 1986 rainfall season started early in pentad 54, while the 1985 season experienced a late onset of seasonal rainfall, starting in pentad 69 (December). Hence, this section and the corresponding subsections, consider 1986 and 1985 rainfall seasons from the 1980-89 decade in the examination of CMAP precipitation pentad data. The atmospheric features associated with seasonal variation in rainfall are examined in chapter 6 and 7.

5.2.1 Rainfall - 20 days Prior to 1986 Early Onset

Figure 5.1 shows the CMAP precipitation distribution 20 days prior to the 1986 seasonal rainfall onset date. Pentad 50 shows the southern Africa regions under low precipitation and this condition appears to change in the subsequent pentad (pentad 51) wherein a northward march of precipitation emanating from the South Indian Ocean is observed leading to an increase in the value of precipitation (about 2.5 mm/day) over the south eastern part of South Africa. The study area recieved very little precipitation. A similar pattern of precipitation persisted into pentad 52 with a slight increase in the value of precipitation by about 1 mm/day. The southeast oriented precipitation axis is apparent five days before the onset pentad (pentad 53) but the values of precipitation over the district declined.

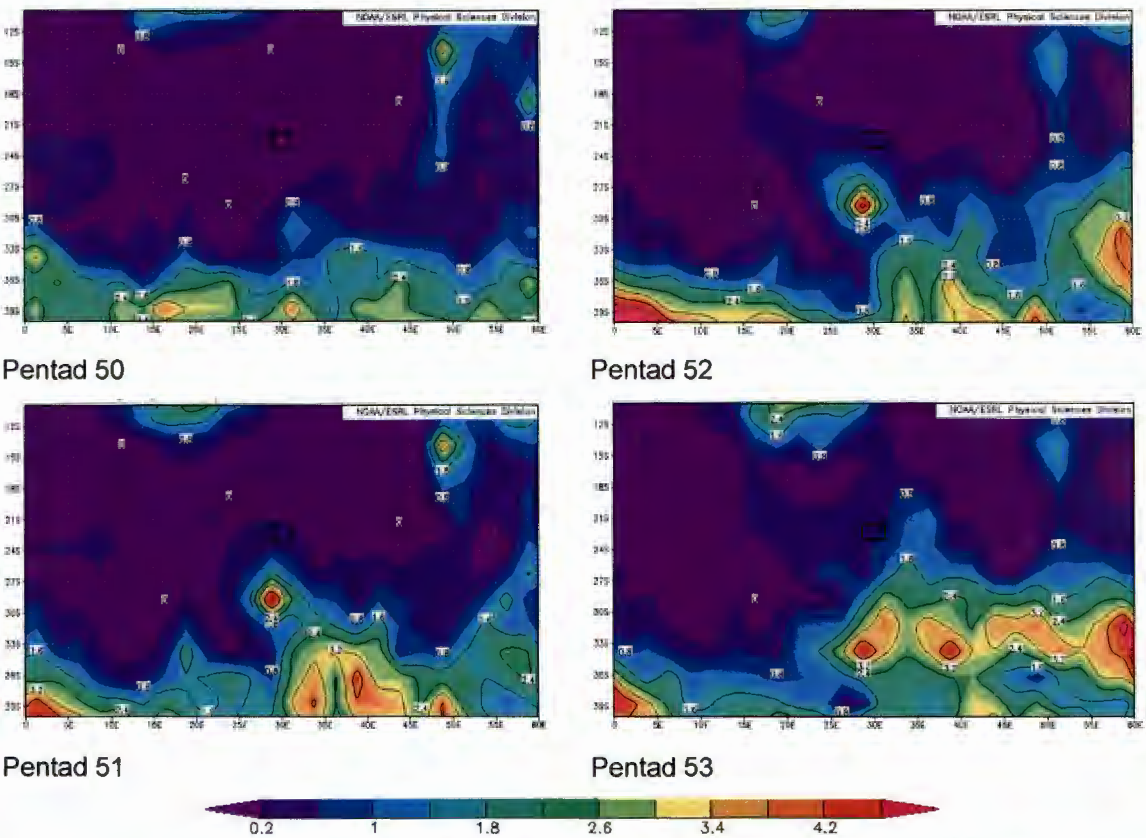

Figure 5.1: Pentad mean rainfall 20 days prior to the 1986 seasonal rainfall onset in the humid zone. Contour intervals are 0.4 mm/day. The study area is centred at the square in the middle of the map

5.2.2 Rainfall - During 1986 Early Onset

On the onset pentad (pentad 54), which is in late September, a relatively moderate amount of rainfall (with the centre > 4 mm day^{-1}) can be observed over southeast parts of South Africa and northwestern parts of southern Africa. The rainfall appears to originate from the Indian Ocean and the tropical regions.

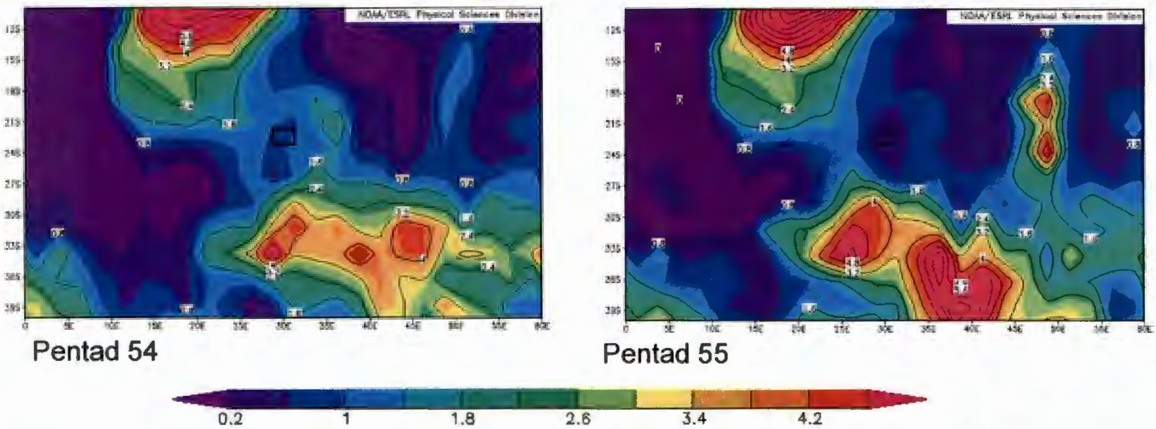

Figure 5.2: Pentad mean rainfall during 1986 seasonal rainfall onset in the humid zone. Contour intervals are 0.4 mm/day. The study area is centred at the square in the middle of the map

5.2.3 Rainfall - 20 days prior to 1985 Late Onset

During the 1980 – 89 decade, the 1985 rainfall season started late (pentad 69). Figure 5.3 represents five-day CMAP composite fields for 20 days prior to the seasonal rainfall onset. Pentad 65 shows the southeastward march of precipitation originating from the tropics. The mean precipitation of about 3 mm/day can be seen over the northeastern part of South Africa with the highest amount concentrated over the Indian Ocean and the periphery of Mozambique. A sudden increase in precipitation over most parts of the southern Africa region occurred in the subsequent pentad with centres of high amount of precipitation located in Mozambique, Madagascar and the Indian Ocean. A slight increase in precipitation is evident over the study region that is between 1 to 3 mm/day. In pentad 67, the atmosphere over Vhembe District shows precipitation of < 2 mm/day, and the same condition holds a pentad before the onset date.

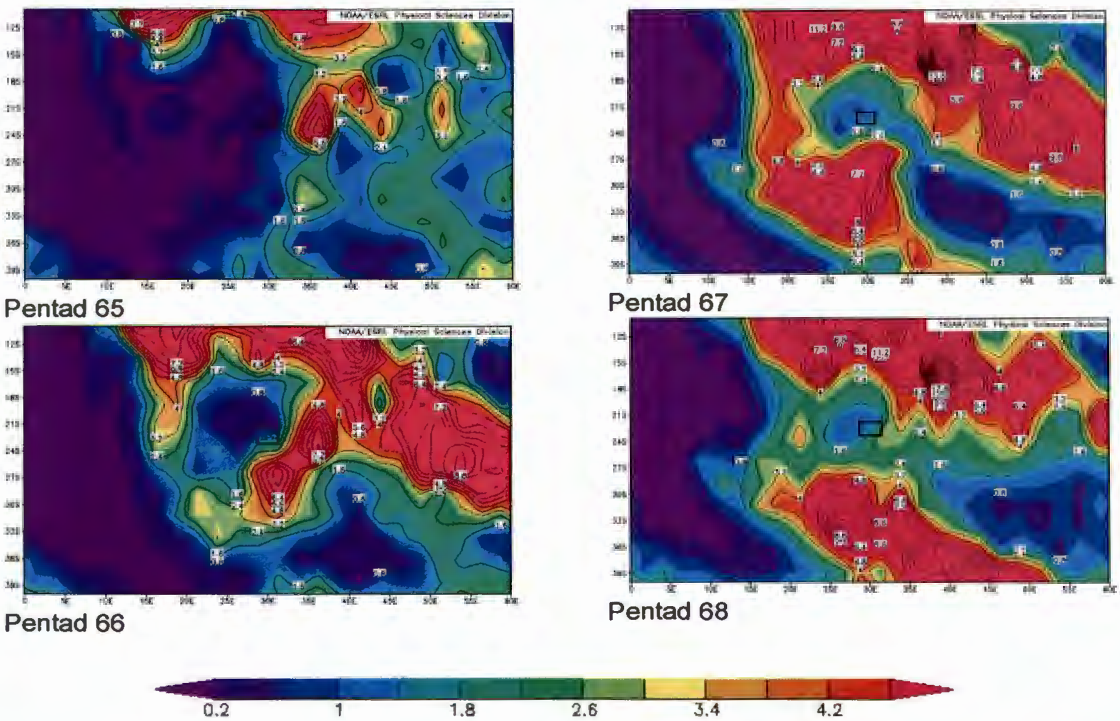

Figure 5.3: Pentad mean rainfall 20 days prior to the 1985 seasonal rainfall onset in the humid zone. Contour intervals are 0.4 mm/day. The study area is centred at the square in the middle of the map

5.2.4 Rainfall - During 1985 Late Onset

In pentad 69 (Figure 5.4), which is the onset pentad, north to southeast propagation of precipitation is evident, forming an axis of precipitation that appears to be a result of the connection of the tropical-Africa sources of precipitation with that of the Indian Ocean. The highest amount of precipitation occurred over the periphery of Madagascar and the surrounding ocean followed by Mozambique and Malawi. The atmosphere over the northeastern parts of South Africa and the study area is characterised by precipitation values ranging from 2 to 5 mm/day, and a slight increase in precipitation is evident in the successive pentad.

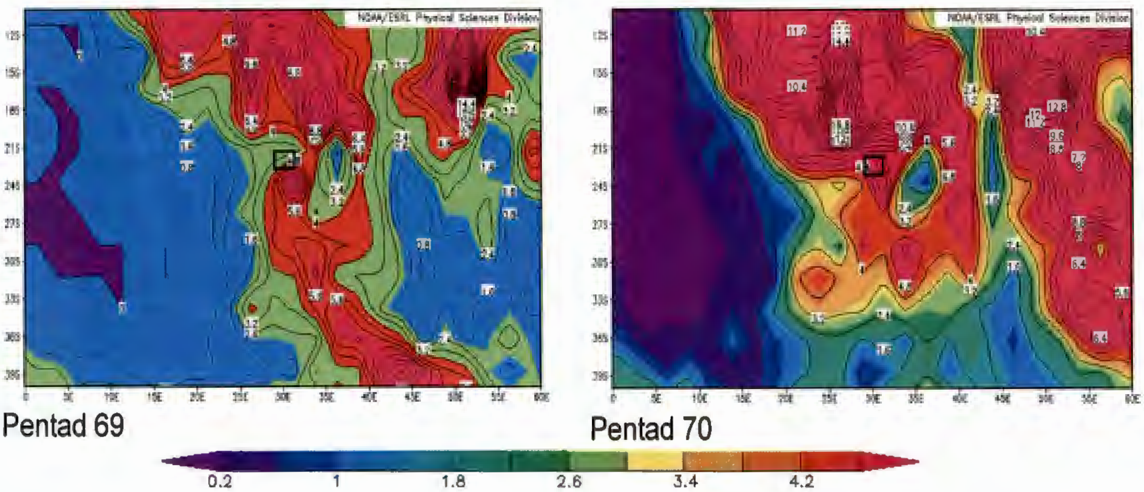

Figure 5.4: Pentad mean rainfall during 1986 seasonal rainfall onset in the humid zone. Contour intervals are 0.4 mm/day. The study area is centred at the square in the middle of the map

5.2.5 Rainfall - 20 days prior to 2001 Early Onset

Figure 5.5 presents the evolution of CMAP pentad fields composite 20 days prior 2001 seasonal rainfall, which is the earliest onset season for 2000-09 decade. Pentad 52 shows pronounced southeast propagation of rainfall across South Africa with relatively weak northwest extensions that provide large areas of the country with about 1 – 4 mm/day of rainfall; the study area observed ~ 1 mm/day of rainfall. Centres with high amount of rainfall are located over the Indian Ocean followed by the southernmost part of the country. A break in the northwest extension and a substantial reduction in rainfall values over northeastern parts of the country can be seen in pentad 53. This conditions progresses over pentad 54 and 55 leading to a further decline in rainfall over the land areas.

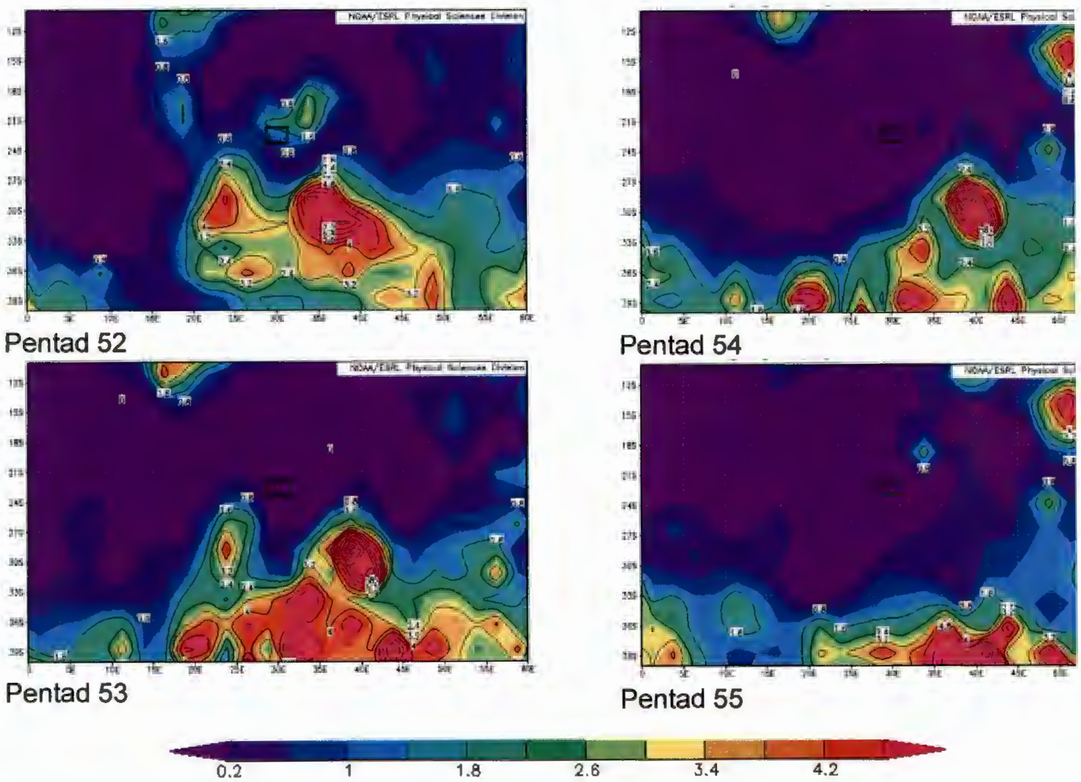

Figure 5.5: Pentad mean rainfall 20 days prior to the 2001 seasonal rainfall onset in the humid zone. Contour intervals are 0.4 mm/day. The study area is centred at the square in the middle of the map

5.2.6 Rainfall - During 2001 Early Onset

As seen in Figure 5.6, rainfall of about 0.5 mm/day exists over most parts of South Africa during the onset date, which is early October (pentad 56). Centres of relatively moderate amounts of rainfall appear to be located over Botswana and Indian Ocean. The pentad after the onset shows a southeast extension of rainfall linking with the Botswana centre, which leads to a slight increase in rainfall values over the northeastern and southeastern parts of the country.

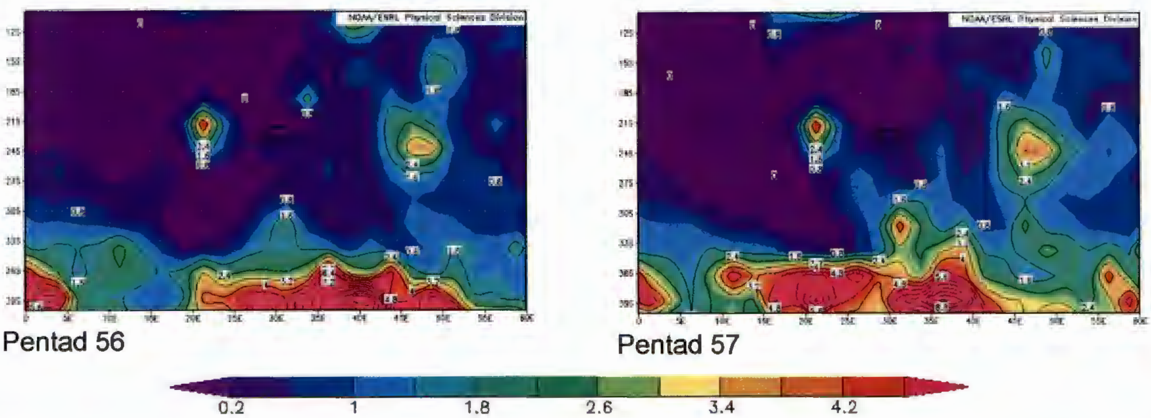

Figure 5.6: Pentad mean rainfall during 2001 seasonal rainfall onset in the humid zone. Contour intervals are 0.4 mm/day. The study area is centred at the square in the middle of the map

5.2.7 Rainfall - 20 Days Prior to 2006 Late Onset

In 2006, a late rainfall onset season for the 2000 – 09 decade, rainfall started in mid-December (pentad 71). Figure 5.7 presents the evolution of CMAP pentad field composites for the 20 days prior to the onset. A northeast-elongated rainfall distribution from tropical Africa across Madagascar linking with the Indian Ocean is evident in pentad 67. The South African countryside remains under very low rainfall values between 2 and 3 mm/day. In the subsequent pentad, the distribution of rainfall progresses westward, increasing rainfall amounts over the north and southeastern parts of the country. At this stage, Vhembe District appears to be experiencing about 2 mm/day of rainfall. A similar pattern persists in pentad 69; however, a slight increase in rainfall amount to about 2 mm/day is evident. During pentad 70, SWIO rainfall reduced to < 2 mm/days.

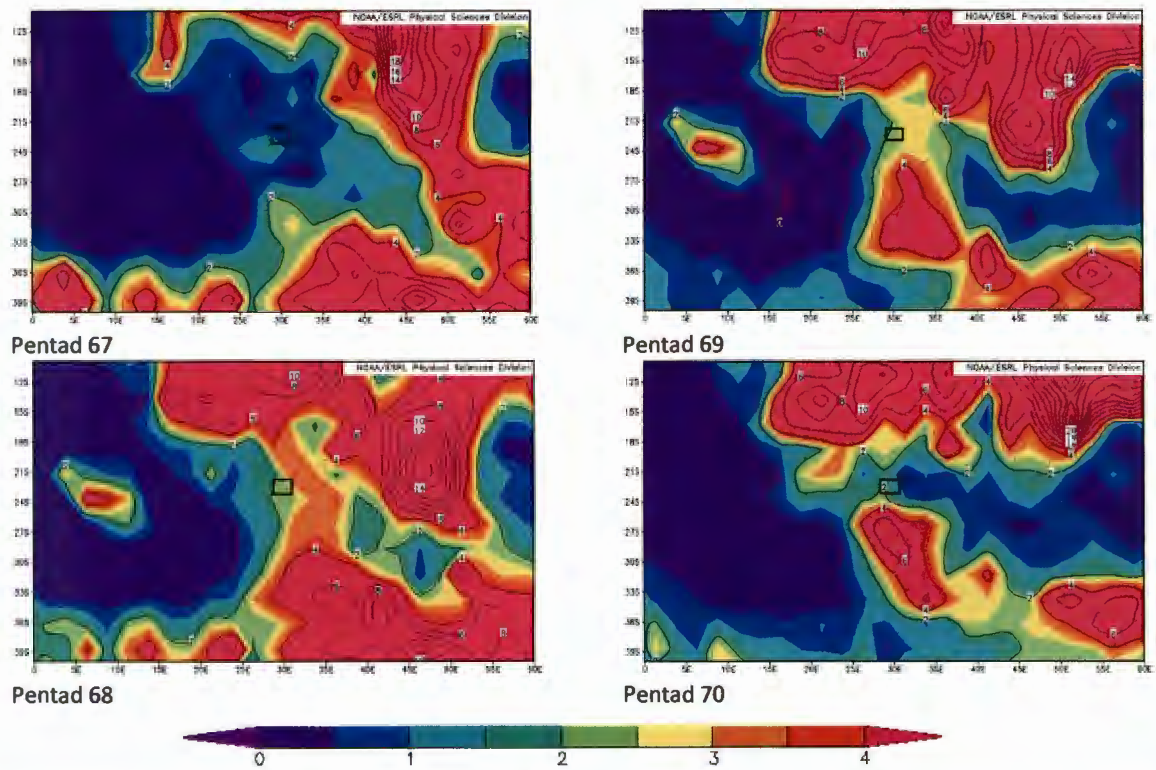

Figure 5.7: Pentad mean rainfall during 2006 seasonal rainfall onset in the humid zone. Contour intervals are 2 mm/day. The study area is centred at the square in the middle of the map

5.2.8 Rainfall - During 2006 Late Onset

During pentad 71, the north-south distribution pattern weakened considerably with a decline in rainfall values over the countryside (Figure 5.8). Vhembe District recorded ~ 2 mm/day rainfall. In the subsequent pentad, a northeast propagation of rainfall emanating from tropical Africa and Madagascar leads to an increase in rainfall values (between 2 - 4 mm/day) over the northeastern parts of South Africa.

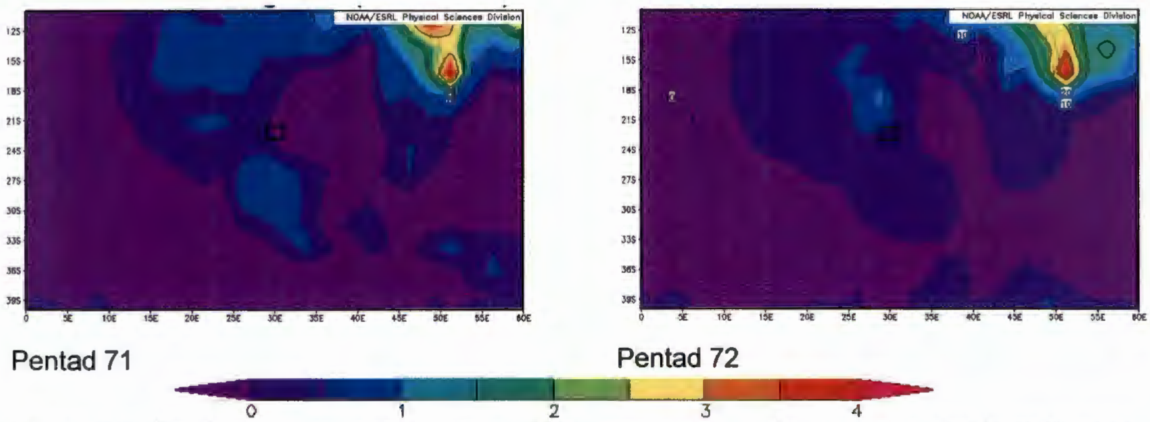

Figure 5.8: Pentad mean rainfall during 2006 seasonal rainfall onset in the humid zone. Contour intervals are 1.5 mm/day. The study area is centred at the square in the middle of the map

5.3 Semi-arid Zone

The analysis of seasonal rainfall onset in sub-section 4.5.1 showed that at a decadal scale, the seasonal rainfall of the semi-arid zone of Vhembe District begins in early November (pentad 63) on average. The observations also showed that during the1980 – 89 decade, the earliest seasonal rainfall onset was experienced in 1984 at the end of October, while the late onset season was reported in 1981/2 early January of the following year (pentad 1). In the 2000 – 09 decade, the earliest onset was in 2001, when seasonal rainfall started in mid-October. The late season rainfall onset was in 2007 and it started in mid-December (pentad 69). The subsequent sections present the corresponding CMAP analysis, which relate to the season's onset of the semi-arid zone.

5.3.1 Rainfall - 20 Days Prior to 1984 Early Onset

Figure 5.9 shows the systematic evolution of pentad precipitation composites 20 days prior to the seasonal rainfall onset during 1984. It is the earliest season onset in the 1980 – 89 decade. The observations show an extension of rainfall from northwest Africa and the southeast Indian Ocean tilted across most areas in South Africa with about 1 mm/day of rainfall registered over the study area early October (pentad 57). In the following pentad, extension appears to be weakening in both the northwest and southeast, but the northeastern part of South Africa remains under a rainy atmosphere. Vhembe District registers from 1 to 1.5 mm/day of rainfall around this time. During pentad 59, there is evidence of a widespread reduction of rainfall over the Southern Africa region in general. Conditions improved in late October a pentad before the onset date of seasonal rainfall (pentad 60). During this time, there was an establishment of a pronounced link between northwest and southeast sources of rainfall across South Africa. This led to an increase in the rainfall recorded over the study area to between 1 and 2 mm/day.

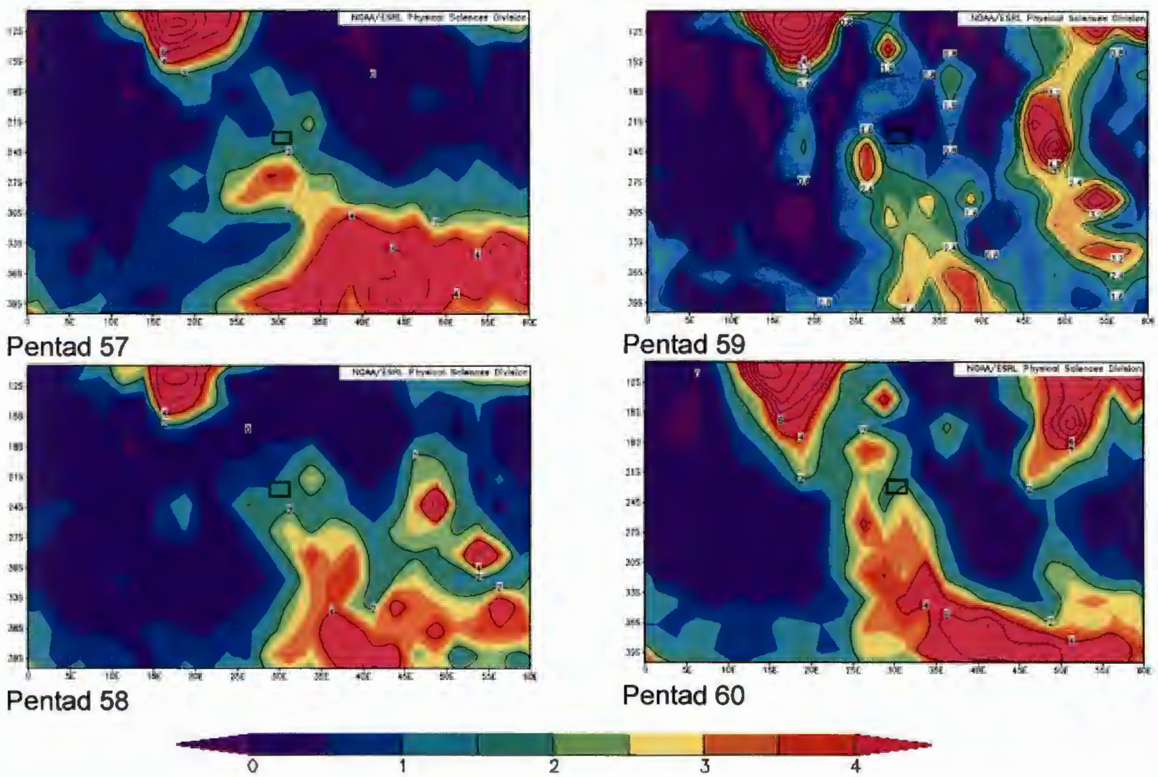

Figure 5.9: Pentad mean rainfall 20 days prior to the 1984 seasonal rainfall onset in the semi-arid zone. Contour intervals are 1 mm/day. The study area is centred at the square in the middle of the map

5.3.2 Rainfall - During 1984 Early Onset

In early November (pentad 61), which is the onset date of seasonal rainfall in the semi-arid zone, the atmosphere over the northeastern part of South Africa is characterised by high amounts of rainfall. This time around, an established connection between the northwest, southeast and Madagascar appears to be feeding the area under investigation with rain. A rainfall band which is tilted across northwest-southeast of Southern Africa regions is evident five days after the onset date (pentad 62) and an amount of rainfall ranging between 4 and 6 mm/day is recorded over the study area (Figure 5.10).

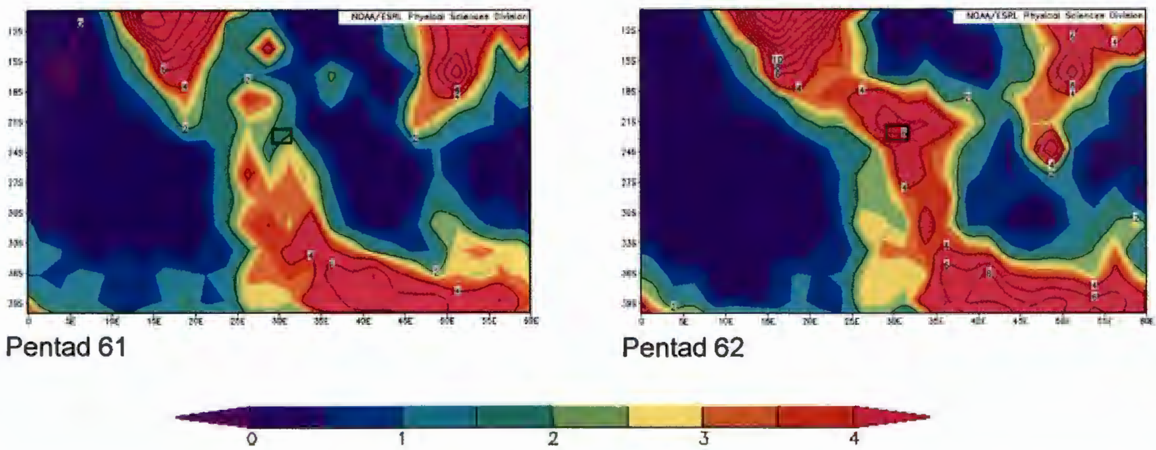

Figure 5.10: Pentad mean rainfall during 1984 seasonal rainfall onset in the semi-arid zone. Contour intervals are 0.5 mm/day. The study area is centred at the square in the middle of the map

5.3.3 Rainfall - 20 Days Prior to 1981 Late Onset

The CPC's precipitation field composites in figure 5.11 show the amount of rainfall registered over the study area 20 days prior to the season onset in the semi-arid zone. Pentad 70 shows a very low amount of rainfall over the southern Africa regions in general, with about 1 mm/day of rainfall over the study area. Similar conditions prevail in the following pentad (pentad 71) which shows the beginning of a southward march of rainfall from the Congo and Madagascar. A band of rainfall that extends from the Congo across Zambia, Mozambique and Madagascar is evident in pentad 72. As a result, the amount of rainfall registered over the study area increases substantially to about 3 to 4 mm/day. A pronounced north to southeast band of rainfall is apparent five days before the onset of rainfall in the semi-arid zone, with a slight increase in rainfall amount.

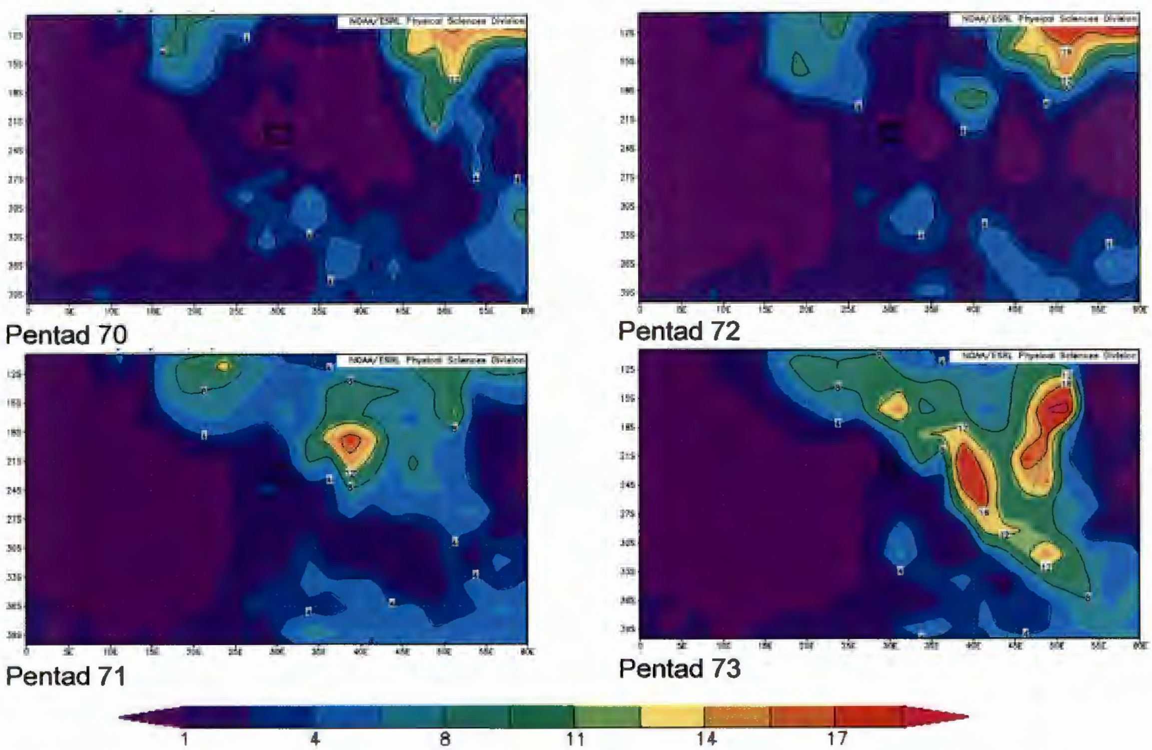

Figure 5.11: Pentad mean rainfall 20 days prior to 1981 seasonal rainfall onset in the semi-arid zone. Contour intervals are 2 mm/day. The study area is centred at the square in the middle of the map

5.3.4 Rainfall - During 1981 Late Onset

During the onset date, which started in pentad 1 in 1982, a spread of a high amount of rainfall towards the land areas is apparent. The maintenance of similar rainfall patterns continued, keeping a centre of high values of rainfall in Madagascar a pentad later (Figure 5.12).

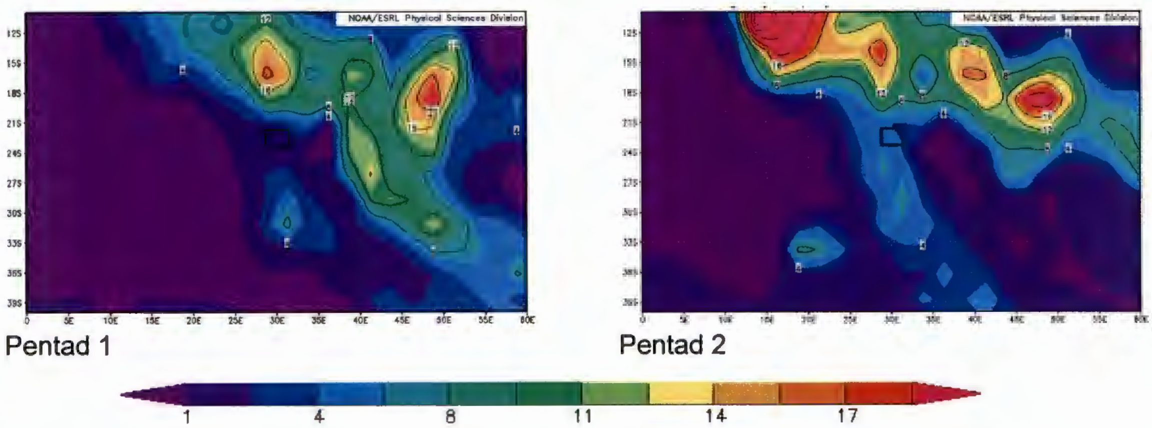

Pentad 1 Pentad 2

Figure 5.12: Pentad mean rainfall during 1981 seasonal rainfall onset in the semi-arid zone. Contour intervals are 2 mm/day. The study area is centred at the square in the middle of the map

5.3.5 Rainfall - 20 Days Prior to 2001 Early Onset

In Figure 5.13, most parts of South Africa recorded a very low amount of rainfall starting late September to early October (pentad 55). However, the atmosphere over the surrounding Ocean and some parts of Madagascar during the same period is characterised by rainfall amounts ranging from 1 to 3 mm/day. Similar conditions prevailed in the following pentad (pentad 56) but with a development of a rainfall centre over Botswana/South African border, with rainfall values ~ 1.5 mm/day. During pentad 58, a rainfall link between tropical Africa, Indian Ocean and Madagascar is apparent. The record shows an increase in rainfall to ~ 1.5 mm/day over the study area.

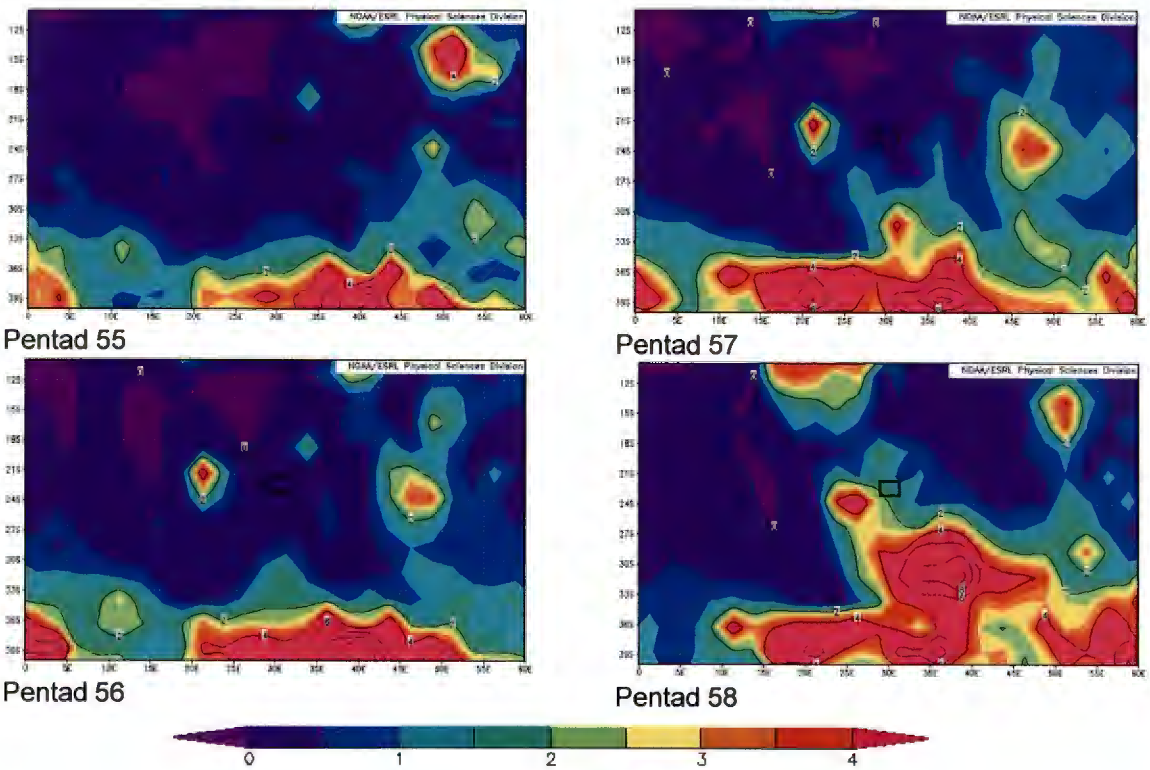

Figure 5.13: Pentad mean rainfall 20 days prior to the 2001 seasonal rainfall onset in the semi-arid zone. Contour intervals are 0.5 mm/day. The study area is centred at the square in the middle of the map

5.3.6 Rainfall - During 2001 Early Onset

The 2001 rainfall season started in mid-October (pentad 59) according to the local gauge data. As indicated in Figure 5.14, an intense flow of rainfall from the southeast Indian Ocean towards inland South Africa is evident with areas of high rainfall located on the east coast of South Africa and the Indian Ocean. Five days after the onset of rainfall (pentad 60), the area of high values of rainfall is located over the countryside and the study area experienced 1 to 2 mm/day of rainfall.

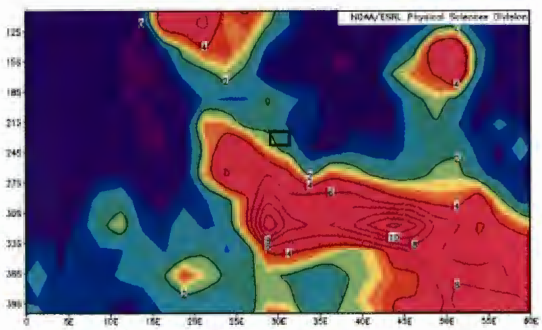

Pentad 59

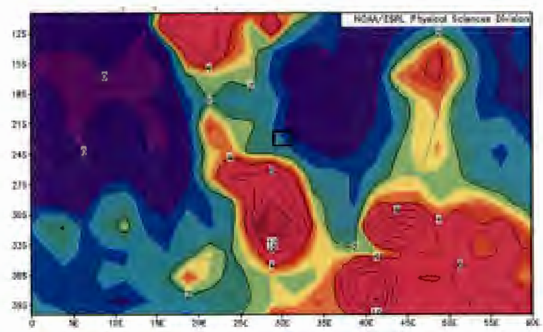

Pentad 60

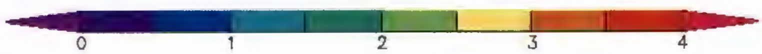

Figure 5.14: Pentad mean rainfall during 2001 seasonal rainfall onset in the semi-arid zone. Contour intervals are 0.5 mm/day. The study area is centred at the square in the middle of the map

5.3.7 Rainfall - 20 Days Prior to 2007 Late Onset

Figure 5.15 indicates the evolution of rainfall 20 days prior to the late onset season in the semi-arid zone during the 2000 – 09 decade. At pentad 66, there is a north-southeast elongated rainfall band across southern Africa with a central value of ~ 4 mm/day of rainfall over the study area. The following pentad shows an increase in rainfall values over the area under study from 4 to about 5 mm/day. Mozambique and eastern South Africa also are areas of high levels of rainfall during that period. By pentad 68, rainfall over southeastern South Africa has reached ~ 8 mm/day, and that has extended to Vhembe District.

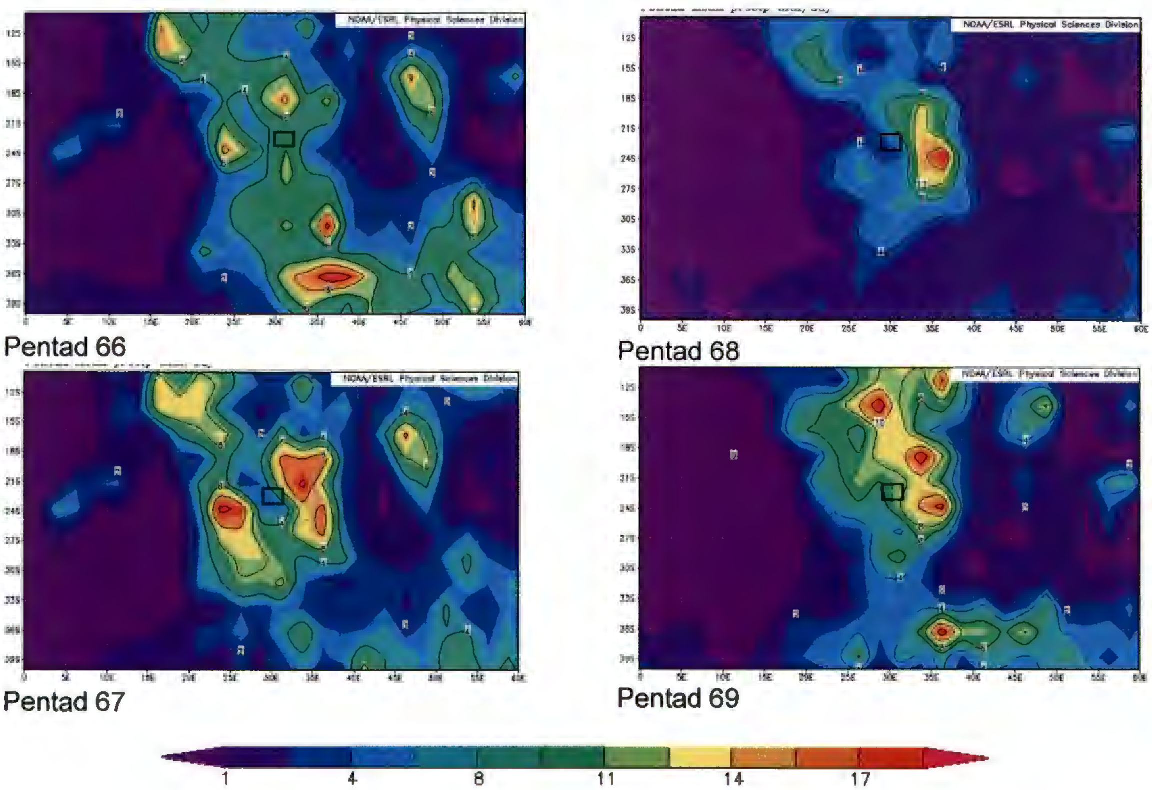

Figure 5.15: Pentad mean rainfall 20 days prior to the 2007 seasonal rainfall onset in the semi-arid zone. Contour intervals are 0.5 mm/day. The study area is centred at the square in the middle of the map

5.3.8 Rainfall - During 2007 Late Onset

Figure 5.16 shows the rainfall patterns during onset time in the 2007 rainfall season (pentad 70). A tongue of rainfall distribution that emanated from the tropics reached Vhembe District with an isohyet value ≥ 6 mm/day. By pentad 71, rainfall distribution of ≥ 4 mm/day has surrounded eastern South Africa and SWIO including Madagascar.

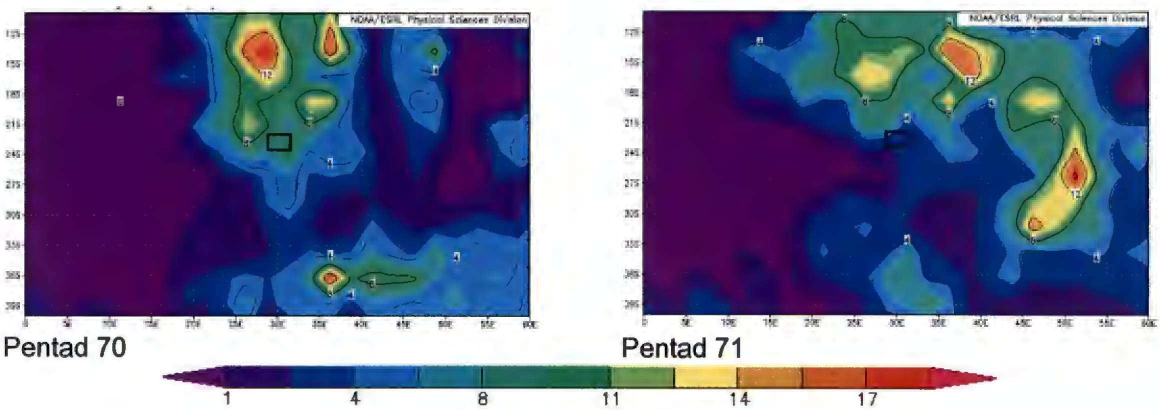

Figure 5.16: Pentad mean rainfall 20 days prior to the 2007 seasonal rainfall onset in the semi-arid zone. Contour intervals are 2 mm/day. The study area is centred at the square in the middle of the map

5.4 Chapter Summary

Using the onset dates established in Chapter 4, the analysis of CMAP data in Chapter 5 provided the rainfall evolution in the 20 days prior to and during the seasonal rainfall onset for two decades 1980 – 89 and 2000 – 09. The purpose was to establish the degree to which the local rainfall gauge data captures the signal of large-scale climate forcing of the study area. Comparisons between the rain gauge rainfall data and CMAP datasets (Table 5.1 & 5.2) show that the overall distribution of the pentad rainfall is largely consistent, although some discrepancies are seen.

Table 5.1 presents the comparisons for the humid zone. The early onset in 1986 indicates a gradual increase of rainfall in both gauge and CMAP data, with maximum rainfall reported during the onset pentad (pentad 54). Substantial amounts of rainfall continued to fall five days later. In 1985, the late-onset season of the same decade, CMAP data estimated rainfall of ~ 0.5 and 1.5 mm/day in pentad 65 and 66 (20 day and 15 day prior to onset) when local gauge station recorded no rain. CMAP estimates increased to about 4 mm/day on the onset date when local gauge station reported heavy rainfall (~ 78.5 mm). Five days after the onset CMAP estimate was ~ 6 mm/day when the local station rainfall increased to ~ 112 mm.

In the 2001 rainfall season, which represents the early season onset during 2000 decade, there was no rainfall recorded over the local rainfall stations throughout the 20 days before the onset date. Nevertheless, the CMAP data sets show a very little amount of rainfall (0.2 mm/day) over the study area at the same time. It increased to ~ 0.5 mm/day by the onset date (pentad 57) when the local gauge registered 11mm.

Table 5.1: Local Station and CMAP Rainfall Prior and During Onset Date in Humid Zone

	Period	Early Onset 1986			Late Onset 1985		
		Pentad	Station gaug Rainfall (mm)	CMAP Rainfall (mm/day) Distribution	Pentad	Station gauge Rainfall (mm)	CMAP Rainfall (mm/day) Distribution
Humid Zone		P50	0	0.15	P65	0	0.5
		P51	3.2	0.15	P66	0	1.5
		P52	4.3	0.25	P67	4.9	2
		P53	0	0.25	P68	0	2
	During Onset	P54	29.7	1.0	P69	78.5	4
	During Onset + 1	P55	5.3	0.5	P70	112.2	6
		Early Onset 2001			Late Onset 2006		
		P52	0	1	P67	0	1
		P53	0	0.25	P68	0	1.5
		P54	0	0.25	P69	0	2
		P55	0	0.25	P70	0	2
	During Onset	P56	11	0.5	P71	12	2
	During Onset + 1	P57	21	0.25	P72	3.5	3-6

Table 5.2 shows the comparison between the local rainfall station gauge records and CMAP rainfall prior to and during onset in semi-arid zone. The early onset season occurred in 1984, while the late onset was in 1981. In 1984, the local rainfall station gauges were mostly dry before the onset date except for an isolated rainfall event of about 6 mm in pentad 58. At the same time, the CMAP estimates ranged between 1 and 2 mm/day. Onset pentad (pentad 61), reported 36 mm and CMAP increased to ~4 mm/day.

The late onset (1981) season rainfall pattern featured persistently dry conditions in the 20 days prior to the onset (pentad 70-73), while at same time the CMAP estimates rainfall of between 1 and 3 mm/day. Increased rainfall (60 mm and 4 mm/day) featured in both station gauge and CMAP data respectively.

Table 5.2 represents the 2000 decade, which features early onset in 2001 and late onset in 2007. Through early onset (2001), local station-gauge and CMAP show similarities in rainfall patterns whereby there is a gradual increase of rainfall reaching a maximum in pentad 59 (onset pentad). However, the late onset (2007) did not show any clear corresponding pattern between the two datasets. For instance, the gauge data showed consistently dry in four pentads (pentads 66 - 69) while CMAP depicted increase from 4.0-6.5 mm/day during the same period. Both datasets, however, indicated presence of substantial amount of rainfall.

Table 5.2: Local Station and CMAP Rainfall Prior and During Onset Date in Semi-arid Zone

	Period	Early Onset 1984			Late Onset 1981		
		Pentad	Station gauge Rainfall (mm)	CMAP Rainfall (mm/d) Distribution	Pentad	Station gauge Rainfall (mm)	CMAP Rainfall (mm/d) Distribution
Semi-arid Zone		P57	0	1	P70	0	1
		P58	4.5	1-1.5	P71	0	2
		P59	0	1	P72	0	2-4
		P60	0	1.5-2	P73	0	2-3
	During Onset	P61	36	4	P1	60	3-4
	During Onset + 1	P62	4.5	4	P2	2.5	4
		Early Onset 2001			Late Onset 2007		
		P55	0	0.25	P66	0	4
		P56	0.7	0.5	P67	0	4
		P57	0	0.5	P68	0.8	6.5
		P58	2	1.25	P69	0	6.5
	During Onset	P59	26.2	2-3	P70	38.1	6
	During Onset + 1	P60	0.9	1-2	P71	59.3	4

The distinctive observations obtained from Table 5.1 and 5.2 are that:

- CMAP precipitation data appears to underestimate the actual magnitude of rainfall over the study area in general. This may be possibly due to the coarse resolution of CMAP precipitation datasets or the sparse gauge data used as base (Yatagai et al., 2008). Global scale gridded precipitation datasets with coarse grid resolution have difficulty capturing daily rainfall events realistically at local scales particularly in areas of significant topography (Huggel et al., 2015) - Vhembe District features prominent topography in the form of Soutpansberg mountains which runs northeast and southwest. They have a mean ridge height of approximately 800-1200 m with various peaks reaching 1500 m above the surroundings.

- The estimated amounts of rainfall of CMAP precipitation data are averages over a large area, which may result in overestimation or underestimation of rainfall at a local level. The problem of CMAP estimating smaller precipitation amounts in some areas is attributed to the differences in the algorithms used to define the merged analyses and the input data sources (Gruber et al., 2000; Adler et al. 2001; Chen et al., 2002; Xie et al., 2003; Huggel et al., 2015). Thus, CMAP precipitation values of about 3 mm/day may in fact indicate heavy rainfall on the ground.

- The CMAP datasets do not capture the amounts of rainfall reported by local station-gauge adequately during the early onset of seasonal rainfall over the humid zone. This may be because the local scale rainfall has the component of orographic inducement due to the unique topographical features in the area (Kabanda, 2004). Gridded precipitation datasets have the tendency of underestimating the magnitude of orographic rainfall and local scale induced convective precipitation (Huggel et al., 2015). They are most representative of large-scale rain producing systems, which the satellite can capture easily. All these observations are in agreement with New et al. (2001), who said that precipitation data derived from local gauge and satellite-gauge merged sources provide contrasting opportunities for rainfall variability analysis over space and time.

- Local station gauge and CMAP rainfall analysis revealed relatively high rainfall prior to and during early and late season in the semi-arid zone as compared to the humid zone. We can attribute this observation to the later arrival of rainfall in the semi-arid zone, which means that there has been enough time for the rainfall mechanism in the whole of Vhembe District and at synoptical-scale level to advance further. In order to understand this, there is a need to explore the evolution of synoptic indicators in southern Africa. This will lead to determining their influence on the seasonal rainfall onset in Vhembe District. It is important to identify the synoptic-scale features (meteorological characteristics) because their positions over southern Africa, which will be dynamically changing between seasons (Kabanda, 2004) will directly influence the rainfall onset in Vhembe District. Chapters 6 and 7 will examine this in detail.

Chapter Six

Meteorological characteristics during the rainfall onset

6.1 Introduction

Some factors which might be associated with the variability of seasonal rainfall onset in Vhembe District have been identified as the physical features in the area such as orography (Kabanda, 2004; Kabanda & Munyati 2010; Nenwiini, 2012; Nenwiini & Kabanda 2015) anthropogenic effects (deforestation and urban sprawling) (Munyati & Kabanda, 2009; Kephe et al., 2015). The availability of a large quantity of moisture in the atmosphere provides great potential for rainfall development. Nevertheless, for rainfall to occur, a lifting mechanism is required to force the air near the earth's surface to rise and cool for moisture to condense. In this regard, the analysis of vertical motion (omega) will indicate areas of rising and subsiding motion and their magnitude, while the analysis of specific humidity and moisture flux will indicate the source, sink, trajectory and magnitude of the moisture needed for rainfall in Vhembe District.

The analysis of the above-mentioned meteorological systems corresponds to the early, late and mean seasonal onset dates per decade. In order to track the evolution of the systems associated with rainfall onset, the period of analysis starts in September and end in April for each season (1980 to 2009). The analysis included the first twenty days prior to the seasonal rainfall onset dates (at pentad scale) for all variables in order to capture the meteorological features as the seasonal rainfall onset evolves from the non-seasonal rainfall events. In this way, the study will avoid or minimise false alarms that rainfall has started when in fact it has not.

The study domain extends from 10°S to 40°S and from 0°E to 60°E. It includes the adjacent oceans - southwest Indian Ocean in the east and southeast Atlantic Ocean in the west. It is necessary to consider such a large domain because the weather systems that affect Vhembe District, especially those of the synoptic scale, seldom form in situ (Kabanda, 2004). Monitoring a larger area will capture and highlight the geographical and temporal characteristics of the weather systems (source of activities) that are in play during the particular seasonal rainfall onset in the local study area.

6.2 Atmospheric Specific Humidity

Generally, moisture in the atmosphere starts as water vapour, water droplets and ice crystals, and is sometimes expressed as humidity. According to Trenberth (2005), water vapour determines the weather and climate of the earth; it acts as the main source of precipitation in the lower troposphere. Water vapour in the atmosphere varies geographically and seasonally; a larger amount of water vapour is concentrated in the tropics (lower latitudes) than in the polar regions (higher latitudes), and the warm season is associated with more water vapour than the cold season (Bonan, 2008).

The three main measurements of atmospheric humidity are absolute, relative and specific humidity. Absolute humidity is the mass of water vapour in a given volume of air Relative humidity measures the amount of water vapour in the air expressed as a percentage of the amount of water vapour the air can hold given its present temperature; it is a measure of how close the air is to saturation. It is worth mentioning that high relative humidity does not automatically imply a large amount of water vapour in the air (Ahrens, 2002).

Specific humidity measures the actual mass of water vapour per mass of air, usually expressed as number of grams of water vapour contained in a kilogram of natural air (Misra et al., 2012). Specific humidity is important in meteorology because it is a measure of water vapour in the atmosphere. Water vapour and the processes that control its abundance in the lower atmosphere (troposphere) play a major role in the global climate system (Seidel, 2002). The condensation of water vapour and release of latent heat is one of the main sources of energy driving the atmosphere's circulation. Water vapour also modulates the transfer of radiation within the atmosphere, and because of its great mobility and brief atmospheric residence time, it is a central component of the global hydrological cycle.

When determining the magnitude of a rainfall event, the most important factor is not the process that brings the air to saturation, but the amount of water vapour available for conversion to liquid water (Hewitson, 1999). Therefore, from these perspectives, the specific humidity is probably the best measure of atmospheric water content, and is the measure used in this study.

According to Liu and Kalnay (2007), the atmospheric humidity relates directly with cloud coverage, precipitation processes and the release of latent heat. For rain to fall there must be sufficient moisture in the atmosphere, but the availability of moisture in the atmosphere is not the only condition for rainfall to occur. There are other mechanisms required to promote moisture lifting, cooling and condensation, including, convection, frontal uplift and orographic effect. In the study area, the wet season rainfall, which is of interest, is largely dependent on deep convection processes and water vapour convergence in the troposphere (Vigaud et al., 2007). Furthermore, the steep topography (Soutpansberg mountain range as well as the northern part of the Drakensberg mountains) in the area promotes the uplift of moist air. Therefore, specific humidity of the air is an ideal parameter to use in tracing the evolution of moisture prior to and during the rainfall onset. According to Monteith and Unsworth (2007), calculation of specific humidity is as follows:

$$Q = \frac{R_L}{R_W} \frac{e}{p+e \quad (R_L / R_W - 1)}$$

Eq. 6.1

where:

$$\frac{R_L}{R_W} = 0.62197$$

(Ratio of gas constants, air/water vapour)

On substituting in equation 6.1, we get equation 6.2

Q = (0.622 x e) / (p-[0.378 x e]) Eq. 6.2

where:

e = vapour pressure

p = air pressure (hPa)

Humidity data from NCEP-NCAR is available at a global scale from 1948 to present; however, in this study, the period of analysis was restricted to 1979 - 2008. This is because NCEP-NCAR specific humidity data before 1973 was unreliable due to instrumental changes that took place (Elliott & Gaffen, 1991).

6.3 Specific Humidity Analysis in the Humid Zone (1980-89)

This section used two seasons (1986 and 1985) from the 1980 – 89 decade data set for analysis, since they represented the early and late seasonal rainfall onset date respectively. In Chapter 4, pentad 57 represented the mean onset pentad in the humid zone of Vhembe District. In this chapter, NCEP reanalysis (Bradley et al., 1987) data for pentad 57 of 1982, 1984, 1988 and 1989 (mean onset seasons) were composited to determine the mean characteristics of the specific humidity and other meteorological fields during seasonal rainfall onset. On all figures the specific humidity are in kg/kg, while in the text g/kg is used (note: kg/kg = g/kg*1000).

6.3.1 Specific Humidity - 20 Days Prior to 1986 Early Onset

In order to establish the evolution of moisture build-up in the study area, the study used four pentads (50, 51, 52 and 53), that is, the 20 days prior to the seasonal rains onset (Figure 6.1). In this way, the dominant features could be captured as they evolved and progressed. It is evident that initially (pentad 50) a tongue of dry air emanating from the Indian Ocean engulfed the study area and remained there for the following two pentads (51 and 52). From 18th to 22nd September (pentad 53), an incursion of moist air (4 g/kg) from the tropics through Zambia and Angola penetrated southwards occupying most of southern Africa. However, Vhembe District and much of the northeastern part of South Africa remained under dry atmosphere with maximum specific humidity at 700 hPa of 2.5 g/kg during that period.

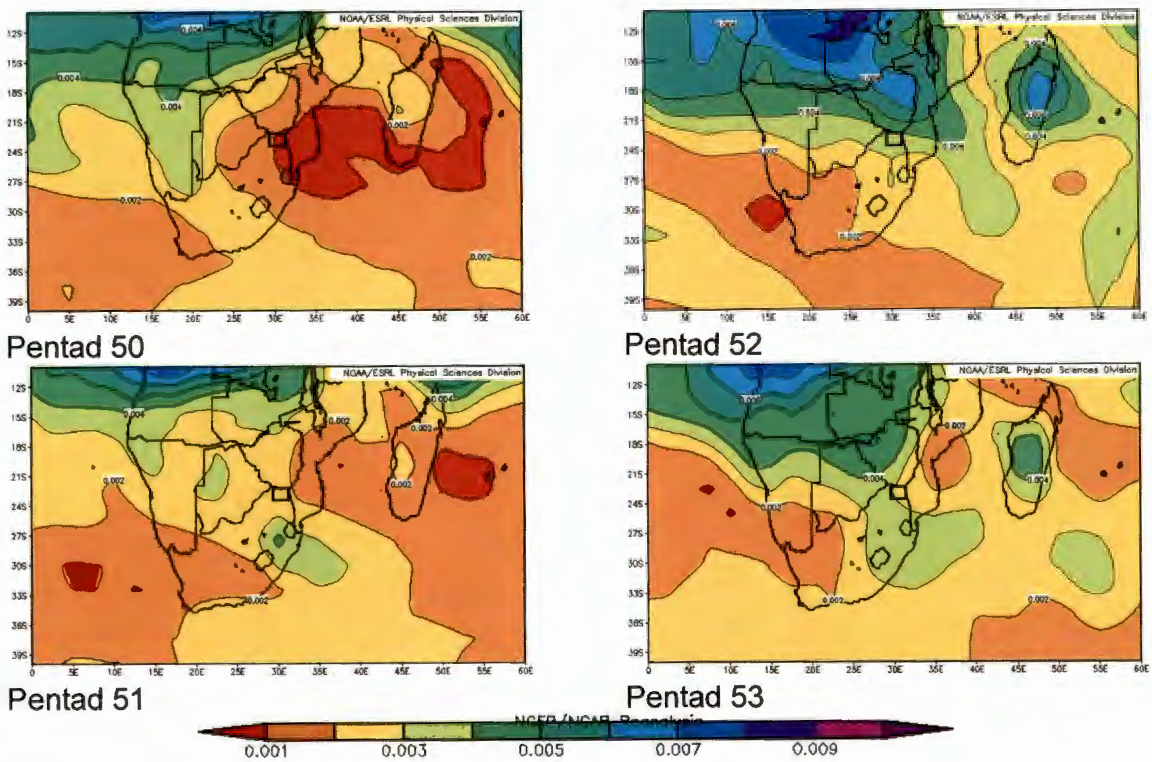

Figure 6.1: Specific humidity 20 days prior to 1986 seasonal rainfall onset. The contour intervals are 0.001 kg/kg.

6.3.2 Specific Humidity - During 1986 Early Onset

Figure 6.2 represents rainfall season onset for 1986, which started in pentad 54 (23 to 27 September). During this time, Vhembe District and its environs experienced a moisture surge of > 4.5 g/kg. At the onset stage (pentad 54) a center of moisture over central Madagascar recorded specific humidity of > 6 g/kg. This center of moisture was separated by a dry Mozambique Channel from moist continental southern Africa. Extending the analysis after the seasonal rainfall onset allows inferences to be drawn about the start and continuation of the seasonal rains with normal alternating dry spells. A significant feature observed so far is that moisture emanated from the tropics and propagated southward to Vhembe District and beyond.

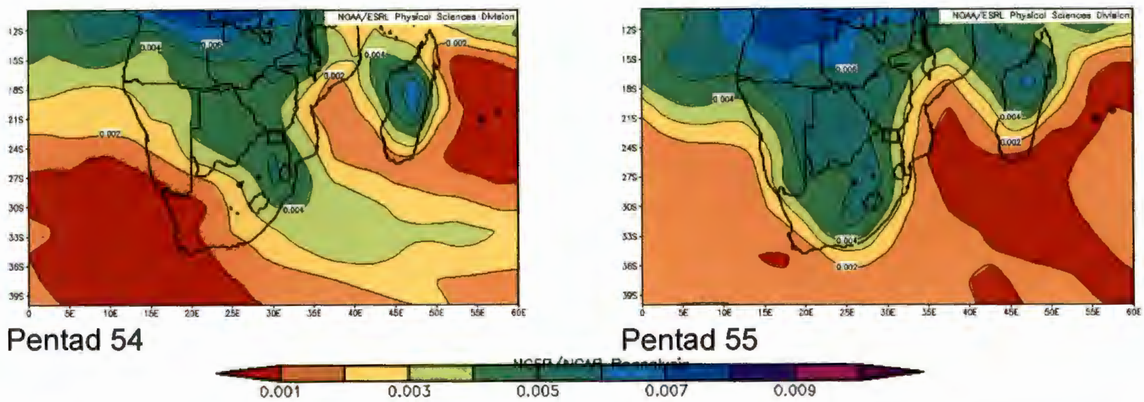

Figure 6.2: Specific humidity during 1986 seasonal rainfall onset. The contour intervals are 0.001 kg/kg.

6.3.3 Specific Humidity - 20 Days Prior to 1985 Late Onset

In 1985, the seasonal rainfall in the humid zone started in pentad 69 (7th to 11th December 1985), making this the late onset season in the 1980 – 89 decade. Figure 6.3 show the specific humidity composites 20 days prior to the onset (pentad 65, 66, 67 and 68). Dry air (≈ 1 g/kg) from the east (over the Indian Ocean) extended westward covering Vhembe District. In the subsequent pentad (22nd to 26th November), the centre of dry air appears to have suddenly moistened and become enclosed by areas of moist air (5 g/kg) extending from central Africa. In pentad 67, moisture intensified in central South Africa and central Africa (≥ 8 g/kg), Vhembe District remained relatively dry with moisture in the range of 3.5 g/kg. Centres of dry air over the Indian Ocean and Atlantic Ocean increased and moved towards the study area, reducing the moisture to ≤ 3 g/kg in Vhembe District a pentad before the rainfall onset.

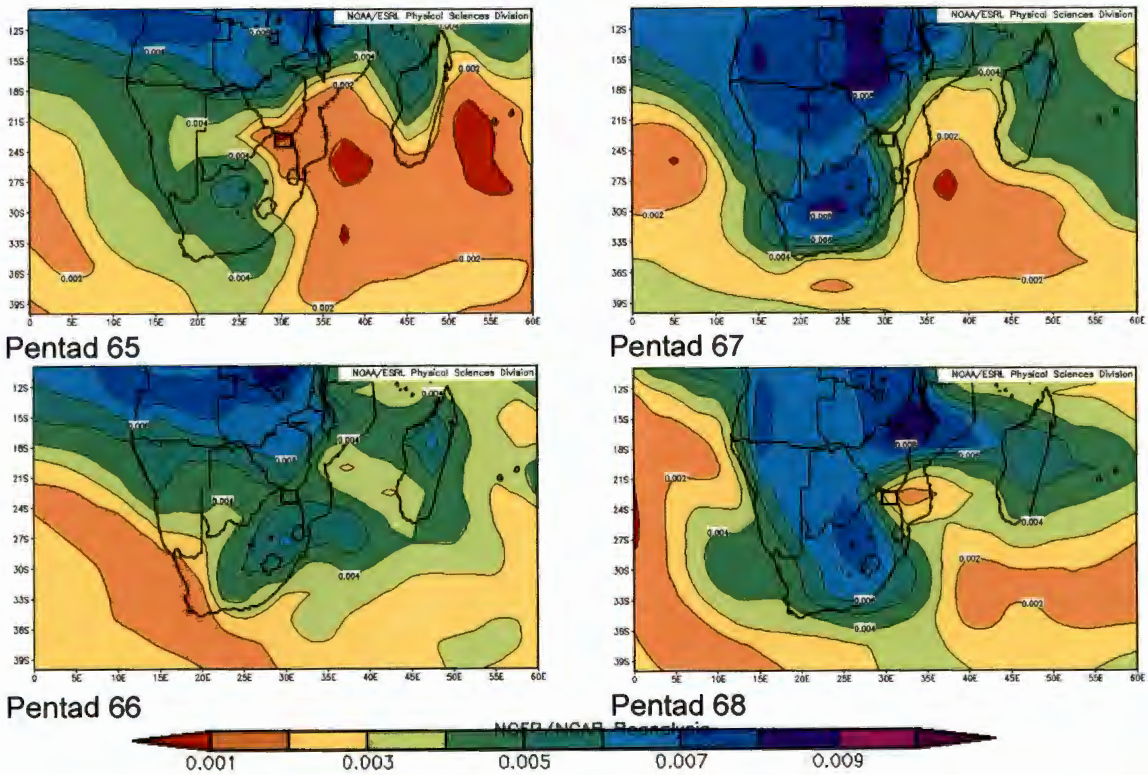

Figure 6.3: Specific humidity 20 days prior to 1985 seasonal rainfall onset. The contour intervals are 0.001 kg/kg.

6.3.4 Specific Humidity - During 1985 Late Onset

Figure 6.4 highlights the gradual development and evolution of moisture during the rainfall onset of 1985, which is characterised as late onset (pentad 69). Moisture activities cantered in Zambia and Botswana directs its low-level moisture into Northwest and Limpopo provinces in South Africa. This incursion of moisture resulted in a build-up of about 4 to 5 g/kg over Vhembe District. In the following pentad after the onset (Pentad 70), it is clear that the values of specific humidity has increased from 3 to 7 g/kg.

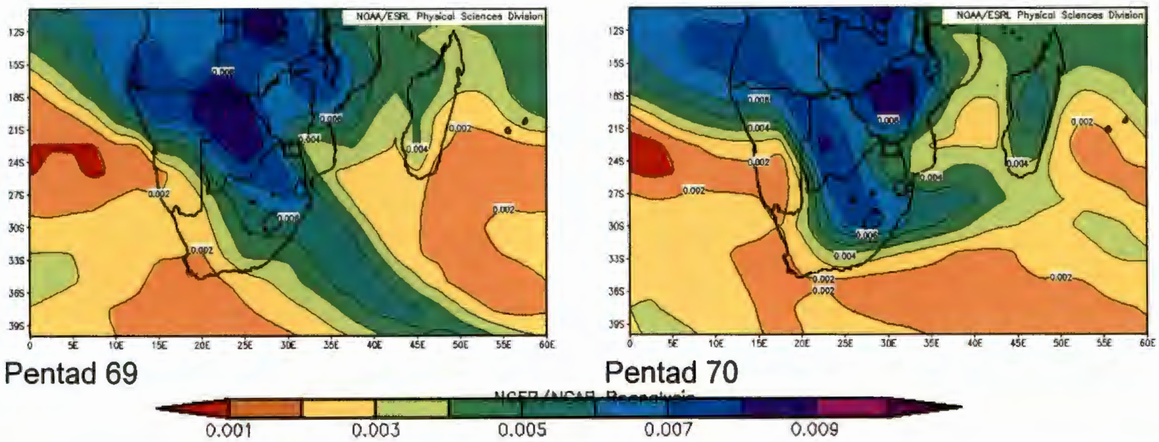

Figure 6.4: Specific humidity during 1985 seasonal rainfall onset. The contour intervals are 0.001 kg/kg

6.4 Specific Humidity Analysis in the Humid Zone (2000-2009)

The period 2000 to 2009 is the third decade from 1980. It is one of the major recent significant studies for South African climate since the original South African Country Studies carried out during the 1990s (DEA, 2013). According to the DEA (2013) report, which is one of the major contributions to the South Africa climate research, rainfall trends were below average in the early 2000s, reverting to normal towards 2010. This observation was generalised for the whole South Africa. The same report observed that there is a tendency towards an increase in the intensity of rainfall events and increased dry spell duration in South Africa. However, what was not certain was the rainfall onset in the different hydrological zones considered. This section considers the evolution of specific humidity during early onset (2001) and late onset (2006) incidents of rainfall in Vhembe District.

6.4.1 Specific Humidity - 20 Days Prior to 2001 Early Onset

Four pentads (52, 53, 54 and 55) prior to the seasonal rains onset are used to observe the evolution of moisture build-up in the study area. From Figure 6.5 an incursion of moisture emanating from the north is evident over the study area (pentad 52). This condition is short lived (pentad 53) due to a strong pool of dry air over the Indian Ocean which appears to be causing a decline in the levels of moisture over the study area. However, from 23[th] to 27[th] September (Pentad 54) an incursion of moist air (> 5 g/kg) from the tropics penetrates southwards occupying most of Vhembe District and northeastern parts of South Africa. This moisture presence lasted for only one pentad while the preceding pentad (pentad 55) shows a dry atmosphere with maximum specific humidity of about 2 g/kg.

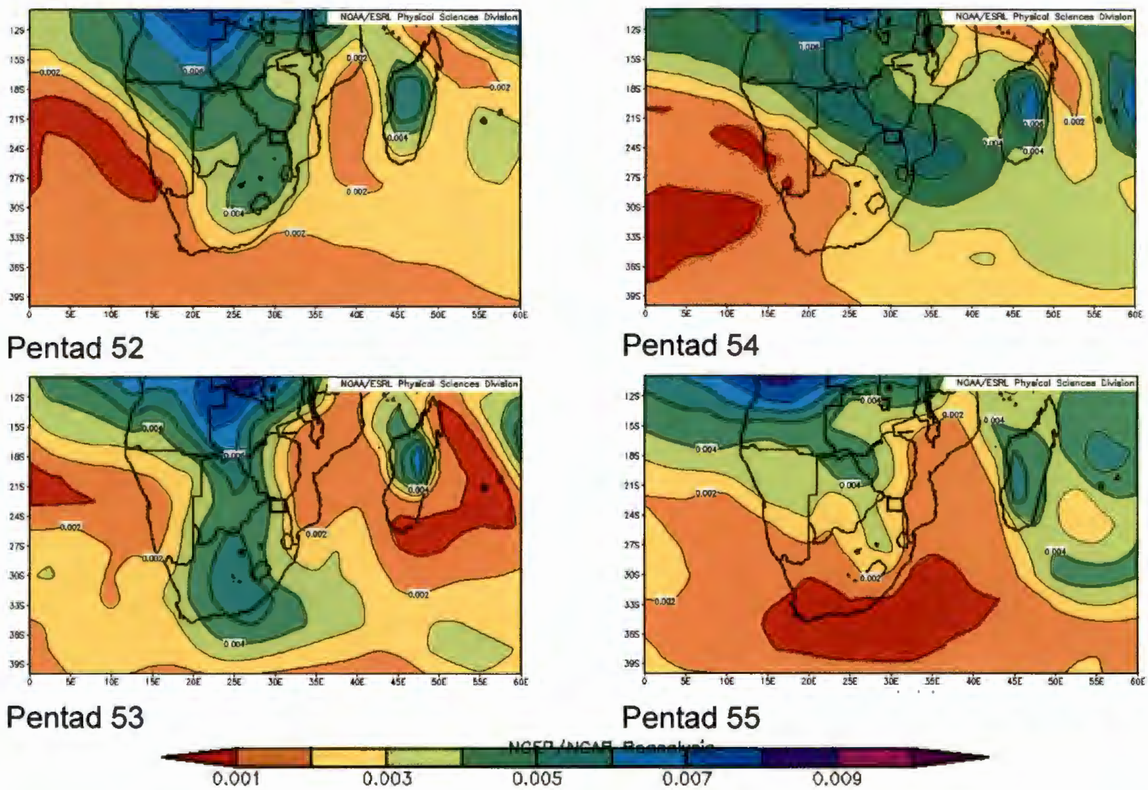

Figure 6.5: Specific humidity 20 days prior to 2001 seasonal rainfall onset. The contour intervals are 0.001 kg/kg

6.4.2 Specific Humidity - During 2001 Early Onset

From pentad 56 (Figure 6.6), which represents the rainy season onset date for the year 2001 in the humid zone, a tongue of moisture originating from the north penetrates southwards across South Africa. However, Vhembe District was under low levels of moisture with the maximum specific humidity of about 2 g/kg; and that appears to be due to a centre of dry air, which is covering over parts of Mozambique, Zimbabwe and the Indian Ocean. By pentad 57, the moisture has increased slightly over the northeastern interior of South Africa (~ 4 g/kg).

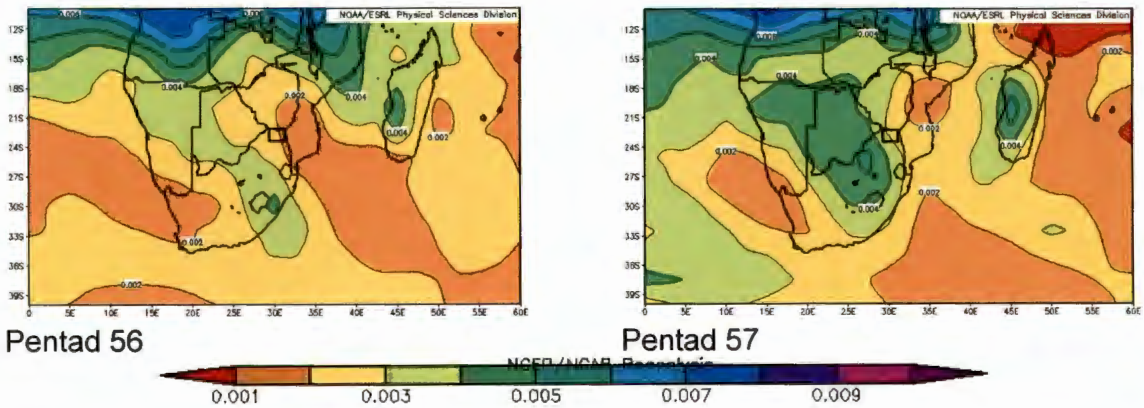

Figure 6.6: Specific humidity during 2001 seasonal rainfall onset. The contour intervals are 0.001 kg/kg

6.4.3 Specific Humidity - 20 Days Prior 2006 Late Onset

The evolution of specific humidity 20 days prior to the 2006 seasonal rainfall onset, which represent the late onset season of 2000 – 09 decade, is presented in Figure 6.7. During pentad 67 (27th November to 1st of December), the maximum concentration of moisture was centred north of the 12°S latitude and it showed a southward oscillation. The southern surge of maximum moisture reached northeastern South Africa by pentad 68 with a magnitude of 7.5 g/kg of moisture. The situation was relaxed in the two following pentads, and the atmosphere over Vhembe District revealed low moisture of 2.5 g/kg during pentad 70. The analysis indicates that 20 days prior to the rainfall onset the maximum specific humidity values were mostly concentrated in central Africa, while the surrounding maritime (Indian and Atlantic oceans) experienced relatively dry atmospheres (~ 3 g/kg).

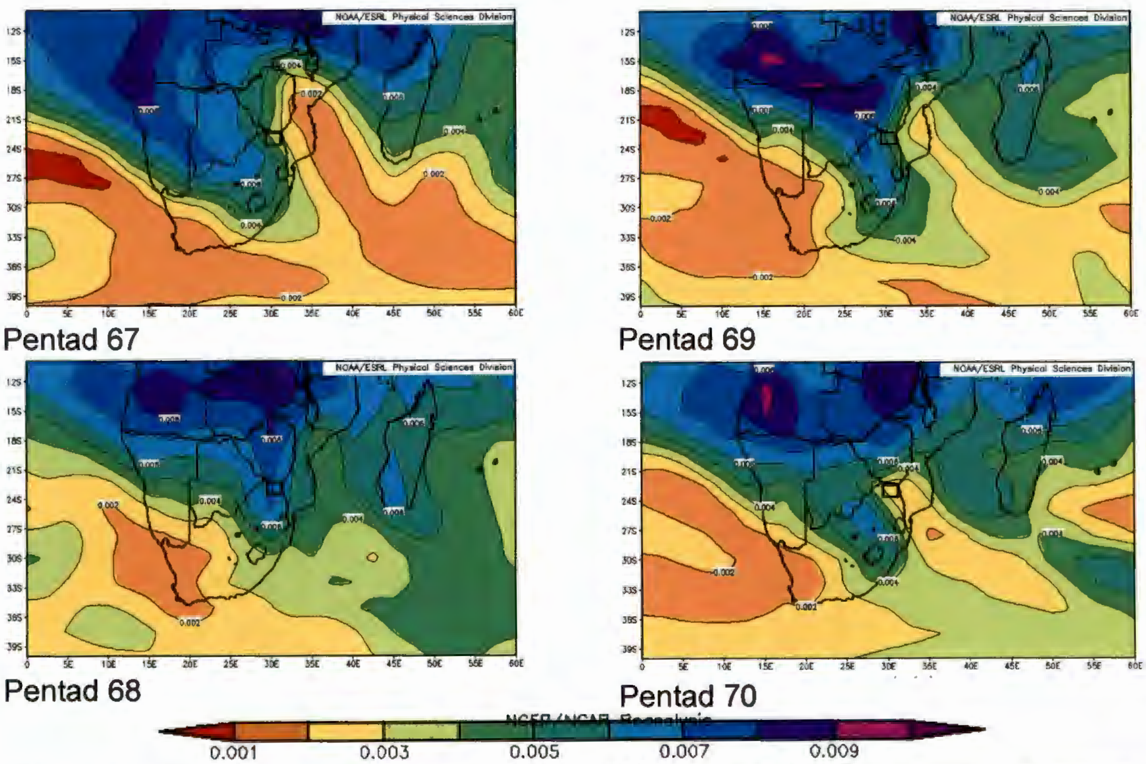

Figure 6.7: Specific humidity 20 days prior to 2006 seasonal rainfall onset. The contour intervals are 0.001 kg/kg

6.4.4 Specific Humidity - During 2006 Late Onset

The rainfall season for 2006 represents the late rainfall onset for the 2000-09 decade. The time of rainfall initiation was in pentad 71 (17th to 21st December) which is somewhat late for the seasonal rainfall in Vhembe District to start. At the beginning of the season (Figure 6.8) the moisture with maximum of 10 g/kg is centred over northeastern Namibia. It advanced further southeastward and contributed moisture to central South Africa and part of the southeast quadrant of southern Africa (mainly Limpopo Province, Mozambique and Zimbabwe). This southeastward propagation of moisture led to moisture accumulation of about 5 g/kg over Vhembe District. In the following pentad, a broad band of moisture from central Africa spread southward and covered the whole of eastern southern Africa. Most areas, including Vhembe District, experienced increasing specific humidity to the tune of 7 g/kg by pentad 72. In both cases (pentads 71 and 72), the dry air is confined to the oceans.

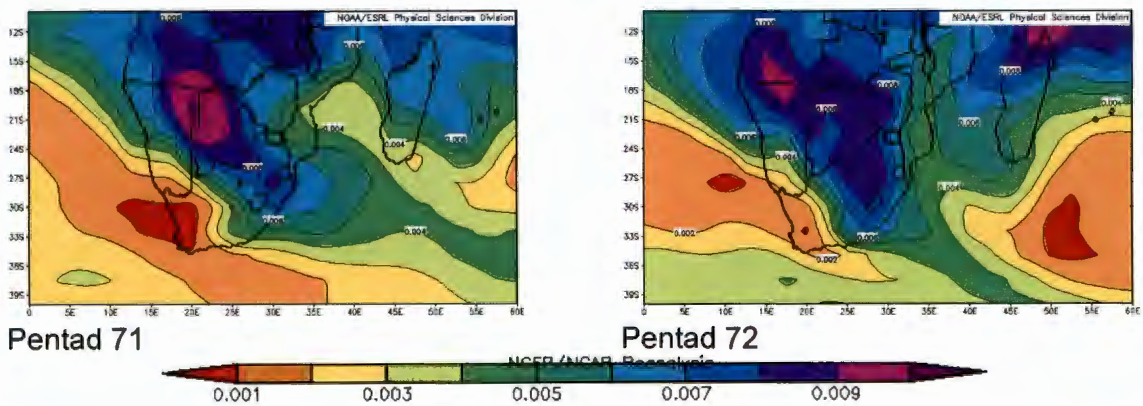

Figure 6.8: Specific humidity during 2006 seasonal rainfall onset. The contour intervals are 0.001 kg/kg

6.5 Semi-Arid Zone Specific Humidity Analysis

This section presents the specific humidity analysis for the earliest and latest rainfall season onset in the decades 1980-89 and 2000-09. 1984 and 1981 are the earliest and latest onset for the1980-89 decade; while 2001 and 2007 are the earliest and late onset for the 2000-09 decade.

6.5.1 Specific Humidity - 20 Days Prior to 1984 Early Onset

Figure 6.11 shows the patterns of the specific humidity 20 days prior to the 1984 rainfall season onset, which is the early onset season in the 1980-89 decade. High moisture presence (8 g/kg) is located over Angola and Zambia during pentad 57. At the same time, the southeast Atlantic Ocean, the southern tip of South Africa and east of Madagascar observed relatively dry atmosphere (1 g/kg). The subsequent pentad (12th to 16th of October 1984) shows an increase in the levels of specific humidity that covers up to northeastern parts of the South Africa with humidity magnitude ranging from 6 g/kg to 6.5 g/kg. A relative dryness (> 3 g/kg) prevailed across Vhembe District in the two pentads prior to the onset date. Meanwhile, the southwest Indian Ocean and southeast Atlantic Ocean maintained a parched atmosphere.

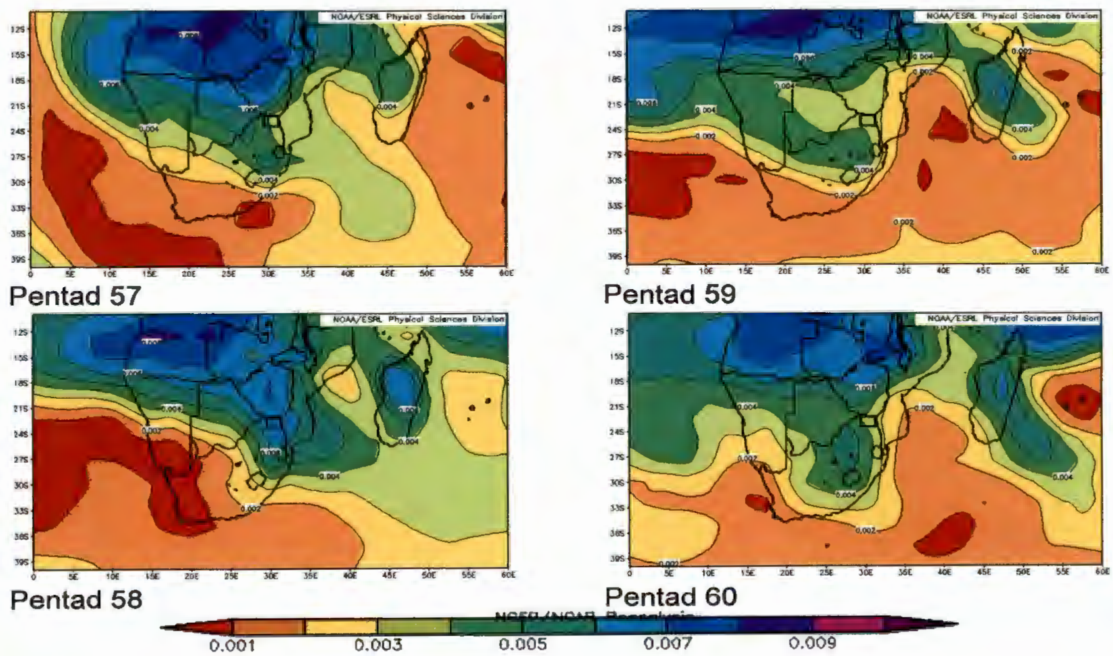

Figure 6.11: Specific humidity 20 days prior to 1984 seasonal rainfall onset. The contour intervals are 0.001 kg/kg

6.5.2 Specific Humidity - During 1984 Early Onset

Rainfall season onset date for 1984 commenced in pentad 61 (27th to 31st October). The onset pentad is characterised by extension of southeastward water vapour from its concentration in the tropics (Figure 6.12). Specific humidity remained high (> 5.5 g/kg) over the northeastern parts of South Africa into the following pentad. The persistence of high humidity for ten days consecutively illustrates the availability of moisture for seasonal rainfall onset.

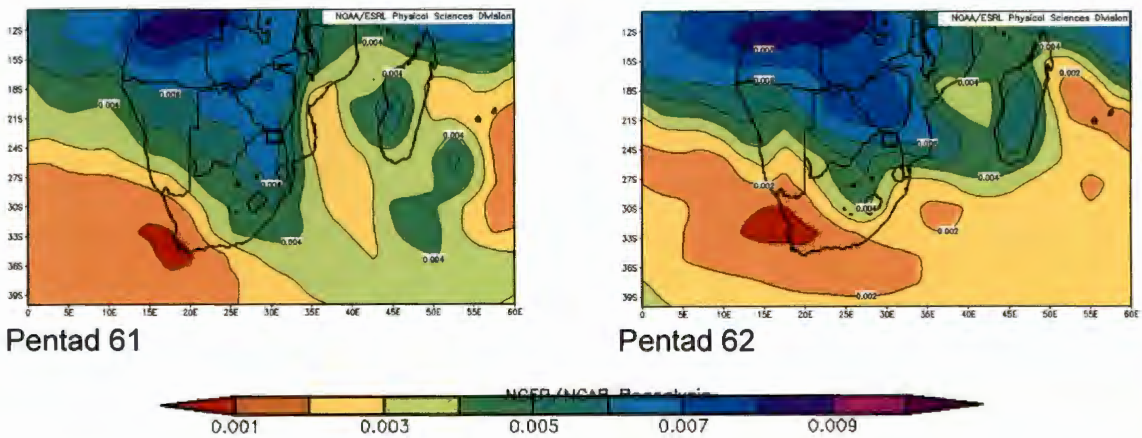

Figure 6.12: Specific humidity during 1984 seasonal rainfall onset. The contour intervals are 0.001 kg/kg

6.5.3 Specific Humidity - 20 Days Prior to 1981 Late Onset

Figure 6.13 below presents the evolution of specific humidity composites 20 days prior to the 1981 late onset season during the 1980-89 decade. In pentad 70 a tongue of moisture emanated from tropical Africa bringing a large amount of moisture into the northern part of South Africa. However, during this time Vhembe District remained under a relatively low amount of moisture (~ 3g/kg). In the following pentad, the moisture continue to spread southeasterly covering northeastern tip of South Africa which increased the specific humidity over the study area to about 5 g/kg and 6 g/kg a pentad later (five days prior to the onset date).

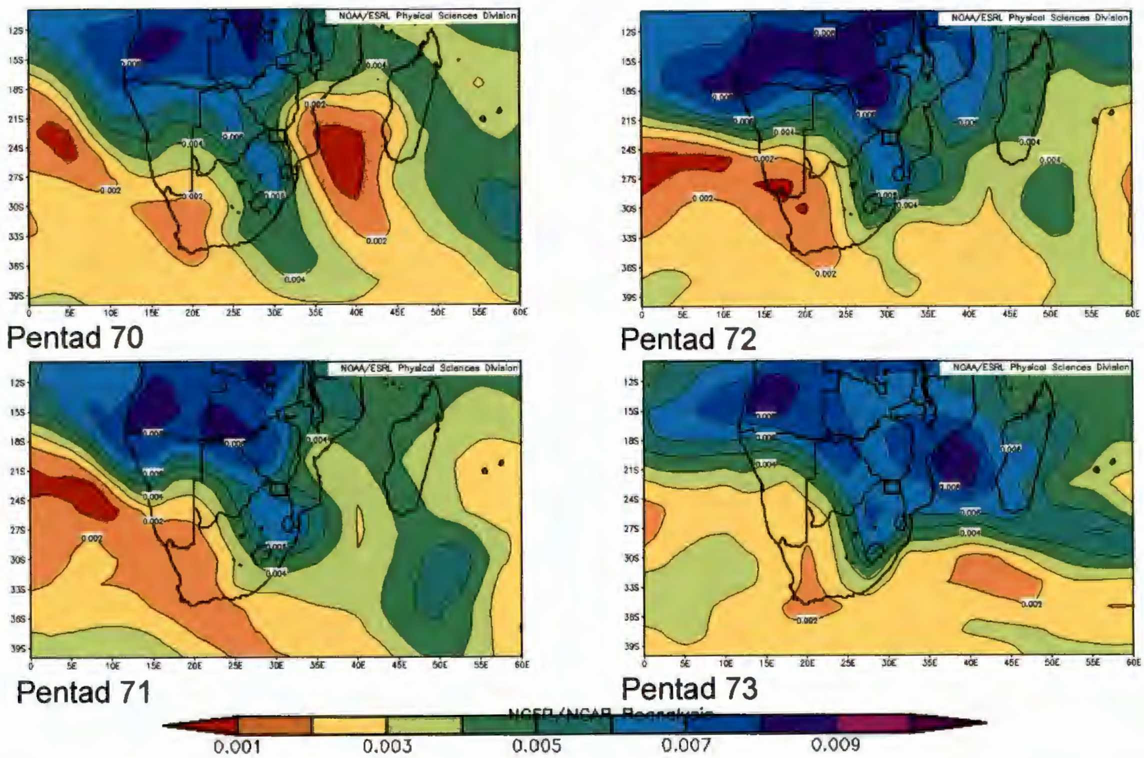

Figure 6.13: Specific humidity 20 days prior to 1981 seasonal rainfall onset. The contour intervals are 0.001 kg/kg

6.5.4 Specific Humidity - During 1981 Late Onset

The seasonal rainfall of the year 2008, which represents a late onset season during 1980 – 89 decade (Figure 6.14), started in the pentad 1 of the following year (1st to 5th January). On the onset pentad, the transport of moisture from the tropical Africa southeasterly into Botswana, Zimbabwe, South Africa, Mozambique, Madagascar and Indian Ocean is evident. The incursion of moisture into South Africa led to an accumulation of about 5.5 g/kg mean specific humidity over the northeastern area. During this time, the Atlantic Ocean maintained dry atmosphere. Five days after the onset date, a reduction in the inflow of moisture over southern Africa is visible with a decrease in the levels of specific humidity over northeastern South Africa (Vhembe District).

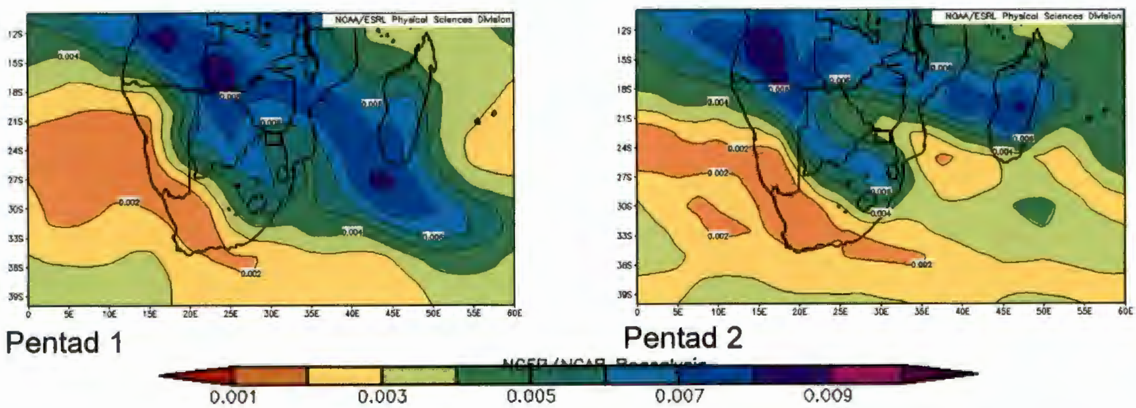

Pentad 1

Pentad 2

Figure 6.14: Specific humidity during 1981 seasonal rainfall onset. The contour intervals are 0.001 kg/kg

6.5.5 Specific Humidity - 20 Days Prior 2001 Early Onset

Figure 6.15 shows the evolution of specific humidity 20 days prior to the 2001 seasonal rainfall onset date (pentad 55, 56, 57 and 58). Pentad 55 shows a rather dry atmosphere over South Africa and the adjacent oceans in general. In the preceding pentad, an extensive area of moist air from the tropics flowed southwards across South Africa moistening the central parts of the country while the Northeast and south Mozambique remained under dry atmosphere. A similar pattern holds during pentad 57. At pentad 58, the inflow of moisture from the tropics strengthened, resulting in the build-up of moisture of about 4 g/kg over the northeastern parts of South Africa. During that time, moisture built up over Madagascar to a central value of > 6g/kg.

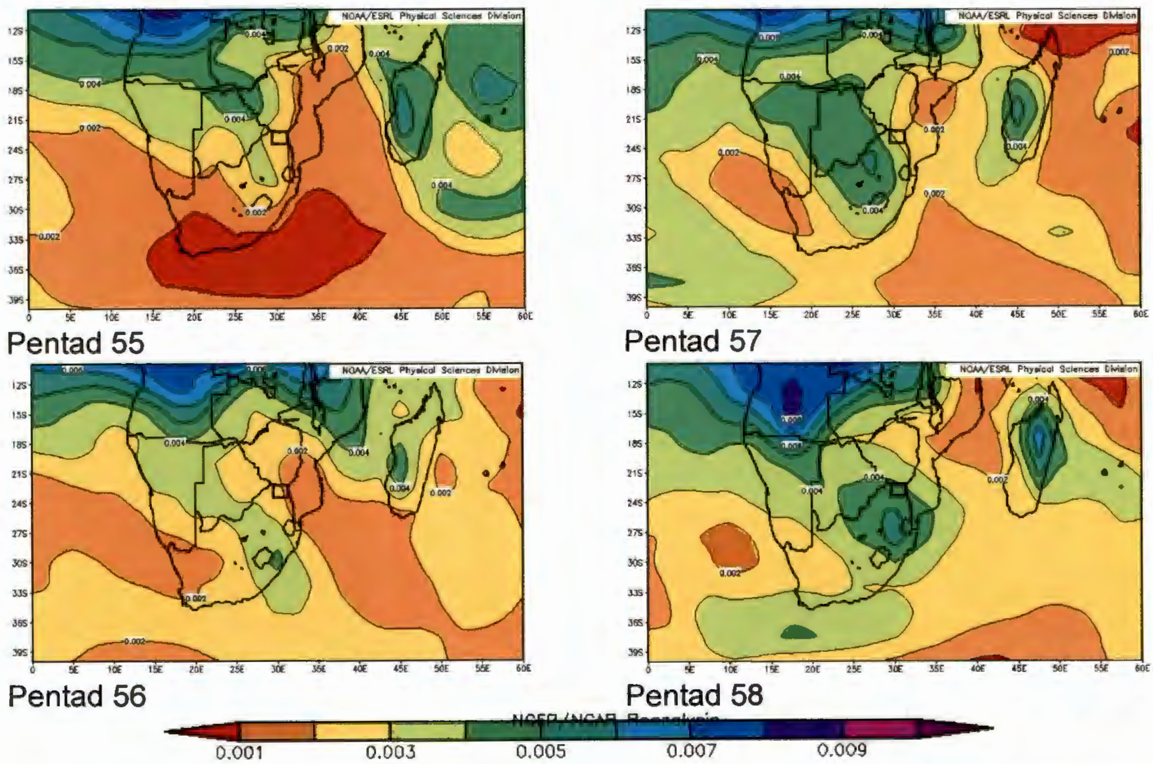

Figure 6.15: Specific humidity 20 days prior to 2001 seasonal rainfall onset. The contour intervals are 0.001 kg/kg

6.5.6 Specific Humidity - During 2001 Early Onset

Figure 5.16 illustrates the sequence for pentad 59 and 60 for early onset of the 2001 rainfall season. The moisture maximum is over the border of Zambia, Democratic Republic of Congo (DRC) and Angola. From there, it spread southwards to South Africa and extends well into the Mozambique Channel during pentad 59. By pentad 60, moisture increase strengthened over southern Africa and over Madagascar, while the Mozambique Channel was parched. Specific humidity level over northeastern South Africa (Vhembe District) was ranging between 5 g/kg and 6 g/kg.

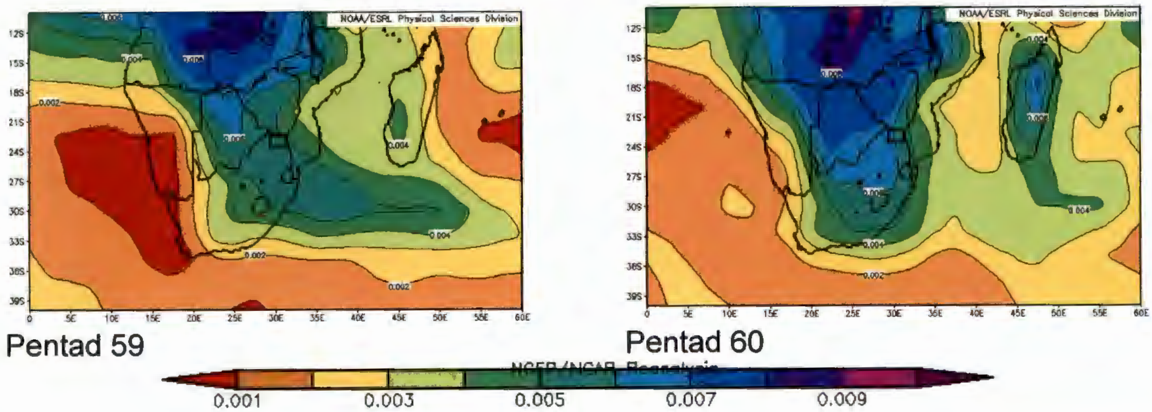

Figure 6.16: Specific humidity during 2001 seasonal rainfall onset. The contour intervals are 0.001 kg/kg

6.5.7 Specific Humidity - 20 Days Prior 2007 Late Onset

The 2007 rainfall season started later in the year relative to the other rainfall seasons in 2000-09 decade within the semi-arid zone of Vhembe. Figure 6.17 represents the evolution of specific humidity 20 days prior to the rainfall season onset. In the figure, the northeastern parts of South Africa and some parts of Indian Ocean experienced a substantial amount of moisture emanating from the tropics with specific humidity values of about 8 g/kg over Vhembe District. A slight decrease in moisture to about 6 g/kg and 7 g/kg over the study area is visible in pentad 67 with the centre of high levels of moisture located in Angola and Congo. From pentad 68, the inflow of moisture from the tropics spread further southeast, moistening the northern parts of South Africa, Zimbabwe and Mozambique. A pentad before the onset date shows an intensive southwards advance of moisture with its centre located over Zimbabwe, resulting in specific humidity values over Vhembe District ranging between 7.5 g/kg and 8 g/kg.

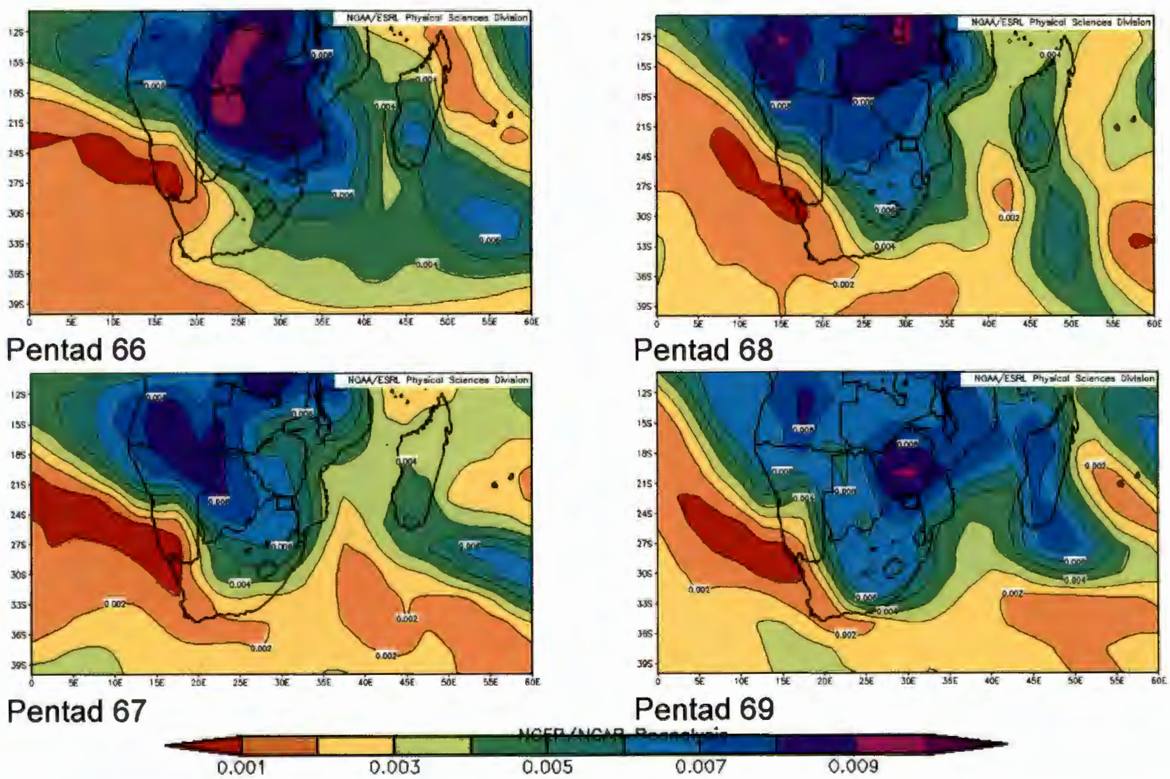

Figure 6.17: Specific humidity 20 days prior to 2007 seasonal rainfall onset. The contour intervals are 0.001 kg/kg

6.5.8 Specific Humidity - During 2007 Late Onset

Pentad 69 maintained the southward moisture flow that emanated from tropical Africa (Figure 6.18). In the meantime, a centre of dry air located over the western Indian Ocean appears to be drying Mozambique and the eastern most part of South Africa leading to a slight decrease in specific humidity levels to about 6 g/kg and 7 g/kg over the study area. In the following pentad, the intensification of the centre of high levels of moisture located in Zimbabwe spread moisture towards the northeastern part of South Africa and Mozambique.

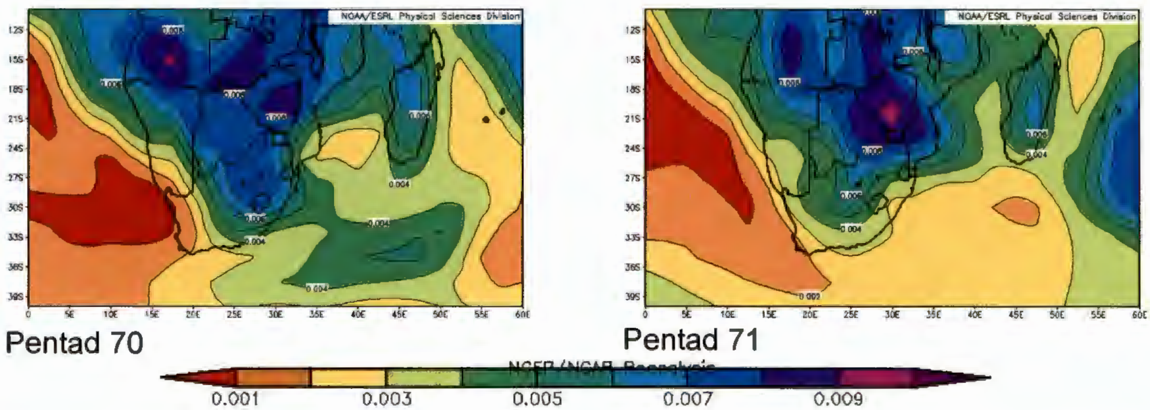

Figure 6.18: Specific humidity during 2007 seasonal rainfall onset. The contour intervals are 0.001 kg/kg

6.7 Atmospheric Moisture Flux

6.7.1 Introduction

Moisture in the atmosphere plays a vital role in the development of rainfall, thus, if there is no moisture or if very small amount of moisture exists in the atmosphere, rain may not form. The supply of water vapour in the atmosphere is through two main processes, namely the surface moisture flux, supplied as surface latent heat flux, and the horizontal moisture flux in the lower free atmosphere (moisture advection). For Vhembe District, which relies largely on large-scale processes for importing moisture to initiate seasonal rainfall (Kabanda, 2004), the latter is important. The large-scale moisture flux transport may be described in terms of the specific humidity and the wind vector components (Peixoto & Oort, 1983). Both of these climatic variables are interactive and play a crucial role in determining other climatic variables such as the various forms of atmospheric energy, in particular, the latent heat transport from the tropics to the mid-latitudes (Peixoto & Oort, 1992).

Atmospheric eddies transport water vapour from the tropics to the middle and high latitudes; this transport of water vapour takes place mostly in the lower troposphere where specific humidity is higher (Hartman, 2015). The magnitude of specific humidity in the lower troposphere varies spatially and temporally. Specific humidity maximum migrates inter-hemispherically as the near equatorial rising branch of Hadley circulation oscillates in response to radiative heating and the lower branch of Hadley circulation transports water vapour into the ITCZ (Peixoto & Oort, 1992). Suzuki (2011) studied the seasonal variation of the ITCZ and its characteristics over central Africa and observed that horizontal moisture flux maintains water vapour within the ITCZ and sustains the deep convection.

Given the importance of atmospheric moisture in the development of rainfall, it is vital to understand the sources and pathways of moisture in order to monitor the progression and arrival of seasonal rains (seasonal rainfall onset). This section focuses on the evolution of moisture prior to and during the seasonal rainfall onset for humid and semi-arid zones in Vhembe District.

6.7.2 Moisture Flux Analysis

This study will analyse moisture flux in conforming to the seasonal rainfall onset dates determined in Chapter 4. Moisture flux (Q) is the flux of volume of water. Q is the advection of moisture through a deep tropospheric layer by horizontal wind and it is obtained through vertical integration. The transport and distribution of moisture in the atmosphere is mostly through the large-scale circulation winds according to Newell et al. (1972) and Chen (1985). The bulk of the horizontal transfer of water vapour takes place below 500 hPa level and in this study the integration is from the surface (P_s) to 700 hPa (P_u) levels (Eq. 6.3).

$$Q = \frac{1}{g}\int_{p_u}^{p_s} qVdp$$ Eq. 6.3

where: q = specific humidity (g kg^{-1})

V = velocity at a particular level

g = acceleration due to gravity (9.81 m s^{-2})

P_s, P_u = lower and upper pressure levels which Q is being determined

The units of Q are kg m^{-1}s^{-1}.

6.8 Moisture Flux Analysis in the Humid Zone

The seasonal evolution of the lower atmospheric moisture flux over the humid and semi-arid zone in Vhembe District prior to and during the seasonal rainfall onset was evaluated for the two decades (1980–89 and 2000–09).

6.8.1 Moisture Flux - 20 Days Prior to 1986 Early Onset

Figure 6.19 summarises the evolution of lower tropospheric moisture flux fields up to 700 hPa, for 20 days (pentad 50 to 53) prior to the early onset, which occurred in the 1986 rainfall season. During pentad 50, the moisture flux over southern Africa north of 30°S and east of 20°E is advected westwards from the Indian Ocean (southeasterlies) because of an established Mascarene anticyclone cell over Madagascar. Generally, the moisture flows over southern Africa for the following pentads (51, 52 and 53) are anticyclonic with a curvature over the eastern Atlantic Ocean. Ahead of the curvature, a flow from the southeast Atlantic Ocean converges with a flow from the tropics creating a weak moisture flux over southern Africa of the order 100 kg $m^{-1}s^{-1}$ throughout the 20 days. The significant development however, is the slight increase of moisture flux toward central southern Africa while Vhembe District and the south of Zimbabwe maintain low moisture.

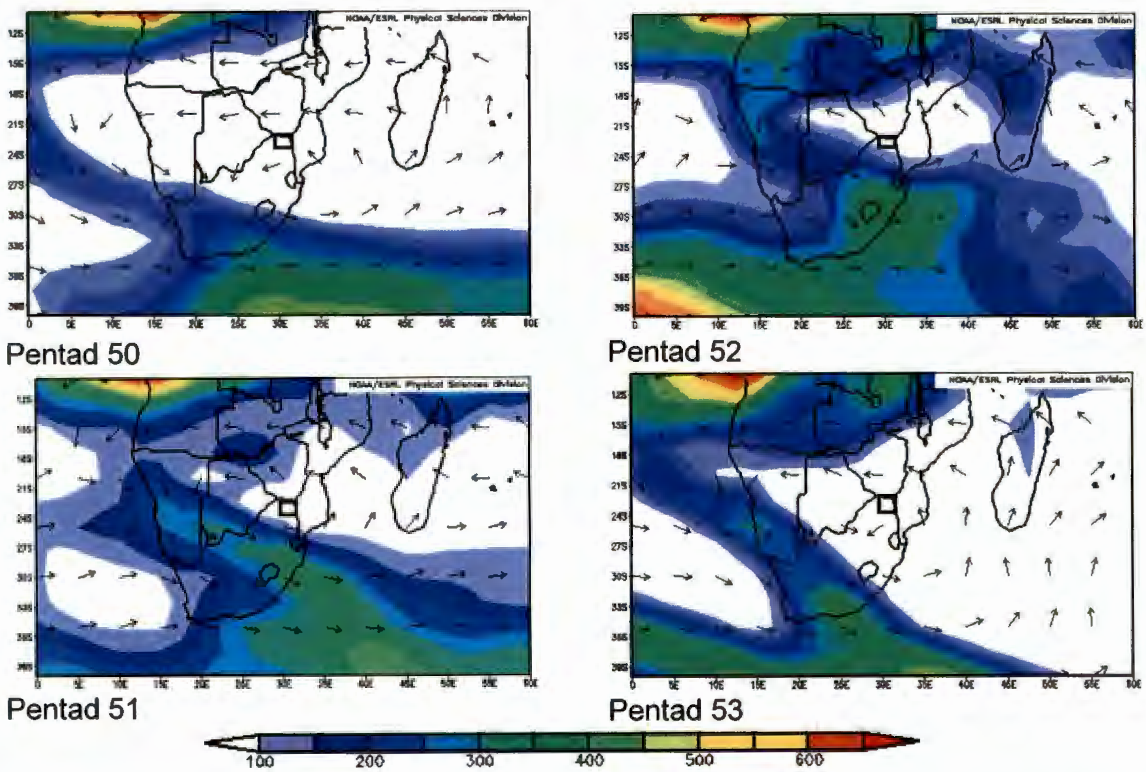

Figure 6.19: Moisture flux (kg $m^{-1}s^{-1}$) analysis for 20 days prior to 1986 seasonal rainfall onset

6.8.2 Moisture Flux - During 1986 Early Onset

The early onset of seasonal rainfall (1986) started in pentad 54 (September 23 – 27), by which time centres of maximum moisture (Zambia and Angola) have deepened resulting in moisture advection over southern Africa (Figure 6.20). At pentad 55, an anticyclonic moisture transport with weak intensity is evident over southern Africa. The area of significant water vapour transport is over Zambia and Angola, which implies that most of the atmospheric water vapour is concentrated in tropical southern Africa. In the southwest Indian Ocean (SWIO) the curvature of the anticyclone over southern Africa is responsible for moisture advection to the subcontinent. Although it is a weaker southeasterly flux from SWIO, it shows that the source of moisture is from the Indian Ocean region where the flow started weakly at ~ 100 kg $m^{-1}s^{-1}$.

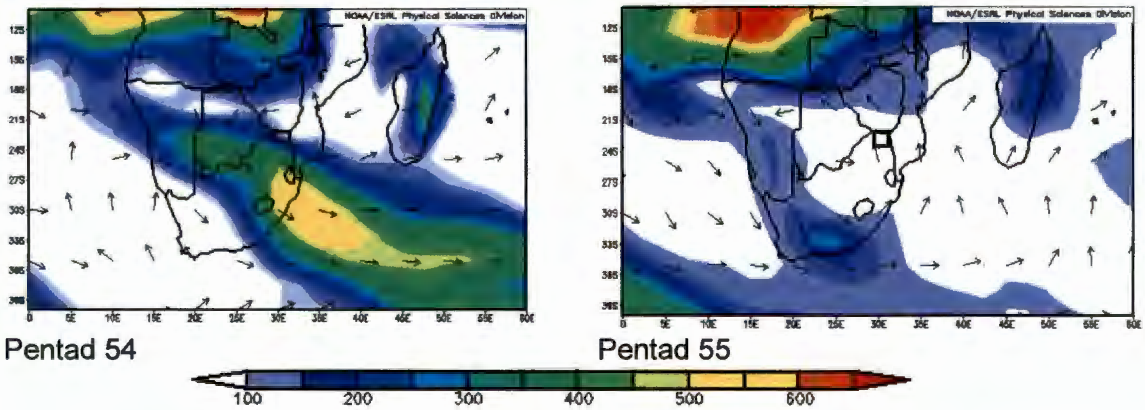

Figure 6.20: Moisture flux (kg $m^{-1}s^{-1}$) analysis for during 1986 seasonal rainfall onset

6.8.3 Moisture Flux - 20 days prior 1985 Late Onset

Figure 6.21 shows the late onset moisture flux (pentad 65 to 68). During pentad 65 (17th to 21st November) an anticyclonic cell of water vapour transport with a curvature in the SWIO and a centre near the border of South Africa and Botswana is evident over southern Africa. Flow over central southern Africa (northeastern South Africa, south Mozambique, Zimbabwe and Botswana), is dominated by southeasterly moisture transport of ≤ 200 kg $m^{-1}s^{-1}$. Five days later (pentad 66), an anticyclonic moisture configuration is centred over the Namibia/Botswana border (22°S, 20°E), and a resulting vector transport of moisture over Limpopo Province, South of Botswana and South Mozambique is dominated by a southwesterly which curves to southeasterly over Zimbabwe. These flow patterns are usually associated with dry air from the Kalahari and Namib Deserts and tend to deplete moisture over South Africa.

Of particular interest during pentad 67 is the observed southerly moisture flow over Limpopo and the divergent flow with axis over south Mozambique and Zimbabwe along 30°S, 21°E – 24°E, where the left (westward) arm feeds central Africa while the right (eastward) arm feed the moisture accumulation in the Indian Ocean through Madagascar. The westward arm moisture flow recurves westward through Zambia and Angola to the Atlantic Ocean, while the eastward arm recurves eastward to the Indian Ocean through central Mozambique. Generally, the moisture flux is persistently low over the study area throughout, even 5 days prior to the seasonal rainfall onset.

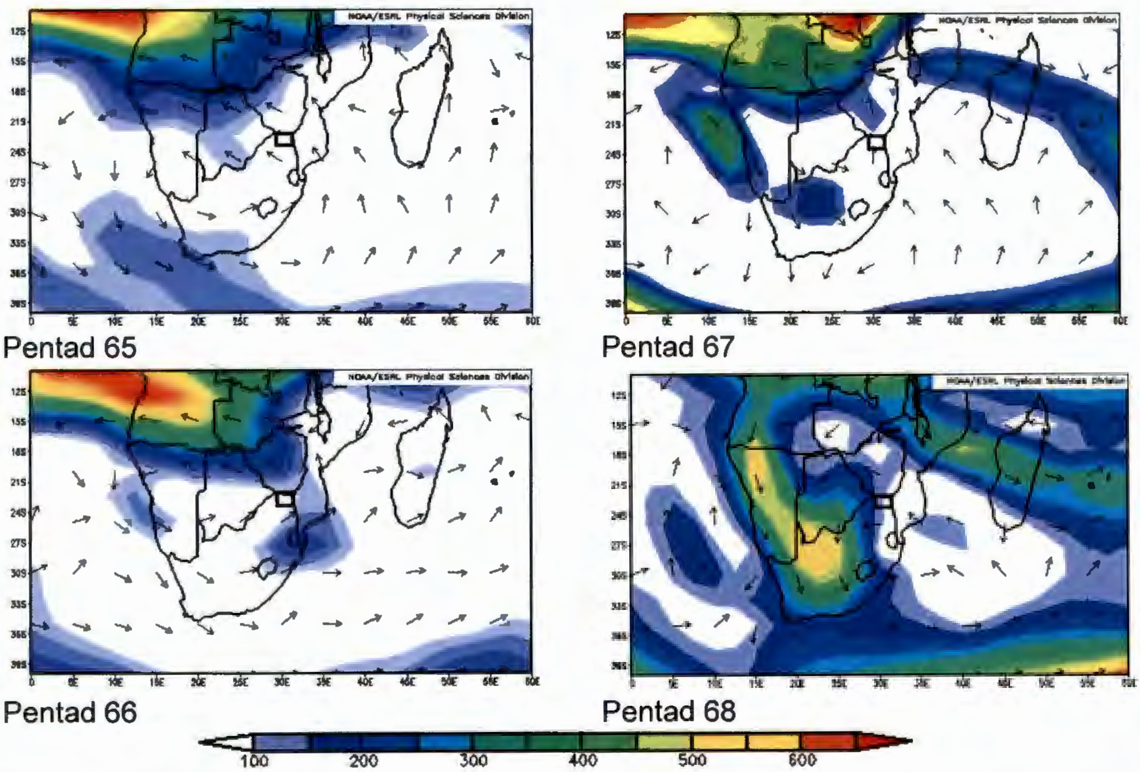

Figure 6.21: Moisture flux (kg $m^{-1}s^{-1}$) analysis for 20 days prior 1985 seasonal rainfall onset

6.8.4 Moisture Flux - During 1985 Late Onset

Seasonal rainfall started in Pentad 69 (Figure 6.22). Areas of higher moisture flux (> 650 kg $m^{-1}s^{-1}$) are confined north of 21°S and west of 30°E into the Atlantic Ocean. At the same time a weak flux convergence is observed over the northeast of South Africa and south of Mozambique. This situation is conducive to low-level uplifting and subsequent rainfall occurrence. Five days later (pentad 70), an easterly flow along 15°S through Madagascar advected moisture into Mozambique and northeast South Africa as north easterly. Meanwhile, moisture intensified in southwest Angola and the Atlantic Ocean. In the meantime, the moisture flowing into Limpopo province in South Africa is from the Indian Ocean, though relatively dry as compared with Zambia and Angola. In the south of the sub-continent, there is a tongue of eastward moisture flux transport, through Lesotho to the SWIO. Generally, the subsequent pentads (not shown) reveal a persistent anticyclonic moisture flow over southern Africa with a curvature in the south of Mozambique that is responsible for directing the moisture into northeast South Africa (Vhembe District) thus indicating the late seasonal rainfall sustenance.

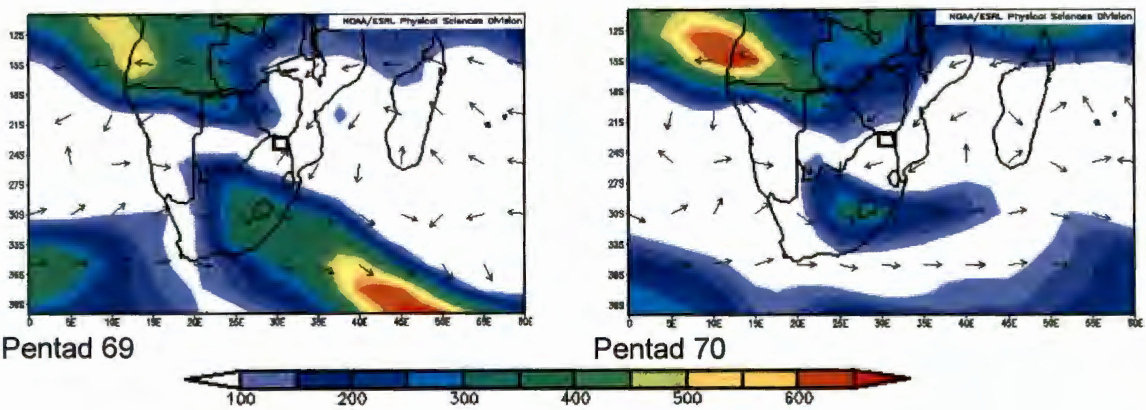

Figure 6.22: Moisture flux (kg $m^{-1}s^{-1}$) analysis during 1985 seasonal rainfall onset

6.8.5 Moisture Flux - 20 Days Prior to 2001 Early Onset

Figure 6.23 represents the evolution of atmospheric moisture flux 20 days prior to the 2001 seasonal rainfall onset, which represents the early onset for the 2000–09 decade. From pentad 52, the northerly flow of moisture from the tropics advances into most parts of South Africa. The anticyclonic moisture transport centred over southern Mozambique propagates the moisture flow that accounts for the northerly flow into the study area. A centre of high moisture flux (≤ 400 kg $m^{-1}s^{-1}$) is over the northern part of South Africa. In pentad 53 (18th to 22nd September), a northwesterly flow of moisture into South Africa created an influx of moisture that intensified moisture sink to ~ 600 kg $m^{-1}s^{-1}$. Westerly flow from the Atlantic Ocean coupled with northwesterly moisture flux from the tropics increased moisture over northeastern South Africa that extended to the Mozambique Channel in the Indian Ocean during pentad 54. Generally, the circulation pattern of moisture flux during the 20 days prior to the rainfall season of 2001 favoured accumulation of moisture in the whole of South Africa. In addition, the moisture flux patterns indicate that the transport of moisture flow from the tropics north of 24°S is the primary source for rainfall over northeastern South Africa (including Vhembe District).

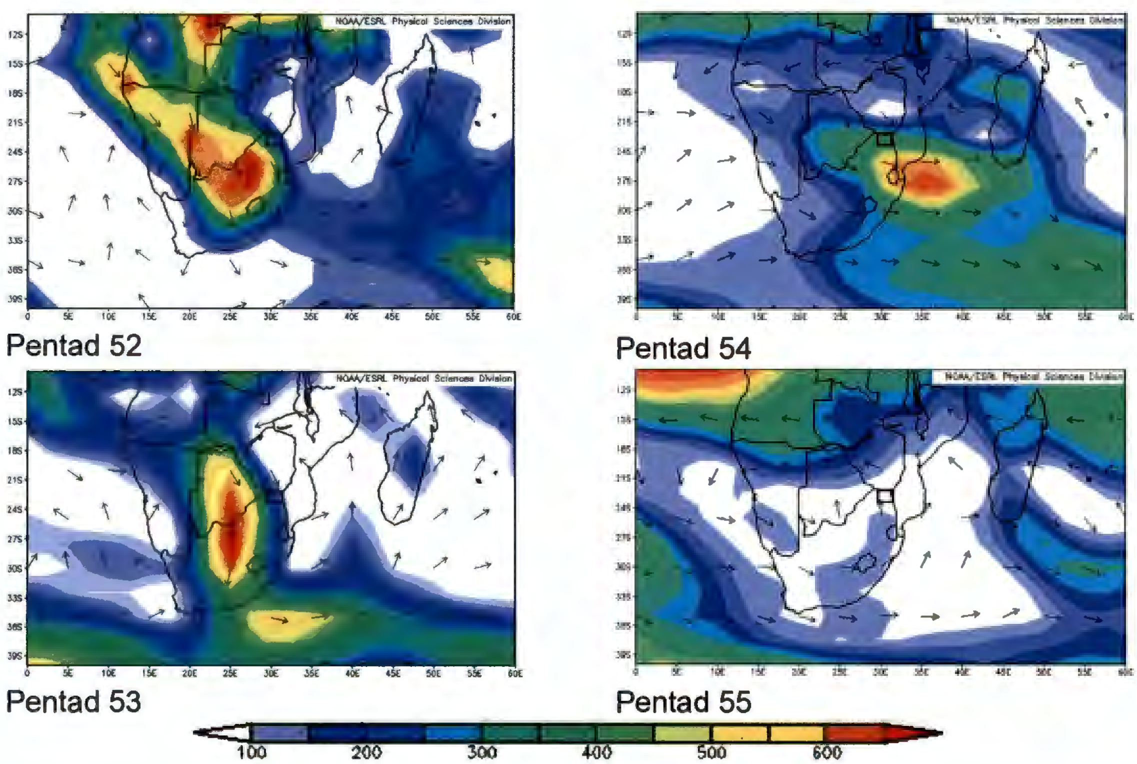

Figure 6.23: Moisture flux (kg $m^{-1}s^{-1}$) analysis 20 days prior to 2001 seasonal rainfall onset

6.8.6 Moisture Flux - During 2001 Early Onset

The onset starts around pentad 56 (3rd to 7th October); a weak signal is observed over northeastern South Africa and south Mozambique (Figure 6.24 – Pentad 56) resulting in moisture advection from the Indian Ocean. The Indian Ocean anticyclone centred between 40 and 55° E at 24° S facilitates the advection. West of 35°E over the whole of southern Africa, another anticyclone moisture circulation exists and contributes to the moisture flux confluence over northeastern South Africa. For the duration of pentad 57, the southwest Indian Ocean (SWIO) supplied moisture over Vhembe District).

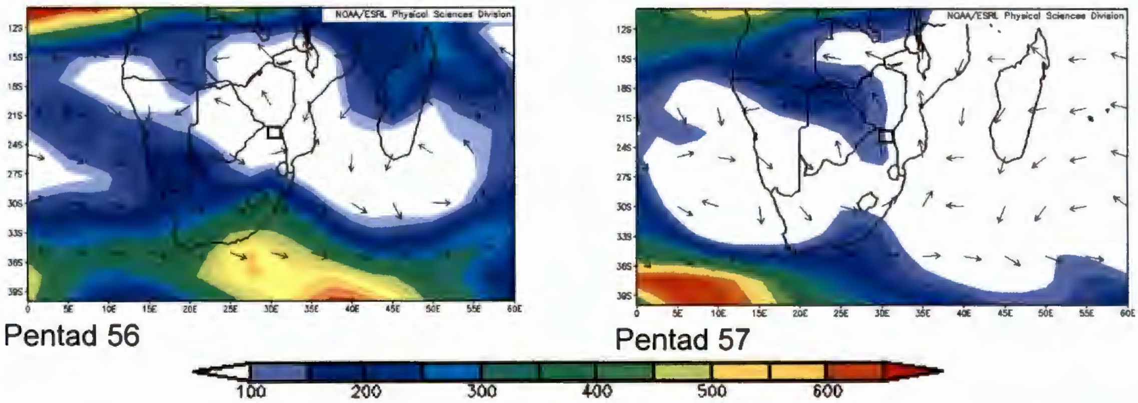

Figure 6.24: Moisture flux (kg $m^{-1}s^{-1}$) analysis during 2001 seasonal rainfall onset

6.8.7 Moisture Flux - 20 Days Prior to 2006 Late Onset

Figure 6.25 displays the analysis of moisture flux evolution prior to the 2006 seasonal rainfall onset, which is a late onset in the 2000 – 09 decade. An anticyclonic circulation of moisture between 15 and 35°E centred over Botswana intensified moisture flow (≥ 150 kg $m^{-1}s^{-1}$) over southern Africa providing a southerly flow into northeastern South Africa during pentad 67. The moisture increased to ~ 250 kg $m^{-1}s^{-1}$ in the following 15 days (27th November to 11th December). However, this is not a substantial amount of moisture, due to the source being the south West Atlantic Ocean, which is cold, and also a passage through Kalahari Desert which tends to diminish the moisture. Generally, the moisture flux over southern Africa during the 20 days prior to the onset of the 2006 rainfall season came from both oceans (Atlantic and Indian Ocean).

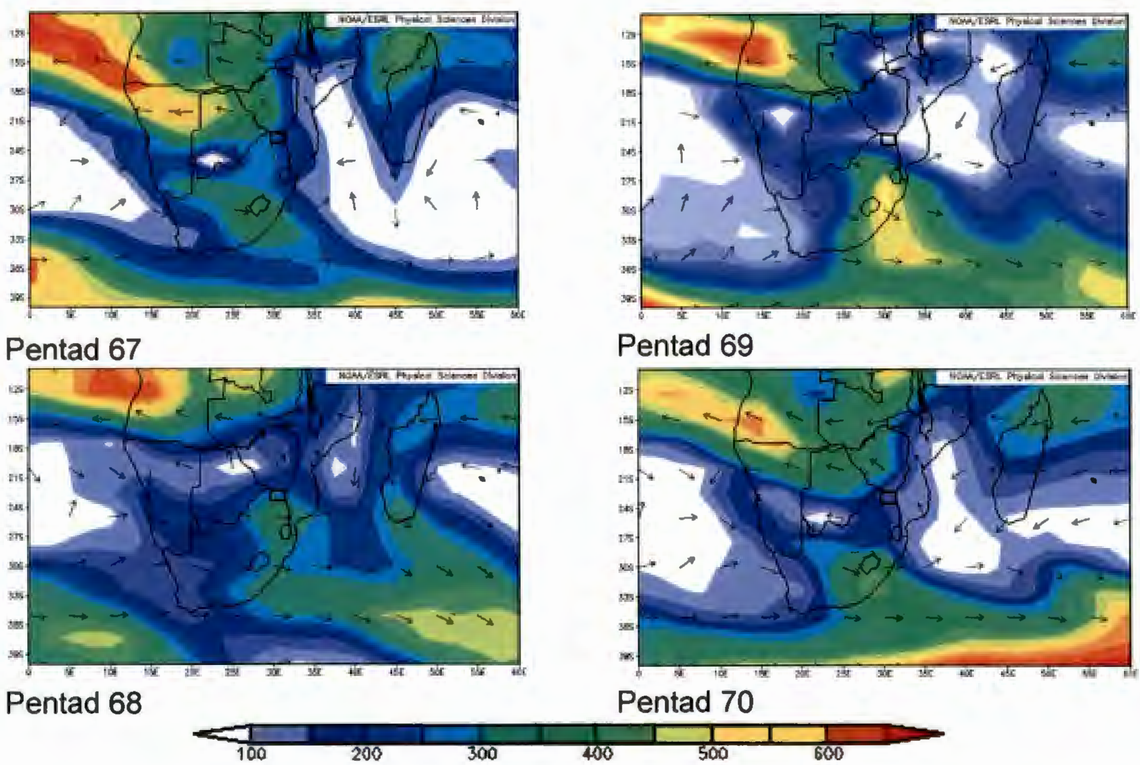

Figure 6.25: Moisture flux (kg $m^{-1}s^{-1}$) analysis 20 days prior to 2006 seasonal rainfall onset

6.8.8 Moisture Flux - During 2006 Late Onset

Figure 6.26 shows the evolution of moisture flux at rainfall season onset in 2006 (a late-onset season in the 2000 – 09 decade). The figure for onset (pentad 71) shows a southeasterly transport of water vapour bringing moisture across South Africa, with the Indian Ocean the main source of moisture. The highest moisture flux (≥ 550 kg $m^{-1}s^{-1}$) is over the southeastern part of South Africa and Lesotho border during the onset. Over northeastern South Africa, Namibia and Botswana, the levels of moisture flow are much lower (~ 100 kg $m^{-1}s^{-1}$).

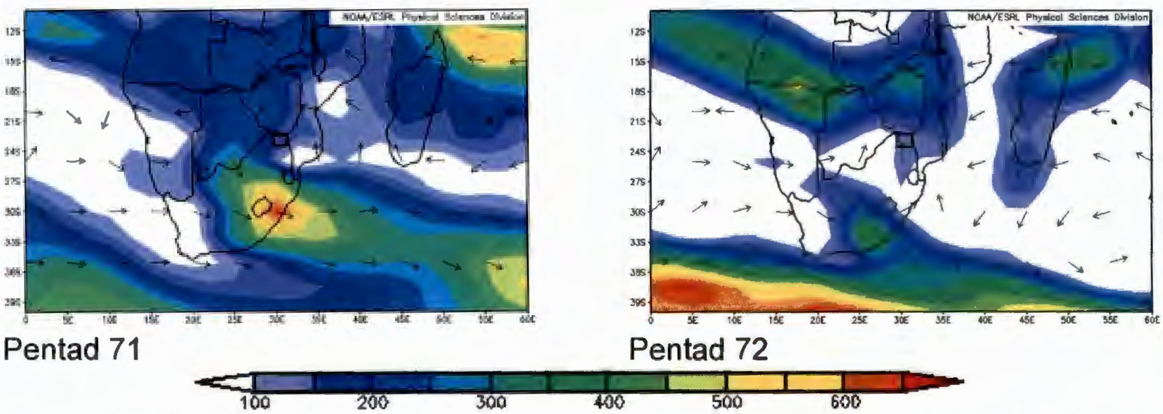

Figure 6.26: Moisture flux (kg $m^{-1}s^{-1}$) analysis during late onset (2006) seasonal rainfall onset

6.9 Moisture Flux Analysis in the Semi-arid Zone

In the semi-arid zone, the moisture flux was evaluated for the early (1984, 1986, 2001) late, (1981, 1985, 2006, 2007) and mean (1982, 2001, 2004, 2008) seasonal rainfall onset in the two decades (1980-89 and 2000-09). These years were selected based solely on their seasonal rainfall onset dates, where they appear as early, late and mean season onset. The later subsections and figures exhibit the evolution of lower tropospheric moisture flux fields up to 700 hPa within the semi-arid zone.

6.9.1 Moisture Flux - 20 Days Prior to 1984 Early Onset

Figure 6.27 presents the moisture flux circulation 20 days prior to the semi-arid early onset season in 1984. In pentad 57, an anticyclonic flow of moisture flux over southern Africa appears to be drawing moisture from tropical Africa with a southeastward tongue of moisture across central parts of South Africa and through Lesotho to the south Indian Ocean. An intense moisture convergence over Angola extends to the southeast Atlantic Ocean. An intense eastward flow of moisture flux in the south conveys moisture through Lesotho to the SWIO during pentad 58. A reduction in moisture over South Africa is evident as the westerlies from the South Atlantic Ocean strengthen. The moisture field composite five days before the onset date shows a rather dry atmosphere over the South Africa in general.

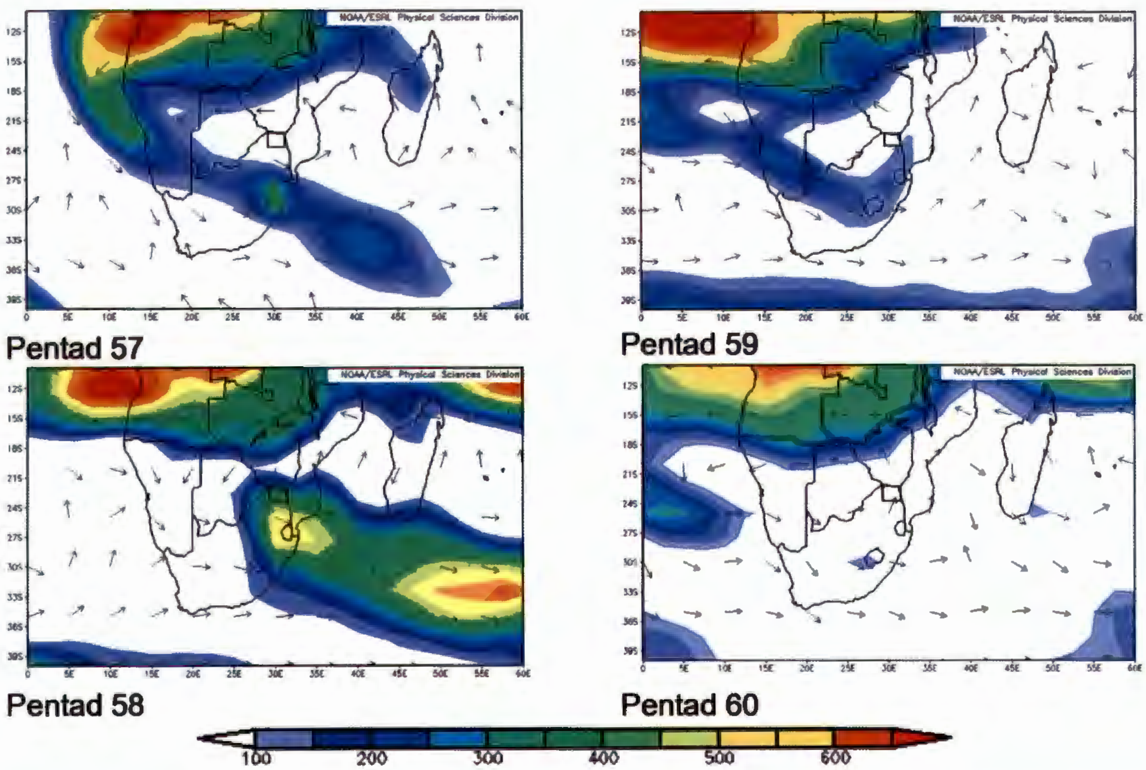

Figure 6.27: Moisture flux (kg $m^{-1}s^{-1}$) analysis 20 days prior to 1984 seasonal rainfall onset

6.9.2 Moisture Flux - During 1984 Early Onset

The first stage of onset starts around pentad 61 (27th to 31st October), as depicted in Figure 6.28, an anticyclonic circulation over southern Africa with a curvature in Namibia bringing moisture towards the southeastern parts of South Africa. The northeasterly flux from the tropics is the source of moisture toward the study area. Five days after the seasonal rainfall onset, the moisture flux is generally low over South Africa.

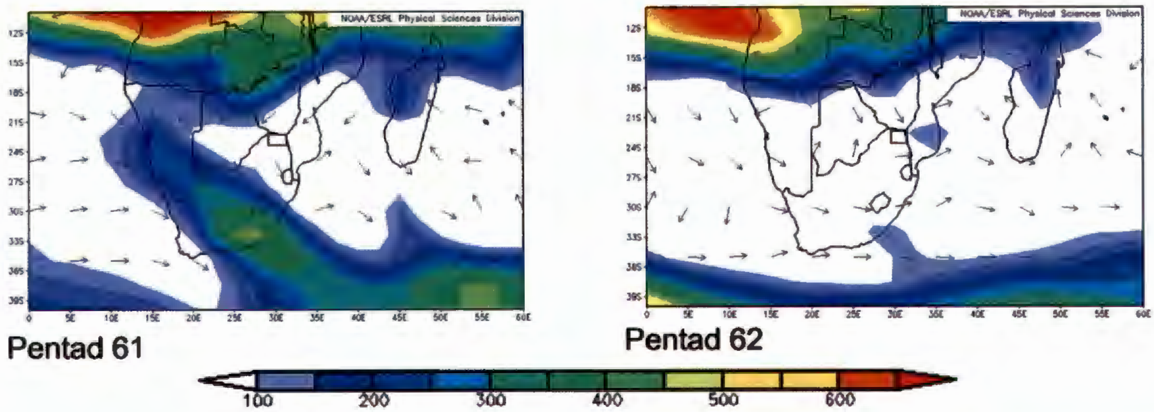

Figure 6.28: Moisture flux (kg $m^{-1}s^{-1}$) analysis during 1984 seasonal rainfall onset

6.9.3 20 Moisture Flux - Days Prior to 1981 Late Onset

As indicated in Figure 6.29, during pentad 70 (12th to 16th December) an anticyclonic transport of moisture with a curve in the south Atlantic Ocean and a centre between the borders of Namibia and Botswana is evident over southern Africa. Most regions of southern Africa experience westerly flow from the Atlantic Ocean, which does not bring much moisture. Therefore, it is not surprising that rainfall onset was delayed, because the moisture flux remained low over the northeastern part of South Africa (Vhembe District) throughout the four pentads. During pentads 72 and 73, the moisture convergence was in the Indian Ocean, which prevented the accumulation of moisture over the study area. Centres of maximum moisture convergence remained in Angola and the Atlantic Ocean throughout the 20 days prior to the rainfall onset.

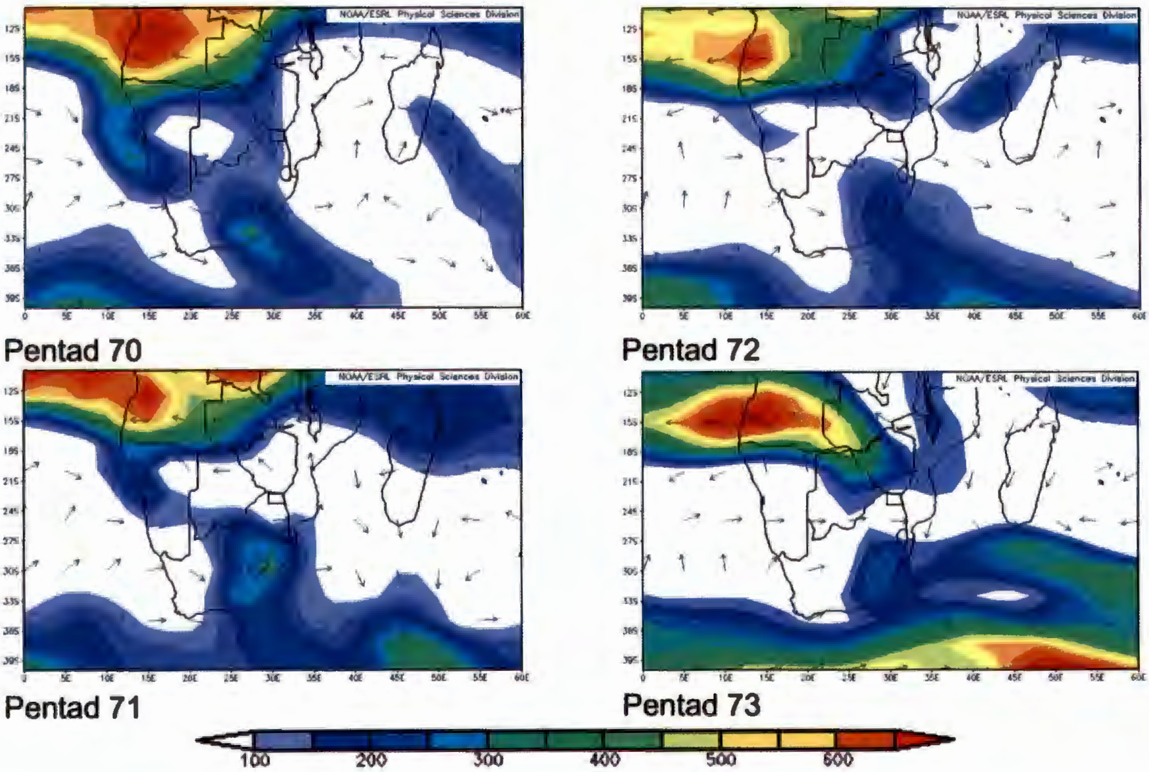

Figure 6.29: Moisture flux (kg $m^{-1}s^{-1}$) analysis 20 days prior to 1981 seasonal rainfall onset

6.9.4 Moisture Flux - During 1981 Late Onset

Figure 6.30 shows the moisture flux for this period. There is a southeasterly flow of water vapour bringing moisture over the study area, with levels of moisture flow over Vhembe of about ≥ 250 kg $m^{-1}s^{-1}$. The area with highest level of moisture (≥ 400 kg $m^{-1}s^{-1}$) is over the Atlantic Ocean.

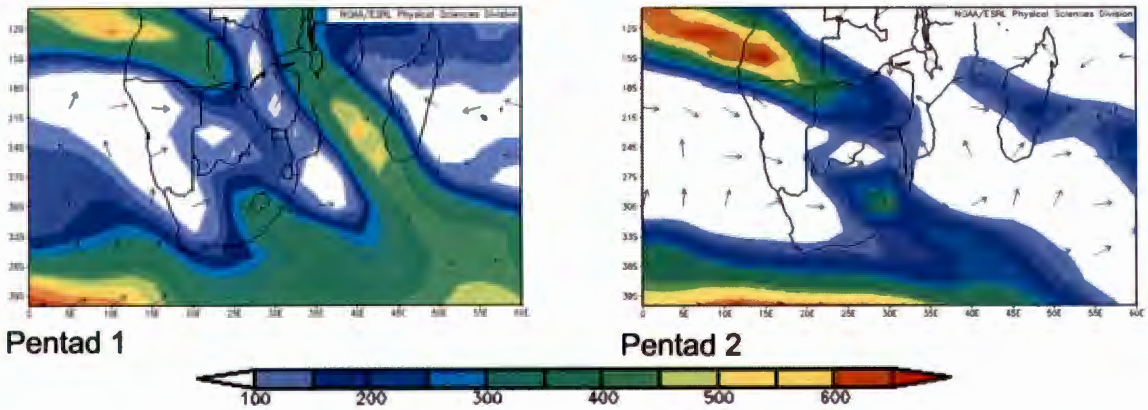

Figure 6.30: Moisture flux (kg $m^{-1}s^{-1}$) analysis during 1981 seasonal rainfall onset

6.9.5 Moisture Flux - 20 Days Prior to 2001 Early Onset

Figure 6.31 below illustrates the moisture flux 20 days prior to the 2001 seasonal rainfall onset, which represents the early onset for the semi-arid zone during 2000 – 09 decade. An anticyclonic transport of water vapour with a curvature in the South Atlantic Ocean and another one with a curvature over Madagascar are evident over southern Africa. In pentad 56, a weak flux convergence appears over northeastern South Africa and south Mozambique, resulting in moisture advection from Indian Ocean. The Indian Ocean anticyclone, centred between 40 and 55°E at 24°S, facilitates the moisture advection. The westward flow of moisture, with a curvature over Mozambique and the Indian Ocean, enhanced moisture over the study area in the five days prior to the onset. The whole of South Africa experienced high levels of moisture during pentad 58.

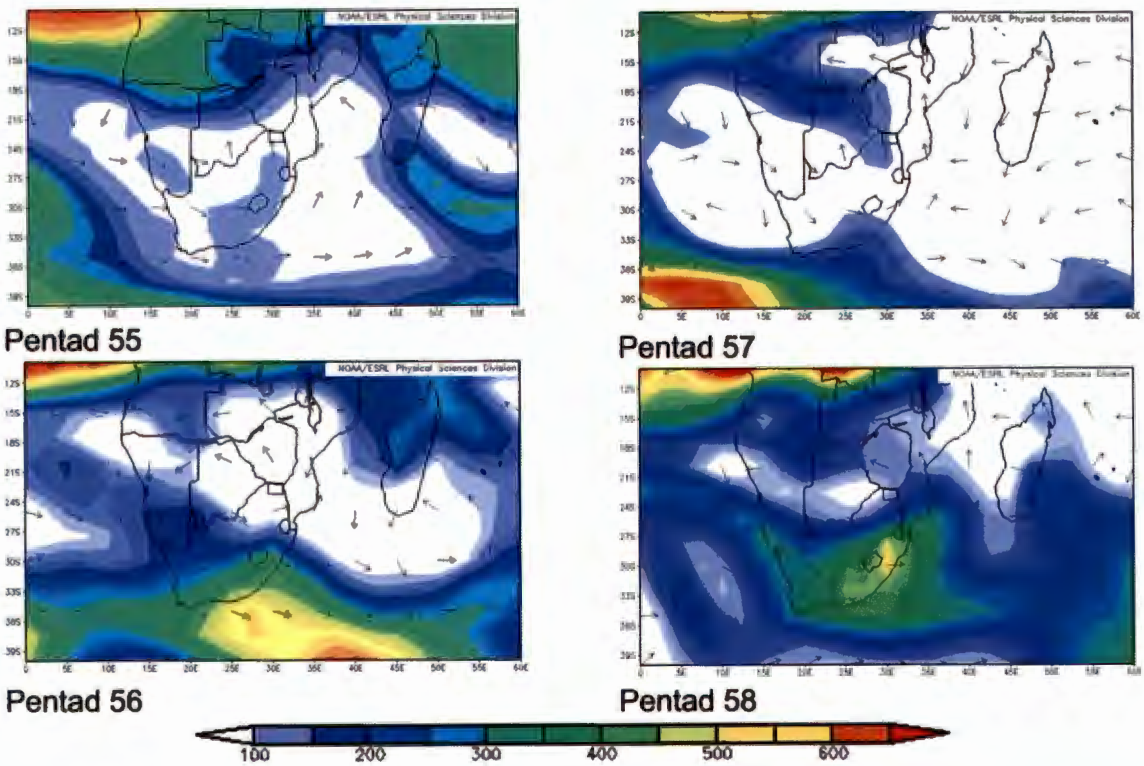

Figure 6.31: Moisture flux (kg $m^{-1}s^{-1}$) analysis 20 days prior to 2001 seasonal rainfall onset

6.9.6 Moisture Flux - During 2001 Early Onset

During the onset pentad (Figure 6.32 - pentad 59), an anticyclonic gyre over southern Africa brought in tropical and Atlantic Ocean air that led to an increase of moisture in Zambia, Botswana, Zimbabwe and a large part of South Africa. A centre of high level of moisture flux (≥ 700 kg $m^{-1}s^{-1}$) exists over the border between South Africa, Botswana and Namibia (covering the Trans Kalahari Corridor (TKC)) five days into the onset.

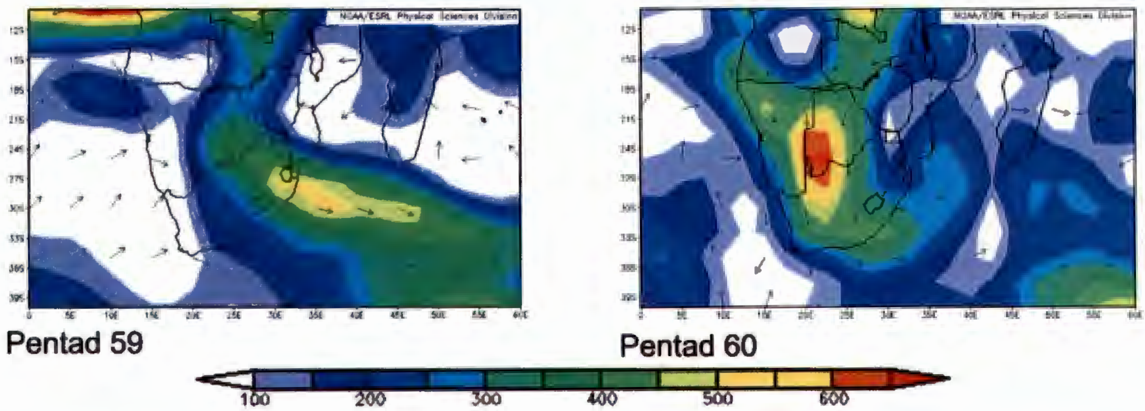

Figure 6.32: Moisture flux (kg $m^{-1}s^{-1}$) analysis during 2001 seasonal rainfall onset

6.9.7 Moisture Flux - 20 Days Prior to 2007 Late Onset

Displayed in Figure 6.33 is the development of atmospheric moisture flux 20 days prior to the 2007 seasonal rainfall onset in the semi-arid zone during 2000 – 09 decade. In pentad 66, an anticyclonic circulation of water vapour with a centre between northeastern South Africa, Zimbabwe and Mozambique brought moisture from the tropics to northern South Africa. Through pentad 69, moisture converged over Vhembe District from both an easterly flow from the Indian Ocean and northerly flow from the tropics. Generally, the circulation pattern of moisture flux 20 days prior to the rainfall season of 2007 led to a build-up of moisture in South Africa.

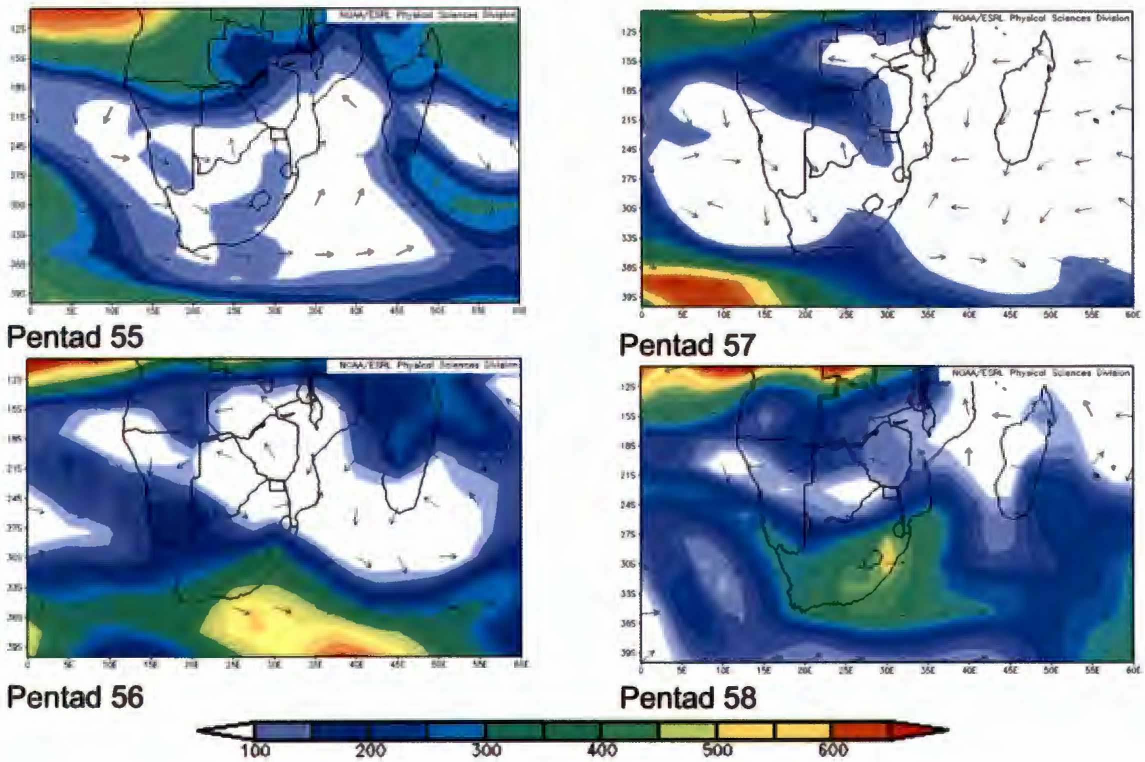

Figure 6.33: Moisture flux (kg $m^{-1}s^{-1}$) analysis 20 days prior 2007 seasonal rainfall onset

6.9.8 Moisture Flux - During 2007 Late Onset

Figure 6.34 shows the moisture flux during the 2007 late onset season of the semi-arid zone. In pentad 70, southeasterly and northerly transport of water vapour converged over northern South Africa, making both the Indian Ocean and tropical Africa the source of moisture. In addition, there is an area with a high level of moisture (≥ 500 kg $m^{-1}s^{-1}$) is over the southeastern part of South Africa, Lesotho boarder, South Indian Ocean and between Angola and Namibian boarder. During the five days after the onset, the levels of moisture flow over the northeastern South Africa and Zimbabwe appear to have decreased to ~ 100 kg $m^{-1}s^{-1}$, while Madagascar maintained moisture convergence.

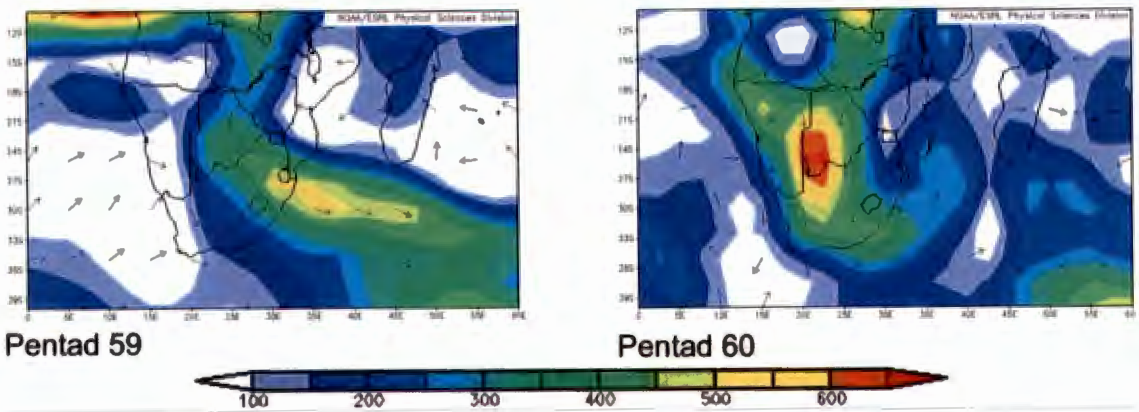

Figure 6.34: Moisture flux (kg $m^{-1}s^{-1}$) analysis during 2007 seasonal rainfall onset

6.10 Vertical Motion (Omega)

The previous sections dealt with the availability of moisture in the atmosphere in the form of specific humidity and moisture flux. However, the availability of moisture alone does not automatically imply rainfall — other factors such as vertical movement of air are also essential components in rainfall formation (Cotton, Bryan & Van den Heever, 2010). Rose and Lin (2003) stressed that prediction of rainfall without any measure of available moisture will always be uncertain.

Vertical motion fields show areas of precipitation activity and of non-precipitation through the rising and sinking of air. Rising air in the atmosphere may lead to the development of clouds and precipitation when the rising moist air cools and reaches condensation level. Sinking air tends to produce warm, dry conditions and so may indicate a lack of rainfall. Mechanisms that lift moist air, and so lead to condensation and rainfall, include convergence, topography, fronts and convection. Previous studies (Kabanda, 2004; Kabanda, 2011; Nenwiini & Kabanda, 2013) described factors which influence Vhembe District rainfall, including local-scale and large-scale convective activities.

This section provides an analysis of the vertical movement of air prior to and during the early and late seasonal rainfall onset within the humid and semi-arid zones of the study area. The vertical motion (Omega) field composites construction at 500 hPa is from the NCEP/NCAR reanalysis data at pentad scale. The data is available on a global scale at 6-hourly 2.5° x 2.5° grid spacing. According to Rose and Lin (2003), vertical motion measured on a coarse scale grid characteristic of a general circulation model is a measure of synoptic scale forcing for uplift and subsidence. Furthermore, vertical motion fields represent rainfall produced by large-scale atmospheric dynamics better than rainfall produced by local convective systems. In the analysis, the negative values indicate upward movement of air parcels while positive values indicate downward movement of air parcels. In mathematical terms, the vertical movement (vertical velocity) ω, with pressure as a vertical coordinate is:

$\omega = dp/dt$ (time rate of change of pressure) (6.6)

Omega (ω) can be approximated by the following equation

$\omega = -g\rho w$ (6.7)

where the symbols are:

t = time

p = pressure

ρ = density

g = acceleration due to gravity (9.81 m s^{-2})

w = vertical velocity component in (x, y, z) coordinates

6.10.1 Vertical Motion Analysis in the Humid Zone

The following sections examine the evolution of vertical motions prior to and during early and late seasonal onset in the humid zone of the study area. NCEP reanalysis vertical motions composites for the pentads that represent the early (1986 and 2001) and late (1985 and 2006) rainfall seasons during the 1980s and 2000s decades were composited to determine the mean characteristics of the vertical motion prior and during seasonal rainfall onset.

6.10.2 Vertical Motion - 20 Days Prior to 1986 Early Onset

Figure 6.35 illustrates the evolution of vertical motion composite fields for 20 days prior to the seasonal rainfall onset of 1986 that represents early onset of 1980 – 89 decade in the humid zone. During pentad 50, SWIO features subsidence while south of 36°S along 25°E there is a centre of maximum ascent. This situation continued throughout the following 15 days, such that the study area remained under weak subsidence.

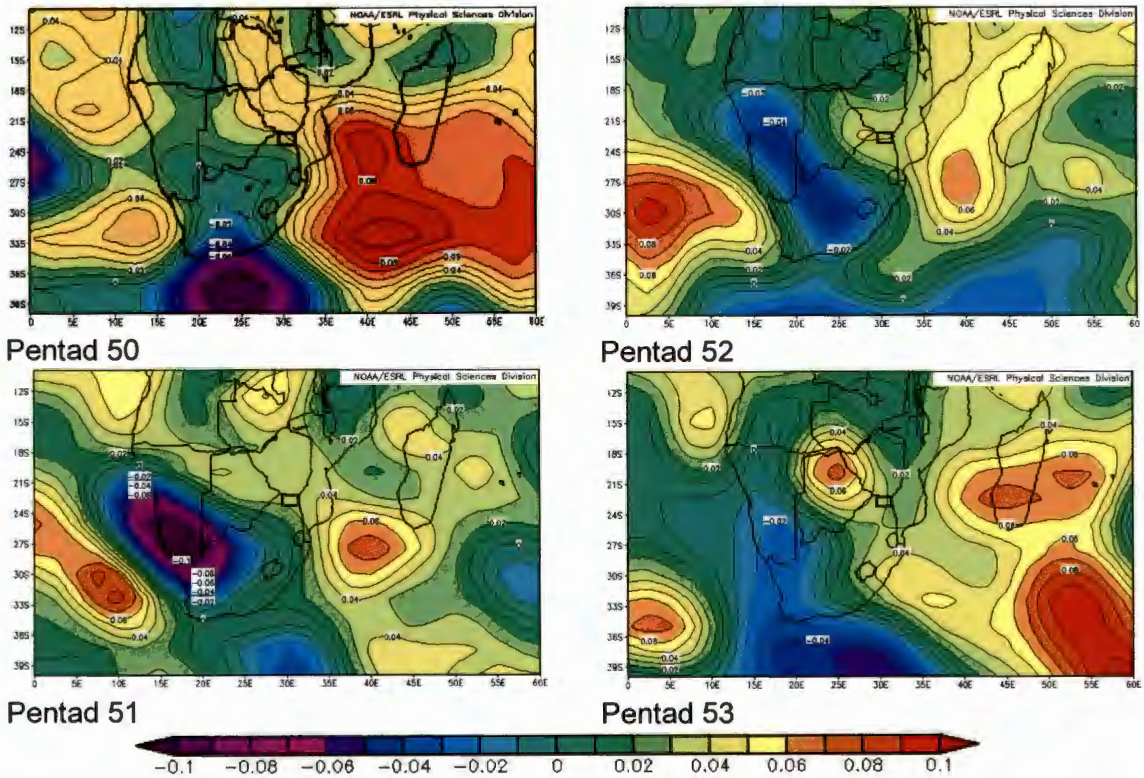

Figure 6.35: Vertical motion (Pa s^{-1}) 20 days prior to 1986 seasonal rainfall onset

6.10.3 Vertical Motion - During 1986 Early Onset

Figure 6.36 shows the vertical motion during the onset date of 1986; the most striking feature is the ascent – descent dipole that exists over central South Africa and south Atlantic Ocean. Meanwhile, the study area features a sinking motion of ~ 0.06 Pa s^{-1}. Five days after the onset date, a tongue of weak descending air (~ 0.04 Pa s^{-1}) is evident over the study site with a strong descending motion south of Madagascar.

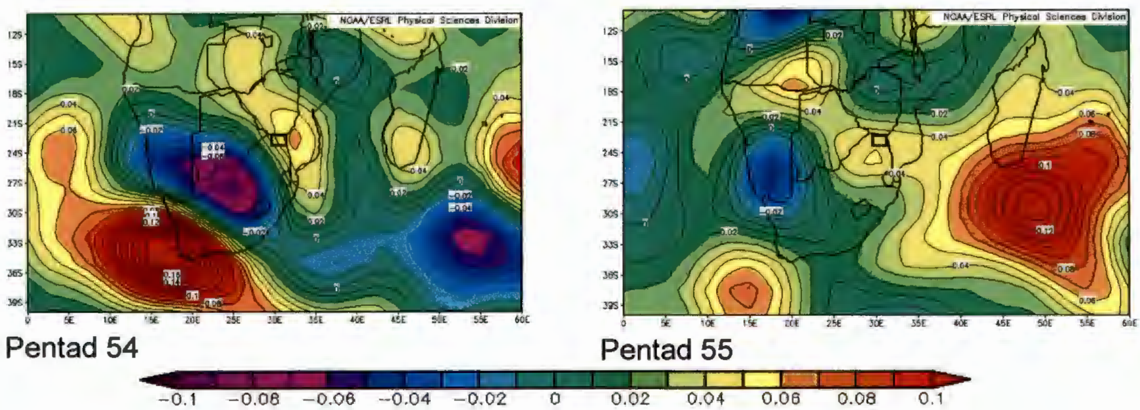

Figure 6.36: Vertical motion (Pa s^{-1}) during 1986 seasonal rainfall onset

6.10.4 Vertical Motion - 20 Days Prior to 1985 Late Onset

This subsection analyses the 20 days prior to the 1985 seasonal rainfall onset, which represents the late season onset for the 1980 – 89 decade (Figure 6.37). Initially (pentad 65), areas of maximum rising motion occur over the Atlantic Ocean and southern parts of South Africa and Indian Ocean, and subsidence areas are across the central regions of Southern Africa extending to the Indian Ocean. A reduction in the strength of vertical motion is evident in the subsequent pentad. In pentad 67, a strong ascending motion is over Madagascar. However, the study area remained under weak subsidence during the course of the four pentads.

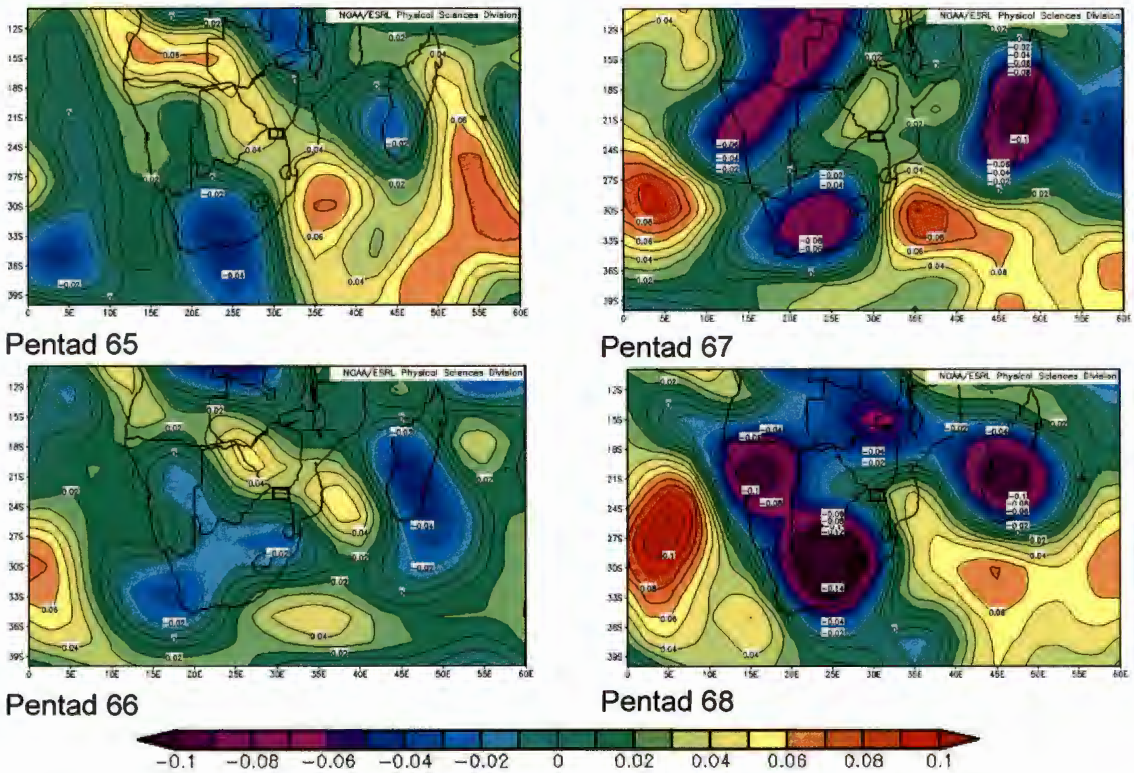

Figure 6.37: Vertical motion (Pa s^{-1}) 20 days prior 1985 seasonal rainfall onset

6.10.5 Vertical Motion - During 1985 Late Onset

During the onset pentad (pentad 69 - Figure 6.38), an increase in the magnitude of the upward motion (-0.08 Pa s^{-1}) over southern Africa in general is evident. An area of strong ascending motion is located over the Indian Ocean while strong subsidence motion is visible over the Atlantic and east Madagascar. The mean vertical motion over the study area is approximately -0.06 Pa s^{-1}, which is high compared to the 20 days prior to onset. Five days after the onset date, strong rising motion occurs in most regions of southern Africa; Vhembe District features the strongest upward motion (~ -0.12 Pa s^{-1}).

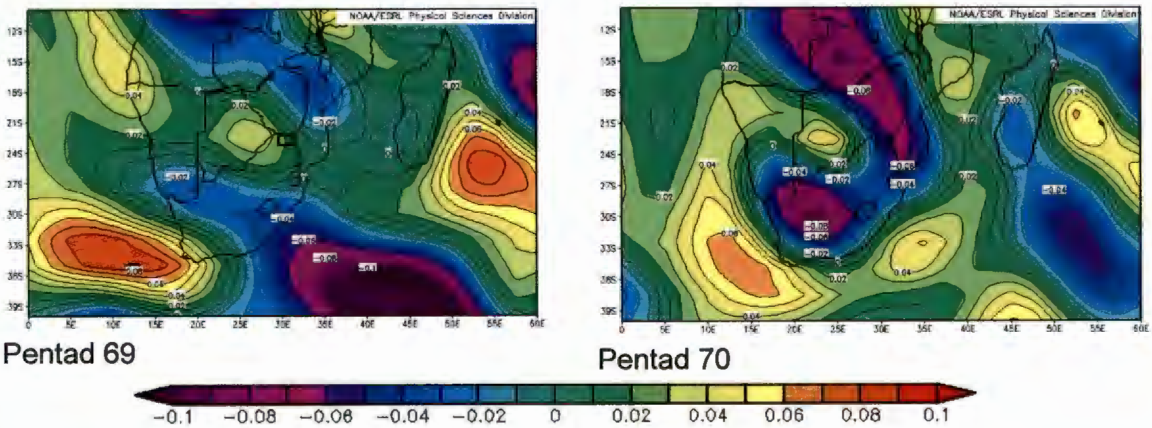

Figure 6.38: Vertical motion (Pa s^{-1}) during 1985 seasonal rainfall onset

6.10.6 Vertical Motion - 20 Days Prior to 2001 Early Onset

The features noteworthy during the evolution of the 20 days prior to the 2000 – 09 decade early onset (Figure 6.39) include strong ascending motion (~ -0.09 Pa s^{-1}) occurring over southern Africa during pentad 52, strong descending motion on both adjacent oceans (SAO and SWIO) and a strong ascent over southern Africa by pentad 52. A dipole (ascent–descent) feature exists between southern Africa-SWIO and SAO during pentad 53. Five days later, SWIO experiences strong subsidence, which spread to the northeastern part of South Africa, covering the study area.

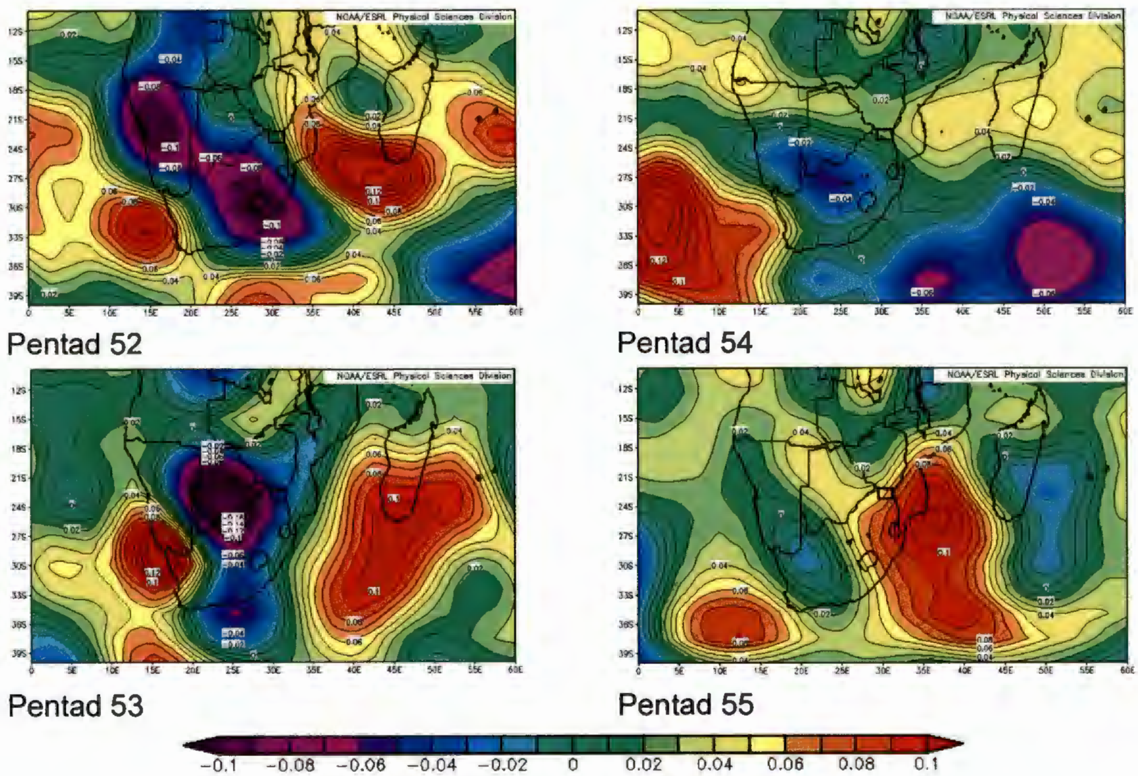

Figure 6.39: Vertical motion (Pa s^{-1}) 20 days prior to 2001 seasonal rainfall onset

6.10.7 Vertical Motion - During 2001 Early Onset

Pentad 56 (Figure 6.40) depicts rising motion over the southern Africa regions in general. Areas of northeastern South Africa, Mozambique, Zimbabwe and west Atlantic Ocean are under sinking motion of ≥ -0.04 Pa s^{-1} magnitude. A pentad later, the noteworthy feature is the centre of Intense sinking motion (-0.12 Pa s^{-1}) over Vhembe District and rising motion over Madagascar and Northern Cape. This kind of pattern over southern Africa does not favour rainfall formation during pentad 57.

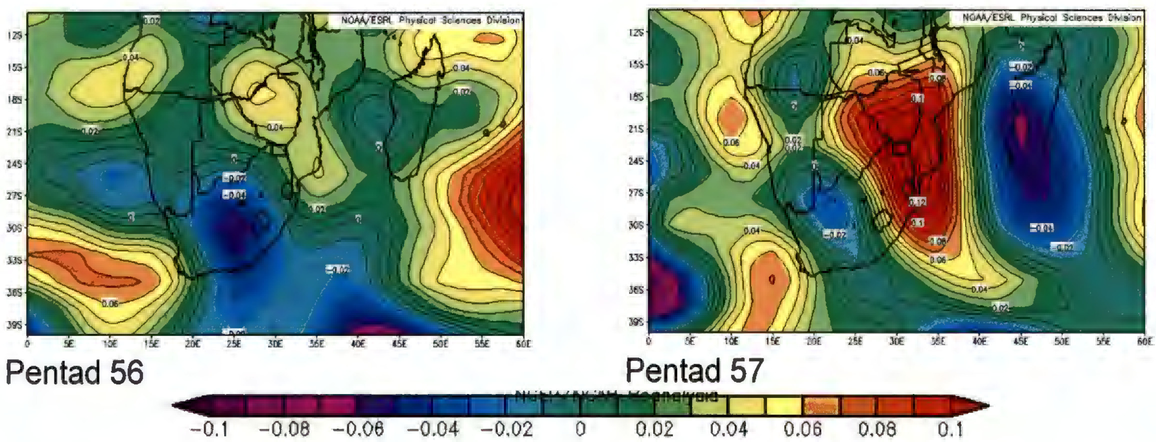

Figure 6.40: Vertical motion (Pa s^{-1}) during 2006 seasonal rainfall onset

6.10.8 Vertical Motion - 20 Days Prior to 2006 Late Onset

In pentad 67, a subsidence motion (≥ -0.04 Pa s^{-1}) occupies Vhembe District and its environs (Figure 6.41), while areas of ascending motion are over the southernmost parts of South Africa and SWIO, and with a relatively strong centre over Madagascar. The striking development, which occurred during pentad 69 is a major subsidence in SAO.

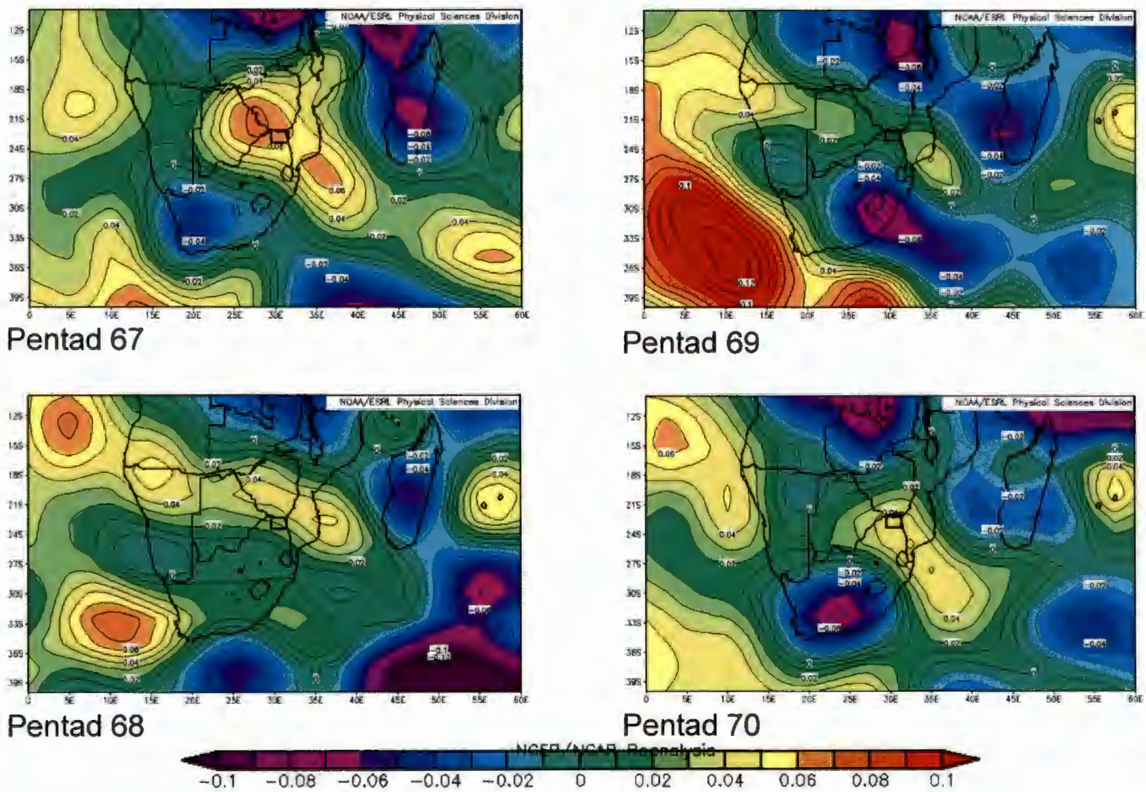

Figure 6.41: Vertical motion (Pa s^{-1}) 20 days prior to 2006 seasonal rainfall onset

6.10.9 Vertical Motion - During 2006 Late Onset

During pentad 70 (Figure 6.42), the whole of southern Africa shows enhanced rising motion (negative Omega values), except in the study area and the Mozambique Channel. The Atlantic Ocean in general shows subsidence.

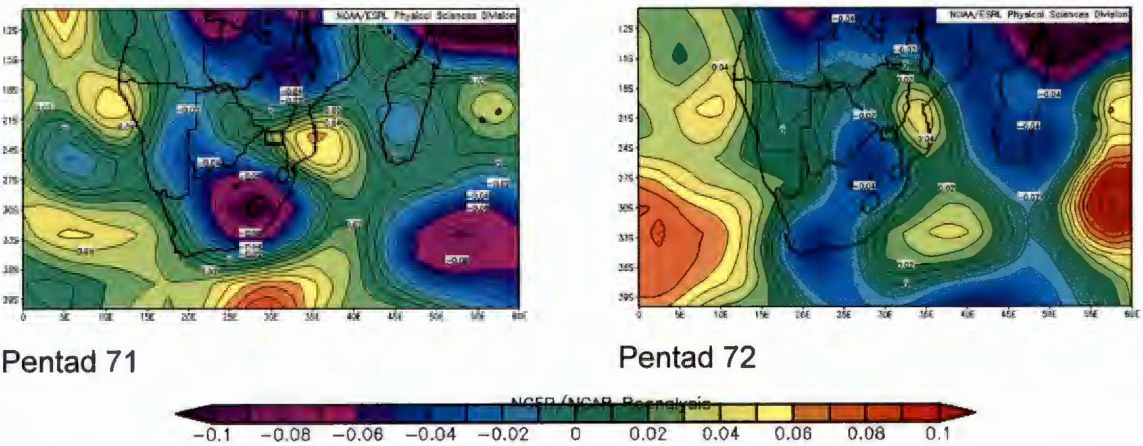

Pentad 71 Pentad 72

Figure 6.42: Vertical motion (Pa s^{-1}) during 2006 seasonal rainfall onset

6.11 Semi-Arid Zone Vertical Motion Analysis

For the two decades 1980 – 89 and 2000 – 09, the early-onset rainfall seasons in 1984 and 2001, and late-onset seasons in 1981 and 2007 were analysed.

6.11.1 Vertical Motion - 20 Days Prior 1984 Early Onset

Figure 6.43 presents the vertical motion in the 20 days prior to the semi-arid early onset season, which occurred in 1984. During pentad 57, ascending motion is evident during over Namibia, the adjacent Atlantic Ocean, and southward to the south Indian Ocean. Meanwhile, relatively strong subsidence is visible over the south Atlantic Ocean, and a slightly weak sinking motion is over Madagascar. In pentad 58, north-south propagation of rising motion over most Southern African regions is evident. In addition, there is enhanced subsidence in the Atlantic Ocean and sinking motion over Madagascar. The situation changes completely in the subsequent pentads (pentad 59 and 60), and a sinking motion occupies the northern part of South Africa, Mozambique and Zimbabwe.

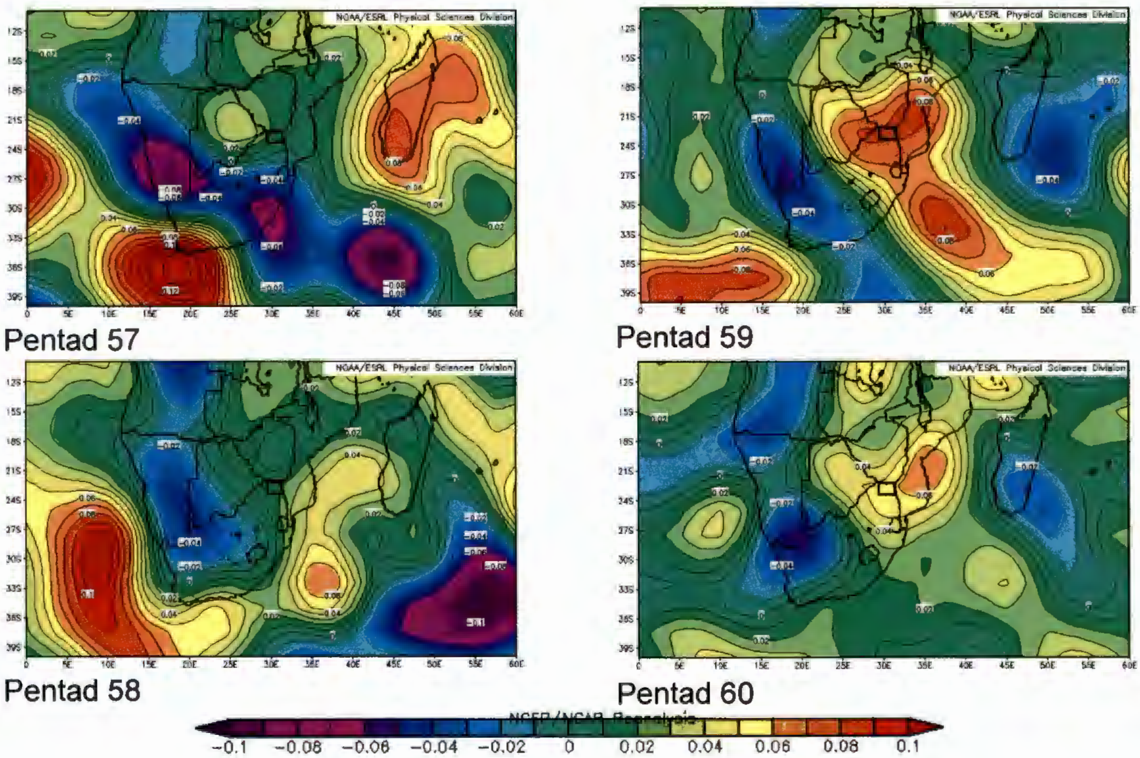

Figure 6.43: Vertical motion (Pa s^{-1}) 20 days prior 1984 seasonal rainfall onset

6.11.2 Vertical Motion - During 1984 Early Onset

On the date of onset (pentad 61), ascending motion over Namibia, Botswana and South Africa intensifies and extends towards the Indian Ocean (Figure 6.44). Meanwhile, the study area experienced rising motion (~ -0.01 Pa s^{-1}), which was maintained throughout the following five days.

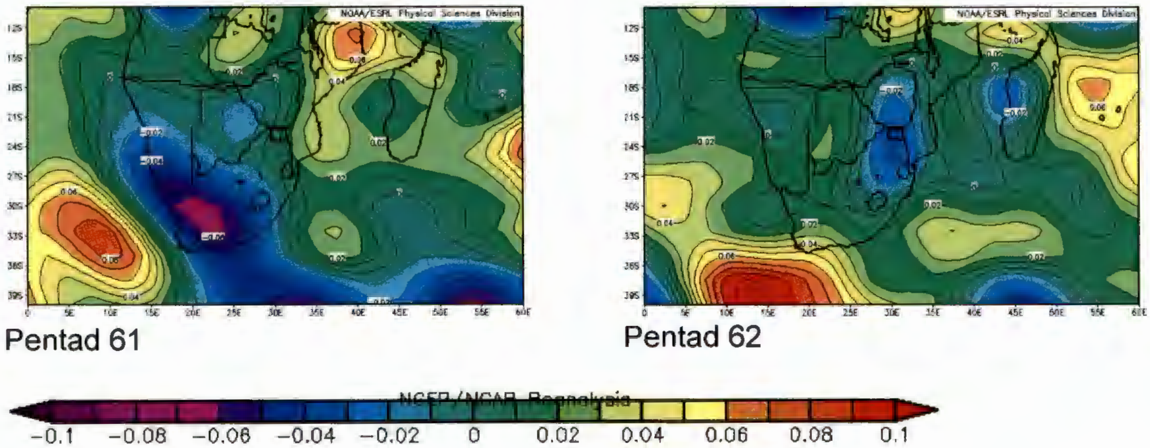

Pentad 61

Pentad 62

Figure 6.44: Vertical motion (Pa s^{-1}) during 1984 seasonal rainfall onset

6.11.3 Vertical Motion - 20 Days Prior to 1981 Late Onset

At pentad 70 (Figure 6.45), sinking motion dominates the southern Africa regions with three distinct cell structures found in the Atlantic Ocean, northern South Africa and Indian Ocean. Rising motion with a tropical origin dominated pentad 73; it covered the study area and most of the Mozambique Channel. There are subsidence centres of ~ 0.06 Pa s^{-1} magnitude over the southeast Atlantic Ocean and Namibia.

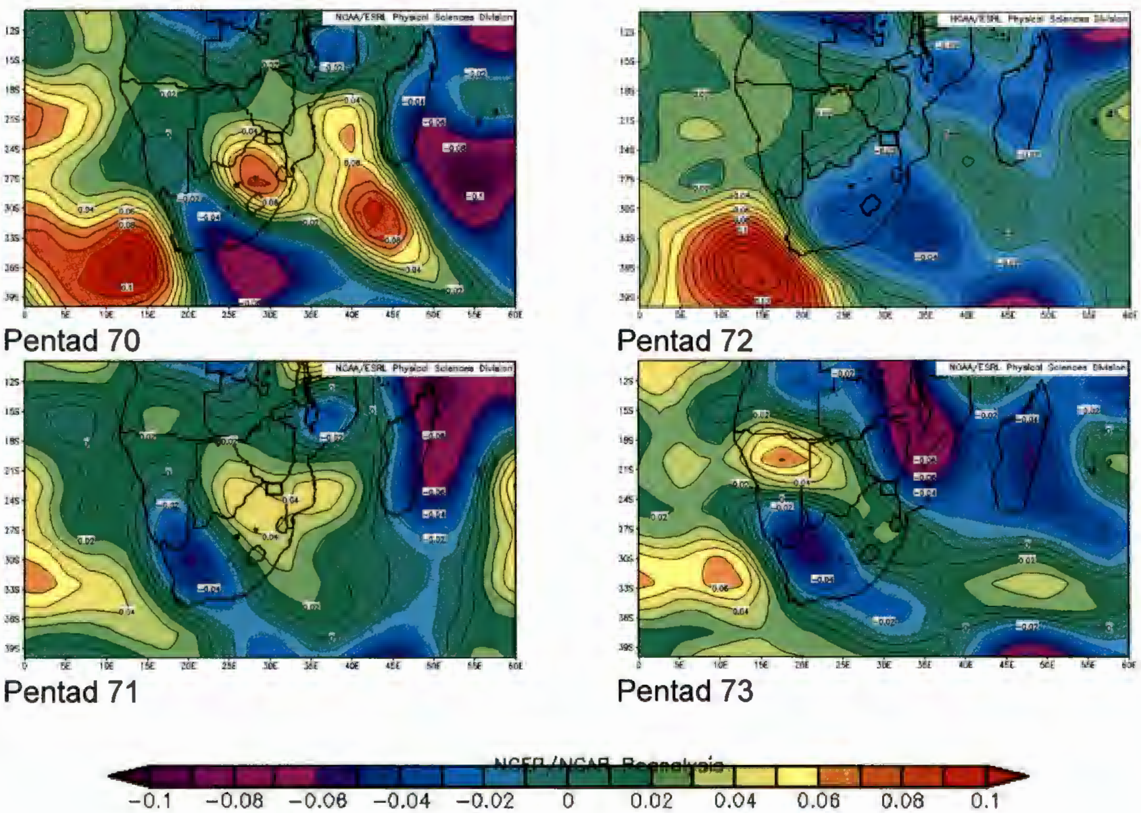

Figure 6.45: Vertical motion (Pa s^{-1}) 20 days prior to 1981 seasonal rainfall onset

6.11.4 Vertical Motion - During 1981 Late Onset

The 1981 seasonal rainfall was late; it started in January of 1982 (Figure 6.46). In pentad 1, the most striking feature is an intense rising motion (with centre value > -0.2 Pa s^{-1}) over the Mozambique Channel. Southeast Atlantic Ocean featured sinking motion. In addition, most of the tropics north of 15°S experienced rising motion that extended to the study area and reached a maximum over Vhembe District during pentad 2.

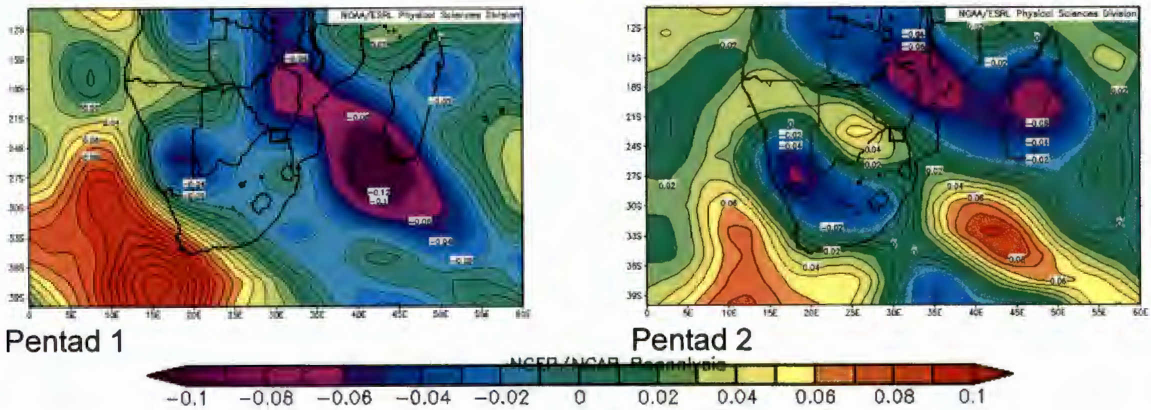

Figure 6.46: Vertical motion (Pa s^{-1}) during 1981 seasonal rainfall onset

6.11.5 Vertical Motion - 20 Days Prior to 2001 Early Onset

There are several interesting features in the patterns seen during the 20 days prior to the 2001 seasonal rainfall onset. (Figure 6.47). In pentad 55 there is quite intense subsidence (0.12 Pa s^{-1}) centred over the Channel and extending to northeastern South Africa, Zimbabwe and Mozambique. Madagascar and southwest South Africa feature weak rising motion. Pentad 57, shows sinking motion and over northeastern South Africa and Mozambique Channel, while the rest of southern Africa has weak rising motion. The other striking feature is the ascent-descent dipole between South Africa and Indian Ocean during pentad 58. Meanwhile, the vertical motion over the study area shows weak ascent.

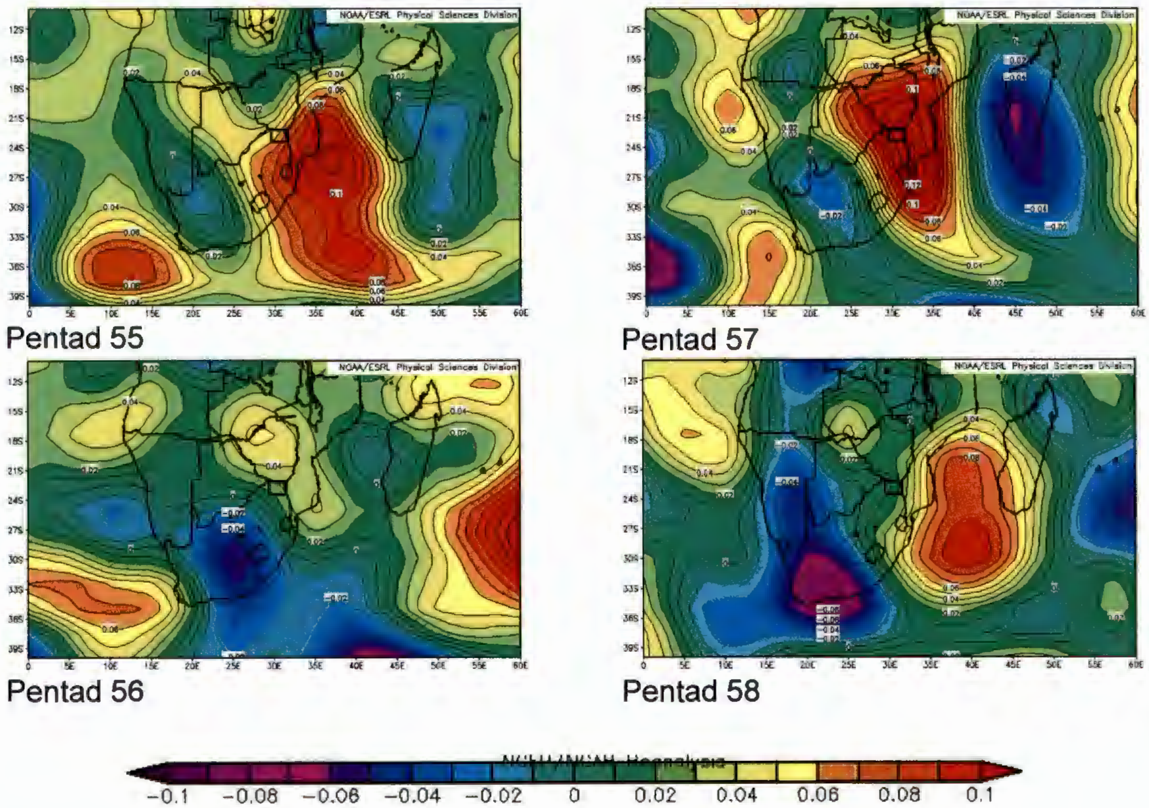

Figure 6.47: Vertical motion (Pa s^{-1}) 20 days prior 2001 seasonal rainfall onset

6.11.6 Vertical Motion - During 2001 Early Onset

In Figure 6.48 (pentad 59), the prominent structure is the enhanced ascent (with centre value -0.2 Pa s^{-1}) over South Africa, which links with enhanced descent over SAO. The pattern in the SWIO through the Mozambique Channel exhibits a narrow tongue of sinking motion. The study area maintained a weak ascending motion throughout the onset period.

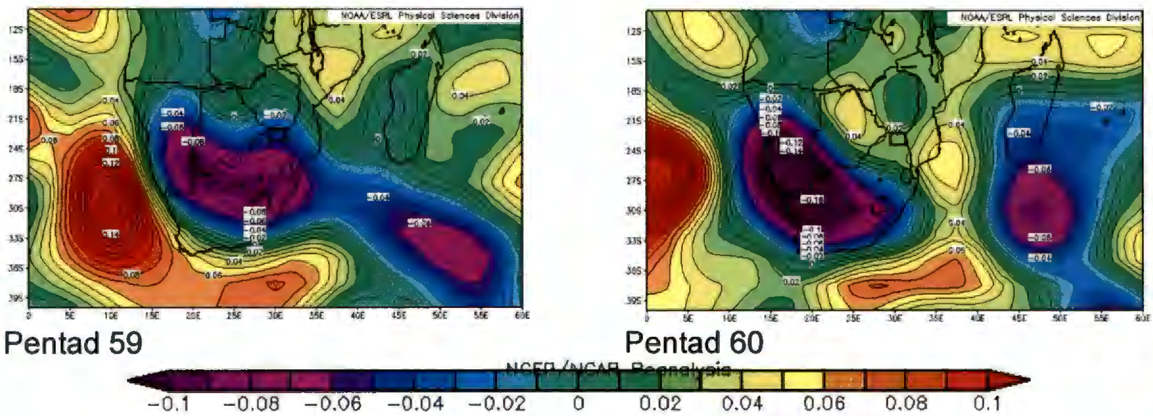

Figure 6.48: Vertical motion (Pa s^{-1}) during 2001 seasonal rainfall onset

6.11.7 Vertical Motion - 20 Days Prior to 2007 Late Onset

The late onset of the 2000 – 09 decade in the semi-arid zone occurred in the 2007 season. Figure 6.49 illustrates the patterns for the 20 days prior to the onset date. The striking features are apparent in pentad 68 and 69 where a concentration of major ascent emanating from the tropics extends southward covering the whole of Southern Africa. Another prominent centre of action, albeit of opposite sign (i.e. strong subsidence), exists in the Atlantic Ocean. When the dominant sinking motion is in the Atlantic Ocean, the corresponding rising motion over southern Africa is generally weak.

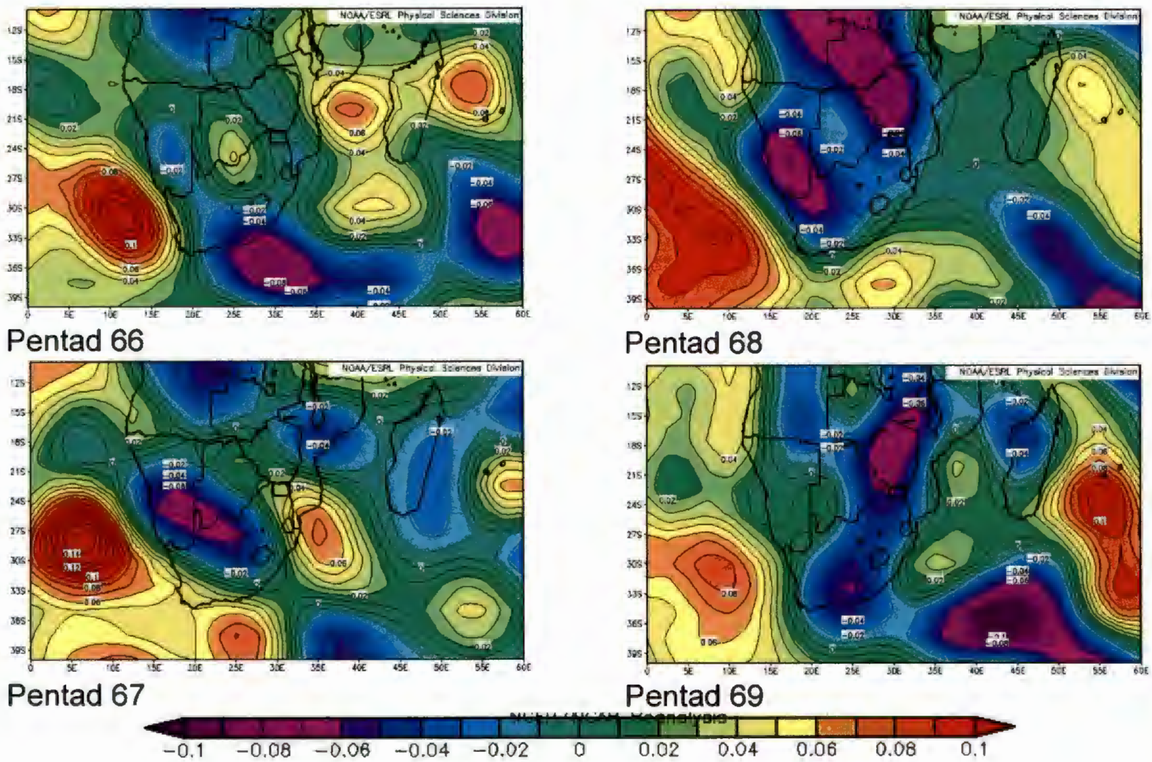

Figure 6.49: Vertical motion (Pa s^{-1}) 20 days prior 2007 seasonal rainfall onset

6.11.8 Vertical Motion - 20 During 2007 Late Onset

During the onset date of seasonal rainfall (pentad 70), the vertical velocity over northeastern South Africa is ~ -0.06 Pa s^{-1} (Figure 6.50). The Atlantic Ocean depicts an enhanced subsidence. It plays an important role in influencing the rising motion over land (southern Africa). The other player in that effect is the SWIO.

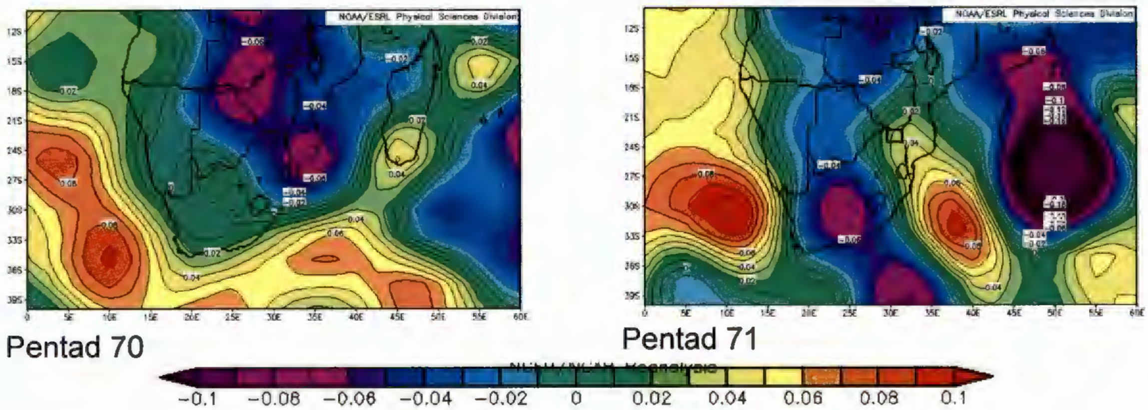

Figure 6.50: Vertical motion (Pa s^{-1}) during 2007 seasonal rainfall onset

6.6 Chapter Summary

In this chapter, specific humidity patterns indicated the location and amount of water vapour present in atmosphere over the domain prior to and during the onset of seasonal rainfall in the study area. Moisture flux composites for the corresponding period were analysed in order to identify the location of moisture sources and the transport pathways associated with the evolution of seasonal rainfall onset. The analysis of vertical motion (Omega) revealed potential areas of convection activities. The selection of these three parameters was based on the hypothesis that more accurate large-scale fields of moisture and vertical motion will have a stronger relationship with observed rainfall (Kennedy, Dong & Xi, 2011). The composite analysis of the aforementioned synoptic meteorological variables associated with the seasonal rainfall onset in Vhembe District revealed different patterns of atmospheric features during early and late seasonal rainfall period of the humid and semi-arid zones. These are summarised below in Table 6.1 and Table 6.2.

Table 6.1 shows the observed station rainfall per pentad and the evolution of associated meteorological variables prior to and during the onset of both early and late onset of seasonal rainfall in the humid zone in Vhembe District. Overall, the onset of rainfall in the early seasons of the humid zone is associated with the relatively weak moisture build-up prior to the onset compared to the semi-arid zone. About 0.02 to 0.04 Pa/s vertical motion dominated the early onset in the humid zone while the late onset is associated with near zero values of vertical motion. In contrast, both the early and late onset seasons in the semi-arid zone are associated with negative vertical motion values (Table 6.2), which indicates relatively strong ascending vertical motion. The observed pattern of vertical motion during the onset of seasonal rainfall in the semi-arid zone agrees well with the amount of rainfall reported at the rainfall stations.

In contrast with late-onset seasons in the humid zone, late-onset seasons in the semi-arid zone showed relatively high moisture build-up prior to the onset date. An increase in the amount of specific humidity in the atmosphere is apparent on the date of onset. The generally earlier onset of rainfall in the humid zone occurs when specific humidity in the atmosphere is between 3-4 g/kg while ≥ 5 g/kg specific humidity is necessary for the rainfall onset in the semi-arid zone.

During the onset of early season period in the humid zone, the atmosphere is characterised by relatively low water vapour (about 2 g/kg) in the 20 days before the onset date. About 3-4 g/kg of water vapour was necessary to trigger the early onset of seasonal rainfall in this zone. The early rainfall onset over the humid zone is associated with the southeasterly flux from SWIO which imports moisture from the Indian Ocean region at ~ 150 kg $m^{-1}s^{-1}$. An anticyclone in the southwest Indian Ocean (SWIO) with a curvature over southern Africa was responsible for moisture advection to the study area. During this period, areas of maximum ascending motion were observed in the central parts of South Africa and over the Indian Ocean. The early onset of seasonal rainfall in the humid zone is associated with weak downward vertical motion of about 0.02 -0.04 Pa/s. This suggests that the vertical motion does not signify the rainfall during the onset of early season rainfall in the humid zone.

However, near zero values of vertical motion characterise the atmosphere over the study site during the onset of late season in the humid zone. Persistently low moisture was observed in the 20 days prior to the 1981 late onset season. However, the 2006 late season displayed a different pattern; the build-up of specific humidity appeared to be relatively higher than that of 1981.

Table 6.1 Local station rainfall and meteorological variables prior and during onset date in the humid zone

		Early Onset 1986					Late Onset 1985				
	Period	Pentad	Station Rainfall (mm)	Specific Humidity (g/kg)	Moisture Flux (kg $m^{-1}s^{-1}$)	Vertical Motion (Pa/s)	Pentad	Station Rainfall (mm)	Specific Humidity (g/kg)	Moisture Flux (kg $m^{-1}s^{-1}$)	Vertical Motion (Pa/s)
Humid Zone		P50	0	1	100	0.02	P65	0	1	150	0.04
		P51	3.2	2.5	100	0.02	P66	0	5	150	0.02
		P52	4.3	2.5	100	0.03	P67	4.9	3-4	150	0.03
		P53	0	2.5	100	0.06	P68	0	2-3	100-150	0-0.2
		P54	29.7	4	150	0.04	P69	78.5	4.5	150	0
		P55	5.3	4	100	0.04	P70	112.2	4.5	150	>-0.04
		Early Onset 2001					Late Onset 2006				
		P52	0	4	150	0-0.4	P67	0	3-4	200	0.06
		P53	0.7	2-4	150	-0.02	P68	0	7	150	0.02
		P54	0	5	250	0.02	P69	0	4.5	150	0.02
		P55	2	2-3	100	>0.4	P70	0	2	225	0.04
		P56	26.2	2-2.5	100	0.02	P71	12	5	150	0
		P57	0.9	3	100-150	>0.08	P72	3.5	6	150	<0

Table 6.2: shows the observed station rainfall per pentad and the evolution of associated meteorological variables prior to and during the onset of both early and late onset of seasonal rainfall in the semi-arid zone. The analysis of meteorological variables in the 20 days prior the onset of late season rainfall in 1981 showed persistent southeasterly moisture transport over southern Africa, signifying both the south Indian Ocean and tropical Africa as sources of moisture. Nevertheless, abundant amount of moisture was concentrated over tropical Africa. The observed inflow brought in the moisture needed for the onset of rainfall over the northeastern part of South Africa. Rainfall onset date was characterised by moisture flow of about ≥ 250 kg $m^{-1}s^{-1}$. The observed ascending motion of about -0.02 Pa/s and specific humidity of about 5.5 g/kg over the atmosphere of the study area during the period of onset coincides with the rainfall observed by rainfall stations on the ground.

Table 6.2: Local station rainfall and meteorological variables prior and during onset date in the semi-arid zone

	Period	Early Onset 1984					Late Onset 1981				
		Pentad	Station Rainfall (mm)	Specific Humidity (g/kg)	Moisture Flux (kg $m^{-1}s^{-1}$)	Vertical Motion (Pa/s)	Pentad	Station Rainfall (mm)	Specific Humidity (g/kg)	Moisture Flux (kg $m^{-1}s^{-1}$)	Vertical Motion (Pa/s)
Semi-arid Zone		P57	0	4	200	0.02	P70	0	3-4	250	0.04
		P58	6	6	200	0.02	P71	0	5-6	200	0.03
		P59	0	3-4	450	0.08	P72	0	5-6	200	-0.01
		P60	0	3	200	0.05	P73	0	6	200	0 to -0.01
		P61	36	6	200	0 - 0.1	P1	60	5.5	200	-0.01
		P62	4.5	6	200	-0.01	P2	2.5	3-4	250	0.02
		Early Onset 2001					Late Onset 2007				
		P55	0	2-3	200	>0.06	P66	0	7	500	-0.02
		P56	0	2-3	200	0.02	P67	0	6	200	0.04
		P57	0	3	200	0.12	P68	0.8	6	200	-0.04
		P58	0	4	200	0.01	P69	0	7	250	-0.06
		P59	11	5	300	-0.04	P70	38.1	6	200	-0.04
		P60	21	5.5	100-150	0.01	P71	59.3	8	100-150	-0.08

This chapter managed to establish distinctive patterns of atmospheric variables, which are unique for a particular zone (humid zone and semi-arid zone). In summary;

1) Specific humidity showed these characteristics:

- Specific humidity is low in the humid zone during onset pentad and it is limited to a small area. In the semi-arid zone, humidity is moderate to high during onset, and is spread over a large area

- Moisture distribution originates from the tropics and spreads southward
- Moisture deficiency (dryness) emanates from the Indian Ocean and extends eastward

2) Moisture Flux Patterns;

- A large-scale anticyclonic gyre is over southern Africa with an eastern curvature over the Indian Ocean during the early rainfall onset in humid zone, and since the atmosphere over the Indian Ocean was found to be relatively dry, it implies that relatively little moisture is advected towards Vhembe from the east
- A weak convergence of southerlies and northwesterly moisture flow over northeastern South Africa during late rainfall onset in humid zone, but due to moisture scarcity in the southerlies, this convergence produces little moisture over the study area.
- Vhembe District is more influenced by northwesterly/northerly flow emanating from tropical areas which have abundant moisture during early and late rainfall onset in the semi-arid zone

3) As far as vertical motion is concerned, distinctive characteristics observed in the Vertical Motion (Omega Patterns)are mainly;

- Weak subsidence occupied Vhembe District during early rainfall onset in the humid zone, while strong upward motion is evident in late rainfall onset, which is accompanied by a strong subsidence in the Mozambique Channel, creating a dipole pattern with overland uplifting motion. During early rainfall onset in the semi-arid, the ascent-descent continues to occupy the south Atlantic, southern Africa and southwest Indian Ocean, providing Vhembe District with modest ascent regime during early and late onset.
- From these observations it is suggested that, during the early and late onset in the humid zone, it is the local forcing (i.e., orographic lifting developing along the Soutpansberg mountains with weak synoptic-scale support) which is more likely to cause rainfall. This observation is in good agreement with Dong et al. (2010). By contrast, in the semiarid zone, large-scale atmospheric systems drive the local rainfall variability at the seasonal rainfall onset time. This significant association is more clearly exhibited in Table 6.2, where the increase in the

magnitude of the meteorological parameters relates well with increase in rainfall during onset – and it is well captured by the reanalyses. The same does not hold true for the humid zone. Generally, rainfall values show stronger and clearer relationships with the large-scale meteorological systems in the semi-arid zone than in the humid zone. Rainfall starts earlier in the humid zone, since the necessary specific humidity is reached earlier. This is due to upslope flow lifting the air, causing cooling and condensation and increasing the air moisture aloft from 4-5 to 6-7 g/kg. On the other hand, it takes longer for the moisture to increase to the level of precipitating in the semi-arid zone and this is generally initiated by the large-scale atmospheric circulation and vertical motion.

Chapter Seven
Atmospheric Anomalies

7.1 Introduction

The previous chapter analysed the synoptic climatological systems such as specific humidity, moisture flux and vertical motion prior to and during the early and late seasonal rainfall onset in the study area at lower and middle pressure levels (700 and 500 hPa). This chapter presents the atmospheric circulation anomaly field composites for the same variables and pentads analysed in Chapter 6, in order to explore the relationship between seasonal rainfall and the evolution of synoptic scale atmospheric anomalies during early and late season rainfall onset. The anomalies of atmospheric variables (in this case specific humidity, moisture flux and vertical motion) provide information on how they deviate from the climatological mean prior to and during the onset of seasonal rainfall in the study area (Vhembe District). The intention here is to identify any significant early signals that may exist around onset. Knowledge of the significant signals will help identify the drivers of early and late seasonal rainfall onset in the humid and semi-arid zone and improve onset predictability. According to Dirmeyer and Kinter (2010), Bagley et al. (2012) and Spracklen et al. (2012), knowledge of moisture sources that supply rainfall over a particular location could be used to understand how moisture anomalies may affect local hydrology, and potentially to aid prediction.

7.2 Specific Humidity Anomalies

The abundance of specific humidity (positive anomalies) implies that the atmosphere contains an anomalous amount of water vapour that has the potential to cause rainfall, while a specific humidity deficit implies the opposite. The positive anomaly areas are indicative of a moisture evaporative source region, while the negative anomaly areas are moisture sinks. To determine the association between seasonal variations in atmospheric specific humidity anomalies and local rainfall onset over the study area, an analysis of the evolution of specific humidity anomalies corresponding to the early and late season onset is undertaken.

7.2.1 Specific Humidity Anomalies - 20 Days Prior 1986 Early Onset

Figure 7.1 shows the evolution of specific humidity anomalies for the 20 days prior to the 1986 seasonal rainfall onset. In pentad 50, negative specific humidity anomalies (drier than normal) occur over the northeastern regions of southern Africa extending to the Indian Ocean and Madagascar. Meanwhile, positive specific humidity anomalies are visible to the west, centred over south Namibia. In pentad 52, positive specific humidity anomalies progress further to the adjacent oceans and northwards towards Zimbabwe and Botswana. In addition, the northeastern part of South Africa remains under weak positive specific humidity anomalies. The pattern changes from positive moisture distribution anomalies to negative (about -0.1 g/kg) five days before the onset date due to the development of a centre of negative specific humidity anomalies over the Indian Ocean that spread northwestward. At the same time, southeast propagation of positive specific humidity anomalies extending from the Atlantic Ocean through Namibia, Botswana and South Africa to the Indian Ocean is evident.

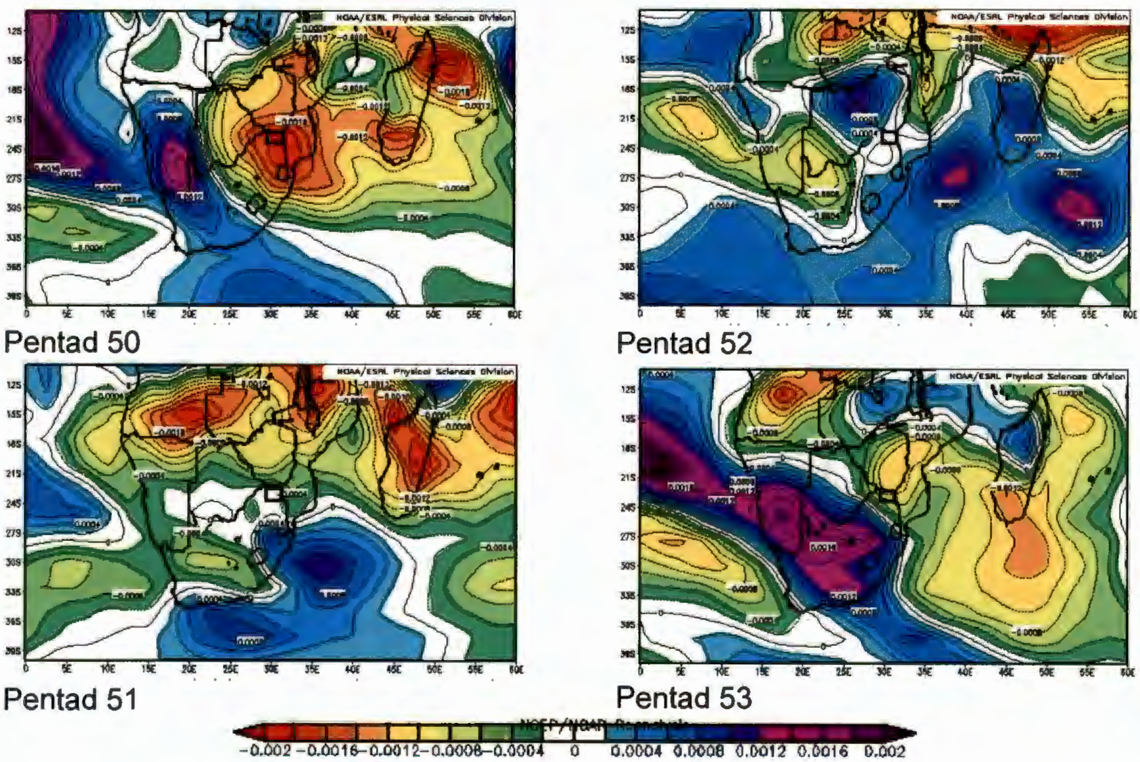

Figure 7.1: Specific humidity anomalies 20 days prior to 1986 seasonal rainfall onset. The contour intervals are 2×10^{-4} kg/kg

7.2.2 Specific Humidity Anomalies - During 1986 Early Onset

On the onset date (pentad 54), the areas of positive anomalies include the study area, Madagascar and SWIO. The Atlantic Ocean is under weak negative specific humidity anomalies. Relatively strong moisture sinks are observed in the east of Madagascar. Five days later, the whole of South Africa is under positive specific humidity, except the northeastern areas, which are influenced by negative values over the Indian Ocean.

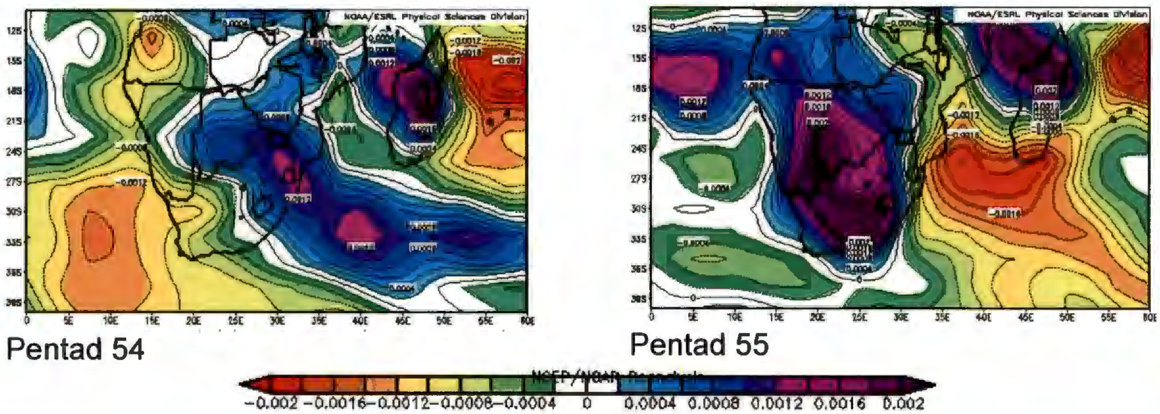

Figure 7.2: Specific humidity anomalies during 1986 seasonal rainfall onset. The contour intervals are $2x10^{-4}$ kg/kg

7.2.3 Specific Humidity Anomalies - 20 Days Prior to 1985 Late Onset

Figure 7.3 displays the evolution of mean specific humidity anomalies for the 20 days prior to the seasonal rainfall onset of 1985, which represents the late onset season during the 1980 – 89 decade. As evident in pentad 65, an anomalous negative specific humidity centre is confined to the border of northeastern South Africa, Botswana and Zimbabwe, while areas of positive anomalous specific humidity are found over the Atlantic Ocean stretching to the southwestern parts of South Africa. Disintegration of the negative specific humidity structure over the Indian Ocean is evident in pentad 66 while strengthening inland. Five days before the onset date (pentad 68), the study area is under anomalous negative specific humidity (-0.3 to -0.4 g/kg), while areas of high specific humidity are found over the Atlantic and much of South Africa as well as west and east of Madagascar.

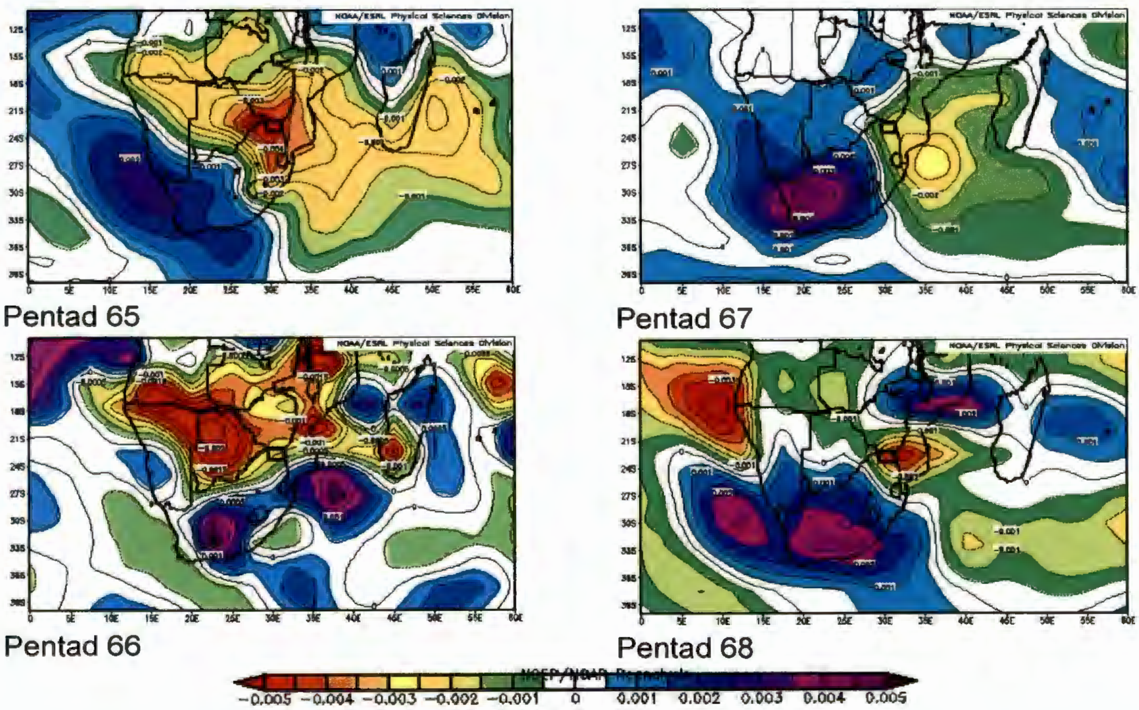

Figure 7.3: Specific humidity anomalies 20 days prior to 1985 seasonal rainfall onset. The contour intervals are $2x10^{-4}$ kg/kg

7.2.4 Specific Humidity Anomalies - During 1985 Late Onset

During the onset (pentad 69), a tongue of negative specific humidity anomalies stretches from a centre of the Indian Ocean across northeastern part of South Africa to Mozambique and Zimbabwe, leading to an accumulation of about -0.1 g/kg specific humidity anomalies in Vhembe District (Figure 7.4). Positive anomalies are observed in the SWIO. Similar conditions prevail five days later, although the high, positive specific humidity anomalies seen over the Indian Ocean earlier have migrated northwards toward the Mozambique Channel. Negative anomalies are still maintained over Vhembe.

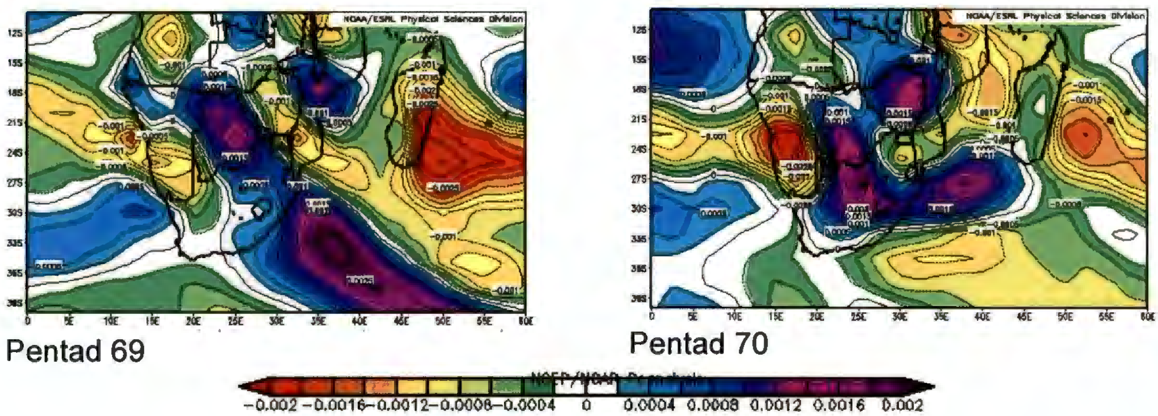

Figure 7.4: Specific humidity anomalies during 1985 seasonal rainfall onset. The contour intervals are $2x10^{-4}$ kg/kg

7.2.5 Specific Humidity Anomalies - 20 Days Prior 2001 (Early Onset)

Figure 7.5 shows a north-south distribution of postive anomalous specific humidity from tropical Africa to southern Africa during pentad 52, with positive moisture anomalies located over the northeastern part of South Africa. Five days before the onset date (pentad 55), negative specific humidity anomalies overlay the whole of southern Africa. Areas of positive specific humidity, which are indicative of moisture evaporative source regions, are found in eastern Madagascar, weakly complemented by the Atlantic Ocean.

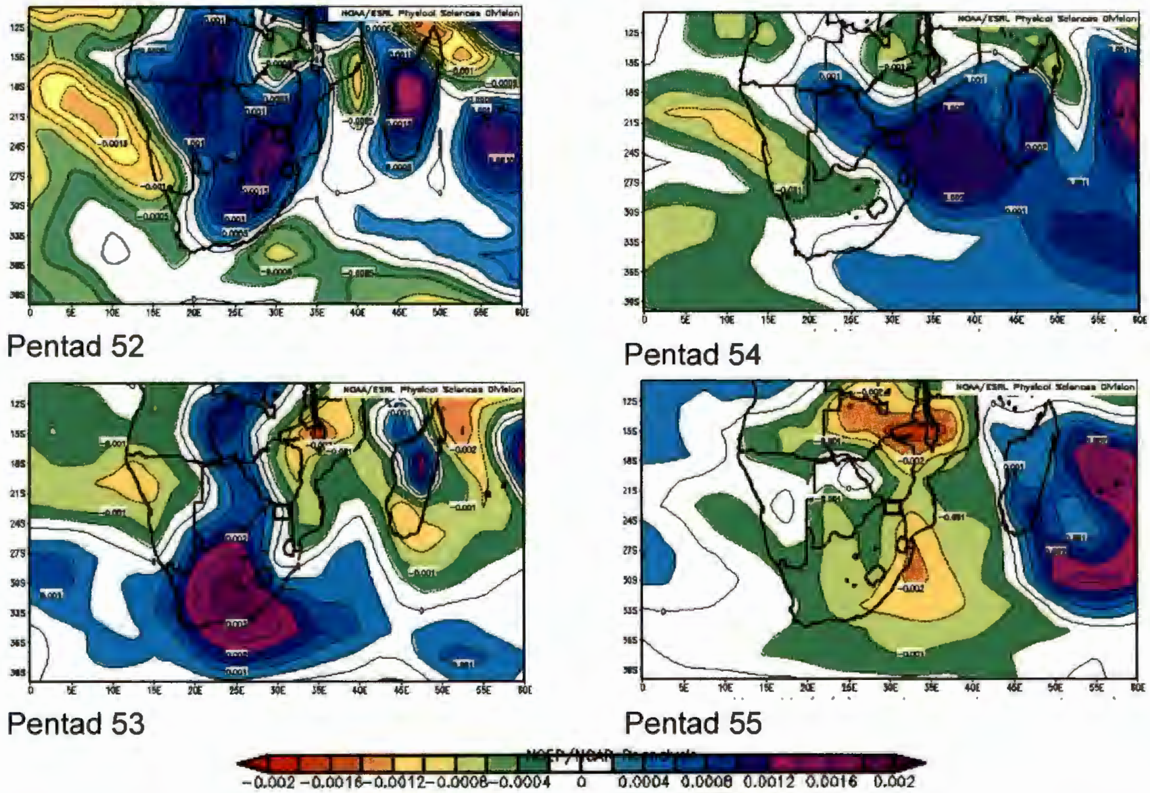

Figure 7.5: Specific humidity anomalies 20 days prior to 2001 seasonal rainfall onset. The contour intervals are 2×10^{-4} kg/kg

7.2.6 Specific Humidity Anomalies - During 2001 (Early Onset)

In Figure 7.6, certain areas in the observing domain (40°S – 10°S and 0°E – 60°E), including the study area, experienced negative specific humidity anomalies. In contrast, a positive specific humidity anomaly stretching from the South Atlantic Ocean across the southernmost parts of South Africa to the Indian Ocean is apparent. Generally, during the onset of seasonal rainfall within the humid zone, the study area remained under negative specific humidity anomalies. Similar conditions continued a pentad after the onset of rainfall with an increase of positive specific humidity anomalies over the Atlantic Ocean.

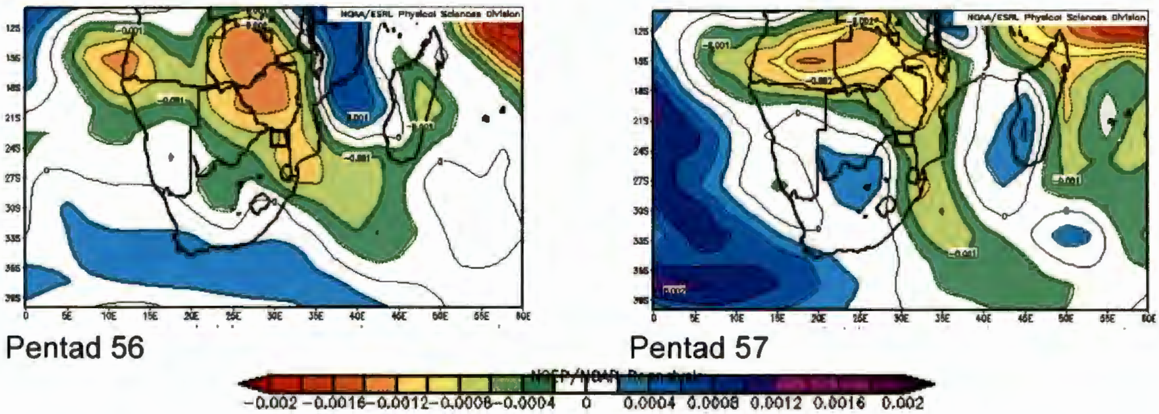

Figure 7.6: Specific humidity anomalies during 2001 seasonal rainfall onset. The contour intervals are $2x10^{-4}$ kg/kg

7.2.7 Specific Humidity Anomalies - 20 Days Prior to 2006 (Late Onset)

In the whole evolution of specific humidity anomalies (pentad 67-70, Figure 7.7), only pentad 68 patterns exhibited positive anomalies over the study area. These conditions can be associated with alternating wet and dry events within the humid zone. At pentad 69, the atmosphere over southern Africa regions is under negative specific humidity anomalies.

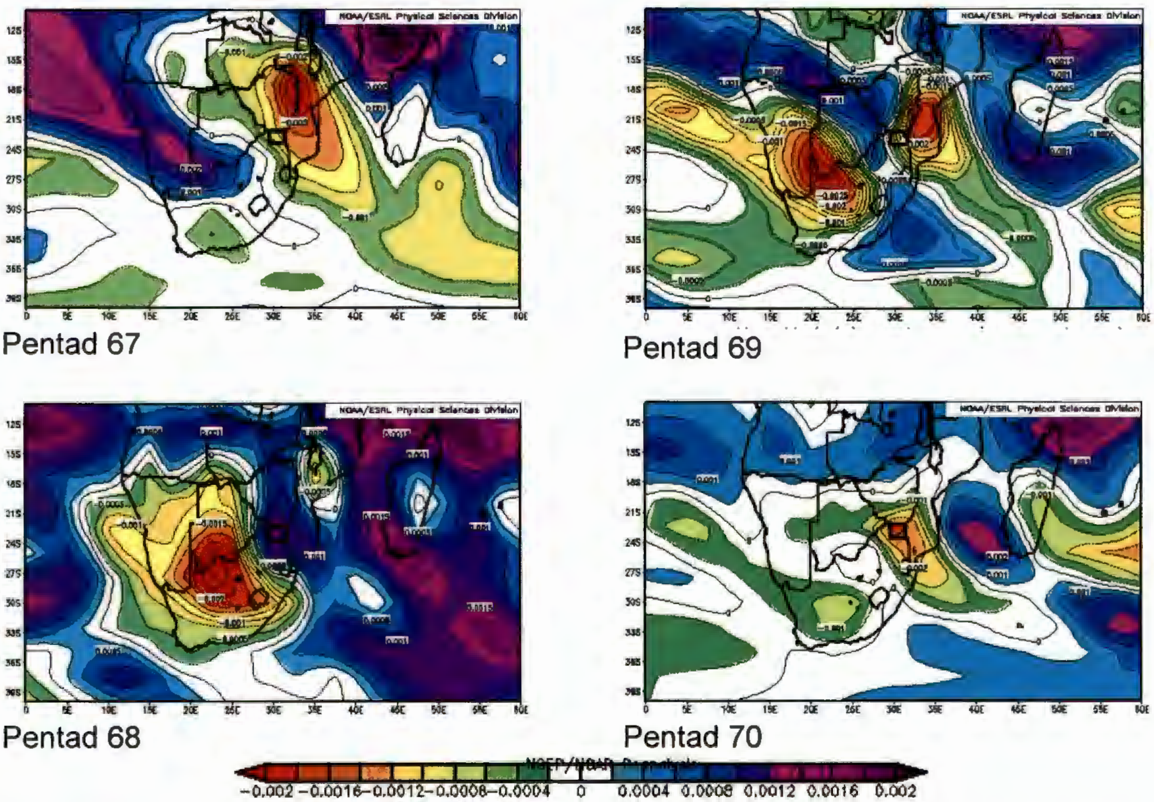

Figure 7.7: Specific humidity anomalies 20 days prior to 2006 seasonal rainfall onset. The contour intervals are $2x10^{-4}$ kg/kg

7.2.8 Specific Humidity Anomalies - During 2006 (Late Onset)

Figure 7.8 shows the patterns of the seasonal rain onset in the humid zone. Positive anomalies stretch from Namibia to the Indian Ocean; at the same time, a narrow band of negative specific humidity anomaly spreads dry air from the Indian Ocean towards Mozambique, Zimbabwe and the northeastern part of South Africa.

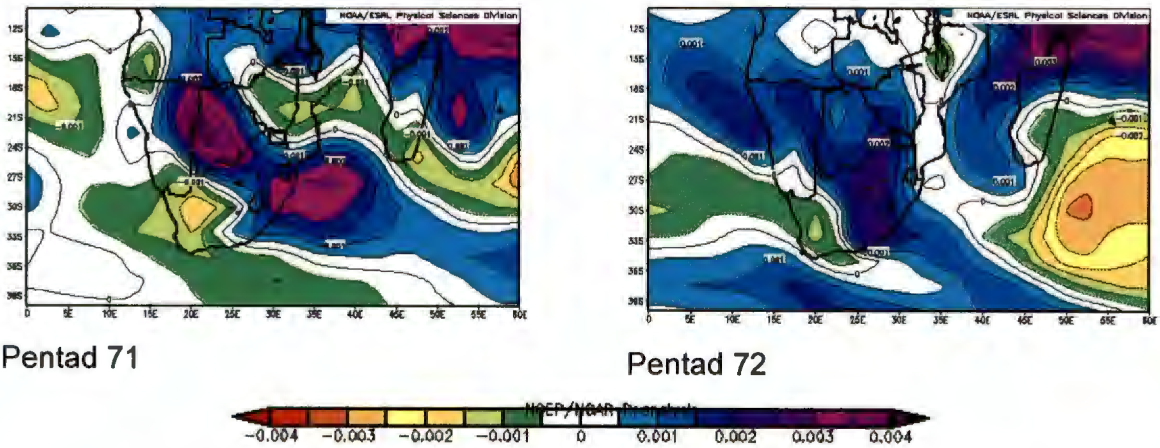

Figure 7.8: Specific humidity anomalies during 2006 seasonal rainfall onset. The contour intervals are $2x10^{-4}$ kg/kg

7.3 Specific Humidity Anomaly Analysis – Semi-arid Zone

7.3.1 Specific Humidity Anomaly 20 Days Prior 1984 (Early Onset)

The mean specific humidity anomaly composites 20 days prior to the seasonal rainfall onset of 1984 (an early-onset season in the 1980 – 89 decade) are shown in Figure 7.9. In pentad 57, the positive anomaly areas north of 27°S in southern Africa are indicative of a moisture evaporative source region. The other areas on the map domain are under negative anomalies excluding the Mozambique Channel. Pentad 59 shows a dry atmosphere over the southern Africa regions in general.

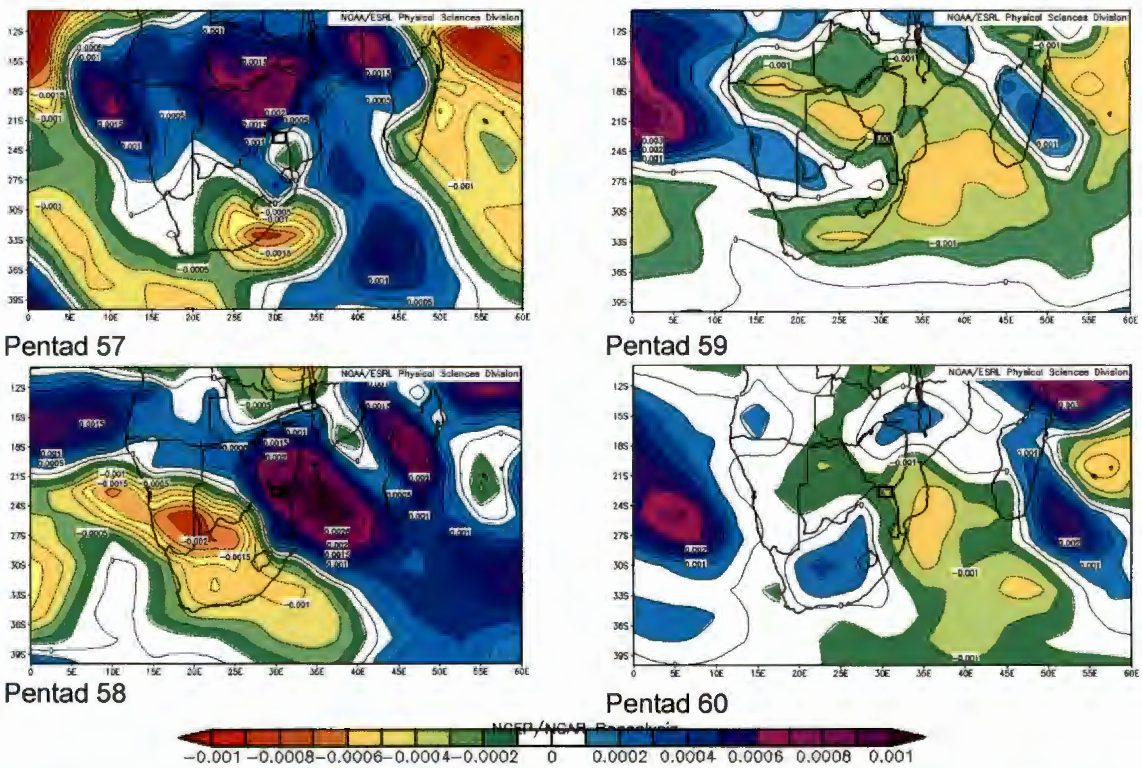

Figure 7.9: Specific humidity anomalies 20 days prior to 1984 seasonal rainfall onset. The contour intervals are $2x10^{-4}$ kg/kg

7.3.2 Specific Humidity Anomalies - During 1984 (Early Onset)

Pentad 61 (Figure 7.10) shows the atmospheric condition during the onset date of seasonal rainfall in the semi-arid zone of the study area. There is a strong evaporative centre (~ 1.5 g/kg) over Vhembe, while the Mozambique Channel and Zambia feature negative specific humidity anomalies. These advances are indicative of large-scale convective activity centred over Vhembe District, while the Mozambique Channel and Zambia are sink areas.

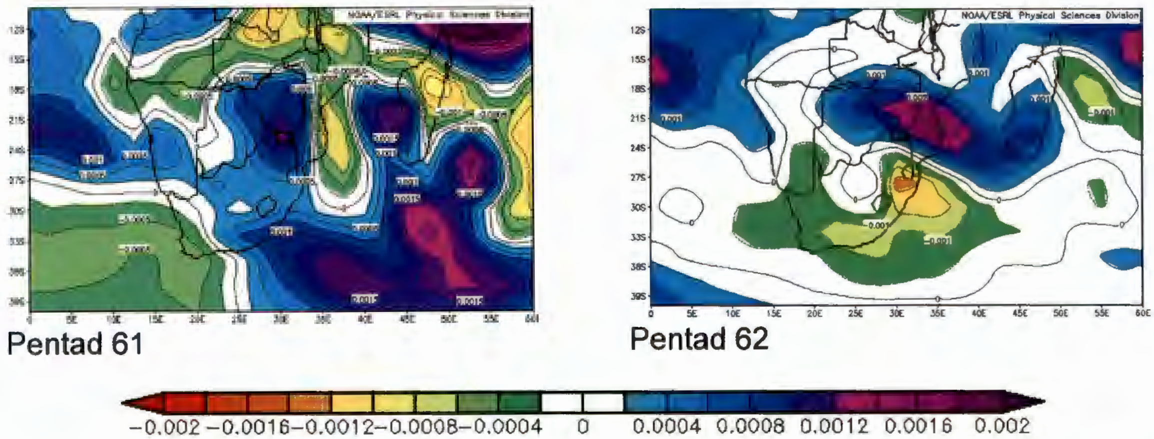

Figure 7.10: Specific humidity anomalies during 1984 seasonal rainfall onset. The contour intervals are $2x10^{-4}$ kg/kg

7.3.3 Specific Humidity Anomalies - 20 Days Prior to 1981 (Late Onset)

Figure 7.11 shows the evolution of mean specific humidity anomalies in the 20 days prior to the onset of seasonal rainfall of the late onset season during 1980 — 89 decade. Negative specific humidity anomalies characterise the atmosphere over the Indian Ocean, Madagascar and southern Africa (pentad 70). Anomalies with high values of negative specific humidity are centred between Mozambique, Mozambique Channel and Madagascar. Alternating positive and negative specific-humidity anomalies exist during the evolution and five days prior the onset, and a dipole of anomalous specific humidity is apparent. The Mozambique Channel has positive anomalies (> 4 g/kg) while negative anomalies (-3.0 g/kg) are over Botswana and Namibia.

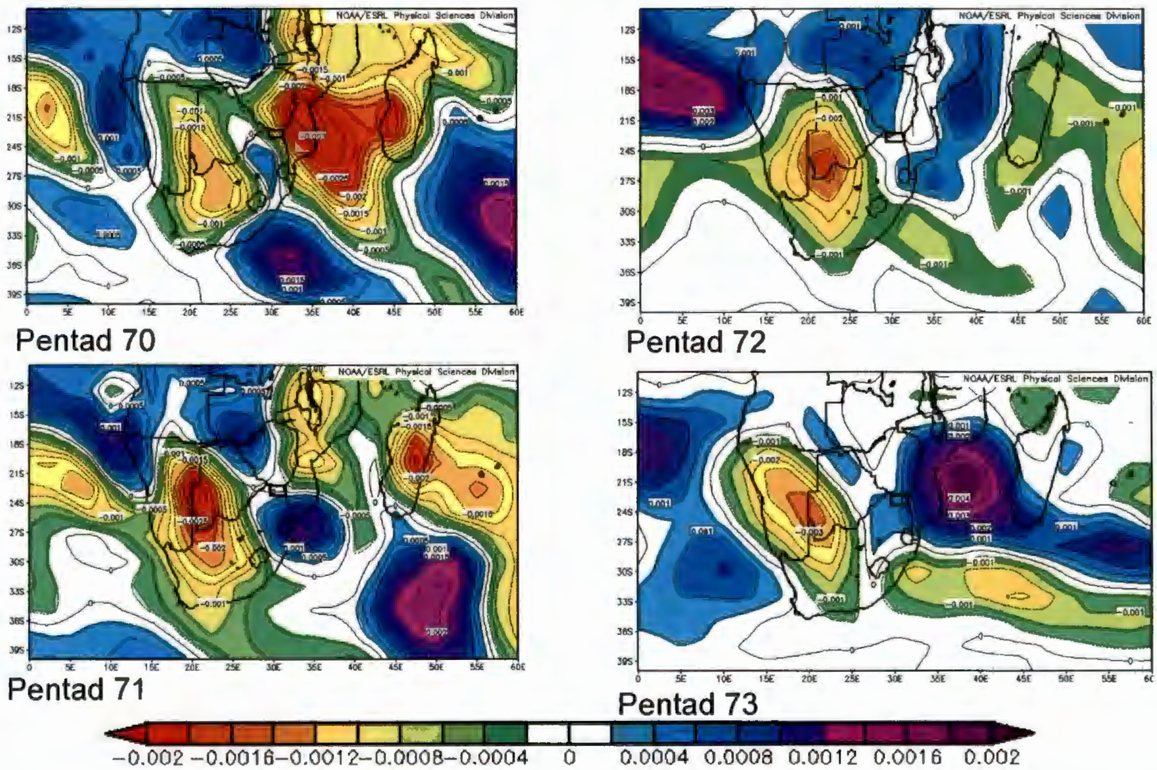

Figure 7.11: Specific humidity anomalies 20 days prior to 1981 seasonal rainfall onset. The contour intervals are $2x10^{-4}$ kg/kg

7.3.4 Specific Humidity Anomalies - During 1981 (Late Onset)

Rainfall in this season was so late that it started in pentad 1 of the following year (1982). From Figure 7.12, the study area was under weak positive specific humidity anomalies. A centre of high positive specific humidity anomalies occurs to the east in the Mozambique Channel. Meanwhile, a centre of high levels of negative specific humidity anomalies is located along the border between Namibia and Angola extending into the Atlantic Ocean. In the subsequent pentad, the area of moisture-evaporative area has shrunk while dry air covers most parts of southern Africa.

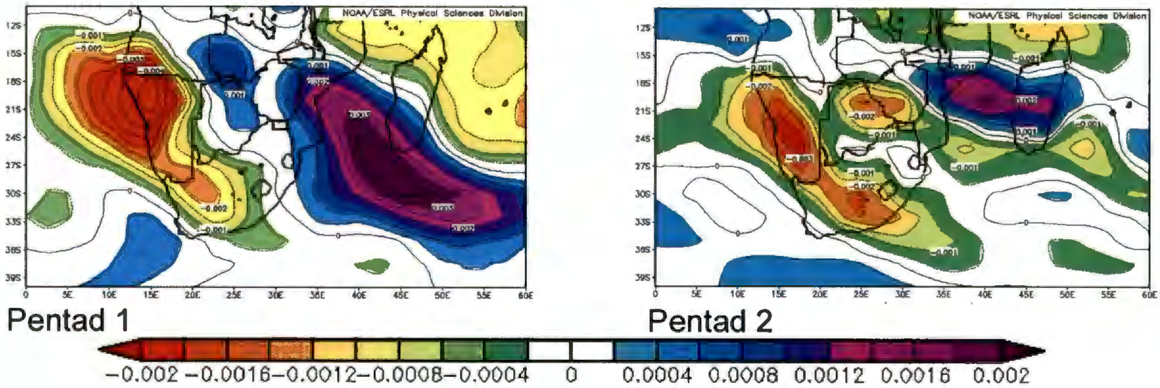

Figure 7.12: Specific humidity anomalies during 1981 seasonal rainfall onset. The contour intervals are $2x10^{-4}$ kg/kg

7.3.5 Specific Humidity Anomalies - 20 Days Prior 2001 (Early Onset)

Figure 7.13 illustrates the distribution of mean specific humidity anomalies in the 20 days prior to the 2001 seasonal rainfall onset – an early-onset season in the 2000 – 09 decade. Pentad 55 shows the distribution of negative specific humidity anomalies throughout the southern Africa region, while centres of positive specific humidity anomalies are over the adjacent oceans with the strongest confined in the Indian Ocean. The positive specific humidity anomalies are mostly confined over the Atlantic Ocean during pentad 57 and 58.

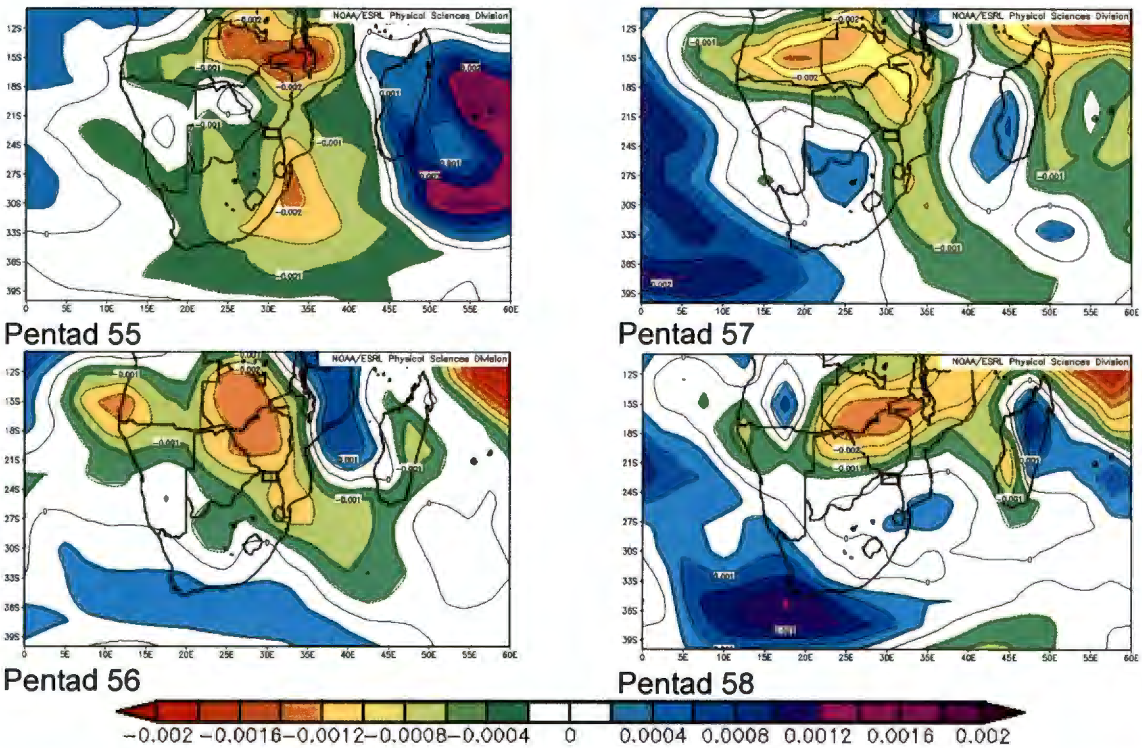

Figure 7.13: Specific humidity anomalies 20 days prior to 2001 seasonal rainfall onset. The contour intervals are $2x10^{-4}$ kg/kg

7.3.6 Specific Humidity Anomalies - During 2001 (Early Onset)

On the date of onset, an increase in the specific humidity anomaly value (~ 1 g/kg) over the study area is evident (Figure 7.14). A centre of high moisture evaporative source region is located in the SWIO, and negative anomalies exist over Namibia and northeastern Madagascar. Five days later, a large part of southern Africa is under high moisture evaporative regime of ~ 2 g/kg. In addition, a centre of high negative anomalies (~ -2.5 g/kg) exists over the Atlantic Ocean.

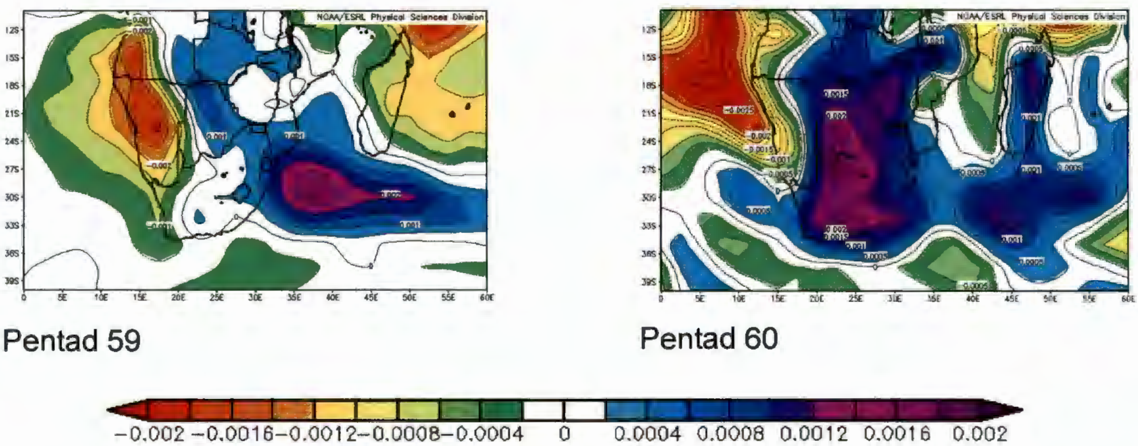

Figure 7.14: Specific humidity anomalies during 2001 seasonal rainfall onset. The contour intervals are 2×10^{-4} kg/kg

7.3.7 Specific Humidity Anomalies - 20 Days Prior 2007 (Late Onset)

Figure 7.15 shows the distribution of mean specific humidity anomaly 20 days prior to the 2007 seasonal rainfall onset in the semi-arid zone. From pentad 66, two centres of high levels of moisture are found in the northeastern part of Southern Africa and the Indian Ocean, while negative specific humidity anomalies occur over the Atlantic Ocean and east of Madagascar. In pentad 67, centres of positive anomalous specific humidity appear to be weakening. Generally, positive specific humidity anomalies occupy the study area in the pentad 20 days prior to onset.

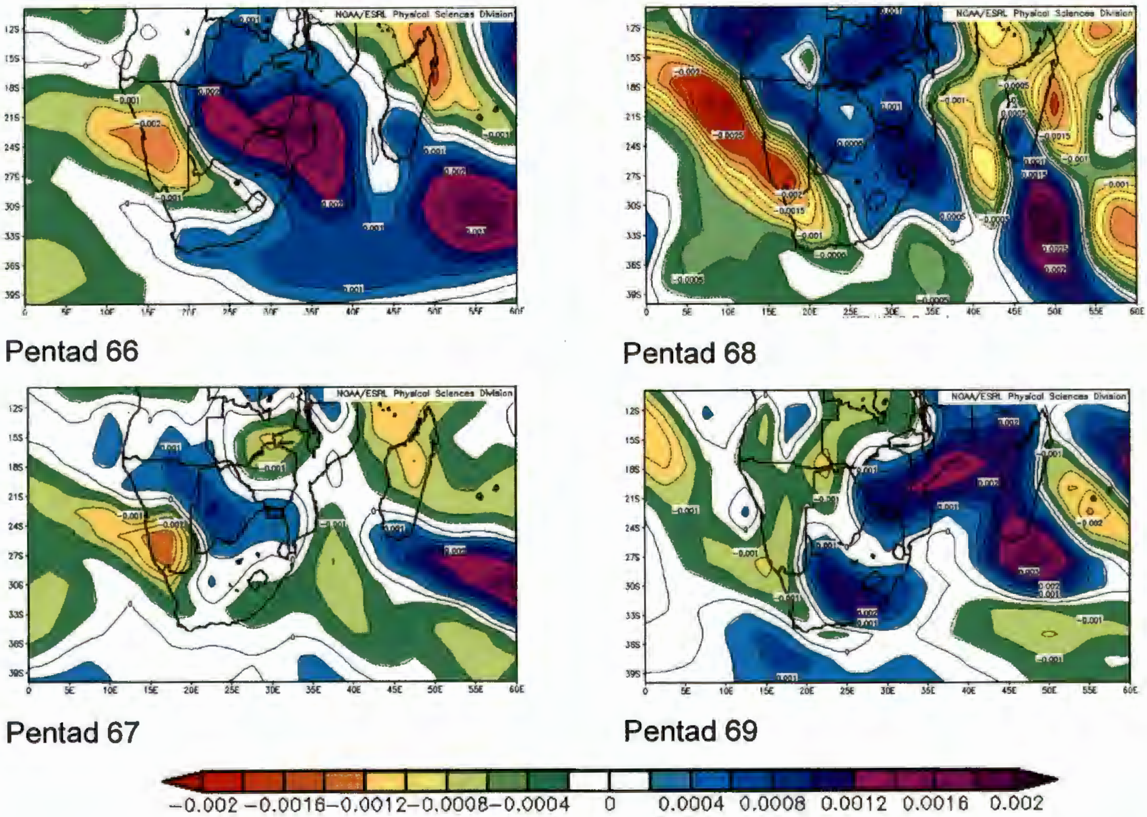

Figure 7.15: Specific humidity anomalies 20 days prior to 2007 seasonal rainfall onset. The contour intervals are 2×10^{-4} kg/kg

7.3.8 Specific Humidity Anomalies - During 2007 (Late Onset)

During the onset (pentad 70, Figure 7.16) in semi-arid zone, large parts of southern Africa remain under positive specific humidity anomalies. The study area features specific humidity anomalies of ~ 2 g/kg. On the other hand, a large area of negative specific humidity anomalies exists over the Atlantic Ocean and east of Madagascar. A pentad later, there is an increase (to ~ 3 g/kg) as a high moisture evaporative source regime occupies the study area.

There is a net increase in rainfall during seasonal rainfall onset in the semi-arid zone, accompanied by a net increase in moisture evaporative regime over the study area.

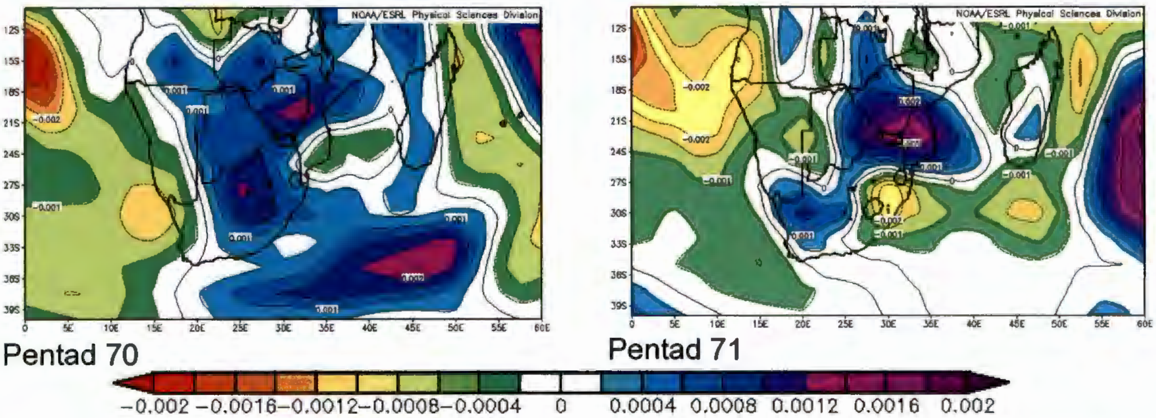

Figure 7.16: Specific humidity anomalies during 2007 seasonal rainfall onset. The contour intervals are $2x10^{-4}$ kg/kg

7.4 Integrated Moisture Flux Anomalies in the Humid Zone

7.4.1 Moisture Flux Anomalies - 20 Days prior 1986 Early Onset

During the evolution of the 20 days prior to the seasonal rainfall onset (Figure 7.17), the moisture flux anomalies in the study area show an easterly component, while a weak anticyclonic flux is maintained over much of South Africa. Patterns five days before the onset date show moderate levels of easterly transport from the Indian Ocean.

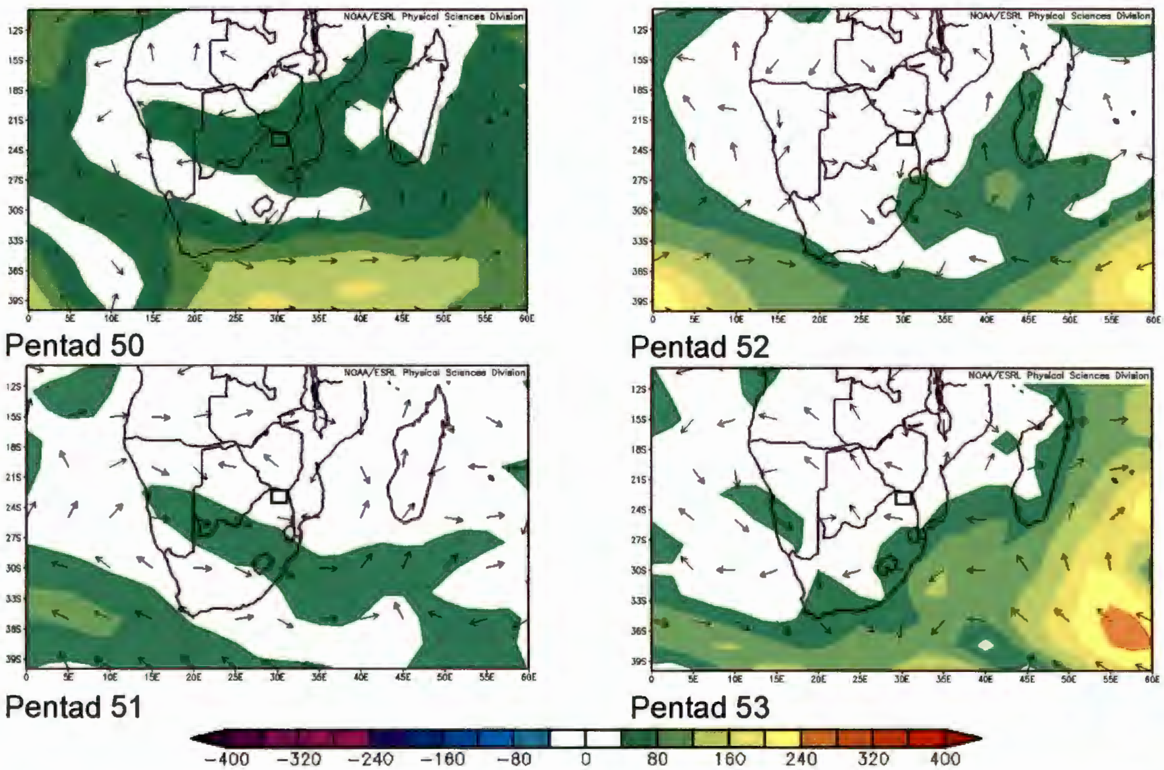

Figure 7.17: Moisture Flux Anomalies (kg s^{-1} m^{-1}) composites 20 days prior to 1986 seasonal rainfall onset.

7.4.2 Moisture Flux Anomalies - During 1986 Early Onset

The moisture flux anomalies (Figure 7.18) show that moisture transport is dominated by westerly flux over the study area during the seasonal onset (pentad 54). The westerly flow suggests that rainfall in the study area is not directly aided by large-scale moisture flow from the Indian Ocean during the onset period.

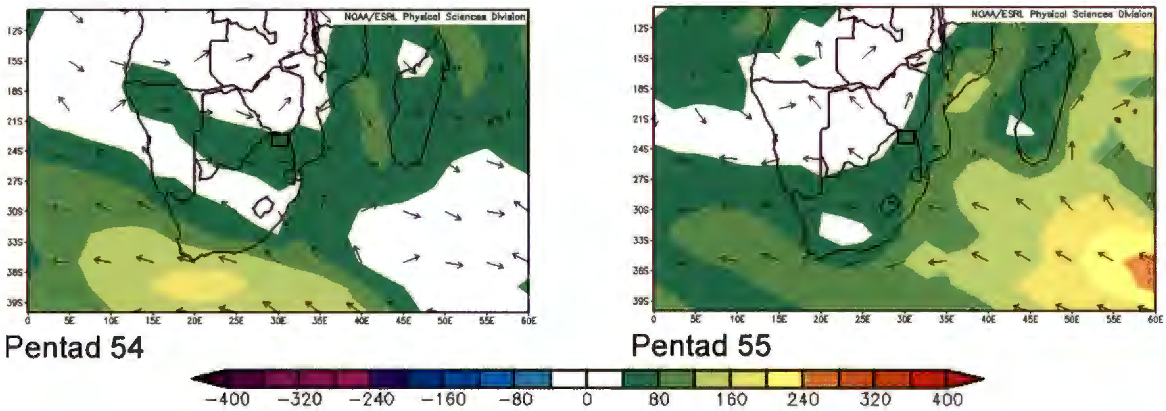

Figure 7.18: Moisture Flux Anomalies (kg m^{-1} s^{-1}) composites during 1986 early onset date

7.4.3 Moisture Flux Anomalies - 20 days prior 1985 Late Onset

In Figure 7.19, pentad 65 shows enhanced flow of moisture flux anomalies from the SWIO approximately 200 kg m^{-1} s^{-1} which appears to be the area of substantial water vapour. In the subsequent pentads, a flow from the southwest Indian Ocean essentially dominates. The most notable patterns are the cyclonic and anticyclonic flow in the SAO and SWIO respectively during pentad 67 and 68.

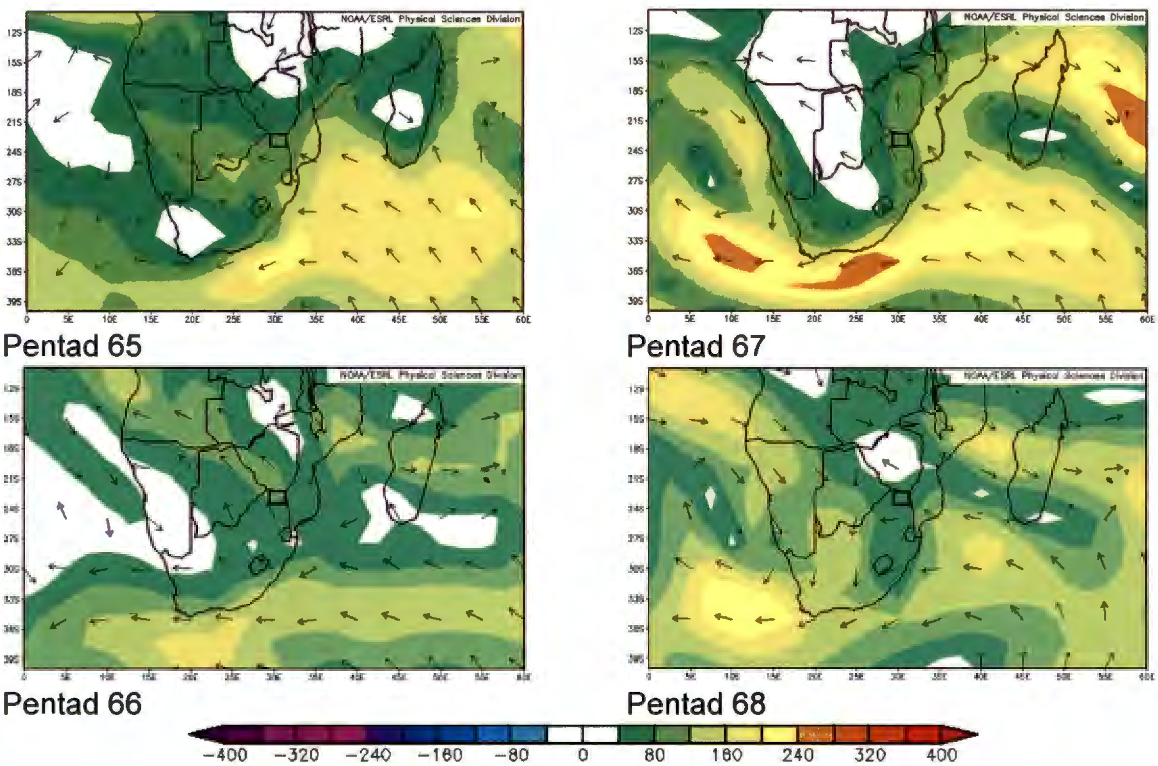

Figure 7.19: Moisture Flux Anomalies (kg m^{-1} s^{-1}) composites 20 days prior to 1985 seasonal rainfall onset.

7.4.4 Moisture Flux Anomalies - During 1985 Late Onset

Figure 7.20 shows that increased moisture transport occurs south of 36°S, 45°E in the SWIO with a northeasterly trajectory through southern Mozambique. Low moisture flux of ~ 50 kg m^{-1} s^{-1} is apparent over Vhembe District. During the following pentad, integrated moisture flux has increased to ~ 80 kg m^{-1} s^{-1} from the tropics and the Indian Ocean.

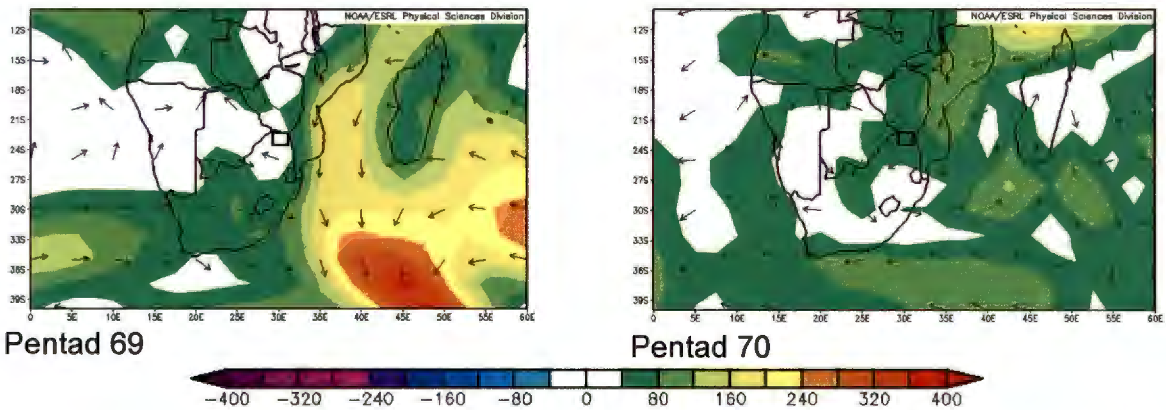

Figure 7.20: Moisture Flux Anomalies (kg $m^{-1}s^{-1}$) composites during 1985 seasonal rainfall onset.

7.4.5 Moisture Flux Anomalies - 20 Days Prior to 2001 Early Onset

Figure 7.21 shows the evolution of moisture flux anomalies for pentads 52, 53, 54 and 55. The most noticeable feature is the enhanced southeasterly-southerly moisture flux (~ 150 kg $m^{-1}s^{-1}$) in the Mozambique Channel at pentad 55 and moisture flux from the tropics in pentad 53. Meanwhile, moisture flux anomalies over the study area rise to ~ 100 kg $m^{-1}s^{-1}$.

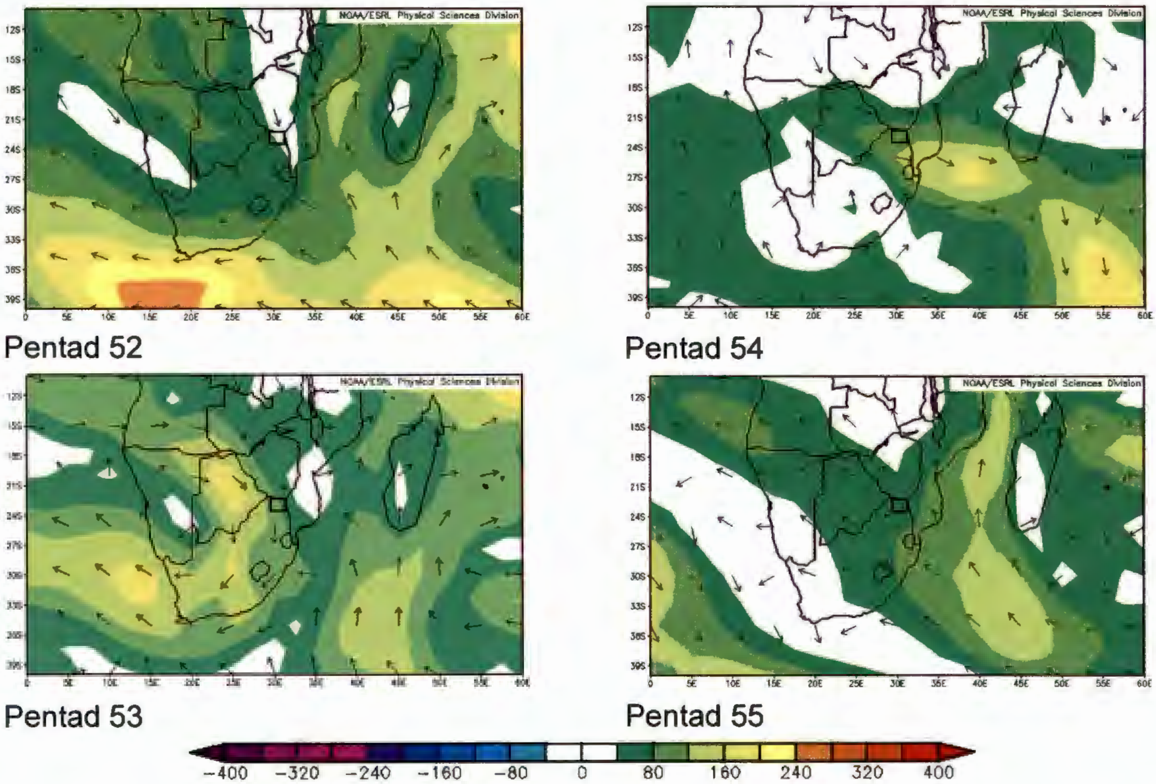

Figure 7.21: Moisture Flux Anomalies (kg $m^{-1}s^{-1}$) composites 20 days prior to 2001 seasonal rainfall onset.

7.4.6 Moisture Flux Anomalies - During 2001 Early Onset

During the onset date (Figure 7.22), a weak cyclonic flow exists over the study area with moisture flux of ~ 60 kg $m^{-1}s^{-1}$. Generally, the moisture flux direction (from east to west) indicates that the moisture flow source is the Indian Ocean with moisture flowing into the study area. In the ensuing pentad (pentad 57), westward propagation of moisture flux anomalies deepens which leads to an increase in the accumulation of moisture into the study area to about 150 kg $m^{-1}s^{-1}$.

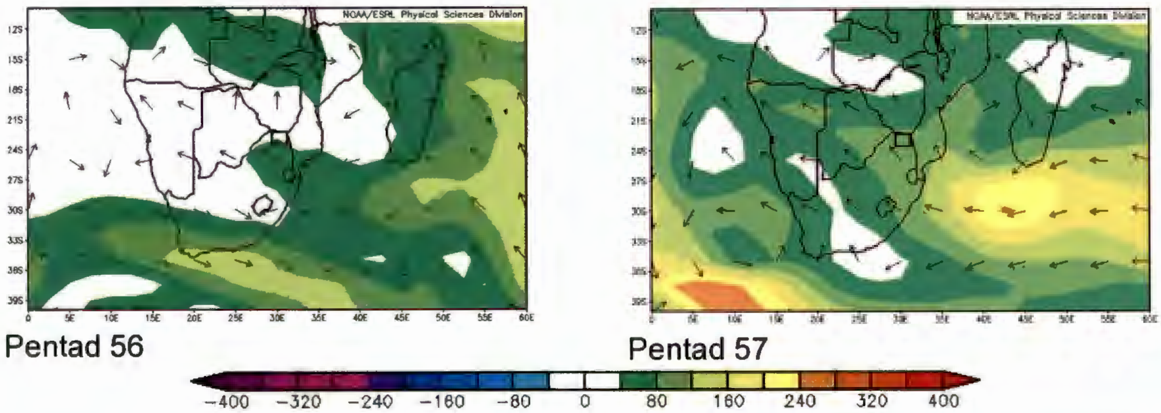

Figure 7.22: Moisture Flux Anomalies (kg $m^{-1}s^{-1}$) composites during 2001 seasonal rainfall onset.

7.4.7 Moisture Flux Anomalies - 20 days Prior 2006 Late Onset

Figure 7.23 depicts the directions and the intensities of moisture flux for 20 days prior to the seasonal rainfall onset in 2006. It demonstrates that almost all the incursions of moisture flux anomalies into the study area result from the Indian Ocean, except for pentad 68 when a southwesterly flux was the dominant component. This is suggests that Indian Ocean is the key source of moisture to Vhembe District prior to the onset of 2006-seasonal rains.

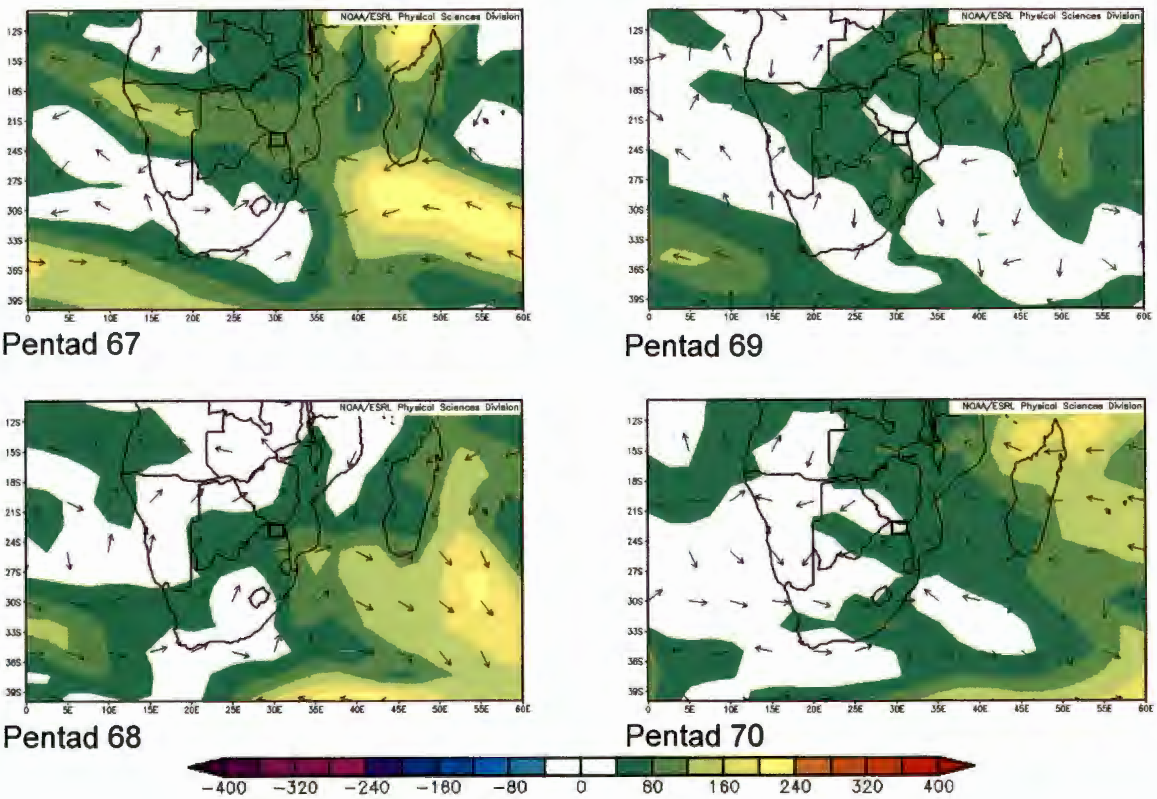

Figure 7.23: Moisture Flux Anomalies (kg $m^{-1}s^{-1}$) composites 20 days prior to 2006 seasonal rainfall onset.

7.4.8 Moisture Flux Anomalies - During 2006 Late Onset

During 2006 seasonal rainfall onset (pentad 71), which is illustrated in Figure 7.24, an anticyclonic transport of moisture with a centre over the Mozambique Channel is apparent. Westward flow of moisture from the Indian Ocean is deflected by the anticyclone cell that leads to the advection of moisture into the northeastern part of South Africa. Meanwhile, the study area experiences ~ 100 kg $m^{-1}s^{-1}$ moisture flux anomalies. In pentad 72, increasing moisture flux anomalies are further enhanced over SWIO. However, westerly flow of dry moisture flux anomalies from the Atlantic Ocean leads to reduced moisture in large parts of South Africa.

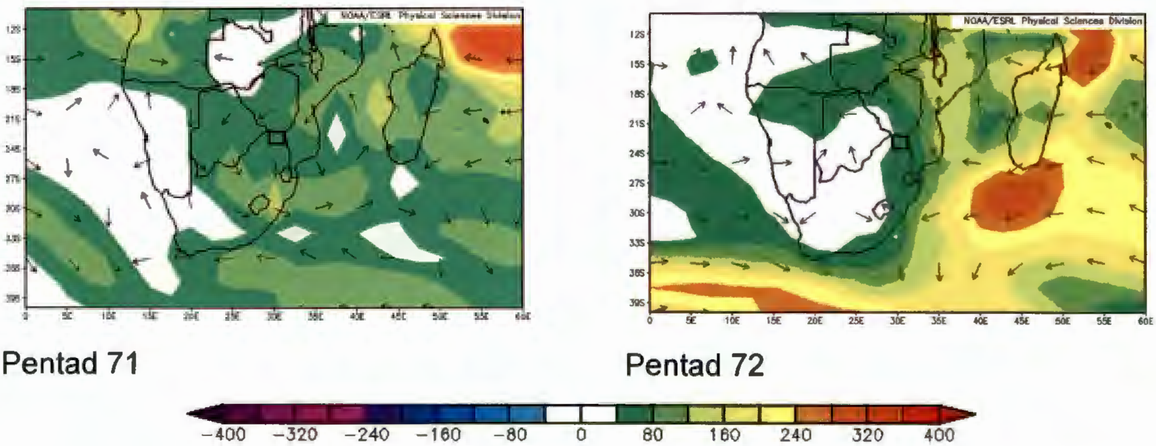

Figure 7.24: Moisture Flux Anomalies (kg $m^{-1}s^{-1}$) composites during 2006 seasonal rainfall onset.

7.5 Moisture Flux Anomalies Analysis - Semi-arid Zone

7.5.1 Moisture Flux Anomalies - 20 Days Prior 1984 Early Onset

In Figure 7.25, pentad 57 shows dry air over northeastern South Africa. At pentad 58, the Indian Ocean south of Madagascar experienced a moisture flux maximum of ~ 240 kg m^{-1} s^{-1}. Pentad 59 and 60 patterns indicate that the moisture advected to the study area prior to the seasonal rainfall onset of 1984 emanated from the Mozambique Channel. This is in agreement with Hewitson et al. (2012).

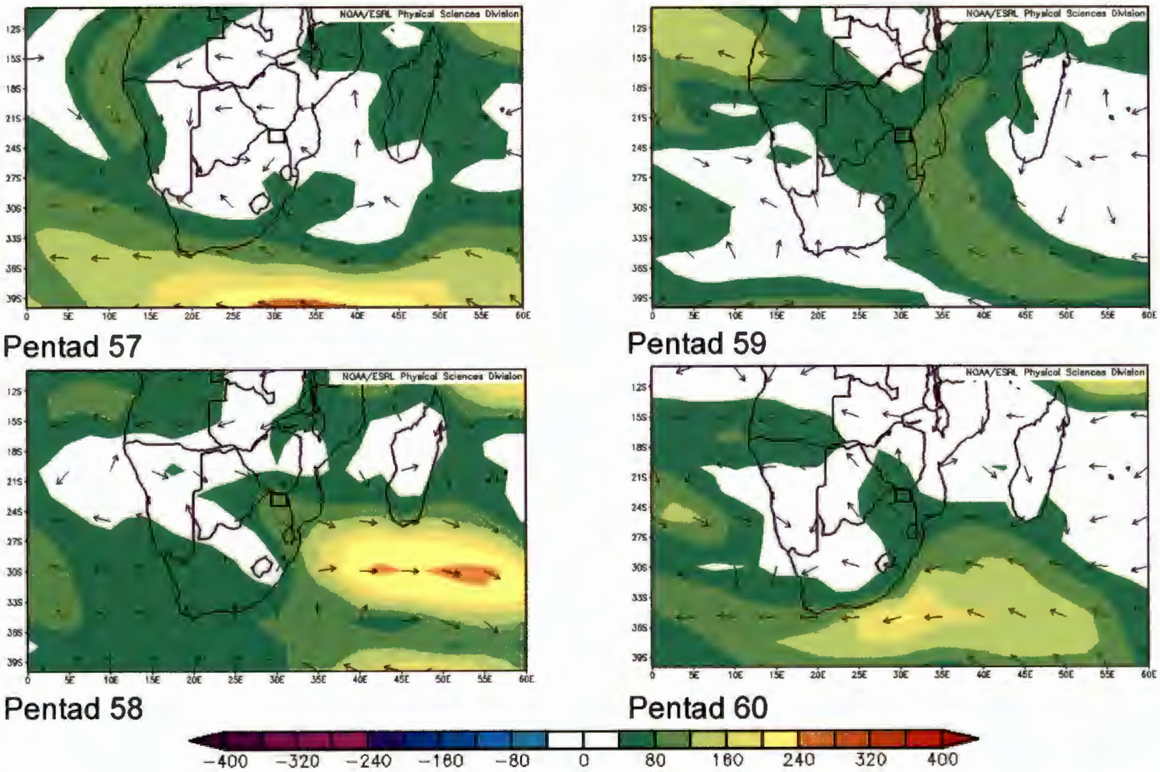

Figure 7.25: Moisture Flux Anomalies (kg $m^{-1}s^{-1}$) composites 20 days prior to 1984 seasonal rainfall onset.

7.5.2 Moisture Flux Anomalies - During 1984 Early Onset

The onset pentad (pentad 61) is characterised by convergence of moisture flux from the Indian Ocean and Atlantic Ocean over eastern South Africa (Figure 7.26). However, these two fluxes have different moisture contents; the Atlantic Ocean flow is relatively dryer than the flow from the Indian Ocean. Therefore, the moisture realised over the study area is lower than that in the Indian Ocean.

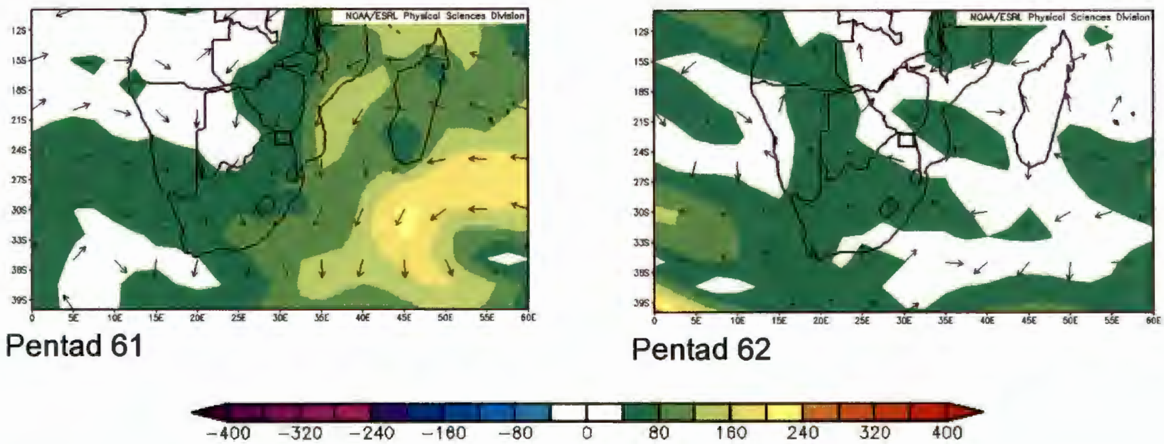

Figure 7.26: Moisture Flux Anomalies (kg $m^{-1}s^{-1}$) composites during 1984 seasonal rainfall onset.

7.5.3 Moisture Flux Anomalies - 20 Days Prior to 1981 Late Onset

Figure 7.27 depicts the directions and the intensities of moisture flux for 20 days prior to the seasonal rainfall onset in 1981. The dominating moisture flux towards Vhembe District is from the west, which suggests that less moisture is available there in the first 15 days (up to pentad 72). Five days before the onset date, a weak convergence accumulates moisture over the northeastern part of South Africa, mainly from the Mozambique Channel.

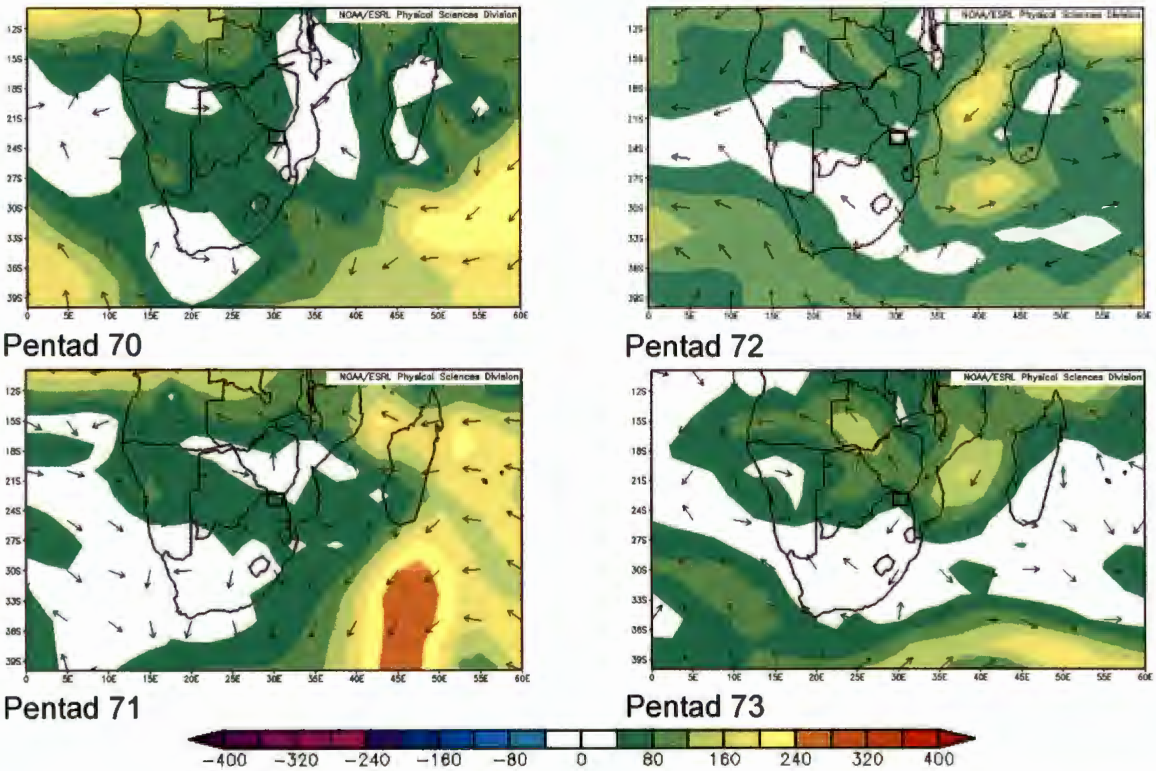

Figure 7.27: Moisture Flux Anomalies (kg $m^{-1}s^{-1}$) composites 20 days prior to 1981 seasonal rainfall onset.

7.5.4 Moisture Flux Anomalies - During 1981 Late Onset

Divergence of moisture over the southernmost part of South Africa (Figure 7.28) results in weak moisture anomalies (100 kg m^{-1} s^{-1}) in most parts of South Africa during the 1981 – 82 season onset, which happened in pentad 1 of 1982. The westerly flow from the Atlantic Ocean brought dry air to the study area. Meanwhile the maximum moisture anomalies were in the Mozambique Channel. Dry air over the study area persisted into the following pentad.

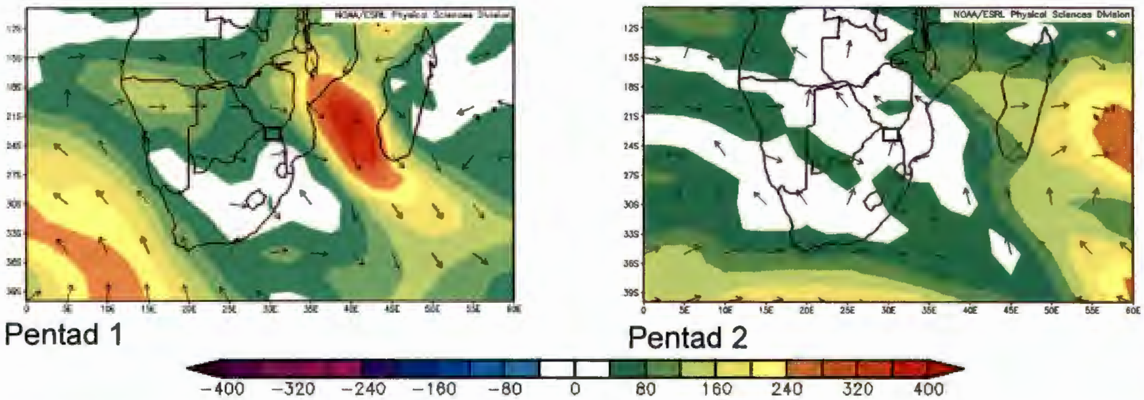

Figure 7.28: Moisture Flux Anomalies (kg $m^{-1}s^{-1}$) composites during 1981 seasonal rainfall onset

7.5.5 Moisture Flux Anomalies - 20 Days Prior to 2001 Early Onset

The integrated flux over the sub-continent exhibits anticyclonic anomalies with the flux changing from southeasterly to southerly over northeastern South Africa during the evolution of 20 days prior to rainfall onset (Figure 7.29). Predominantly, during this evolution, SWIO provided the bulk of the moisture to the study area.

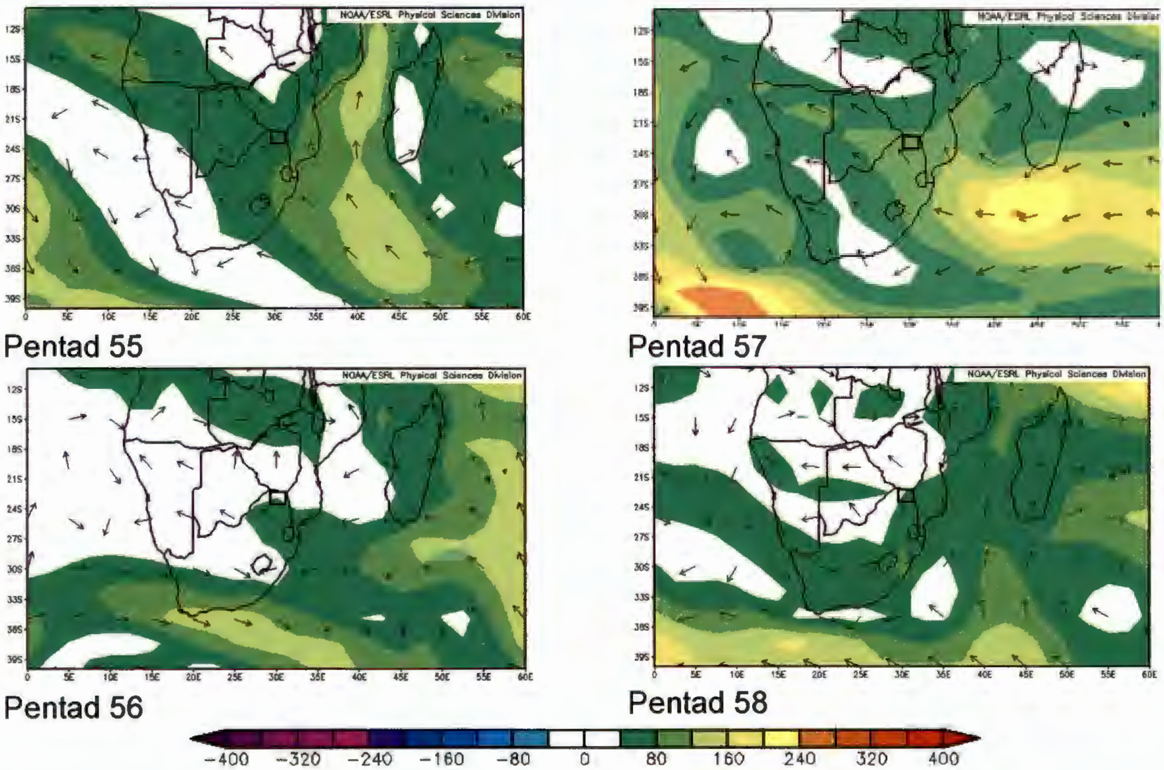

Figure 7.29: Moisture Flux Anomalies (kg $m^{-1}s^{-1}$) composites 20 days prior to 2001 seasonal rainfall onset

7.5.6 Moisture Flux Anomalies - During 2001 Early Onset

Figure 7.30 shows the anomaly of vertically integrated moisture flux during the 2001 onset of seasonal rainfall. The northeasterly flow of moisture is the notable feature over the study area, and persisted to the following pentad. Another distinctive feature is a cyclonic moisture flux over South Africa with a maximum in the Mozambique Channel at the onset initiation stage (pentad 59). These observations suggest that the Indian Ocean together with tropical Africa contributed to the moisture flux over the study area.

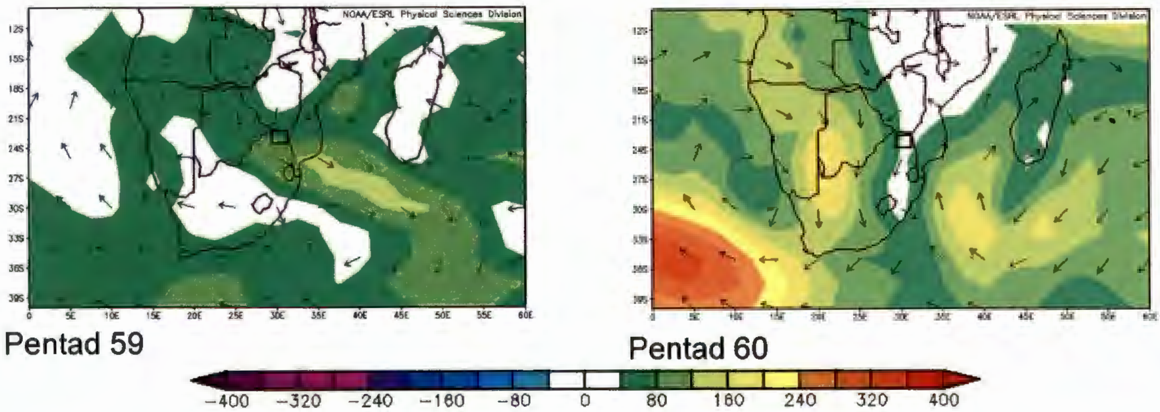

Figure 7.30: Moisture Flux Anomalies (kg $m^{-1}s^{-1}$) composites during 2001 seasonal rainfall onset

7.5.7 Moisture Flux Anomalies - 20 Days Prior to 2007 Late Onset

Figure 7.31 shows the evolution of integrated moisture flux anomalies in the 20 days prior to the 2000 – 08 seasonal rainfall onset – a late - onset season in the 2000 – 09 decade. The outstanding feature was the convergence of Indian Ocean moisture flux with tropical air over the study area during pentad 69. This action indicates that the study area is a recipient of integrated flux from SWIO and tropical Africa.

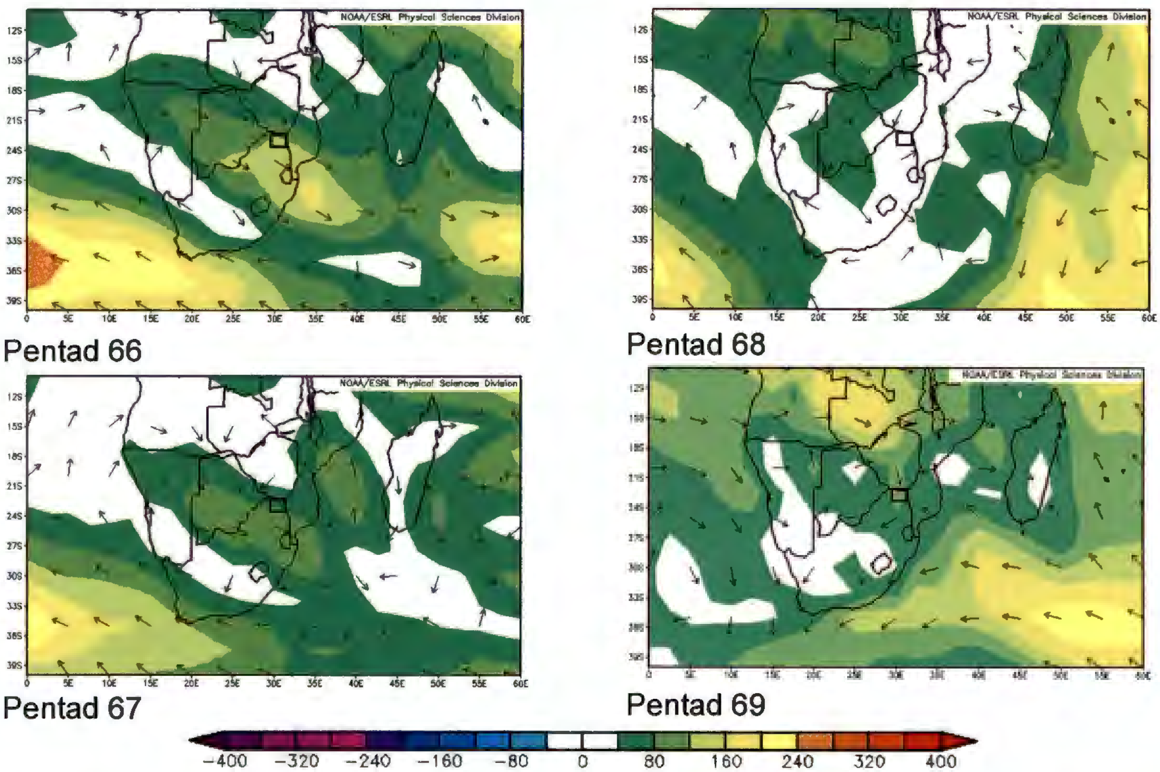

Figure 7.31: Moisture Flux Anomalies (kg $m^{-1}s^{-1}$) composites 20 days prior to 2007 seasonal rainfall onset

7.5.8 Moisture Flux Anomalies - During 2007 Late Onset

During the onset date (Figure 7.32, pentad 70), the dominant flux of Vhembe District is from the tropics with enhanced integrated moisture flux anomalies ~ 100 kg $m^{-1}s^{-1}$. Five days later, weak moisture flux anomalies overlay the study area; this can be associated with a dry spell due to moisture flux divergence near the study area.

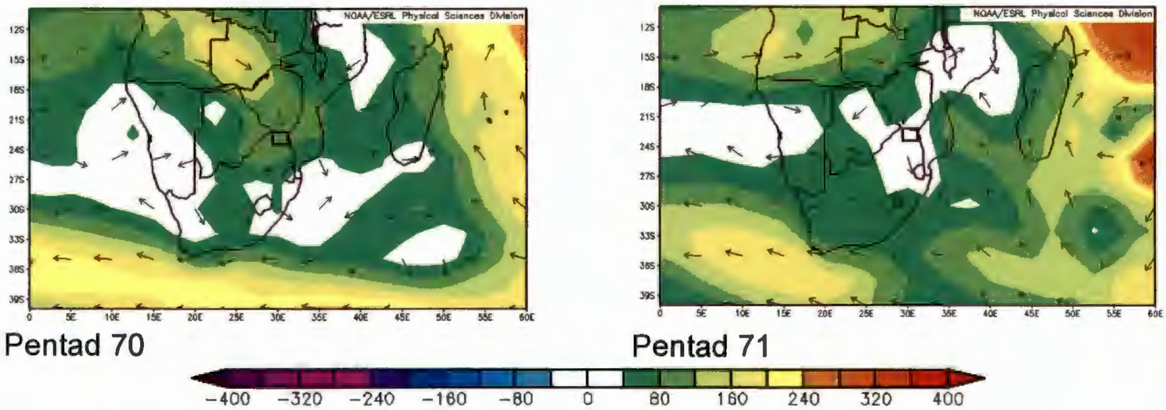

Figure 7.32: Moisture Flux Anomalies (kg $m^{-1}s^{-1}$) composites during 2007 seasonal rainfall onset

7.6 Vertical Motion Anomalies

This section evaluates the reanalysis vertical motion anomalies in relation to the corresponding seasonal rainfall onset dates. Vertical motion anomalies (Q) are movements of moisture per unit area per unit time. The transport and distribution of moisture in the atmosphere is generally through the large-scale circulation winds. The bulk of the horizontal transfer of water vapour takes place from the surface to the 500 hPa level (Newell et al., 1972; Chen, 1985). The vertical motion anomalies usually are complicated to interpret (Kabanda, 2004); therefore, this section will confine itself to significant patterns that are found to influence the rainfall onset in Vhembe District.

7.6.1 Vertical Motion Anomaly - 20 days Prior to 1986 Early Onset

Figure 7.33 presents the evolution of 500hPa vertical motion anomaly fields in the 20 days before the 1986 early season onset in the humid zone. A centre of vertical upward motion anomalies ~ -0.01 Pa s^{-1} is apparent over the northern part of South Africa while a large centre of strong descending motion occupies the southwest Indian Ocean (SWIO) at pentad 50. A strong rising motion occurs over southern Africa with a centre in Namibia (pentad 51). This pattern is short-lived as it is displaced by subsidence during pentad 52. The study area maintained a weak rising motion during the twenty days prior to the seasonal rainfall onset.

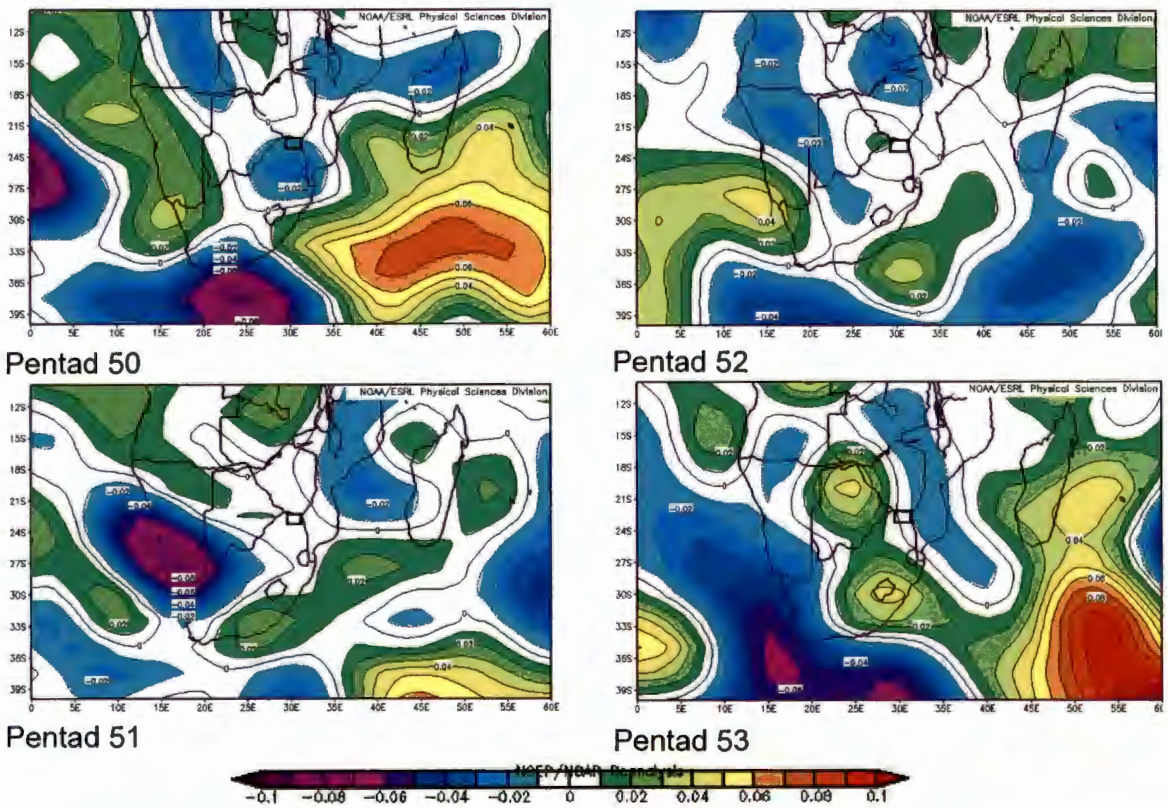

Figure 7.33: vertical motion anomalies (2 x 10^{-4} Pa s^{-1}) 20 days prior to 1986 seasonal rainfall onset

7.6.2 Vertical Motion Anomaly - During 1986 Early Onset

During onset stage (Figure 6.34), Vhembe District experienced weak subsidence. The most striking feature is the anomalous subsidence observed over Western Cape, while offshore in the SWIO rising motion is displayed in a NW-SE band. The study area remained quiescent from the onset pentad to the following one.

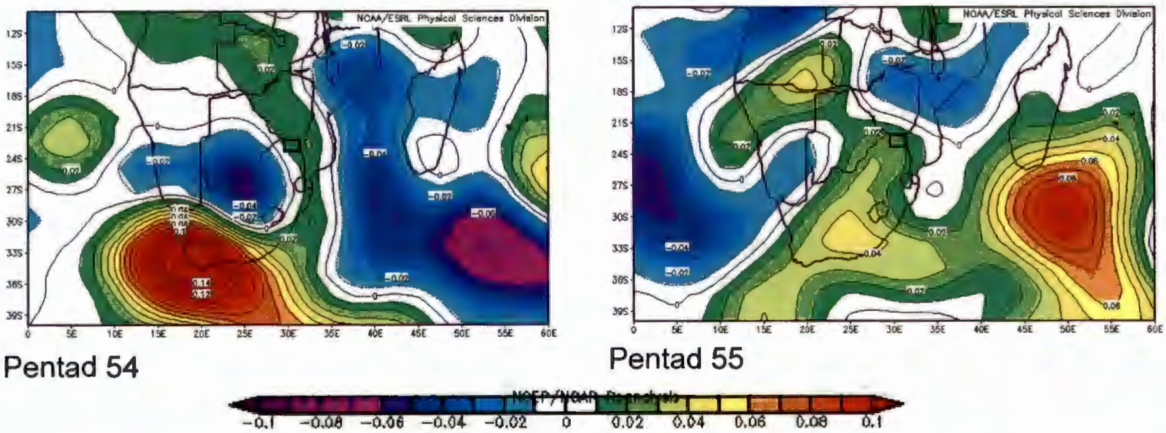

Figure 6.34: Vertical motion anomaly (2 x 10^{-4} Pa s^{-1}) during 1986 seasonal rainfall onset

7.6.3 Vertical Motion Anomaly - 20 days prior to 1985 Late Onset

In Figure 7.35 the prominent feature is that the study area displays positive anomalous vertical motion throughout the 20 days prior to the season onset. Strong rising motion in the interior of South Africa and over Madagascar (pentad 67 & 68) appears as the main feature of the vertical motions. A tongue of sinking motion that emanated from the SWIO and extended to the study area implies Vhembe District is under the influence of moisture divergence.

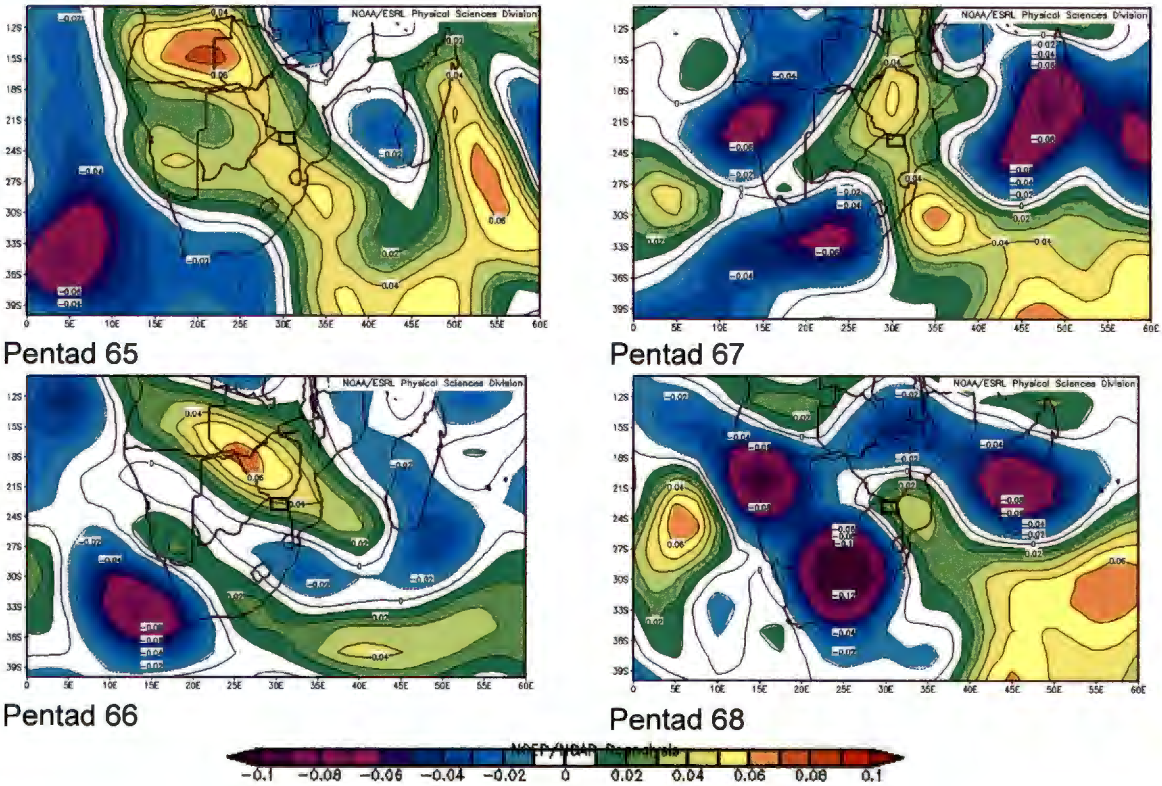

Figure 7.35: Vertical motion anomaly (2 x 10^{-4} Pa s^{-1}) 20 days prior to 1985 seasonal rainfall onset

7.6.4 Vertical Motion Anomaly - During 1985 Late Onset

The major areas of action in Figure 6.36 are the SWIO (located 36-39°S, 40-45°E), which features sinking motion, and southeast of Madagascar, that experienced subsidence, during pentad 69. In addition, the study area obtains the sinking motion that extends north-westward to Zimbabwe, Botswana and Namibia. Five days later, the vertical motion anomalies over the study area progressively changed from sinking to rising motion.

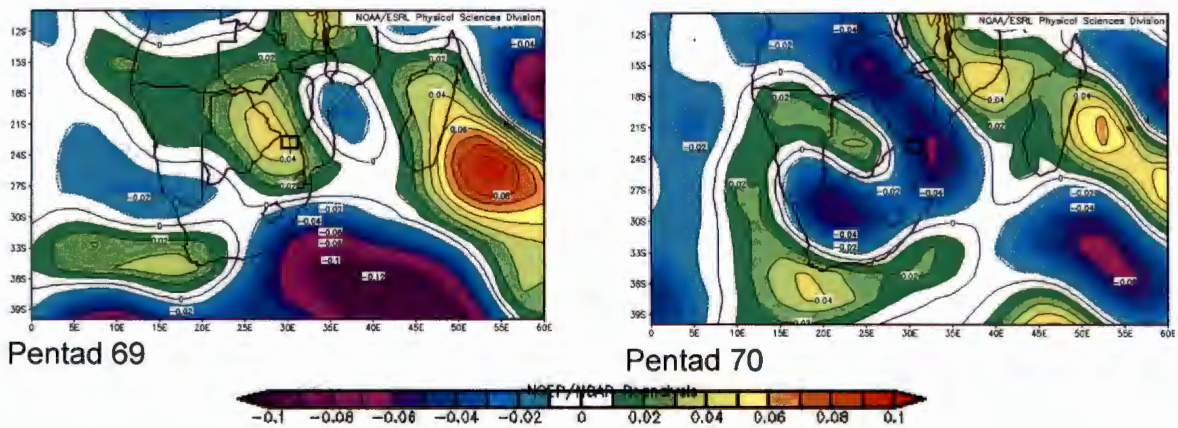

Figure 7.36: Vertical motion anomalies (2 x 10^{-4} Pa s^{-1}) during 1985 seasonal rainfall onset

7.6.5 Vertical Motion Anomaly - 20 Days Prior to 2001 Early Onset

During pentad 52 (Figure 7.37), a NW-SE band of strong ascending motion anomalies occupies much of southern Africa extending to the Indian Ocean. Another strong rising motion exists during pentad 53, centred over Botswana. In pentad 55, the whole of South Africa is dominated by positive vertical anomalies of ~ 0.06 Pa s^{-1}, which have their maximum in the Mozambique Channel. This implies that the study area is part of a moisture divergence (see 7.4.5).

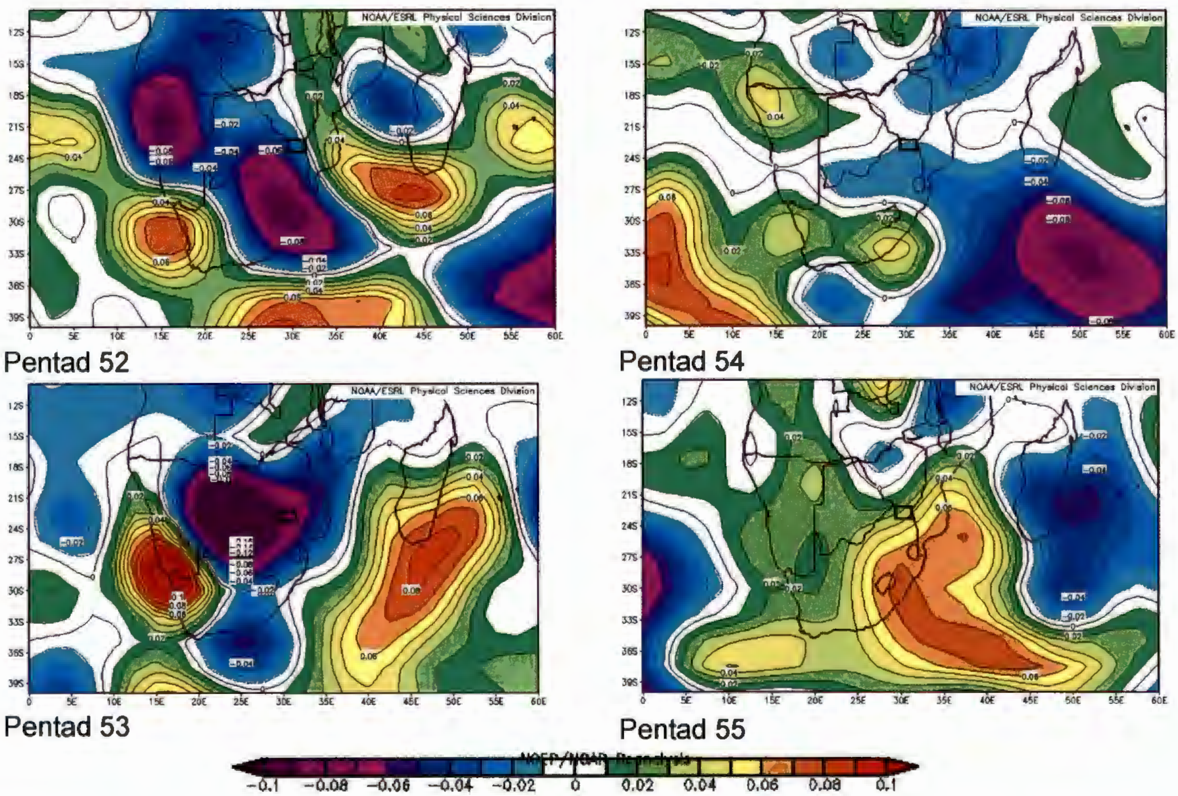

Figure 7.37: Vertical motion anomaly (2 x 10^{-4} Pa s^{-1}) 20 days prior to 2001 seasonal rainfall onset

7.6.6 Vertical Motion Anomaly - During 2001 Early Onset

At the onset stage (pentad 56), a relatively strong narrow band negative vertical motion anomalies developed over the south Indian Ocean and through the Mozambique Channel (Figure 7.38). A tongue of subsidence with its origin further east exists and extends to southeast Madagascar. Continental South Africa is generally under weak subsidence. Five days later, strong negative motion anomalies occur over the Atlantic Ocean and south of Madagascar, with strong positive anomalies over the northeastern part of southern Africa. These observations suggest that the study area is not a recipient of large scale convective forcing during the 2001 seasonal rainfall onset.

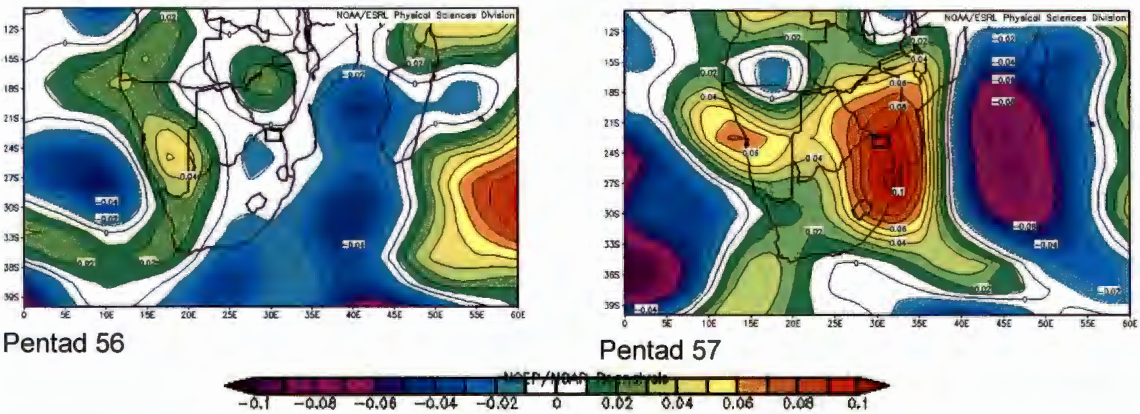

Figure 7.38: Vertical motion anomalies (2 x 10^{-4} Pa s^{-1}) during 2001 seasonal rainfall onset

7.6.7 Vertical Motion Anomaly - 20 Days Prior to 2006 Late Onset

Through the evolution of vertical motion anomaly 20 days before 2006 seasonal rainfall, Vhembe District and most part of South Africa are subsident (Figure 7.39). North of 12°S, especially to the east of 25°E, display a strong rising motion. Some pockets of rising motion are apparent south of 27°S.

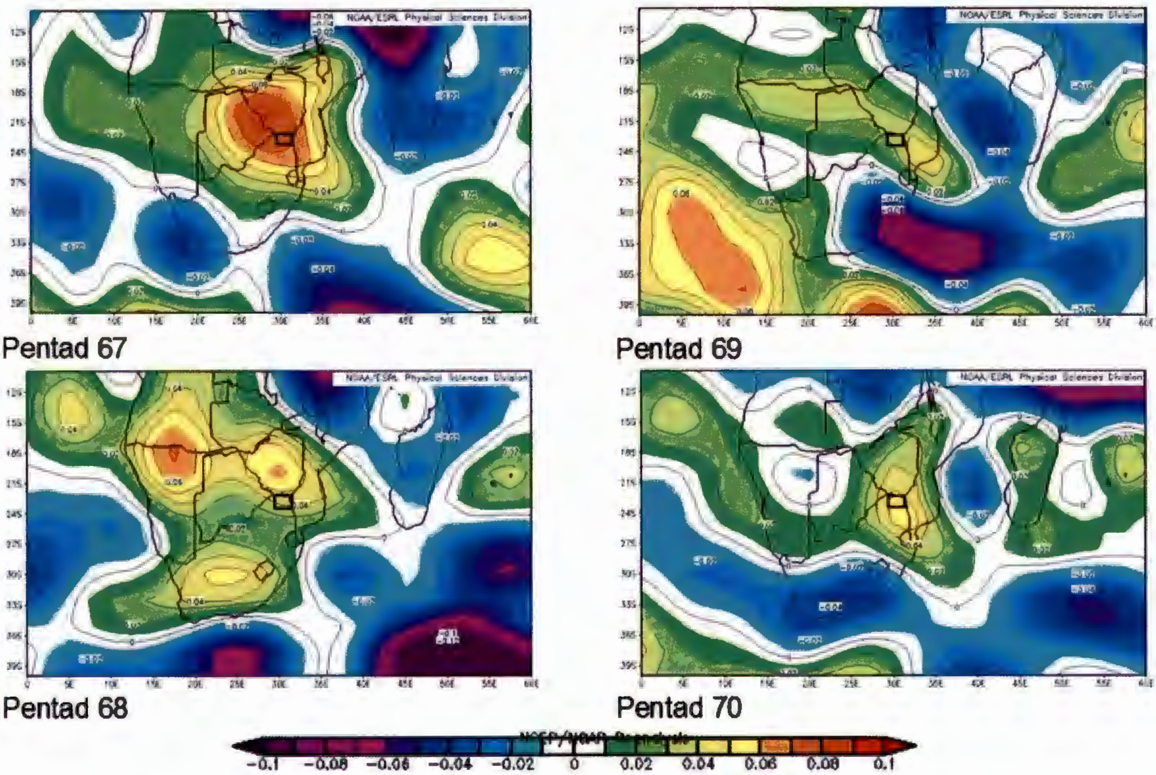

Figure 7.39: Vertical motion anomaly (2 x 10^{-4} Pa s^{-1}) 20 days prior 2006 seasonal rainfall onset

7.6.8 Vertical Motion Anomaly - During 2006 Late Onset

Figure 7.40 displays sinking motion over Vhembe District; meanwhile, distinct cell structures of negative vertical anomalies exist over the Atlantic Ocean, the interior of South Africa and the Indian Ocean. The rising motion, seen emanating from the tropics, as described in the previous section, continue to stretch southwards. This observation indicates that the equatorial trough (ITCZ) was late to arrive near southern Africa. Five days later, the centre of subsidence in the south of Mozambique is displaced northward due to the development of a pocket of relatively weak negative motion over the northern part of South Africa.

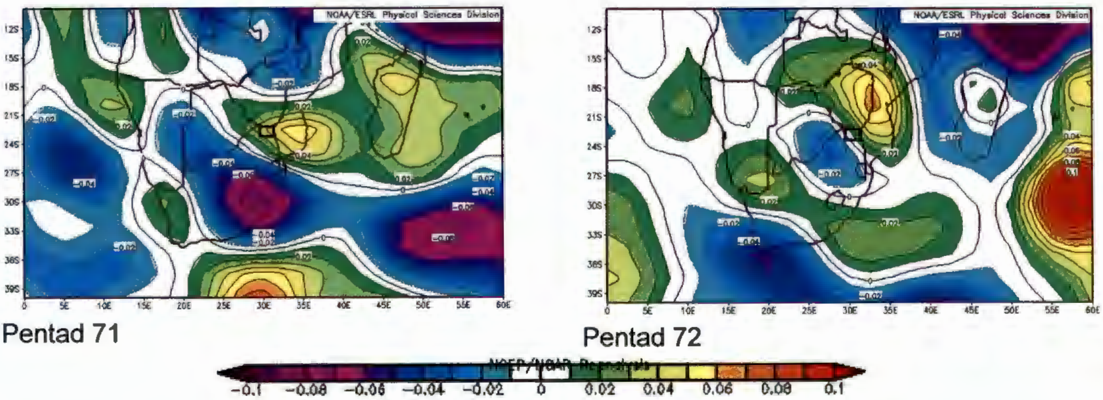

Figure 7.40: Vertical motion anomalies (2 x 10^{-4} Pa s^{-1}) during 2006 seasonal rainfall onset

7.7 Semi-Arid Zone Mean Anomalies Vertical Motion Analysis

7.7.1 Vertical Motion Anomalies - 20 Days Prior to 1984 Early Onset

Figure 7.41 shows the distribution of vertical motion anomalies in the 20 days prior to the 1984 seasonal rainfall onset. From pentad 57, two distinct cell structures of upward vertical anomalies occur over the South Indian Ocean extending to northeast South Africa through the Mozambique Channel. Strong subsidence centred over Western Cape and extending north and south is evident. Meanwhile, Madagascar experienced a strong downward motion. Ten days before the onset stage, sinking motion dominated most southern Africa regions with strong upward motion observed over the Atlantic and Indian Ocean.

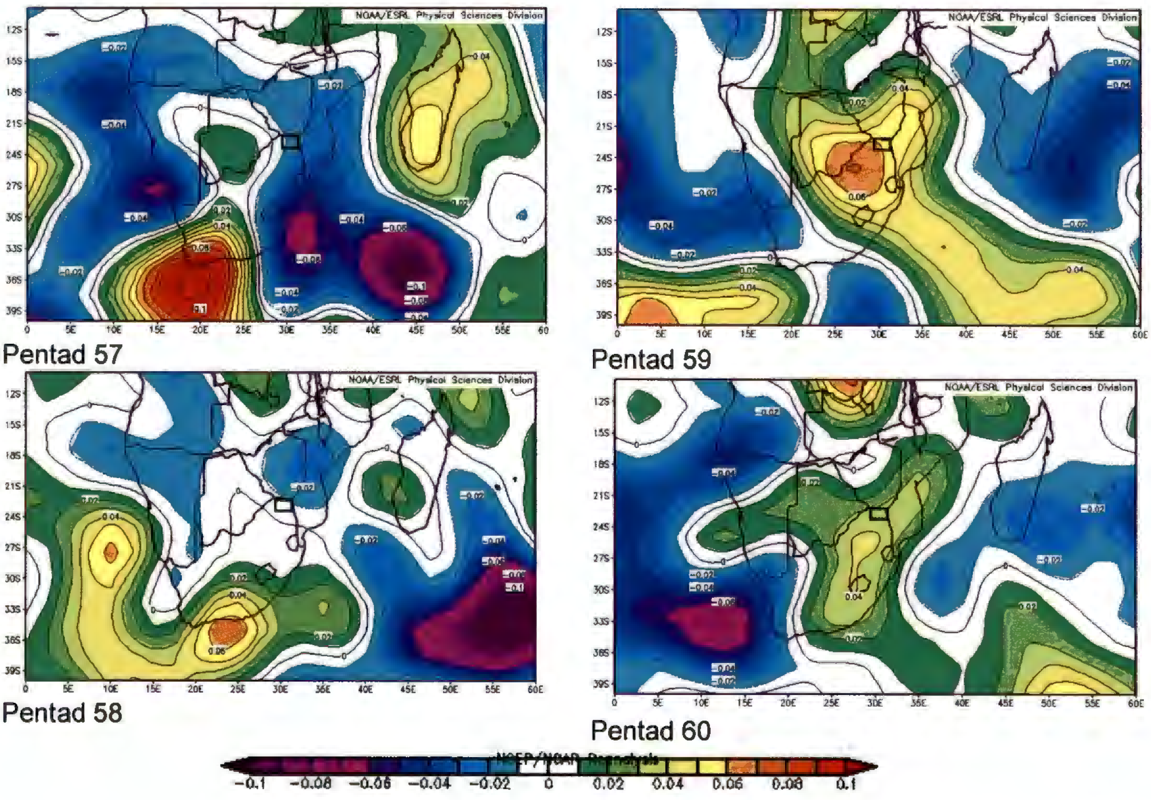

Figure 7.41: Vertical Motion Anomalies (2 x 10^{-4} Pa s^{-1}) 20 days prior 1984 seasonal rainfall onset

7.7.2 Vertical Motion Anomalies - During 1984 Early Onset

Convective activities prevail in southern Africa and in the adjacent ocean part during the onset pentad (Figure 7.42). As a result, the vertical motion anomalies over northeastern South Africa are ~ -0.01 Pa s^{-1}. Five days later, the magnitude of the upward vertical motion anomalies over northeastern South Africa increased to ~ -0.06 Pa s^{-1}. It is apparent from these observations that large-scale convective activities are concomitant with rainfall onset in the semi-arid zone during the early onset.

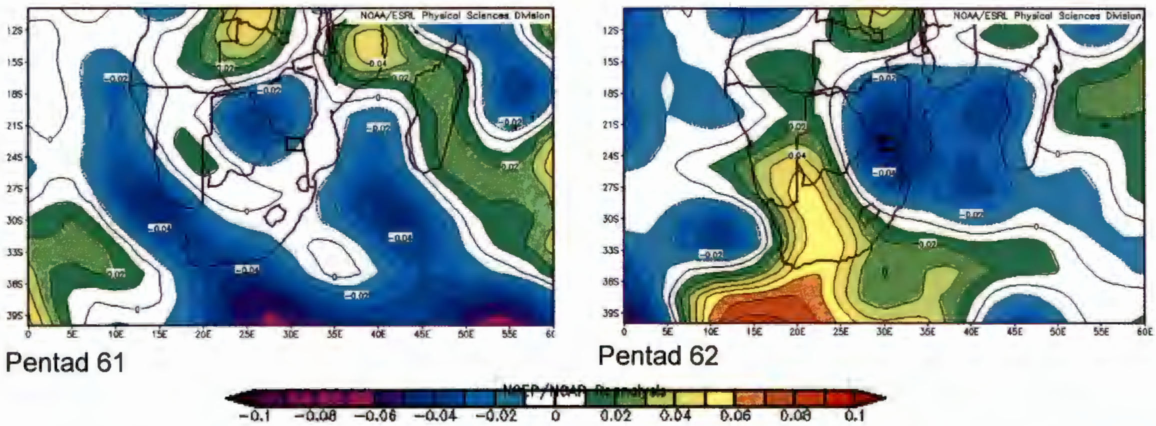

Figure 7.42: Vertical Motion Anomalies (2 x 10^{-4} Pa s^{-1}) during 1984 seasonal rainfall onset

7.7.3 Vertical Motion Anomalies - 20 Days Prior to 1981 Late Onset

The evolution of mean vertical motion anomaly composites 20 days prior to the seasonal rainfall onset of the late season during 1980 – 89 decade are highlighted by Figure 7.43. The most notable feature is that subsidence was maintained over the southern Africa region and various pockets of rising motion especially in the Indian Ocean.

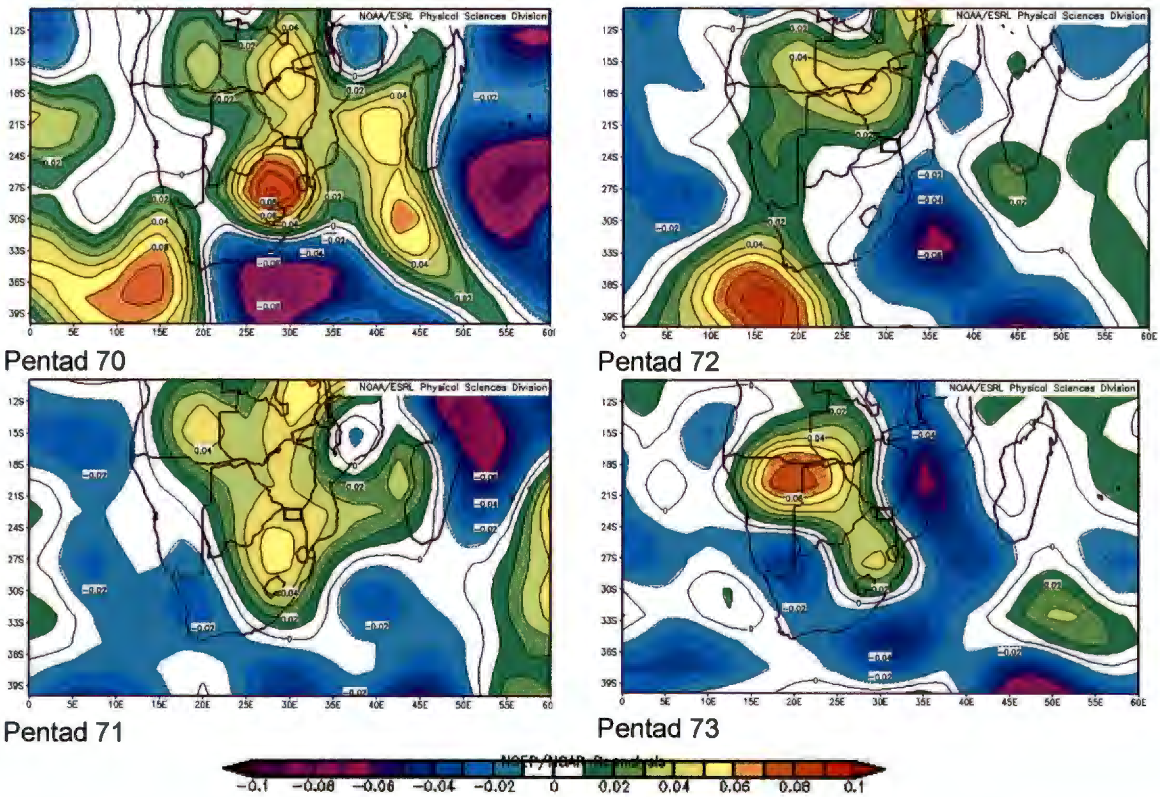

Figure 7.43: Vertical Motion Anomalies (2 x 10^{-4} Pa s^{-1}) 20 days prior 1981 seasonal rainfall onset

7.7.4 Vertical Motion Anomalies - During 1981 Late Onset

During the onset stage (Figure 7.44), which occurred on the first pentad of the following year (1982), a strong rising motion occurs over southern Africa with a centre in the Mozambique Channel. Meanwhile, there are enhanced descending vertical motion anomalies over the southeast Atlantic Ocean.

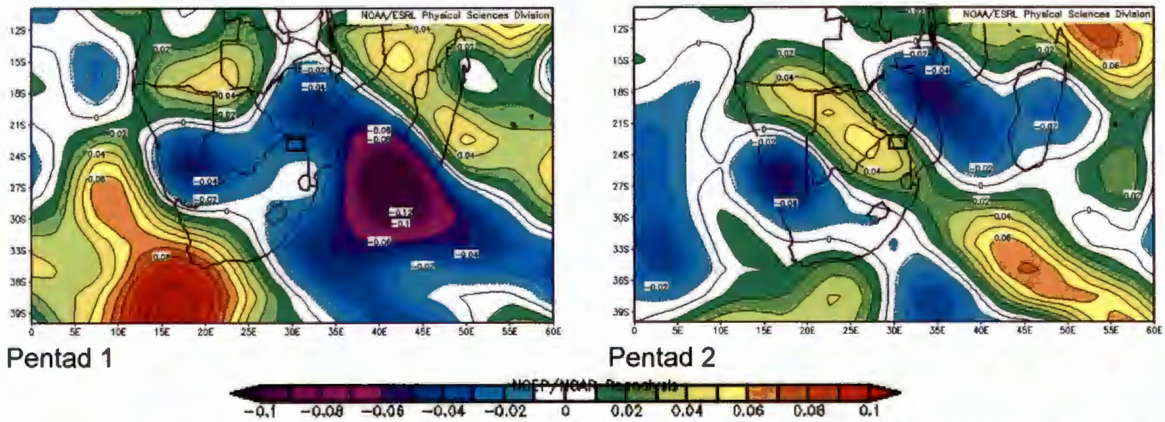

Figure 7.44: Vertical Motion Anomalies (2 x 10^{-4} Pa s^{-1}) during 1981 seasonal rainfall onset

7.7.5 Vertical Motion Anomalies - 20 Days Prior to 2001 Early Onset

Figure 7.45 illustrates a strong subsidence pattern over South Africa, which is sandwiched between rising motion anomalies east of Madagascar and one in the Atlantic Ocean in pentad 55 and 57. The uplifting motion over Madagascar and the sinking motion centred over Vhembe create a spectacular dipole feature in pentad 57, which can be associated with mass (moisture in this case) transport from land to ocean. The patterns of vertical motion anomalies are different in pentad 56, wherein the rising motion is occupying the Mozambique Channel between a subsidence overland (South Africa) and another over the Indian Ocean. In pentad 58, in a mirror image of the pattern in pentad 56, the channel is under sinking motion.

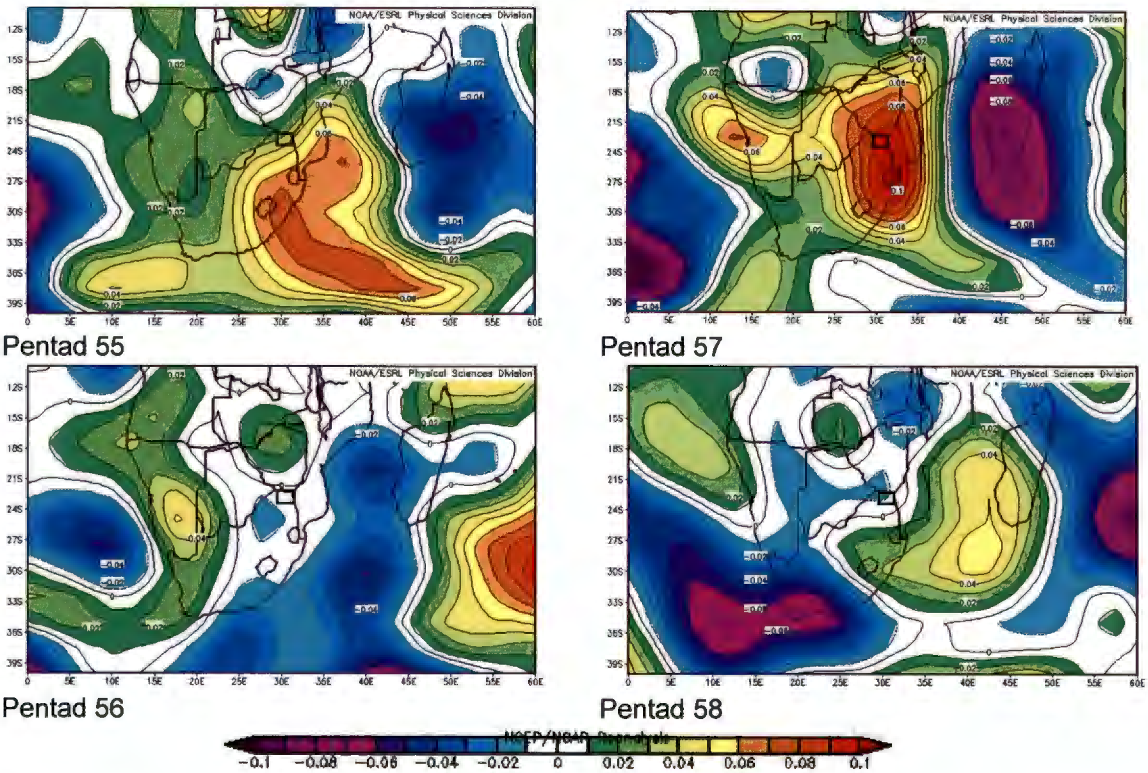

Figure 7.45: Vertical Motion Anomalies (2 x 10^{-4} Pa s^{-1}) 20 days prior 2001 seasonal rainfall onset

7.7.6 Vertical Motion Anomalies - During 2001 Early Onset

At the onset stage (pentad 59), a NW-SE band of strong rising motion anomalies stretches from the south Indian Ocean to South Africa, Lesotho, parts of Mozambique, Zimbabwe, Botswana and Namibia (Figure 7.46). The study area experiences rising motion of 0.04 to – 0.05 Pa s^{-1}. Relatively strong sinking motion is observed in the Atlantic Ocean, and it extends to the Indian Ocean south of 36°S. An anomalous rising motion appears in southwest southern Africa five days after the onset stage. SWIO is occupied by a strong subsidence that is sandwiched by strong rising motion on either side. The study area continued to experience rising motion.

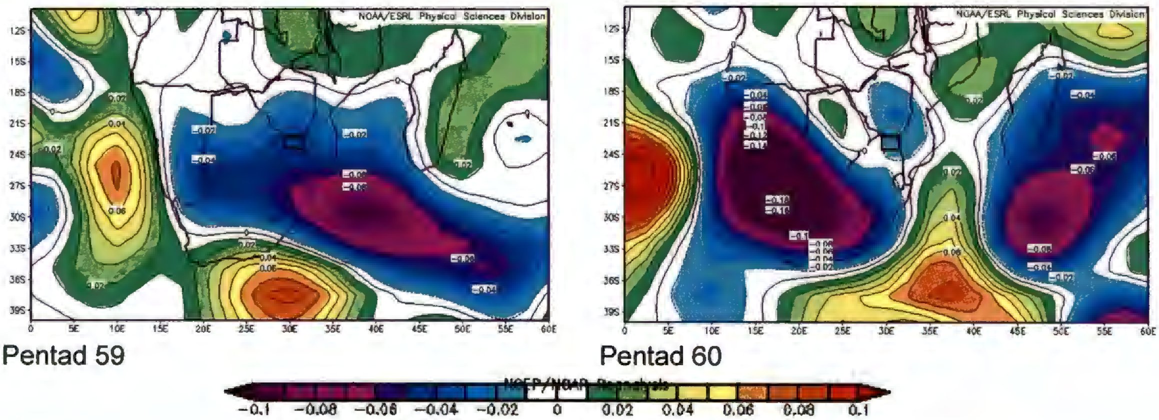

Figure 7.46: Vertical Motion Anomalies (2 x 10^{-4} Pa s^{-1}) during 2001 seasonal rainfall onset

7.7.7 Vertical Motion Anomalies - 20 Days Prior to 2007 Late Onset

Strong positive vertical motion anomalies exist over the Atlantic Ocean and Madagascar in pentad 66 (Figure 7.47). Strong negative vertical motion anomalies are located over SWIO. In five days before the onset, there was rising motion over the study area.

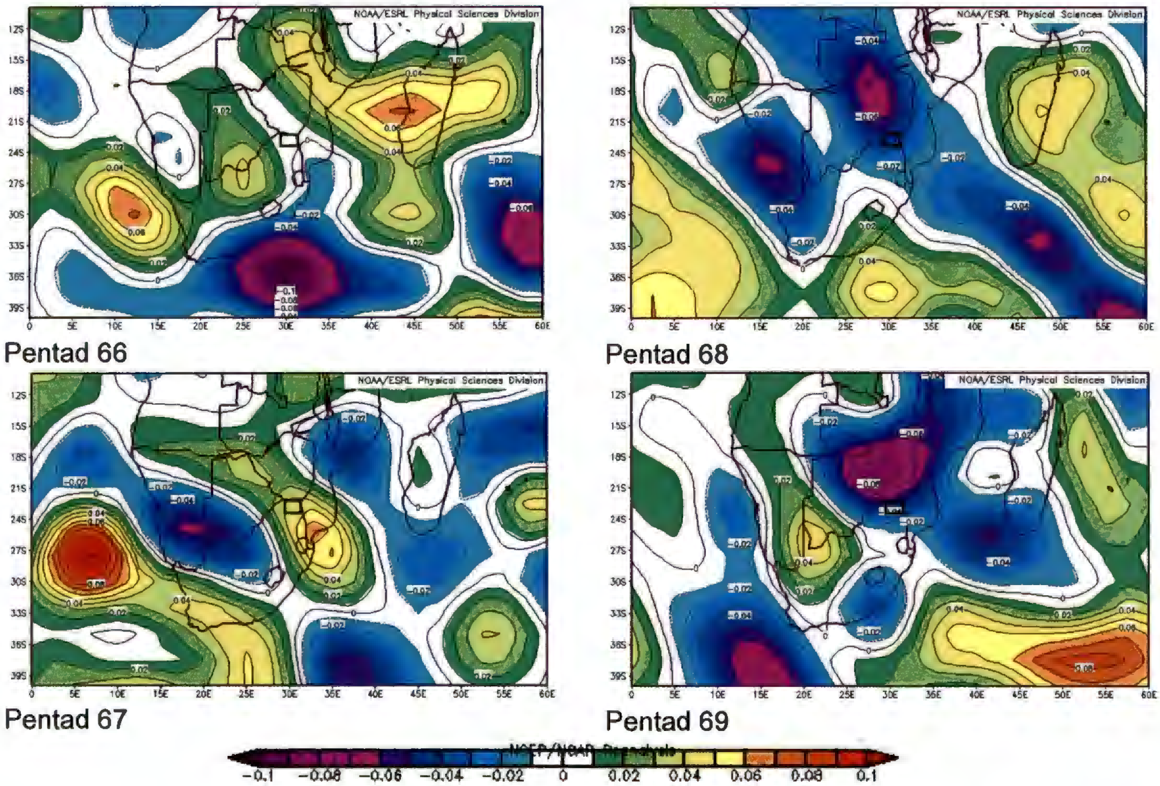

Figure 7.47: Vertical Motion Anomalies (2 x 10^{-4} Pa s^{-1}) 20 days prior 2007 seasonal rainfall onset

7.7.8 Vertical Motion Anomalies - During 2007 Late Onset

In Figure 7.48, pentad 70 shows that the study area is under rising motion. Centres of strong action are in the Indian Ocean, with a sinking motion is centred southeast of Madagascar and a rising motion centred south of Madagascar. Rising motion was maintained over the study area five days later, which intensified to ~ -0.06 Pa s^{-1}.

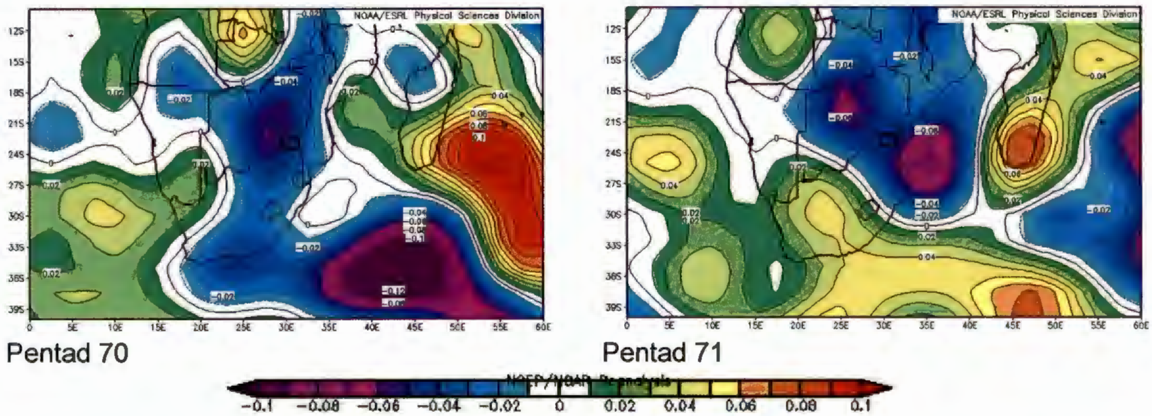

Figure 7.48: Vertical Motion Anomalies (2 x 10^{-4} Pa s^{-1}) during 2007 seasonal rainfall onset

7.9 Chapter Summary

The results of analyses atmospheric anomalies (specific humidity, water vapour flux and vertical motion) are discussed in Chapter 7. The analysis has studied the rainfall onset in the humid and semi-arid zones of Vhembe (Nenwiini, 2010; Nenwiini & Kabanda, 2013) using departures from the long-term period mean. It has identified differences and common denominators between humid and semi-arid zones during early and late seasonal rainfall onset.

More importantly, the investigation has revealed the following over Vhembe:

- In general, rainfall onset in the humid areas is strongly associated with negative specific humidity anomalies and strong persistence of easterlies transporting of moisture from the Indian Ocean, coupled with an anticyclonic anomaly over southern Africa. From the patterns of vertical motion anomalies, the most noticeable feature was the sinking motion over the study area.

- In contrast, it was different with the semi-arid zone, where the rainfall onset was associated with an increase in positive specific humidity anomalies that indicate abundant moisture availability. In addition, the analysis of moisture flux anomalies over the semi-arid zone shows that the early onset seasons in the semi-arid zone are associated with the westward - propagating moisture from the Indian Ocean, which is channelled inland by an anticyclonic circulation over southern Africa. This includes the moisture from the tropics, which end up in the northeastern part of South Africa. The patterns of vertical motion indicate general uplifting during rainfall onset in the semi-arid zone, which is manifested by negative vertical motion anomalies.

- Close similarities between patterns associated with humid and semi-arid zones are observed during late seasonal rainfall onset. In this respect, the seasons that start late (both in humid and semi-arid) are generally characterised by persistent westerly moisture transport anomalies from the Atlantic Ocean to the interior of southern Africa. The westerly anomalies advect dry air from the Atlantic Ocean towards the interior, which leads to a reduction of moisture brought by easterlies from the Indian Ocean. When the westerly flow dominates, rainfall onset over Vhembe District is delayed.

- The significant characteristics shown by each climatological parameter are summarised in Table 7.1 and 7.2. The summary is illustrated using selected seasons in each category (early and late onset) and the notable findings from the relationships among the parameters are listed below:

a) Climatological anomalies in the humid zone:

➢ During the early onset (1986) the rainfall started in pentad 54 (23rd to 27th September). Specific humidity was approximately 1 g/kg, moisture flux was about 60 kg^{-1} ms^{-2} and there was no rising motion (0 Pa s^{-1}) – rainfall accumulated to 29.7 mm (Table 7.1).

➢ During the early onset (2001) the rainfall started in pentad 56 (3rd to 7th October) specific humidity was about 1.5 g/kg but moisture flux was ~ 40 kg^{-1} ms^{-2} and there was no rising motion (0 Pa s^{-1}) – rainfall accumulated to 26.2 mm.

➢ During the late onset (1985) the rainfall started in pentad 69 (7th to 11th December). Specific humidity was about -1 g/kg, moisture flux ~ 50 kg^{-1} ms^{-2} and there was sinking motion (0.04 Pa s^{-1}) – rainfall accumulated to 78.5 mm.

➢ During the late onset (2006) the rainfall started in pentad 71 (17th to 21st December) Specific humidity was ~ 0 g/kg, moisture flux was ~ 100 kg^{-1} ms^{-2} and there was sinking motion (0.04 Pa s^{-1}) – rainfall accumulated to 12 mm.

Table 7.1: Local station rainfall and atmospheric anomalies prior and during onset date in the humid zone

	Period	Early Onset 1986					Late Onset 1985				
		Pentad	Station Rainfall (mm)	Specific Humidity Anomaly (g/kg)	Moisture Flux anomaly (kg m^{-1} s^{-1})	Vertical Motion Anomaly (Pa/s)	Pentad	Station Rainfall (mm)	Specific Humidity Anomaly (g/kg)	Moisture Flux Anomaly (kg^{-1} ms^{-1})	Vertical Motion Anomaly (Pa/s)
Humid Zone		P50	0	-1.5	60	0	P65	0	-4	100	0.03
		P51	3.2	0	30	0.02-0.03	P66	0	-1.25	100	0.04
		P52	4.3	0	20	0-0.01	P67	4.9	-1.5	120	0.02
		P53	0	-1	30	0	P68	0	-2.5	80	0.02
		P54	29.7	1	60	0	P69	78.5	-1	50	0.04
		P55	5.3	0.5	60	0.02	P70	112.2	-0.5	60-80	>-0.03
		Early Onset 2001					Late Onset 2006				
		P52	0	0.5	60	>-0.01	P67	0	-2	100	0.06
		P53	0.7	0	80	-0.1	P68	0	1.5	40	0.03
		P54	0	2	120	0	P69	0	-1	40	0.03
		P55	2	-1	100	>0.04	P70	0	-3	60	0.06
		P56	26.2	1-1.5	40	0	P71	12	0	100	0.06
		P57	0.9	0.1	150	0.09	P72	3.5	1	50-100	0

b) Climatological anomalies in the semi-arid zone:

- During the early onset (1984) the rainfall started in pentad 61 (27th to 31st October) Specific humidity was about 1.5 g/kg, moisture flux was approximately 80 kg^{-1} ms^{-2} and there was rising motion (-0.02 Pa s^{-1}) – rainfall accumulated to 36 mm (Table 7.2).

- During the early onset (2001) the rainfall started in pentad 59 (18th to 22nd October) specific humidity was about -0.5 g/kg, moisture flux was ~ 80 kg^{-1} ms^{-2} and there was rising motion (-0.05 Pa s^{-1}) – rainfall accumulated to 59 mm.

- During the late onset (1981) the rainfall started in pentad 1 (1st to 5th January 1982) specific humidity was 0 g/kg, moisture flux was 100 kg^{-1} ms^{-2} and there was rising motion (-0.04 Pa s^{-1}) – rainfall accumulated to 60 mm.

- During the late onset (2007) the rainfall started in pentad 70 (12th to 16th December) specific humidity was low (1 g/kg), moisture flux was high (120 kg^{-1} ms^{-2}) and there was rising motion (-0.05 Pa s^{-1}) – rainfall accumulated to 38.1 mm

Table 7.2: Local station rainfall and atmospheric anomalies prior and during onset date in the semi-arid zone

Zone	Period	Early Onset 1984					Late Onset 1981				
		Pentad	Station Rainfall (mm)	Specific Humidity Anomaly (g/kg)	Moisture Flux Anomaly ($m^{-1} s^{-1}$)	Vertical Motion Anomaly (Pa/s)	Pentad	Station Rainfall (mm)	Specific Anomaly Humidity (g/kg)	Moisture Flux Anomaly ($kg^{-1} ms^{-1}$	Vertical Motion Anomaly (Pa/s)
Semi-arid Zone		P57	0	0	30	0 - 0.01	P70	0	-1	40	0.06
		P58	6	2.5	120	0	P71	0	0	60	>0.03
		P59	0	-1	80	0.05	P72	0	0	80	0
		P60	0	-1	80	0.06	P73	0	0.5-1	80	-0.02
		P61	36	1.5	60-80	>- 0.01	P1	60	0	100	>-0.04
		P62	4.5	1-1.5	0-60	-0.02	P2	2.5	1	30	0.04
		Early Onset 2001					**Late Onset 2007**				
		P55	0	-1	100	>0.03	P66	0	2.5	120	-0.01
		P56	0	-1	40	0	P67	0	1	40	0.04
		P57	0	-1	90	0.9	P68	0.8	1	30	-0.02
		P58	0	0	60	0	P69	0	2	100	-0.02
		P59	11	-0.5	80	-0.05	P70	38.1	1	120	-0.05
		P60	21	1	60	0	P71	59.3	2	50	-0.06

There are several other noteworthy observations from this chapter, which need to be highlighted:

- The South West Indian Ocean (SWIO) plays a leading role in supplying most of the moisture during both early and late onset of seasonal rainfall in the humid and semi-arid zones; the Mozambique Channel seem to be the primary source. This observation is in agreement with earlier studies (Levey & Jury, 1996; Makarau, 1995; Lindesay & Jury, 1991).

- South Atlantic Ocean (SAO) contributes the westerly flow, which in most cases is dry; hence it contributes to a reduction of moisture over Vhembe District. This is due to the moisture flux-passage over the cold ocean and thereafter through the dry western regions (Namib and Kalahari deserts and Northern Cape and North West Provinces in South Africa).

- The large-scale atmospheric flows such as moisture flux and convective activities play a small role during rainfall onset in the humid areas. However, they are concomitant with rainfall onset in the semi-arid zone. This observation is supported by the larger amount of rainfall that is realised during semi-arid zone seasonal rainfall onset as compared to that in the humid zone. In addition, the absence of large-scale forcing (see Table 7.1) during rainfall onset in the humid zone is another indicator of insignificant influence.

Chapter Eight
Summary and Conclusions

8.1 Summary of Work Presented

8.1.1 Introduction

The principal aim of this study was to establish a meaningful association between the synoptic meteorological systems, their dynamics and the local rainfall characteristics of Vhembe District. To accomplish this aim, the following tasks were undertaken in the respective chapters: Chapter 1 was the introductory chapter that provides the summary of the research and includes issues such as the background, motivation and a description of the study area. A review of the literature on the local and synoptic climatology with much emphasis on meteorological systems that influence the climate of southern Africa was presented in Chapter two. Chapter three described the basic research plan, data sets used, their sources and specific use in this study as well as the statistical analysis techniques employed. Chapters four, five, six and seven provide the original work of this study and each of these chapters includes a chapter summary.

8.1.2 Seasonal rainfall trends and onset (Chapter 4)

This study has provided strong support to conclusions developed in previous work (e.g. Nenwiini, 2012; Nenwiini & Kabanda 2013) that Vhembe District indeed features two prominent climatic zones (humid and semi-arid). In Chapter 4, distinct temporal rainfall trend patterns and rainfall onset dates for the humid and semi-arid zones have been established. Generally, the seasonal rainfall onset dates in the humid zone are different from that of the semi-arid zone, although the rainfall patterns are similar. Trend analysis using Mann-Kendall test and Sen's slope estimator on the 1950-2009 seasonal rainfall of Vhembe District indicated a general decrease over that time. This is in agreement with Kabanda and Nenwiini (2015), who detected a reduction of 50 days in the seasonal rainfall length over 60 years.

The humid zone showed earlier seasonal rainfall onset dates than the semi-arid zone. In some cases, the lag was > 50 days (ten pentads). For instance, during decade 1980-89, the average seasonal rainfall in the humid zone was found to occur in pentad 58 - approximately nine pentads earlier than in the semi-arid zone, which was found to start in pentad 67 on average.

During the 1980s, there was a general declining trend in seasonal rainfall over most stations in the study area. In the 1990s, there was an overall upward trend, and during the 2000s, another general decline. The most plausible explanation of these variations is the ENSO, or the El Niño-Southern Oscillation phenomenon's ability to modulate surface climate (Dambul, 2005; Reason et al., 2005).

8.1.3 CMAP analysis during the rainfall onset (Chapter 5)

The thesis used rainfall analysis, which was provided by CPC Merged Analysis Precipitation (CMAP) to establish the degree to which the local rainfall gauge data captures the signal of large-scale climate forcing over the study area. The following results, based upon Vhembe District pentad data (computed from daily data), present a basis and avenue for further understanding the local rainfall and its relationship with large-scale circulations.

- The local seasonal rainfall at onset stage in the study area is not adequately represented by the CMAP datasets - the difference is most prominent in the humid zone and improves over the semi-arid zone. These observations suggest that the CMAP data sets represent large-scale circulation induced rainfall events rather than locally induced.
- Yatagai et al. (2008) were of the opinion that the disparity was caused by the coarse resolution of CMAP precipitation datasets or the sparse gauge data used as base in developing the CMAP data which were obtained from the area and its environs.
- Vhembe District features prominent topography in the form of the Soutpansberg mountains and according to Huggel et al. (2015), global scale gridded precipitation datasets have difficulty capturing daily rainfall events realistically in a mountainous environment.

The most important finding identified in Chapter 5 is that, CMAP datasets can be useful in the study, especially in manifesting the origin and evolution of the rainfall induced by synoptic modes in the area.

8.1.4 Meteorological characteristics during the rainfall onset (Chapter 6)

The evolution of meteorological fields (specific humidity, moisture flux and vertical motion) associated with four pentads before the seasonal rainfall onset, one during and one after rainfall onset, has revealed distinct atmospheric features in both the humid and semi-arid zones.

- Early onset in the humid zone is preceded by low water vapour in the atmosphere (about 4 g/kg). Rainfall starts earlier in the humid zone, since the necessary specific humidity is reached earlier. This is due to upslope flow lifting the air, causing cooling and condensation and increasing the air moisture aloft from 4-5 to 6-7 g/kg. Meanwhile, it takes longer for the moisture to increase to the level of precipitating in the semi-arid zone – it has to wait for large-scale atmospheric circulation and vertical motion [to deliver sufficient moisture].

- South West Indian Ocean and the Mozambique Channel advects moisture towards Vhembe District (the study area) from the east. This is in agreement with the findings of Hewitson et al. (2004), Makarau (1995), Taljaard (1990) and Tyson (1986). But at the onset stage in the humid zone, the ocean is overlaid by relatively low moisture, which leads to a large-scale flow that is unable to transport enough moisture to Vhembe District.

- A weak convergence of southerlies and north-westerly moisture flow over northeastern South Africa during late rainfall onset in the humid zone, but due to moisture scarcity in the southerlies, this convergence produces little moisture over the study area.

- Large-scale convective activities are absent during early rainfall onset in the humid zone; instead weak subsidence covers the district. There is, by contrast, strong upward motion in late rainfall onset, which is accompanied by a strong subsidence in the Mozambique Channel creating a dipole pattern with overland uplifting motion.

- During early and late rainfall onset in the semi-arid zone, Vhembe District rainfall is influenced by northwesterly/northerly flow emanating from tropical areas, which has abundant moisture.

- During early rainfall onset in the semi–arid zone, the ascent-descent continues to occupy south Atlantic, southern Africa and southwest Indian Ocean, providing Vhembe District with a modest ascent regime during early and late onset.

8.1.5 Atmospheric anomalies linked to seasonal rainfall onset (Chapter 7)

Makarau (1995) observed that large-scale flow and synoptically induced instability reciprocally influence each other during summer rainfall in southern Africa. His observation was referring to a regional-scale environment. What was not shown or understood is how the synoptic meteorological fields control rainfall at a local scale such as rainfall onset in Vhembe District. Chapter 7 examined the evolution of specific humidity anomalies, moisture flux and large-scale convective anomalies (vertical motion) during early and late seasonal rainfall periods within the humid and semi-arid zone of Vhembe District. Moisture sources and pathways associated with the seasonal rainfall onset and its relationship with early and late seasonal rainfall onset have been addressed. The analysis used NCEP/NCAR reanalysis data.

The main results of this chapter are that differences and common denominators between humid and semi-arid zones during early and late seasonal rainfall onset have been identified.

Other important observations to note are:

- No large-scale moisture supply or convective activities are needed in the humid zone for rainfall to commence.
- In the semi-arid zone, large-scale moisture supply and large-scale convective activities initiated seasonal rainfall onset.
- Moisture from the South West Indian Ocean (Mozambique Channel) and the tropics provided enough moisture during seasonal rainfall onset, although at varying magnitude.
- Late onset is simultaneous with persistent westerly flow from South Atlantic Ocean to southern Africa.

8.2 Concluding remarks

The meteorological fields used in this study are in apparent magnitude not comparable with each other; their significance lies in their relative patterns and variability. For example, CMAP data and local rain gauge data differ in their magnitude but are comparable based on their relative structures. This is also true of other parameters.

In summary, this study has identified the most probable drivers of seasonal rainfall onset and rainfall onset disruptions in Vhembe District. The evolution of large-scale meteorological fields in conjunction with local area rain gauge rainfall data has revealed fields associated with different zones and their rainfall onsets and delays in the study area - particularly, the moisture trajectory, their sources and sinks together with the forcing mechanisms. Orographic lifting over the Soutpansberg plays a vital role as a local forcing mechanism in initiating rainfall onset, since it enhances air saturation and initiate rainfall onset in the absence of large-scale moisture supply and large-scale convective activities

Knowledge of the seasonal variability of rainfall in Vhembe District and the associated dynamic climatological features is of interest because of its importance in developing significant predictors. These can assist in making reliable predictions of the seasonal rainfall characteristics in order to ensure sustainable agricultural production, risk management planning, engineering, efficient water resource management and supply (e.g. fog water harvesting - Olivier & Van Heerden, (1999) among others.

When carrying out this study some limitations were encountered, although they have not weakened the study, in terms of attaining the aim and the set objectives. The main one that needs to be mentioned here is that there are few studies, which have been undertaken in southern Africa, which looked at the influence of large-scale atmospheric field forcings on local climate. In addition, very few studies that have been conducted are specifically related to Vhembe District, which limit the climate study references from the area. Besides the unique aspects of Vhembe District, which include its geographic location and its physiographic nature, are other limitations. Geographically, Vhembe District is a recipient of both tropical and extratropical influence. Physiographically, it has an imposing mountain range - the Soutpansberg - in its midst. Thus, to a certain extent, this might have limited the depth of this research, in terms of detailed investigation of certain findings. These limitations can serve as areas of possible further work in the future to advance the knowledge on Vhembe District or on the areas with similar geographical settings.

This type of research is a significant departure from most research done in South Africa, where investigations have dealt with regional climate studies. It has added strength and opportunities for future studies and understanding the local climate of Vhembe District.

9. References

Adedokun, J.A. (1981). Potential instability and precipitation occurrence within intertropical discontinuity. Archiv f˙ur Meteorologie, Geophysile und Broklimatologie, Serie A, Meteorologie und Geophysile, 30, 69–
86.

Adejuwon, J.O., Balogun, E.E. & Adejuwon, S.A. (1990). On the annual and seasonal patterns of rainfall fluctuations in Sub-Saharan West-Africa. International Journal of Climatology, 10, 839848. Retrieved from http://onlinelibrary.wiley.com/doi/10.1002/joc.3370100806/full.

Adler, R.F., Kidd, C., Petty, G., Morissey, M. & Goodman, H.M. (2001). Intercomparison of global precipitation products: The third Precipitation Intercomparison Project (PIP-3). *Bulletin of the American Meteorological Society*, *82*(7), 1377.

Adler, R.F., Huffman, G.J., Chang, A., Ferraro, R., Xie, P., Janowiak, J., Rudolf, B., Schneider, U., Curtis, S., Bolvin, D., Gruber, A., Susskind, J., Arkin, P. & Nelkin E. (2003). The version-2 Global Precipitation Climatology Project (GPCP) monthly precipitation analysis (1979-presient). *Journal of Hydrometeorology, 4, 1147-1167.*

AghaKouchak, A., Behrangi, A., Sorooshian, S., Hsu, K., & Amitai, E. (2011). Evaluation of satellite-retrieved extreme precipitation rates across the central United States. *Journal of Geophysical Research: Atmospheres*, *116*(D2). Retrieved from http://onlinelibrary.wiley.com/doi/10.1029/2010JD014741/full.

Aguado, E. & Burt, J.E. (2001). *Understanding weather and climate.* 2nd ed. Prentice Hall, Upper Saddle River, New Jersey, USA.

Ahrens, C.D. (2000). *Meteorology Today, 6th edn.* Brooks/Cole Publishing: Toronto.

Allan, R., Lindesay, J., & Parker, D. (1996). *El Niño southern oscillation & climatic variability*. CSIRO publishing.

Allan, R.J. (2000). ENSO and climate variability in the last 150 years. *El Niño and the Southern Oscillation: Multiscale variability and its impacts on natural ecosystems and society*, (eds). Cambridge University Press.

Ambrosino C., Chandler R.E. & Todd M.C. (2010). Southern African monthly rainfall variability: an analysis based on generalized linear models. *Journal of Climate, 24*, 4600–4617. Retrieved from journals.ametsoc.org/doi/full/10.1175/ 2010JCLI3924.

Amekudzi, L. K., Yamba, E. I., Preko, K., Asare, E. O., Aryee, J., Baidu, M., & Codjoe, S. N. (2015). Variabilities in rainfall onset, cessation and length of rainy season for the various agro-ecological zones of Ghana. *Climate*, *3*(2), 416-434.

Ampitiyawatta, A.D., & Guol, S. (2009). Precipitation trends in the Kalu Ganga Basin in Sri Lanka. *Journal of Agricultural Science*, Vol. 4(1).

Anyamba, E.K., Kiangi, P.M.R., & Patnaik, J.K. (1982). The mean horizontal motions over the African atmosphere during the southern summer. In *WMO Tech. Conf. on Climate: Africa p 156-170(SEE N 83-12736 03-47)*.

Arkin, P., Xie., P., & National Center for Atmospheric Research Staff (Eds). (2016) *The Climate Data Guide: CMAP: CPC Merged Analysis of Precipitation.* Retrieved from https://climatedataguide.ucar.edu/climate-data/cmap-cpc-merged-analysis-precipitation.

Ati O.F., Stigter C.J. & Oladipupo E.O. (2002). A comparison of methods to determine the onset of growing season in northern Nigeria. *International Journal of Climatology,* 22, 731–742.

Aviad, Y., Kutiel, H. & Lavee, H. (2004). Analysis of beginning, end and length of the rainy season along a Mediterranean arid climate transect for geomorphic purposes. *Journal of Arid Environments*, 59, 189-204.

Ayoade, J. (1983). *Introduction to Climatology for the Tropics.* John Wisley.

Bagley, J.E., Desai, A.R., Dirmeyer, P. A. & Foley, J.A. (2012). Effects of land cover change on moisture availability and potential crop yield in the world's breadbaskets. *Environmental Research Letters*, 7(1), 014009.

Barry, R.G. (1992). *Mountain weather and climate.* 2nd Ed. London: Routledge.

Barry, R.G. & Chorley, R.J. (1992). *Atmosphere, weather and Climate.* New York: Routledge.

Benoit, P. (1977). The start of the growing season in Northern Nigeria. *Agric. Meteorol*, 18, 91-99.

Bewick, V., Cheek, L. & Ball, J. (2003). Statistics review 7. Correlation and regression. *Critical Care*, *7*(6), 1.

Beyer, M., Wallner, M., Bahlmann, L., Thiemig, V., Dietrich, J., & Billib, M. (2016). Rainfall characteristics and their implications for rain-fed agriculture: a case study in the Upper Zambezi River Basin. *Hydrological Sciences Journal*, *61*(2), 321-343. Retrieved from http://www.tandfonline.com/doi/abs/10.1080/02626667.2014.983519

Biasutti, M, Battisti, D.S. & Sarachik, E.S. (2003). The annual cycle over the tropical Atlantic, South America, and Africa. *Journal of Climate,* 16(15): 2491-2508.

Bonan, G.B. (2008). Forests and climate change: forcings, feedbacks, and the climate benefits of forests. *Science, 320*(5882), 1444-1449.

Bowman, K.P. (2005). Comparison of TRMM precipitation retrievals with rain gauge data from ocean buoys. *Journal of Climate*, *18*(1), 178-190. Retrieved from doi: http://dx.doi.org/10.1175/JCLI3259.1.

Bradley, R.S., Diaz, H.F., Eischeid, J.K., Jones, P.D., Kelly, P.M. & Goodess, C.M. (1987). Precipitation fluctuations over Northern Hemisphere land areas since the mid-19th century. *Science*, *237*(4811), 171-175.

Camberlin, P, & Diop, M. (2003). Application of daily rainfall principal component analysis to the assessment of the rainy season characteristics in Senegal. *Climate Research,* **23**, 159–169.

Camberlin P., Moron V., Okoola R., Philippon N. & Gitau W. (2009). Components of rainy seasons variability in Equatorial East Africa: onset, cessation, rainfall frequency and intensity. *Theor Appl Climatol,* 98(3–4):237–249.

Cook C., Reason C.J.C. & Hewitson B. (2004). Wet and dry spells within particularly wet and dry summers in the South African summer rainfall region. *Climate Research*, 26,17–31.

Cotton, W.R., Bryan, G. & Van den Heever, S.C. (2010). *Storm and cloud dynamics* (Vol. 99). Academic press.

Chandler, R. & Scott, M. (2011). *Statistical methods for trend detection and analysis in the environmental sciences*. John Wiley & Sons.

Chen, T. (1985). Global Water Vapor Flux and Maintenance during FGGE *Mon. Weather Review,* 113, 1801-1819.

Chen, M., Xie, P., Janowiak, J.E. & Arkin, P.A. (2002). Global land precipitation: A 50-yr monthly analysis based on gauge observations. *Journal of Hydrometeorology*, *3*(3), 249-266.

Chiara, A., Chandler, R.E. & Todd, M.C. (2011). Southern African Monthly Rainfall Variability: An Analysis Based on Generalized Linear Models. *J. Climate,* 24, 4600–4617.

Cook, C., Reason, C.J.C., & Hewitson B.C. (2004). Wet and dry spells within particularly wet and dry summers in the South African summer rainfall region. *Climate Research,* 26:17–31

Cocheme, J., & Franquin, P. (1967). An agroclimatological survey of a semi-arid area in Africa, South of the Sahara. W.M.O. 86(210): 110–136

D'Abreton, P.C., & Tyson, P.D. (1995). Divergent and Non-Divergent water Vapour Transport over Southern Africa during Wet and Dry Conditions. *Meteorological and Atmospheric Physics*, 55, 47-59.

D'Abreton, P.C., & Lindesay, J.A. (1993). Water vapour transport over southern Africa during wet and dry late summer months. *International J Climatol,* 13:151–170

Dambul, R. (2005). *The Relationships between Large-scale Atmospheric Circulation and Surface Climate* (A PhD thesis, University of East Anglia, England). Retrieved from https://crudata.uea.ac.uk/cru/pubs/thesis/2007-dambul/Thesis_2007.pdf.

David, S., Thomas, G., Twyman, C., Osbah, H. & Hewitson, B. (2007). Adaptation to climate change and variability: farmer responses to intra-seasonal precipitation trends in South Africa. *Climatic change,* 83, 301-322.

DEA (Department of Environmental Affairs). (2013) Long-Term Adaptation Scenarios Flagship Research Programme (LTAS) for South Africa. Climate Trends and Scenarios for South Africa. Pretoria, South Africa.

Dirmeyer, P.A., & Kinter III, J.L. (2010). Floods over the US Midwest: A regional water cycle perspective. *Journal of Hydrometeorology*, *11*(5), 1172-1181.

Dhonneur, G. (1974). Nouvelle approche des realites des realites mateorologiques de l'Afrique occidentale et centrale, Tome: ASECNA.

Dong, X., Xi, B., Kennedy, A., Feng, Z., Entin, J.K., Houser, P.R., ... & Liu, W.T. (2011). Investigation of the 2006 drought and 2007 flood extremes at the Southern Great Plains through an integrative analysis of observations. *Journal of Geophysical Research: Atmospheres*, 116(D3). Retrieved from, doi:10.1029/2010JD014776.

Dunning, C.M., Black, E.C., & Allan, R.P. (2016). The onset and cessation of seasonal rainfall over Africa. *Journal of Geophysical Research: Atmospheres*, *121*(19).

Dzivhani, A.M. (1998). *Temperature and rainfall variability over the Northern Region of the Northern Province for the past 35 years* (BA. Hons. thesis submitted University of Venda).

Elliott, W.P. & Gaffen, D.J. (1991). On the utility of radiosonde humidity archives for climate studies. *Bulletin of the American Meteorological Society*, *72*(10), 1507-1520.

Esteban-Parra, M.J., Rodrigo, F.S. & Castro-Diez, Y. (1998). Spatial And Temporal Patterns Of Precipitation In Spain For The Period 1880–1992. *International. J. Climatol,* 18: 1557–1574.

FAO, (1995). Digital soil map of the world and derived soil properties. Food and Agriculture Organization of the United Nations, Rome.

Fauchereau, N., Trzaska, S., Rouault, M., & Richard, Y. (2003). Rainfall variability and changes in southern Africa during the 20th century in the global warming context. *Natural Hazards*, *29*(2), 139 154. Retrieved from doi: 10.1023/A:102363092 41.

Fauchereau, N., Pohl, B., Reason, C., Rouault M. & Richard, Y. (2008). Recurrent daily OLR patterns in the Southern Africa/ Southwest Indian Ocean region, implications for South African rainfall and teleconnections. *Climate Dynamics,* 32, 575–591.

Fernando, M.A., Samita, S. & Abeynayake, R. (2012). Modified factor analysis to construct composite indices: illustration on urbanization index. *Tropical Agricultural Research*, 23(4).

Folland, C.K. (1983). Regional-scale interannual variability of climate – A north-west European perspective. *Meteorol. Mag*azine, 112, 163 –183.

Fowler, H.J., Blenkinsop, S. & Tebaldi, C. (2007). Linking climate change modelling to impacts studies: recent advances in downscaling techniques for hydrological modelling. *Int. J. Climatol*, 27 (12), 1547–1578.

Gong, D. &. Ho C (2003). Arctic oscillation signals in the east Asian summer monsoon. *J. Geophysics Research*, 108(D2), 4066. Retrieved from doi:10.1029/2002JD002193.

Göbel, W., Ouali, A.E.I. & Singh. M. (1996). Spatial interpolation of precipitation data: an example from Morocco, Workshop on Spatialization, E.U. Cost and Météo France, 24-25 September, Toulouse, France.

Goswami, P. & Gouda, K.C. (2007). Objective determination of the date of onset of monsoon rainfall over India based on duration of persistence. CSIR Centre for Mathematical Modelling and Computer Simulation. Research Report RR CM 0711.

Grist, J.P., & Nicholson. S.E. (2001). A study of the dynamic factors influencing the interannual variability of rainfall in the West African Sahel. *Journal of Climate*, 14, 1337– 359.

Gruber, A., Su, X., Kanamitsu, M. & Schemm, J. (2000). The comparison of two merged rain gauge–satellite precipitation datasets. *Bull. Amer. Meteor. Soc*, **81,** 2631–2644.

Hahn, N. (2002). *Endemic flora of the Soutpansberg* (MSc thesis, University of Natal, Pietermaritzburg).

Hanssen-Bauer, I., Farland, E.J., Tveito, O.E., & Nordli, P.O. (1997). Estimating Regional Precipitation Trends Comparison of two Methods. *Nordic Hydrology,* 28, 1997, 21 -36.

Harangozo, S.A. & Harrison, M.S.J. (1983). On the use of synoptic data in indicating the presence of cloud bands over southern Africa. *South African Journal of Science,* 79(10):413–414.

Harrison, M.S.J. (1984). A generalized classification of South African rain-bearing synoptic systems. *J Climatol,* 4:547–560.

Harrison, M.S.J. (1986). A synoptic climatology of South African rainfall variations (PhD
thesis, University of Witwatersrand, Johannesburg). Retrived from http://www.reposit ory.up.ac.za/handle/2263/23300.

Hart, N., Reason, C.J.C. & Fauchereau, N. (2010). Tropical-extratropical interactions over southern Africa: three cases of heavy summer season rainfall. *Monthly Weather Review,* 138:2608–2623.

Hart, N., Reason, C.J.C., & Fauchereau, N. (2012). Cloud bands over southern Africa: Seasonality, contribution to rainfall variability and modulation by the MJO. *Climate Dynamics,* 41, 1199–1212. Retrieved from doi:10.1007/s00382-012-1589-4.

Hartmann, D.L. (2015). *Global physical climatology.* (Vol. 103). Newnes.

Hastenrath, S., & J. Kutzbach. (1985). Late Pleistocene climate and water budget of the South American Altiplano.*Quat. Res,* 24,249-256.

Haylock, M.R., Cawley, G.C., Harpham, C.R., Wilby, L. & Goodess, C. (2006). Down scaling heavy precipitation over the UK: A comparison of dynamical and statistical methods and their future scenarios. *Int. J. Climatol,* **26**, 1397 1415, doi:10. 1002/joc.1318.

Hewitson, B.C. (1999). *Deriving Regional Precipitation Scenarios from General Circulation Models.* Water Research Commission, South Africa. Report No. 751/1/99

Hewitson, B.C., Tennant, W. & Walawege R. (2004). Atmospheric moisture transport and sources for southern Africa. WRC Report No. 1012/1/04. Pretoria: Water Research Commission.

Hirsch, R.M., Alexander, R.B., & Smith, R.A. (1991). Selection of methods for the detection and estimation of trends in water quality. *Water resources research*, *27*(5), 803-813.

Huang, Y., Cai, J., Yin H & Cai, M. (2009). Correlation of precipitation to temperature variation in the Huanghe River (Yellow River) basin during 1957–2006. *Journal of Hydrology*, vol. 372, 1–4.

Huggel, C., Carey, M., Clague, J. J. & Kääb, A. (Eds.). (2015). *The High-Mountain Cryosphere*. Cambridge University Press.

Hulme, M., Osborn, T.J. & Johns, T.C. (1998). Precipitation sensitivity to global warming: comparison of observations with HADCM2 simulations. *Geophysical Research Letters,* 25: 3379–3382.

Ilesanmi, O.O. (1972a). An empirical formulation of the onset, advance and retreat of rainfall in Nigeria. *J Tropical Geography*, 34: 17–24.

Ilesanmi, O.O. (1972b). Aspect of the precipitation climatology of the July–August rainfall minimum of Southern Nigeria. *Journal of Tropical Geography*, 35: 51–59.

Jones, P.D. & Hulme, M. (1996). Calculating regional climatic time series for temperature and precipitation: methods and illustrations. *Intern. J. Climatol*, 16, 361-377 (4.2).

Jury, M.R. & Pathack, B. (1991). A study of climate and weather variability over the tropical Southwest Indian Ocean. *Meteorology and Atmospheric Physics*, 47, 37-48.

Jury, M.R., Pathack, B. & Sohn, B.J. (1992). Spatial structure and interannual variability of summer convection over southern Africa an SW Indian Ocean. *South Africa Journal of Science*, 275-280.

Jury, M.R. & Mpeta, E.J. (2009). African climate variability in the satellite era. *Theor Appl Climato,* 98:279–29.

Kabanda, T.A. (2003). Climate. Pp. 10–11. *In*: Berger, K., Craffort, J.E., Gaiger, I., Gaiger, M.J., Hahn, N. and MacDonald, I. (eds.). *A first synthesis of the environmental, biological and cultural assets of the Soutpansberg*. Leach Printers and Signs, Makhadu.

Kabanda, T.A. (2004). *Climatology of long-term drought in the northern region of the Limpopo Province of South Africa* (PhD thesis, University of Venda).

Kabanda, T.A., & Munyati, C. (2010). Anthropogenic-induced climate change and the resulting tendency towards land conflict: the case of the Soutpansberg region, South Africa. *Climate change and Natural Resources Conflicts in AfricaMonograph*, (170), 139-155.

Kabanda, T.A. (2011). Impacts of Climate Change on Agriculture: Collapsing of dry Land Potato Farming in North East South Africa. *J Soc Sci,* 29 (1): 57-62.

Kabanda, T.A, & Nenwiini, S.C (2015). Impacts of climate variation on the length of the rainfall season: an analysis of spatial patterns in North-East South Africa. *Theoretical and Applied Climatology*, *125*(1-2), 93-100. Retrieved from doi:10.1007/s00704-015-1498-7.

Kabanda, T.A. (2017). Geographical Variability of Drought in Northern South Africa. *Journal of Geography and Geology*, *9*(1), 53. Retrieved from https://doi.org/10.5539/jgg.v9n1p53.

Katz, R.W. & Brown, B.G. (1992). Extreme events in a changing climate. Variability is more important than averages. *Climatic Change*, 21: 289–302.

Kaufman, C.E. (1998). Determinants and Consequences of Fertility; Contraceptive use in South Africa under apartheid. *Demography*, Volume 35, Number 4 (1998), 421-434.

Kalnay, E., Kanamitsu, M., Kistler, R., Collins, W., Deaven, D., Gandin, L., ... & Zhu, Y. (1996). The NCEP/NCAR 40-year reanalysis project. *Bulletin of the American meteorological Society*, *77*(3), 437-471.

Kennedy, A., Dong, X.Q. & Xi, B.K. (2011). A comparison of MERRA and NARR reanalyses with the DOE ARM SGP data. *Journal of Clim*, 24 (17), 4541–4557.

Kephe, P.N. (2014). Impacts of Anthropogenic Climate Change on the Vegetation of the Soutpansberg Region of South Africa (MSc Dissertation. North West University, Mafikeng, South Africa).

Kephe, P.N., Petja, B.M. & Kabanda, T.A. (2016). Spatial and inter-seasonal behaviour of rainfall in the Soutpansberg region of South Africa as attributed to the changing climate. *Theoretical and Applied Climatology*, 1-13.

Kiangi, P.M.R. (1989). The Weather systems affecting eastern-southern Africa. In Seminar on Tropical Meteorology, WMO/TD -No. 277.

Kistler, R., E. Kalnay, W. Collins, S. Saha, G. White, J. Woollen, M. Chelliah, W. Ebisuzaki, M. Kanamitsu, V. Kousky, H. van den Dool, R. Jenne, and M. Fiorino, (2001). The NCEP-NCAR 50 year reanalysis: Monthly means CD-ROM and documentation. *Bull. Amer. Meteor. Soc*, **82**, 247-268.

Kostopoulou, E. (2003). The relationships between atmospheric circulation patterns and surface climatic elements in the eastern Mediterranean (University of East Anglia, Ph.D. thesis). Retrieved from http://ethos.bl.uk/OrderDetails.do?uin=uk.bl.eth os.405217.

Kowal, J.M. & Knabe, D.T. (1972). An agro-climatic atlas of the northern states of Nigeria. Ahmadu Bello University Press, Zaria, Nigeria.

Kruger, A.C. 2006). Climate of South Africa, Precipitation, WS47. South African Weather Service: South Africa.

Lengoasa, J.R. (1991). Surface Temperature Fields and Circulation Variations over Southern Africa. *South African Geographical Journal, 73, 41-47.*

Levey, K.M., & Jury, M.R. (1996). Composite intraseasonal oscillations of convection over southern Africa. *Journal of Climate*, *9*(8), 19101920. Retrieved from http://dx.doi .org/10.1175/1520-0442(1996)009<1910:CIOOCO>2.0.CO;2.

Liebmann, B., & Marengo, J.A. (2001). Interannual variability of the rainy season and rainfall in the Brazilian Amazon Basin. *J Climate, 14:4308–4318.*

Lima, C.H.R., & Lall, U. (2009). Hierarchical Bayesian modeling of multisite daily rainfall occurrence: rainy season onset, peak and end. *Water Resour Res,* 45:1–14.

Limpopo, D.F.E.D. (2004). Limpopo State of the environment report (Phase 1) *(Limpopo Department of Finance and Economic Development).*

Lindesay, J.A. (1988). South African rainfall, the Southern Oscillation and a Southern Hemisphere semi-annual cycle. *Journal of Climatology*, *8*(1), 17-30. Retrieved from http://onlinelibrary.wiley.com/doi/10.1002/joc.3370080103/full.

Liu, J. & Kalnay, E. (2007). Simple Doppler wind lidar adaptive observation experiments with 3D-Var and an ensemble Kalman filter in a global primitive equations model. *Geophysical Research Letters*, *34*(19).

Liu, S. (1998). Estimation of rainfall storage capacity in the canopies of cypress wetlands and slash pine uplands in North-Central Florida. *Journal of Hydrology*, *207*(1-2), 32-41.

Makarau, A. (1995). Intra-Seasonal Oscillatory Modes of the Southern Africa Summer Circulation (Ph.D. Thesis, University of Cape Town).

Mapande, A.T. & Reason, C. (2005). Interannual rainfall variability over western Tanzania. *Int. J. Climatol,* 25, 13551368. Retrieved from http://onlinelibrary.wiley.co m/doi/10.1002/joc.1193/pdf.

Maragatham, R.T. (2012). Trend analysis of rainfall data -a comparative study of existing methods. International *Journal of Physics and Mathematical Sciences,* Vol. 2 (1) 13-18.

Marengo, J.A., Liebmann, B., Kousky, V.E., Filizola, N. & Wainer, I.C. (2001). Onset and end of the rainy season in the Brazilian Amazon Basin. *Journal of Climate,* 14:833–852.

Marshall, G.J. & Harangozo, S.A. (2000). An appraisal of NCEP/NCAR reanalysis MSLP data viability for climate studies in the South Pacific. *Geophysical Research Letters*, *27*(19), 3057-3060.

Mason, S.J. (1996). Climate Change over the Lowveld of South Africa. *Climate change*, 32, 35-54.

Mearns, L.O., Rosenzweig, C., & Goldberg, R. (1996). The effect of changes in daily and interannual climatic variability on CERES-Wheat: a sensitivity study. *Climatic Change*, 32: 257–292.

Misra, V., Pantina, P., Chan, S. C., & DiNapoli, S. (2012). A comparative study of the Indian summer monsoon hydroclimate and its variations in three reanalyses. *Climate dynamics*. *39*(5), 1149-1168.

Mitchell, T.P. & Wallace, J.M. (1992). The annual cycle in equatorial convection and sea surface temperature. *Journal of Climate*, 5, 1140– 1156.

Mo, K.C. & Higgins, R.W. (1996). Large-scale atmospheric moisture transport as evaluated in the NCEP/NCAR and the NASA/DAO reanalyses. *Journal of Climate*, *9*(7), 1531-1545.

Moeletsi, M.E., Mellaart, E.A.R., Mpandeli, N.S., & Hamandawana, H. (2013). The use of rainfall forecasts as a decision guide for small-scale farming in Limpopo Province, South Africa. *The Journal of Agricultural Education and Extension*, *19*(2), 133-45. Retrieved from http://www.tandfonline.com/doi/full/10.1080/1389224X.2012.734253

Monteith, J. & Unsworth, M. (2007). *Principles of environmental physics*. Academic Press.

Moron, V., Robertson, A.W. & Beer, R. (2009). Spatial coherence and seasonal predictability of monsoon onset over Indonesia. *Journal of Climate,* 22, 840–850.

Mostert, T.H.C. (2006). *Vegetation ecology of the Soutpansberg and Blouberg area in the Limpopo Province* (Doctoral dissertation, University of Pretoria) Retrieved from http://www.repository.up.ac.za/dspace/bitstream/handle/2263/23251/Complete.pdf?sequence=12.

Mubiru, D.N., Komutunga, E., Agona, A., Apok, A., & Ngara, T. (2012). Characterising agrometeorological climate risks and uncertainties: Crop production in Uganda. *South African Journal of Science,* 108(3-4), 108-118. DOI: 10.4102/sajs.v108i3/4.470

Mucina, L., & Rutherford, M. C. (2006). The vegetation of South Africa, Lesotho and Swaziland. Strelitzia 19, South African National Biodiversity Institute, Pretoria. *Memoirs of the Botanical Survey of South Africa*.

Mulenga, H.M., Rouault, M. & Reason, C.J.C. (2003). Dry summers over NE South Africa and associated circulation anomalies, *Climate Research*, 25, 29-41. Retrieved from http://www.int-res.com/articles/cr2003/25/c025p029.pdf

Mulugisi, A. (2015). *The impacts of heavy rains on the vegetation cover in the Limpopo Province of South Africa* (Doctoral dissertation, North-West University) Retrieved from https://repository.nwu.ac.za/handle/10394/17385.

Munyati, C. & Kabanda, T.A. (2009). Using multi-temporal Landsat TM imagery to establish land use pressure induced trends in forest and woodland cover in sections of the Soutpansberg Mountains of Venda region, Limpopo Province, South Africa, *Regional Environmental Change,* 9(1).

Mpandeli, S., Nesamvuni, E., & Maponya, P. (2015). Adapting to the Impacts of Drought by Smallholder Farmers in Sekhukhune District in Limpopo Province, South Africa. *Journal of Agricultural Science*, *7*(2), 115.

Mpandeli, S. (2014). Managing climate risks using seasonal climate forecast information in Vhembe District in Limpopo Province, South Africa. *Journal of Sustainable Development*, *7*(5), 68.

Mpandeli, S., & Maponya, P. (2014). Constraints and challenges facing the small scale farmers in Limpopo Province, South Africa. *Journal of Agricultural Science*, *6*(4), 135.

Maponya, P., & Mpandeli, S. (2012). Climate Change Adaptation Strategies used by Limpopo Province Farmers in South Africa. *Journal of Agricultural Science*, *4*(12), 39.

Mphaphuli S, (1999) Management of resources on mountain environments, In Fairhurst, J., Musyoki, A., Saidi, T., & Wilson, D. (2000). Integrating Environment and Society: The Thohoyandou Environs, Northern Province, South Africa.

Mzezewa, J., Misi, T. and van Rensburg, L.D. (2010). Characterisation of rainfall at a semiarid ecotope in the Limpopo province (South Africa) and its implications for sustainable crop production. *Water SA,* 36 (1), 19-26.

Nandargi, S. & Mulye, S. S. (2012). Relationships between rainy days, mean daily intensity and seasonal rainfall over the koyna catchment during 1961–2005. *The Scientific World Journal, 2012.*

Nenwiini, S.C. (2010). *Climate classification of Vhembe District in Limpopo Province of South Africa Using Multivariate Statistical Analysis (MVSA)* (Honours dissertation, University of Venda).

Nenwiini, S.C. (2012). *Delineation of Vhembe District into homogeneous rainfall zones and their climatology* (Masters dissertation, North West University).

Nenwiini, S.C & Kabanda, T.A. (2013). Trends and variability assessment of rainfall in Vhembe South Africa. *J Hum Ecol*, *42*(2), 171-176.

Netshitungulu, D. (1999). *Adaptation to wind erosion at Muswodi area, Ecology and Resource Management* (Third year research Project, University of Venda, South Africa).

Netshitungulu, D. (2001). *Drought and its impacts on the water resources in the Northern Region of Northern Province of South Africa* (*BESc. Hons. Thesis* University of Venda).

New, M., Todd, M., Hulme, M. & Jones, P. (2001). Precipitation measurements and trends in the twentieth century. *International Journal of Climatology,* 21, 1922 – 1999.

Newell, R.E., Kidson J.W., Vincent, D.G. & Boer, G.J. (1972). *The General Circulation of the Tropical Atmosphere and Interactions with Extratropical Latitudes* (Vol 1). MIT Press, Cambridge.

Newman, M., Sardeshmukh, P.D. & Bergman, J.W. (2000). An assessment of the NCEP, NASA, and ECMWF reanalyses over the tropical west Pacific warm pool. Bulletin of the American Meteorological Society, 81(1), 41.

Nicholson, S.E. & Selato, J.C, (2000). The Influence of La Nina on African Rainfall, *Int. Journal of Climatology*, 20: 1761–1776.

Odekunle, T.O. (2004). Rainfall and the length of the growing season in Nigeria. *International Journal of Climatology,* 24: 467–479.

Odekunle, T.O. (2006). Determining rainy season onset and retreat over Nigeria from precipitation amount and number of rainy days. *Theoretical and Applied Climatology*, 83, 193– 201.

Ojo, O. (1977).*The Climate of West Africa*. Heineman: London.

Olaniran, O.J. (1983). The onset of the rains and the start of the growing season in Nigeria. *Nigerian Geographical Journal,* 26: 81–88.

Olivier, J. & Rautenbach, C.J. (2002). The implementation of fog water collection systems in South Africa. *Atmospheric Research,* 64(4): 227–239.

Olivier, J. & Van Heerden, J. (2003). Implementation of an operational prototype fog water collection system: Project implementation. Report to the Water Research Commission. WRC Report No 902/1/02. Pretoria.

Olivier, J. & Van Heerden, J. (1999). The South African Fog Water Collection Project, Report to the Water Research Commission by the Department of Geography, University of the North. WRC Report No 67.

Olofintoye, O., Adeyemo, J. & Otieno, F. (2012). Impact of Regional Climate Change on Freshwater Resources and Operation of the Vanderkloof Dam System in South Africa. *Global Warming–Impacts and Future Perspective.*

Omotosho, J.B., Balogun, A.A., & Ogunjobi, K. (2000). Predicting monthly and seasonal rainfall, onset and cessation of the rainy season in West Africa using only surface data. *International Journal of Climatology*, *20*(8), 865-880.

Önöz, B. & Bayazit, M. (2002). Troughs under threshold modeling of minimum flows in perennial streams. *Journal of Hydrology*, *258*(1), 187-197.

Päädam, K., & Post, P. (2011). Temporal variability of precipitation extremes in Estonia 1961–2008. *Oceanologia*, *53*, 245-257.

Partal, T. & Kahya, E. (2006). Trend analysis in Turkish precipitation data. Hydrology Process, 20, 2011–2026.

Paul, D.K. (1991). Interaction between Tropical and Extra-Tropical Systems during Monsoon. In The WMO/IMD Training Course in Monsoon Meteorology WMO/TD - No. 496.

Paltridge, G., Arking, A. & Pook, M. (2009). Trends in middle-and upper-level tropospheric humidity from NCEP reanalysis data. *Theoretical and Applied Climatology*, *98*(3-4), 351-359.

Pearce, R.P. (2002). Meteorology at the Millennium. Academic Press. ISBN 978-0-12-548035-2.

Peixóto, J.P., & Oort, A.H. (1983). The atmospheric branch of the hydrological cycle and climate. In Variations in the global water budget. Springer Netherlands.

Peixoto, J.P. & Oort, A.H. (1992). Physics of climate.

Platzky, L. & Walker, C. (1985). The Surplus People: Forced Removals in South Africa. Johannesburg: Ravan Press.

Qian, B., Corte-Real, J. & Xu, H. (2002). Multisite stochastic weather models for impact studies. *International Journal of Climatology*, 2002:1377–1397

Rajeevan, M., Pai, D.S. & Thapliyal, V. (1998). Spatial and temporal relationships between global land surface air temperature anomalies and indian summermonsoon rainfall. *Meteorology and Atmospheric Physics*, vol. 66, no. 3-4, 157–171.

Randel, W.J., Wu, F., & Gaffen, D. J. (2000). Interannual variability of the tropical tropopause derived from radiosonde data and NCEP reanalyses. *Journal of geophysical research*, *105*(D12), 15-509.

Rasmusson, E.M. & Carpenter, T.H. (1982). Variations in tropical sea surface temperature and surface wind fields associated with the Southern Oscillation/El Nin˜o. *Monthly. Weather Review,* **110,** 354–384.

Reason, C.J.C., Allan, R.J., Lindesay, J.A., & Ansell, T.J. (2000). ENSO and climatic signals across the Indian Ocean basin in the global context: Part I, Interannual composite patterns. *International Journal of Climatology*, *20*(11), 1285-1327.

Reason, C.J.C., & Keibel, A. (2004). Tropical cyclone Eline and its unusual penetration and impacts over the southern African mainland. *Weather and forecasting*, *19*(5), 789-805.

Reason, C.J.C., Hachigonta, S. & Phaladi, R.F. (2005). Interannual variability in rainy season characteristics over the Limpopo region of southern Africa. *International Journal of Climatology*, 25, 1835-1853.

Reid, P.A., Jones, P.D., Brown, O., Goodess, C.M. & Davies, T.D. (2001). Assessments of the reliability of NCEP circulation data and relationships with surface climate by direct comparisons with station based data. *Climate Research*, 17, 247-261.

Rocha, A. & Simmonds, I. (1997). Interannual variability of south-eastern African Summer rainfall. Part 1: Relationships with air-sea interaction processes. *International Journal of Climatology,* 17 235-265.

Rocha, A., & Simmonds, I. (1997b). Interannual variability of south-eastern African Summer rainfall. Part II: Modelling the impact of Sea Surface Temperature on Rainfall and Circulation. *International Journal of Climatology*, 17, 267-290.

Root, T.L. & Schneider, S.H. (1995) Ecology and Climate: Research Strategies and Implications. *Science,* 269, 334–341.

Ropelewski, C.F. & Halpert, M.S. (1987). Global and regional-scale precipitation patterns associated with the El-Nino/Southern Oscillation. *Monthly Weather Review*, 115:1606–1626.

Ropelewski, C.F., & Halpert, M.S. (1989). Precipitation patterns associated with the high index phase of the southern Oscillation. *Journal of Climate*, 2:268–284.

Ropelewski, C.F. & Halpert, M.S. (1996). Quantifying Southern Oscillation–precipitation relationships. *Journal of Climate*, 9: 1043–1059.

Rose, C.W. (1998). *Modeling erosion by water and wind* (pp. 57-88). CRC Press.
Rose, B.E. & Lin, C.A. (2003) Precipitation from vertical motion: a statistical diagnostic scheme. *International journal of climatology*, *23*(8), 903-919.

Rudolf, B. & Schneider, U. (2005). Calculation of gridded precipitation data for the global land-surface using in-situ gauge observations. Proceedings of the 2nd Workshop of the International Precipitation Working Group IPWG, Monterey, October 2004, 231-247.

Salmi, T., Maatta., A, Anttila, P., Ruoho-Airola, T. & Amnell, T. (2002). Detecting trends of annual values of atmospheric pollutants by the Mann–Kendall test and Sen's slope estimates-the Excel template application MAKESENS. In Publications on Air Quality no. 31 (ed. Finnish Meteorological Institute), Finnish Meteorological Institute.

Schamm, K., Ziese, M., Becker, A., Finger, P., Meyer-Christoffer, A., Schneider, U., Schröder, M. & Stender, P. (2014). Global gridded precipitation over land: a description of the new GPCC First Guess Daily product. *Earth System Science Data*, 6, 49–60. Retrieved from doi:10.5194/essd-6-49-2014.

Serrano, A., Garcia, J., Mateos, V., Cancillo, M. & Garrido, J. (1999). Monthly modes of variation of precipitation over the Iberian Peninsula. *Journal of Climate*, 12: 2894–2919.

Seidel, D.J. (2002). *Water vapor: Distribution and trends.* Encyclopedia of Global Environmental Change. John Wiley & Sons, Ltd, Chichester.

Shongwe, M.E., van Oldenborgh, G.J., van den Hurk, B.J.J., de Boer, M.B., Coelh, A. S. & van Aalst, M.K. (2009). Projected changes in mean and extreme precipitation in Africa under global warming. Part I: Southern Africa *Journal of Climate*, **22**, 3819–3837.

Shongwe, M.E., Van Oldenborgh, G.J., Van den Hurk, B. & Van Aalst, M, (2011). Projected Changes in Mean and Extreme Precipitation in Africa under Global Warming. Part II: East Africa. *Journal of Climate*, 24, 3718–3733.

Sneyers, R. (1992) On the use of statistical analysis for the objective determination of climate change. *Meteorologische Zeitschrift, 1*(5), 247-256.

Singh, B. & Sharma, M.K. (2003). A study of pattern of rainfall of crop research station-Masodha (U.P.). *Mausam*, 54 (2): 552-556.

Singo, L.R. (2008). *Temporal characteristics of rainfall and their influence on river discharge: the case of Luvuvhu River Catchment in Limpopo Province of South Africa* (Masters Dissertation, University of Venda).

Singleton, A.T. & Reason, C.J.C. (2007). A numerical model study of an intense cutoff low pressure system over South Africa. *Monthly Weather Review*, 135:1128–1150.

Sinthumule, N.I., (2001). *A comparative analysis of the pattern and effects of wetlands utilization in urban versus rural areas of Thohoyandou, Northern Province* (Honours Dissertation, University of Venda, South Africa).

South African Weather Service, (2011). Specialist Information.

Sparrow, G.W.A. (1987). The Meteorology and Climatology of Africa, Dept. of Geography, UNIVEN, pp.138-163.

Spracklen, D.V., Arnold, S.R. & Taylor, C.M. (2012). Observations of increased tropical rainfall preceded by air passage over forests. *Nature*, *489*(7415), 282-285.

Stringer, E. (1972). *Foundations of Climatology. An Introduction to Physical, Dynamic, Synoptic and Geographical Climatology*. San Francisco, WH Freeman & Co.

Suzuki, T. (2011). Seasonal variation of the ITCZ and its characteristics over central Africa. *Theoretical and Applied Climatology*, *103*(1-2), 39-60.

Swinscow, T.D.V., & Campbell, M.J. (2002). *Statistics at square one* (pp. 119-132). London: Bmj.

Symes, C.T., Venter S.M. & Perrin M.R. (2000). Afromontane forest avifauna of the eastern Soutpansberg mountain range, Northern Province, South Africa. *The Southern African Forestry Journal*, 189:1, 71 80. Retrieved from doi: 10.1080/102959 25.2000.9631282.

Tadross, M.A., Hewitson, B.C. & Usman, M.T. (2005). The interannual variability of the onset of the maize growing season over South Africa and Zimbabwe. *Journal of Climate,* 18, 3356–3372.

Tadross, M., Suarez, P., Lotsch, A., Hachigonta, S., Mdoka, M., Unganai, L., ... & Muchinda, M. (2007, June). Changes in growing-season rainfall characteristics and downscaled scenarios of change over southern Africa: implications for growing maize. In *IPCC regional Expert Meeting on Regional Impacts, Adaptation, Vulnerability, and Mitigation, Nadi, Fiji* (pp. 193-204).

Taljaard, J.J. (1985). *Cut-off lows in the South African region.* Government Printer, South Africa.

Tennant, W. (2004). Considerations when using pre-1979 NCEP/NCAR reanalyses in the southern hemisphere. *Geophysical research letters*, *31*(11).

Tennant, W.J., & Hewitson, B.C. (2002). Intra-seasonal rainfall characteristics and their importance to the seasonal prediction problem. *International Journal of Climatology*, *22*(9), 1033-1048. Retrieved from http://onlinelibrary.wiley.com/doi/10.1 02/joc.778/pdf.

Thomas, J.J. (1983). *An introduction to statistical analysis for economists (second edition).* Weidenfeld and Nicolson: London, 228-276.

Timiza, W. (2011). Climate variability and satellite – observed vegetation responses in Tanzania. Master thesis Physical Geography and Ecosystem Analysis, Lund University, Seminar series 205, 30 ECTS.

Todd, M. & Washington, R. (1999). Circulation anomalies associated with tropical-temperate troughs in Southern Africa and the south west Indian Ocean. Climate Dynamics, 15, 937–951.

Todd, M., Washington, R. & Palmer, P.I. (2004). Water vapour transport associated with tropical-temperate trough systems over southern Africa and the southwest Indian Ocean. *International Journal of Climatology*, 24, 555–568.

Tomozeiu, R., Busuioc, A., Marletto, V., Zinoni, F. & Cacciamani, C. (2000). Detection of changes in the summer precipitation time series of the region Emilia-Romagna, Italy. *Theoratical Applied Climatology*, 67, 193-200.

Traore, B., Corbeels, M., Van Wijk, M. T., Rufino, M. C., & Giller, K. E. (2013). Effects of climate variability and climate change on crop production in southern Mali. *European Journal of Agronomy*, *49*, 115-125.

Trenberth, K.E. & Guillemot, C.J. (1995). Evaluation of the global atmospheric moisture budget as seen from analyses. *Journal of Climate*, *8*(9), 2255-2272.

Trenberth, K.E., Stepaniak, D.P., Hurrell, J.W. and Fiorino, M. (2001). Quality of Reanalyses in the Tropics. *Journal of Climate*, 14, 1499-1510.

Trenberth, K.E. (2005). The impact of climate change and variability on heavy precipitation, floods, and droughts. *Encyclopedia of hydrological sciences.*

Tshitangoni, M., Okorie, A., & Francis, J. (2010). Assessment of challenges facing poverty alleviation projects in Vhembe District of Limpopo Province in South Africa. *Scientific Research and Essays*, *5*(17), 2375-2383.

Tyson, P.D. & Preston-Whyte, R.A. (2000). *The Weather And Climate Of Southern Africa*. Oxford Universty Press, Cape Town.

Tyson, P.D. (1986). *Climate Change Variability in South Africa.* Oxford University Press, Cape Town.

Van den Heever, S.C., D'Abreton, P.C. & Tyson, P.D (1997). Numerical simulation of tropical-temperate troughs over Southern Africa using the CSU RAMS model. *South African Journal of Science,* 93, 359-365.

Vigaud, N., Richard, Y., Rouault, M. & Fauchereau, N. (2007). Water vapour transport from the tropical Atlantic and summer rainfall in tropical southern Africa. *Climate dynamics*, *28*(2-3), 113-123.

Vila, D.A., de Goncalves, L.G.G., Toll, D.L. & Rozante, J.R. (2009). Statistical evaluation of combined daily gauge observations and rainfall satellite estimates over continental South America. Journal of Hydrometeorology, 10: 533–542.

Von Storch, H., & Navarra, A. (1993). Analysis of Climate Variability Applications of Statistical Techniques Proceedings of an Autumn School organized by the Commission of the European Community on Elba from October 30 to November 6, 1993 2nd updated and extended edition.

Von Storch, H. & Navarra, A. (1999). *Analysis of climate variability: applications of statistical techniques*. Springer Science & Business Media.

Waliser, D.E. & Gautier, C. (1993). A satellite-derived climatology of the ITCZ. *Journal of. Climate*, 6, 2162– 2174.

Walter, M.W. (1968). Length of the rainy season in Nigeria. Institute of Agriculture Research, Ahmadu Bello University, Samaru, Zaria, Nigeria.

Washington, R. & Preston (2006). Extreme wet years over southern Africa: Role of Indian Ocean sea surface temperatures. *Journal of Geophysics Research*, 111, D15104. Retrieved from doi:10.1029/2005JD006724.

Wilbanks, T.J. & R.W. Kates, (1999). Global Change in Local Places: How Scale Matters. *Climate Change*, 43(3):601-628.

Wilby, R.L. (1998). Statistical downscaling of daily precipitation using daily airflow and seasonal teleconnection indices. *Climate Research*, 10:163–178.

Williams, C.J. & Kniveton, D.R. (Eds.). (2011). *African climate and climate change: physical, social and political perspectives* (Vol. 43). Springer Science & Business Media.

Wu, X, Liang, X.Z. & Zhang, G.J. (2003). Seasonal migration of ITCZ precipitation across the equator: Why can't GCMs simulate it? *Geophysical Research Letters*, Vol. 30, NO. 15, 1824.

Whitbread, A., MacLeod, N., McDonald, C., Pengelly, B., Ayisi, K., & Mkhari, J. (2011). Farming Systems, Emerging Farmers and Land Reform in the Limpopo Province of South Africa. In *Rainfed Farming Systems* (pp. 433-449). Springer Netherlands.

Xie, S.P. (1996). Westward propagation of latitudinal asymmetry in a coupled ocean-atmosphere model. *Journal of Atmospheric Science,* 53, 3236– 3250.

Xie, P. & Arkin, P.A. (1997). Global precipitation: A 17-year monthly analysis based on gauge observations, satellite estimates, and numerical model outputs. Bull. *Amer. Meteor. Soc,* 78, 2539 - 2558.

Xie, P., Janowiak, J., Arkin, P., Adler, R., Gruber, A., Ferraro, R., Huffman, G. & Curtis, S. (2003). GPCP Pentad Precipitation Analyses: An Experimental Dataset Based on Gauge Observations and Satellite Estimates. *Journal of Climate,* **16**, 2197–2214. Retrieved from doi: 10.1175/2769.1.

Xie, P., Yatagai, A., Chen, M., Hayasaka, T., Fukushima, Y., Liu, C. & Yang, S. (200 7). A gauge-based analysis of daily precipitation over East Asia. J. Hydrometeor, 8, 607–627.

Yatagai, A., Xie, P. & Alpert, P. (2008). Development of a daily gridded precipitation data set for the Middle East. *Advance in Geoscience,* 12, 165–170.

Appendix 1

List of Rainfall Stations in Vhembe District

Station Name	Latitude	Longitude	Height (m)
Mara	2309	2934	897
Una Agric	2307	2940	899
Bandelierkop	2319	2948	1128
Zwartrandjes	2314	2951	1036
Louis Trichardt	2303	2954	961
Hangklip	2301	2955	1036
Soekmekaar	2329	2956	1172
Elim Hos	2310	3003	808
Setali	2320	3003	884
Goedehoop	2305	3006	811
Klein Australie	2303	3013	702
Levubu	2305	3017	706
Tshakhuma	2303	3018	1158
Tsianda	2303	3020	1120
Kruger	2310	3057	427
Tolwe	2259	2835	793
Alldays	2241	2906	823
Tshipise	2236	3010	579
Entabeni Bos	2300	3016	1376
Matiwa	2259	3017	1311
Vondo Bos	2256	3020	1130
Palmaryville	2259	3026	570
Rambuda	2247	3028	762
Folovhodwe	2232	3029	610
Messina	2216	2954	525
Mphephu	2252	3007	768
Legraal	2322	2932	1014
Mara Pol	2305	2923	914
Roondewal Bos	2300	3001	1133
Saamboubrug	2234	2834	695
Sheffeera	2303	3012	1214
Nooitgedacht	2304	3012	762
Messina Pol	2221	3003	538
Pont Drift	2213	2909	580

Appendix 2

Standard World Meteorological Organisation (WMO) Annual Pentads Format

Pentads	Day of Year	Date- Ordinary years (1)	Date- Leap Years (2)
1	01-05	01-Jan-05-Jan	01-Jan-05-Jan
2	06-10	06-Jan-10-Jan	06-Jan-10-Jan
3	11-15	11-Jan-15-Jan	11-Jan-15-Jan
4	16-20	16-Jan-20-Jan	16-Jan-20-Jan
5	21-25	21-Jan-25-Jan	21-Jan-25-Jan
6	26-30	26-Jan-30-Jan	26-Jan-30-Jan
7	31-35	31-Jan-04-Feb	31-Jan-04-Feb
8	36-40	05-Feb-09-Feb	05-Feb-09-Feb
9	41-45	10-Feb-14-Feb	10-Feb-14-Feb
10	46-50	15-Feb-19-Feb	15-Feb-19-Feb
11	51-55	20-Feb-24-Feb	20-Feb-24-Feb
12	56-60	25-Feb-01-Mar	25-Feb-29-Feb
13	61-65	02-Mar-06-Mar	01-Mar-05-Mar
14	66-70	07-Mar-11-Mar	06-Mar-10-Mar
15	71-75	12-Mar-16-Mar	11-Mar-15-Mar
16	76-80	17-Mar-21-Mar	16-Mar-20-Mar
17	81-85	22-Mar-26-Mar	21-Mar-25-Mar
18	86-90	27-Mar-31-Mar	26-Mar-30-Mar
19	91-95	01-Apr-05-Apr	31-Mar-04-Apr
20	96-100	06-Apr-10-Apr	05-Apr-09-Apr
21	101-105	11-Apr-15-Apr	10-Apr-14-Apr
22	106-110	16-Apr-20-Apr	15-Apr-19-Apr
23	111-115	21-Apr-25-Apr	20-Apr-24-Apr
24	116-120	26-Apr-30-Apr	25-Apr-29-Apr
25	121-125	01-May-05-May	30-Apr-04-May
26	126-130	06-May-10-May	05-May-09-May
27	131-135	11-May-15-May	10-May-14-May
28	136-140	16-May-20-May	15-May-19-May
29	141-145	21-May-25-May	20-May-24-May
30	146-150	26-May-30-May	25-May-29-May
31	151-155	31-May-04-Jun	30-May-03-Jun
32	156-160	05-Jun-09-Jun	04-Jun-08-Jun
33	161-165	10-Jun-14-Jun	09-Jun-13-Jun
34	166-170	15-Jun-19-Jun	14-Jun-18-Jun
35	171-175	20-Jun-24-Jun	19-Jun-23-Jun
36	176-180	25-Jun-29-Jun	24-Jun-28-Jun
37	181-185	30-Jun-04-Jul	29-Jun-03-Jul
38	186-190	05-Jul-09-Jul	04-Jul-08-Jul
39	191-195	10-Jul-14-Jul	09-Jul-13-Jul
40	196-200	15-Jul-19-Jul	14-Jul-18-Jul
41	201-205	20-Jul-24-Jul	19-Jul-23-Jul
42	206-210	25-Jul-29-Jul	24-Jul-28-Jul
43	211-215	30-Jul-03-Aug	29-Jul-02-Aug
44	216-220	04-Aug-08-Aug	03-Aug-07-Aug
45	221-225	09-Aug-13-Aug	08-Aug-12-Aug
46	226-230	14-Aug-18-Aug	13-Aug-17-Aug
47	231-235	19-Aug-23-Aug	18-Aug-22-Aug

48	236-240	24-Aug-28-Aug	23-Aug-27-Aug
49	241-245	29-Aug-02-Sep	28-Aug-01-Sep
50	246-250	03-Sep-07-Sep	02-Sep-06-Sep
51	251-255	08-Sep-12-Sep	07-Sep-11-Sep
52	256-260	13-Sep-17-Sep	12-Sep-16-Sep
53	261-265	18-Sep-22-Sep	17-Sep-21-Sep
54	266-270	23-Sep-27-Sep	22-Sep-26-Sep
55	271-275	28-Sep-02-Oct	27-Sep-01-Oct
56	276-280	03-Oct-07-Oct	02-Oct-06-Oct
57	281-285	08-Oct-12-Oct	07-Oct-11-Oct
58	286-290	13-Oct-17-Oct	12-Oct-16-Oct
59	291-295	18-Oct-22-Oct	17-Oct-21-Oct
60	296-300	23-Oct-27-Oct	22-Oct-26-Oct
61	301-305	28-Oct-01-Nov	27-Oct-31-Oct
62	306-310	02-Nov-06-Nov	01-Nov-05-Nov
63	311-315	07-Nov-11-Nov	06-Nov-10-Nov
64	316-320	12-Nov-16-Nov	11-Nov-15-Nov
65	321-325	17-Nov-21-Nov	16-Nov-20-Nov
66	326-330	22-Nov-26-Nov	21-Nov-25-Nov
67	331-335	27-Nov-01-Dec	26-Nov-30-Nov
68	336-340	02-Dec-06-Dec	01-Dec-05-Dec
69	341-345	07-Dec-11-Dec	06-Dec-10-Dec
70	346-350	12-Dec-16-Dec	11-Dec-15-Dec
71	351-355	17-Dec-21-Dec	16-Dec-20-Dec
72	356-360	22-Dec-26-Dec	21-Dec-25-Dec
73	361-365	27-Dec-31-Dec	26-Dec-31-Dec

Appendix 3

Homogeneous Rainfall Zones Rainfall Zones in Vhembe District

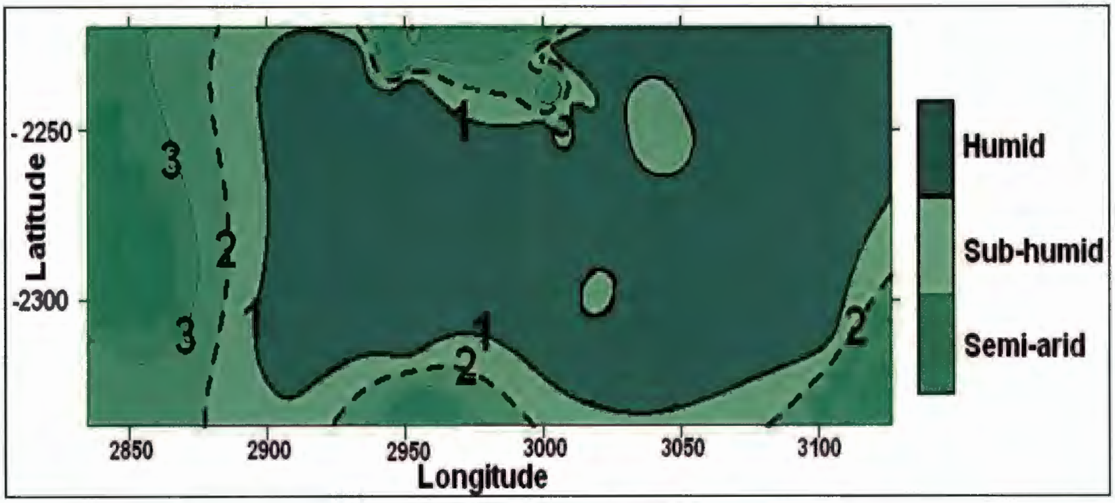

Appendix 4

Rainfall stations per Classified Rainfall Zones in Vhembe District

Humid Zone (1)	Semi-arid Zone (3)	Sub-Humid Zone (2)
Tsianda	Mara	Goedehoep
Palmaryville	Saambouberg	Zwartrandjes
Entabeni	Mara	Klein Astralie
Rambuda	Tshipise	Soekmekaar
Levubu	Banderliekop	Shefeere
Tshakhuma	Tolwe	Hanglip
Matiwa	Unagric	Roodeval Bos
Kruger	Pontdrift	
Vondo bos	Legraal	
Mphephu	Messina	
Nooitgedacht	Elim	
	Folovhodwe	